ลักษณะสมบัติเชิงหน้าที่ของโปรตีนในระบบภูมิคุ้มกันจากกุ้งกุลาดำ *Penaeus monodon* ในการตอบสนองต่อการติดเชื้อก่อโรค

นางสาวภัทรันดา จารีย์

วิทยานิพนธ์นี้เป็นส่วนหนึ่งของการศึกษาตามหลักสูตรปริญญาวิทยาศาสตรดุษฎีบัณฑิต
สาขาวิชาชีวเคมีและชีววิทยาโมเลกุล ภาควิชาชีวเคมี
คณะวิทยาศาสตร์ จุฬาลงกรณ์มหาวิทยาลัย
ปีการศึกษา 2556
ลิขสิทธิ์ของจุฬาลงกรณ์มหาวิทยาลัย

FUNCTIONAL CHARACTERIZATION OF IMMUNE-RELATED PROTEINS FROM BLACK TIGER SHRIMP *Penaeus monodon* IN RESPONSE TO PATHOGEN INFECTION

Miss Phattarunda Jaree

A Dissertation Submitted in Partial Fulfillment of the Requirements
for the Degree of Doctor of Philosophy Program in Biochemistry and Molecular Biology
Department of Biochemistry
Faculty of Science
Chulalongkorn University
Academic Year 2013

Thesis Title	FUNCTIONAL CHARACTERIZATION OF IMMUNE-RELATED PROTEINS FROM BLACK TIGER SHRIMP *Penaeus monodon* IN RESPONSE TO PATHOGEN INFECTION
By	Miss Phattarunda Jaree
Field of Study	Biochemistry and Molecular Biology
Thesis Advisor	Professor Anchalee Tassanakajon, Ph.D.
Thesis Co-Advisor	Assistant Professor Kunlaya Somboonwiwat, Ph.D.
	Professor Chu-Fang Lo, Ph.D.

Accepted by the Faculty of Science, Chulalongkorn University in Partial Fulfillment of the Requirements for the Doctoral Degree

.....Dean of the Faculty of Science

(Professor Supot Hannongbua, Dr.rer.nat.)

THESIS COMMITTEE

.....Chairman

(Professor Aran Incharoensakdi, Ph.D.)

.....Thesis Advisor

(Professor Anchalee Tassanakajon, Ph.D.)

.....Thesis Co-Advisor

(Assistant Professor Kunlaya Somboonwiwat, Ph.D.)

.....Thesis Co-Advisor

(Professor Chu-Fang Lo, Ph.D.)

.....Examiner

(Associate Professor Teerapong Buaboocha, Ph.D.)

.....Examiner

(Assistant Professor Rath Pichyangkura, Ph.D.)

.....External Examiner

(Saengchan Senapin, Ph.D.)

ภัทรันดา จารีย์ : ลักษณะสมบัติเชิงหน้าที่ของโปรตีนในระบบภูมิคุ้มกันจากกุ้งกุลาดำ *Penaeus monodon* ในการตอบสนองต่อการติดเชื้อก่อโรค. (FUNCTIONAL CHARACTERIZATION OF IMMUNE-RELATED PROTEINS FROM BLACK TIGER SHRIMP *Penaeus monodon* IN RESPONSE TO PATHOGEN INFECTION) อ.ที่ปรึกษาวิทยานิพนธ์หลัก: ศ. ดร.อัญชลี ทัศนาขจร, อ.ที่ปรึกษาวิทยานิพนธ์ร่วม: ผศ. ดร.กุลยา สมบูรณ์วิวัฒน์, Prof. Chu-Fang Lo Ph.D., 166 หน้า.

ในระบบภูมิคุ้มกันของกุ้งมีโปรตีนหลายชนิดที่มีการแสดงออกและทำหน้าที่ตอบสนองต่อสิ่งกระตุ้นรวมทั้งเชื้อก่อโรคในกุ้ง ในงานวิจัยนี้สนใจศึกษาโปรตีนที่เกี่ยวข้องกับระบบภูมิคุ้มกัน 2 ตัว คือ Anti-lipopolysaccharide factor isoform 3 (ALF*Pm*3) และ Viral responsive protein 15 (*Pm*VRP15) ที่พบในกุ้งกุลาดำ จากผลงานวิจัยที่ผ่านมาพบว่าโปรตีน ALF*Pm*3 มีความสามารถในการต้านเชื้อแบคทีเรียแกรมลบและแกรมบวก เชื้อรา และไวรัสได้ ในงานวิจัยนี้ สนใจที่จะศึกษาผลของโปรตีน ALF*Pm*3 ต่อเชื้อแบคทีเรียก่อโรคในกุ้ง *Vibrio harveyi* จากการทดลองพบว่าโปรตีน ALF*Pm*3 สามารถจับกับแบคทีเรีย *V. harveyi* ส่งผลให้เกิดการรั่วของผนังเซลล์เมมเบรนของแบคทีเรีย ทำให้เกิดการรั่วของสารจากในเซลล์ออกมานอกเซลล์ จากนั้นได้ทำการศึกษาโครงสร้างภายนอกของแบคทีเรีย *V. harveyi* หลังจากบ่มกับโปรตีน ALF*Pm*3 ด้วยเครื่องจุลทรรศอิเล็กตรอนแบบส่องกราดและแบบส่องผ่าน พบว่าเซลล์เมมเบรนของแบคทีเรียถูกทำลายให้มีลักษณะเปลี่ยนแปลงไป เช่นเกิดการโป่งของเมมเบรน (bleb formation) เมมเบรนเป็นรู (pore formation) และยังมีการรั่วของสารประกอบจากภายในเซลล์ออกมานอกเซลล์ จากผลการทดลองสามารถสรุปได้ว่า โปรตีน ALF*Pm*3 สามารถฆ่าแบคทีเรียก่อโรค *V. harveyi* โดยการแทรกผ่านเซลล์เมมเบรน และทำให้เกิดการรั่วของเซลล์เมมเบรน ในส่วนของโปรตีน *Pm*VRP15 ที่มีการแสดงออกเพิ่มมากขึ้นหลังจากกุ้งติดเชื้อไวรัสตัวแดงดวงขาว (White spot syndrome virus, WSSV) พบว่าในกุ้งที่ติดเชื้อไวรัสตัวแดงดวงขาวที่ถูกยับยั้งการแสดงออกของยีน *Pm*VRP15 โดยเทคนิค RNA interference มีการแสดงออกของยีนไวรัสตัวแดงดวงขาวในระยะต่างๆได้แก่ ยีน ie-1 ซึ่งแสดงออกในช่วง immediate early stage ยีน wsv477 ซึ่งแสดงออกในช่วง early stage และยีน vp28 ซึ่งแสดงออกในช่วง late stage ลดลง 83.5% 85.5% และ 94.8% ตามลำดับ หลังการติดเชื้อเมื่อเทียบกับกลุ่มควบคุม และเมื่อตรวจสอบอัตราการตายของกุ้งพบว่าในกุ้งที่ไม่มียีน *Pm*VRP15 มีอัตราการตายลดลง เมื่อเทียบกับกุ้งกลุ่มควบคุม จึงสามารถสรุปได้ว่า ยีน *Pm*VRP15 มีความสำคัญกับการเพิ่มจำนวนไวรัสในกุ้ง ในการหาโปรตีนของไวรัสที่สามารถจับกับโปรตีน *Pm*VRP15 ด้วยเทคนิค Yeast two-hybrid และ Co-immunoprecipiation พบว่าโปรตีน WSV399 สามารถจับกับโปรตีน *Pm*VRP15 ได้ และเมื่อทำการตรวจสอบหาตำแหน่งของโปรตีน WSV399 บนไวรัสตัวแดงดวงขาวด้วยเทคนิค Immunobloting analysis และ immunoelectron microscopy พบว่าโปรตีน WSV399 เป็นโปรตีนโครงสร้างที่อยู่ในส่วนของ Tegument นอกจากนี้ได้ ศึกษาการควบคุมการแสดงออกของยีน *Pm*VRP15 เริ่มจากการหาลำดับนิวคลีโอไทด์ของปลาย 5’ ของยีน *Pm*VRP15 ด้วยเทคนิค genome walking ได้ขนาดประมาณ 2 กิโลเบส จากนั้นทำการหาส่วนที่สำคัญที่เกี่ยวข้องกับการควบคุมการแสดงออกของยีน พบว่า บริเวณลำดับนิวคลีโอไทด์ที่ตำแหน่ง -525 ถึง -428 และ ตำแหน่ง -287 ถึง -209 น่าจะเป็นบริเวณที่มี repressor และ activator มาจับและควบคุมการแสดงออกของยีนตามลำดับ จากนั้นใช้โปรแกรมคอมพิวเตอร์ และใช้เทคนิค Site-directed mutagenesis ในการตรวจสอบตำแหน่งที่มีผลต่อการแสดงออกของยีน จากผลการทดลองพบว่าบริเวณลำดับนิวคลีโอไทด์ที่ตำแหน่ง -525 ถึง -428 พบลำดับนิวคลีโอไทด์ที่จำเพาะกับ interferon regulatory factor (IRF) ที่คาดว่าทำหน้าที่เป็น repressor ในการควบคุมการแสดงออกของยีน *Pm*VRP15 และ บริเวณลำดับนิวคลีโอไทด์ที่ตำแหน่ง -287 ถึง -209 พบลำดับนิวคลีโอไทด์ที่จำเพาะกับ octamer transcription factor (Oct-1) and nuclear factor of activated T cells (NFAT) ที่คาดว่าทำหน้าที่เป็น activator ในการควบคุมการแสดงออกของยีน *Pm*VRP15

ภาควิชา ชีวเคมี ลายมือชื่อนิสิต .....

สาขาวิชา ชีวเคมีและชีววิทยาโมเลกุล ลายมือชื่อ อ.ที่ปรึกษาวิทยานิพนธ์หลัก .....

ปีการศึกษา 2556 ลายมือชื่อ อ.ที่ปรึกษาวิทยานิพนธ์ร่วม .....

ลายมือชื่อ อ.ที่ปรึกษาวิทยานิพนธ์ร่วม .....

5272471323 : MAJOR BIOCHEMISTRY AND MOLECULAR BIOLOGY
KEYWORDS: ANTI-LIPOPOLYSACCHARIDE FACTOR / VIBRIO HARVEYI / VIRAL RESPONSIVE PROTEIN / WHITE SPOT SYNDROME VIRUS / PENAEUS MONODON

PHATTARUNDA JAREE: FUNCTIONAL CHARACTERIZATION OF IMMUNE-RELATED PROTEINS FROM BLACK TIGER SHRIMP *Penaeus monodon* IN RESPONSE TO PATHOGEN INFECTION. ADVISOR: PROF. ANCHALEE TASSANAKAJON, Ph.D., CO-ADVISOR: ASST. PROF. KUNLAYA SOMBOONWIWAT, Ph.D., PROF. CHU-FANG LO, Ph.D., 166 pp.

Shrimp immunity comprises of various effector molecules that are expressed and function in response to various stimuli including pathogens. In this research, two immune-related proteins; Anti lipopolysaccharise factor isoform 3 (ALF*Pm*3) and Viral responsive protein 15 (*Pm*VRP15) were characterized. The ALF*Pm*3 has previously been shown to exhibit very active antimicrobial activity against a broad range of Gram-positive and Gram-negative bacteria, fungi and virus. The propose of this research is to study the effects of treating ALF*Pm*3 on membrane of *Vibrio harveyi*. The recombinant ALF*Pm*3 protein was found to localize on the *V. harveyi* cells *in vivo*, followed by inducing membrane permeabilization and leakage of cytoplasmic components. Membrane disruption and damage, bleb and pore formation, and the leakage of cytoplasmic contents were all clearly observed by scanning and transmission electron microscopy. Our results suggested that ALF*Pm*3 effectively kills bacteria through bacterial membrane permeabilization mechanism. Other immune-related protein with unknown function, namely *Pm*VRP15, is of interest among the highly up-regulated gene identified in hemocyte of White spot syndrome virus (WSSV)-infected shrimp. RNAi-mediated silencing of *Pm*VRP15 gene in WSSV-infected shrimp resulted in a significant decreased in the expression of WSSV genes including *ie-1* (immediate early stage), *wsv477* (early stage) and *vp28* (late stage) by 83.5%, 85.5% and 94.8%, respectively. The significant decrease in the cumulative mortality of WSSV-infected shrimp following *Pm*VRP15 knockdown suggested its important role in viral propagation. The interaction between *Pm*VRP15 and WSSV proteins was identified by yeast two-hybrid screening and confirmed by co-immunoprecipitation (Co-IP). WSV399 protein was identified as a *Pm*VRP15 binding protein. Immunobloting analysis (*in vitro*) and immunoelectron microscopy (*in vivo*) identified WSV399 as the tegument protein. Moreover, the regulation of *Pm*VRP15 gene expression was studied. About 2 kbp of 5' flanking promoter sequences of *Pm*VRP15 gene were identified by genome walking technique. Promoter deletion assay identified (-525/-428) and (-287/-209) nucleotide positions as repressor and activator binding sites, respectively. The computational analysis and site directed mutagenesis revealed that the repressor binding site (-525/-428) is regulated by interferon regulatory factor (IRF) and activator binding sites in (-287/-209) region are regulated by octamer transcription factor (Oct-1) and nuclear factor of activated T cells (NFAT).

Department:	Biochemistry	Student's Signature	.....
Field of Study:	Biochemistry and Molecular Biology	Advisor's Signature	.....
		Co-Advisor's Signature	.....
Academic Year:	2013	Co-Advisor's Signature	.....

ACKNOWLEDGEMENTS

On the completion of my thesis, I would like to express my deepest gratitude to my superlative supervisor, Prof. Dr. Anchalee Tassanakajon and my lovely co- supervisor, Asst. Prof Dr. Kunlaya Somboonwiwat, for their excellent guidance, supervision, encouragement and supports throughout my five-year study. The great suggestion and discussion with you have become essential keys for developing my research outcome. Especially, I have to thank you very much for your hard effort to teach, improve and inspire me into an efficient researcher.

To my co-supervisor Prof. Dr. Chu-Fang Lo, thank you for your warm welcome in National Taiwan University as well as your great supports and advises all the time while I was studying in Taiwan. Moreover, I did not only gain a lot of knowledge of science from you but I also got your worth experiences of science that you kindly shared to me. I also would like to thank Dr. Wang-Jing Leu for her valuable suggestion and discussion on my works in Taiwan.

I also thank Assoc. Prof. Dr. Sanong Ekgasit and Dr. Saengchan Senapin, for their help in my research experiment.

Assoc. Prof. Dr. Vichien Rimphanitchayakit, Dr. Premruethai Supungul, Dr. Piti Amparyup, Ms. Sureerat Tang and all of my friends in Thailand and Taiwan are greatly appreciated for their helpful suggestion and discussion.

Additional great appreciation is extended to Prof. Dr. Aran Incharoensakdi, Assoc. Prof. Dr. Teerapong Buaboocha, Assist. Prof. Dr. Rath Pichyangkura and Dr. Saengchan Senapin for giving me your precious time on being my thesis's defense committee and for their valuable comments and also useful suggestions.

I wish to acknowledge contributions of The Chulalongkorn University graduate scholarship to commemorate the 72nd Anniversary of His Majesty King Bhumibol Adulyadej and the Royal Golden Jubilee Ph.D. Program, Thailand Research Fund, for my fellowships.

Finally, I would like to express my deepest gratitude to indispensable people including my parents and my family for their understanding, guide, encouragement, endless love, care and support along my lifetime.

CONTENTS

Page

Page

Page

Page

Page

Page

Page

LIST OF TABLES

Page

LIST OF FIGURES

Page

Page

Page

Page

LIST OF ABBREVIATIONS

ALF3	Anti-lipopolysaccharide factor isoform 3
AMP	Antimicrobial peptide
bp	Base pair
co-IP	Co-immunoprecipitation
Da	Dalton
DNA	Deoxyribonucleic acid
dsRNA	Double-stranded RNA
E. coli	*Escherichia coli*
EST	Expressed sequence tag
FBS	Fetal bovine serum
g	Gram
GFP	Green fluorescence protein
h	Hour, Hours
K	Kilo
l	Liter
LB	Luria-Bertani
m	Milli
M	Molar
min	Minute, Minutes
PAGE	polyacrylamide electrophoresis
PCR	Polymerase chain reaction
PBS	1x phosphate buffered saline

Pl	*Pacifastacus leniusculus*
Pm	*Penaeus monodon*
rALF*Pm*3	Recombinant ALF*Pm*3
r*Pm*VRP15	Recombinant *Pm*VRP15
RNA	Ribonucleic acid
RNAi	RNA interference
RT	Reverse transcription
SEM	Scanning electron microscopy
SD	Standard deviation
sec	Seconds
SPF	Specific pathogen free
SSH	Suppression subtractive hybridization
ssRNA	Single-stranded RNA
TEM	Transmission electron microscopy
µ	Micro
UV	Ultraviolet
V. harveyi	*Vibrio harveyi*
VRP15	Viral responsive protein 15
WSSV	White spot syndrome virus

CHAPTER I
INTRODUCTION

1.1. Shrimp aquaculture in Thailand

In 1970s, shrimp aquaculture started and developed rapidly with a huge increase in the number of hatcheries and farms. The activity concerns tropical countries in South East Asia, Central and South America. Shrimp farming has been practiced in Thailand for more than 30 years, but developed and expanded very rapidly during the mid-1980s (Wyban 2007). The shrimp species mainly produced are the black tiger shrimp (*Penaeus monodon*) and the white shrimp (*Litopenaeus. vannamei*). Unfortunately, during the last decade, the production of the black tiger shrimp has been decreased rapidly due to the main problems including the outbreaks of bacterial and viral diseases as well as the lack of high-quality shrimp broodstock (Mohan *et al.* 1998).

Nowadays, in Thailand, the proportion of the black tiger shrimp farming is less than 10% whereas that of the white shrimp, *L. vannamei* accounts for more than 90% of total shrimp production. The white shrimp has several advantages over the *P. monodon*, including the rapid growth rate, availability of specific pathogen free stocks, disease resistance and high survival rate during larval rearing. However, there are disadvantages of *L. vannamei* is that its ability can act as a carrier of various viral pathogens such as *Baculovirus penaei* and Taura syndrome virus, and these viruses can be transmitted to the native penaeid shrimp, *P. monodon*. Moreover, *L. vannamei* is an alien species, and its broodstock has to be imported mainly from aboard that possibly acts as a carrier of various new pathogens to the culture areas. Recently, the shrimp production in Thailand has been substantially dropped during the period from 2012 to 2013 due to the outbreak of the new emerging disease, the early mortality syndrome (EMS) (Figure 1.1). To solve the disease outbreak problems in shrimp aquaculture, the knowledge of shrimp immunity and the invention of the effective disease control need to be improved.

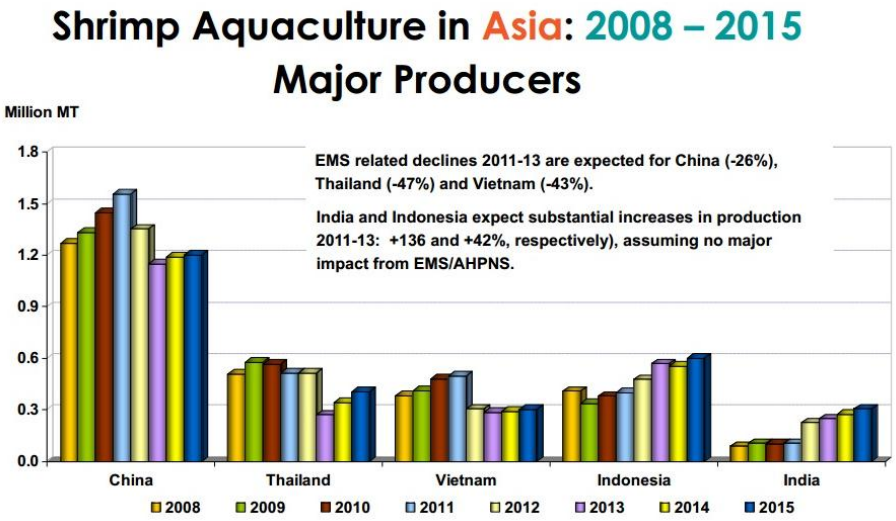

Figure 1.1 The production of shrimp aquaculture in Asia, in the period from 2008 to 2015 (Source: FAO (2013) for 2008-2011, GOAL (2013) for 2012-2015).

1.2. Major diseases in shrimp

The diseases of cultured penaeid shrimp include syndrome with infectious and noninfectious etiologies. Included among the infectious diseases of economic importance to cultured shrimp are those with viral, rickettsial, bacterial, fungal, protistan and metazoan etiologies. A number of noninfectious diseases are also of importance to the industry, and included among these are diseases due to environmental extremes, nutritional imbalances, toxicants, and genetic factors (Lightner and Redman, 1998).

The infectious diseases become serious problems in shrimp industry worldwide. The shrimp farming industry in Thailand encountered a severe problem from uncontrollable viral diseases for over a decade. The bacterial diseases of shrimp are due mainly to Vibrio species (Saulnier *et al.* 2000). On the other hand, the major shrimp viral pathogens are white spot syndrome virus (WSSV), yellow head virus (YHV), hepatopancreatic parvovirus (HPV), monodon baculovirus (MBV), taura syndrome virus (TSV), and hematopoietic virus (IHHNV) (Flegel 2007). In 2009, an emerging disease known as early mortality syndrome (EMS) also later termed acute

hepatopancreatic necrosis syndrome or AHPNS caused significant losses among shrimp farmers in asia. It also reportedly affected shrimp in the eastern Gulf of Thailand in 2012 (Flegel 2012). In this research, we focus on the candidates of bacterial and viral diseases are *Vibrio harveyi* and White spot syndrome virus respectively. Both of them cause damages in shrimp farming, leading to rapid mass mortality of the infected shrimp within few weeks, until now the effective approach for preventing the viral infection has not yet been established.

1.2.1. Vibriosis

V. harveyi is a marine Gram-negative luminous organism with a requirement for sodium chloride (Farmer *et al.* 2005). It is a rod-shaped, 0.5-0.8 μm in width and 1.4-2.6 μm in length. It is capable to emit light of a blue-green color. The penaeid shrimp are typically infected with *V. harveyi* in all life cycle, but mostly in the larvae stage. During the infection, several pathogenic mechnisms of *V. harveyi*, such as quorum sensing factors and biofilm forming, are necessary for the bacteria to circumvent from host immune defenses. The evident symptoms caused by *V. harveyi* in the infected penaied shrimp are called luminous vibriosis (disorder development of basal tissues in the digestive system) and bolitas negricans (glowing in the dark, visible on the thoracic and head part) (Austin and Zhang 2006).

The features of the Vibrio infected shrimps are the milky white body and appendages, weakness, disoriented swimming, lethargy and loss of appetite. Eventually, these lead to death. This bacterial outbreak causes mortality of the affected shrimp up to 100% (Lightner 1993). In Thailand, *V. harveyi* is a causative agent for luminescent shrimp disease in cultivated black tiger shrimp (*P. monodon)* and has caused major losses to shrimp farmers (Jiravanichpaisal *et al.* 1994, Ruangpan *et al.* 1999).

1.2.2. White spot syndrome disease (WSD)

White spot syndrome virus is one of the most severe shrimp pathogens in cultured shrimp. WSSV infection can reach a cumulative mortality of up to 100% within 3–10 days (Lightner 1996). The origin of white spot syndrome outbreak began

in Taiwan shrimp farms in 1992 and rapidly spread throughout Asia, subsequently, the disease crossed over the Pacific Ocean and spread in North, Central and South America, creating by far the greatest economic damage (Chou *et al.* 1995, Flegel 1997, Lotz 1997, Spann and Lester 1997). The clinical signs of WSSV include white spots on the inner side of the carapace, cuticle over abdomen, display signs of lethargy and reddish coloration of the hepatopancreas (Chou *et al.* 1995).

WSSV is the type species of the genus *Whispovirus* in the viral family *Nimaviridae*, containing a circular double-stranded DNA of about 300 Kbp. WSSV is an enveloped rod-shaped particle with a single filamentous appendage-like tail at one end of the nucleocapsid (Yang *et al.* 2001, Vlak *et al.* 2004). The virions contain a rod-shaped nucleocapsid, typically measuring 65-70 nm in diameter and 210-350 nm in length. The nucleocapsids, which contain a DNA-protein core bounded by a distinctive capsid layer giving it a cross-hatched appearance, are wrapped singly into an envelope to shape the virion Figure 1.2A (Durand *et al.* 1997, Nadala and Loh 1998). A tail-like appendage at one end of the WSSV virion is sometimes observed in negatively stained electron micrographs as shown in Figure 1.2B (Wongteerasupaya *et al.* 1995, Durand *et al.* 1996).

(A) (B)

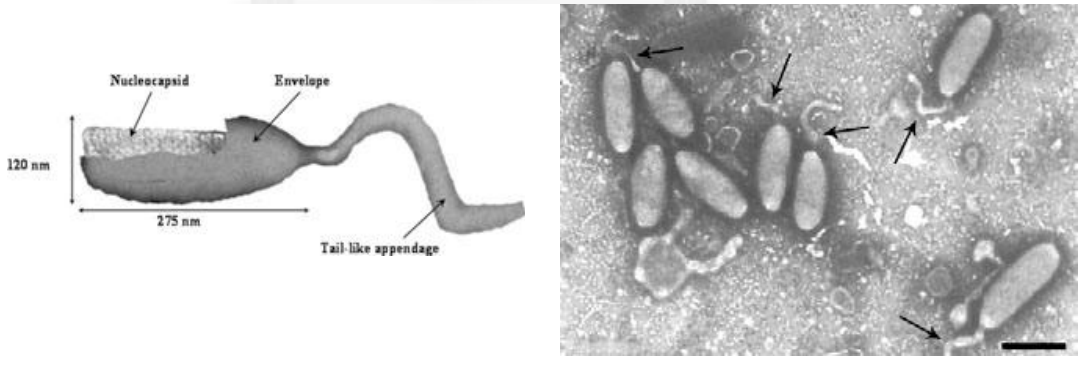

Figure 1.2 White spot syndrome virus (A) The morphology of WSSV virion (B) Negative-staining electron micrograph of WSSV virion with tail-like appendage (arrow). Bar = 250 nm. (Taken from Escobedo-Bonilla *et al.*, 2008)

About 40 WSSV proteins have been characterized as shown in Table 1.2. (Escobedo-Bonilla *et al.* 2008). Most of these proteins are structural proteins in the envelope (VP12B, VP13B, VP14, VP19, VP28, VP31, VP32, VP33, VP38A, VP39B, VP41A, VP41B, VP51A, VP51B, VP53A, VP60A, VP90, VP110, VP124, VP180 and VP187), tegument (VP12A, VP26, VP36A, VP39A and VP95) and nucleocapsid (VP15, VP24, VP35, VP51C, VP60B, VP75, VP76, VP136A, VP190 and VP664) (van Hulten *et al.* 2000, Chen *et al.* 2002, van Hulten *et al.* 2002, Huang *et al.* 2002a, Huang *et al.* 2002b, Tsai *et al.* 2004, Zhang *et al.* 2004, Huang *et al.* 2005, Leu *et al.* 2005, Li *et al.* 2005, Wu *et al.* 2005, Zhu *et al.* 2005, Li *et al.* 2006, Tsai *et al.* 2006, Wu and Yang 2006, Xiao *et al.* 2006, Xie *et al.* 2006, Zhu *et al.* 2006). Some of WSSV proteins act as non-structural proteins are probably involved in transcriptional regulation (VP9) (Liu *et al.* 2006), virus proliferation (WSV021) (Zhu *et al.* 2007) and/or regulation of DNA replication (WSV477) (Han *et al.* 2007).

The morphogenesis of WSSV and route of virus entry have been characterized and are directly related to the development of cellular lesions (Escobedo-Bonilla *et al.* 2008). They have several developmental stages (Figure 1.3). At the early stage of cell infection the WSSV particles entry into host cells and show gently hypertrophied nuclei. A viral nucleosome appears before the formation of viral particles. It composes of viral proteins organized in fibrillar fragments. In the nucleus, the fibrillar material induces the formation of circular membranes that are soon filled with viral core material starting viral assembly. The nucleocapsids appear with low electron density and grow from one end towards the other. The most abundant of viral particles represented in nucleus. Afterwards, the nucleocapsid is completed of globular protein and become completely enclosed by the envelope. At the late stage, the viral particles become egg-shape and a long tail-like projection derived from the envelope is observed. The mature virions lyse the host cell and spread to infect the other cells.

Table 1.1 List of white spot syndrome virus (WSSV) proteins so far characterized (Escobedo-Bonilla *et al.*, 2008)

Protein name	Genbank accession number	Size (aminoacid residues)	Apparent size (kDa)	Putative function	Location in WSSV virion (references)
VP9	2GJIA	79	9	Transcriptional	Non-structural[18]
VP11	AAL89262	433	11	Unknown	Not determined[8]
VP12A (VP95)	AF402996	95	11	Structural	Tegument[8, 9, 21]
VP12B (VP68)	AF411464	68	7	Structural	Envelope[8, 12, 13]
VP13A	AAL89207	100	13	Energy metabolism	Not determined[8]
VP13B (VP16)	AAL89245	117	13	Structural	Envelope[21]
VP14	AAL89217	97	11	Structural	Envelope[21]
VP15	AAL89137	80	15	DNA binding protein	Nucleocapsid/core[8, 11]
VP19	AAL89341	121	19	Structural	Envelope[8, 9, 11]
WSV021	AAL33025	200	23	Regulation virus replication	Non-structural[19]
VP22 (VP184)	AAL89227	891	100	Unknown	Not determined[8]
VP24 (VP208)	DQ902656	208	24	Structural	Nucleocapsid[8, 10, 13]
VP26	EF534253	204	26	Structural	Tegument[8, 10]
VP28	EF534254	204	28	Structural	Envelope[8, 9, 10]
VP31	AY897235	261	31	Cell attachment	Envelope[6, 8, 9]
VP32	AAL89121	278	32	Structural	Envelope[8, 21]
VP35	AY325896	228	26	Structural	Nucleocapsid[1]
VP36A	AAL89002	297	36	Cell attachment	Tegument[8, 9]
VP33 (VP281)	EF534251	281	32	Cell attachment	Envelope[2, 8, 12, 21]
VP38A	AAL89182	309	35	Structural	Envelope[8, 9, 21]
VP38B	AAL89317	321	38	Endonuclease	Not determined[8]
VP39A	AAL89230	419	39	Structural	Tegument[8, 9]
VP39B	AY884234	283	32	Structural	Envelope[8, 15, 21]
VP41A (VP292)	AF411636	292	33	Structural	Envelope[2, 8, 13]
VP41B (VP300)	AF403003	300	34	Structural	Envelope[8, 21]
VP51A	AAL89162	486	51	Structural	Envelope[8, 17, 21]
VP51B (VP384)	AAL89179	384	46	Structural	Envelope[8, 9, 21]
VP51C (VP466)	AAL89232	466	50	Structural	Nucleocapsid[3, 8, 12]
VP53A (VP150)	AAL88935	1301	144	Structural	Envelope[8, 9, 21]
VP53B	AAL89039	968	53	Signal transduction pathway	Not determined[8]
VP53C	AAL89192	489	53	Unknown	Not determined[8]
VP55 (VP448)	AAL88919	448	55	Unknown	Not determined[8]
VP60A (VP56)	AAL89249	465	60	Structural	Envelope[21]
VP60B (VP544)	AAL89342	544	60	Adenovirus fibre-like protein	Nucleocapsid[8, 9, 13, 21]
VP75	AAL89256	786	75	Structural	Nucleocapsid[16]
VP76 (VP73)	AAL89143	675	76	Class 1 cytokine receptor	Nucleocapsid[4, 8, 17, 21]
VP90	AAL89251	856	96	Structural	Envelope[21]
VP95	AAL89370	800	89	Structural	Tegument[21]
VP110	AAL88960	972	110	Cell attachment	Envelope[8, 21]
VP124	AAL89139	1194	124	Structural	Envelope[8, 14, 21]
VP136A	AAL89194	1219	136	Cell attachment	Nucleocapsid[8, 21]
VP136B	AAL89392	1243	136	Unknown	Not determined[8]
VP180 (VP1684)	AAL88920	1684	169	Collagen-like protein	Envelope[8]
VP187	AAL89132	1606	174	Structural	Envelope[7, 21]
VP190	AAL33291	1565	174	Structural	Nucleocapsid[21]
WSV477	DQ121373	208	30	DNA replication	Non-structural[20]
VP664	AAL89287	6077	664	Cell attachment	Nucleocapsid[5, 8, 9]
VP800	AAL02264	800	90	Unknown	Not determined[8]

References: [1]Chen *et al.* 2002b; [2]Huang *et al.* 2002a,b, 2005; [5]Leu *et al.* 2005; [6]Li *et al.* 2005a, 2006b,a, [8]Tsai *et al.* 2004, 2006; [10]van Hulten *et al.* 2000b; [11]van Hulten *et al.* 2002; [12]Wu *et al.* 2005; [13]Zhang *et al.* 2004; [14]Zhu *et al.* 2005; [15]Zhu *et al.* 2006; [16]Xiao *et al.* 2006; [17]Wu & Yang 2006; [18]Liu *et al.* 2006; [19]Zhu *et al.* 2007; [20]Han *et al.* 2007; [21]Xie *et al.* 2006;.

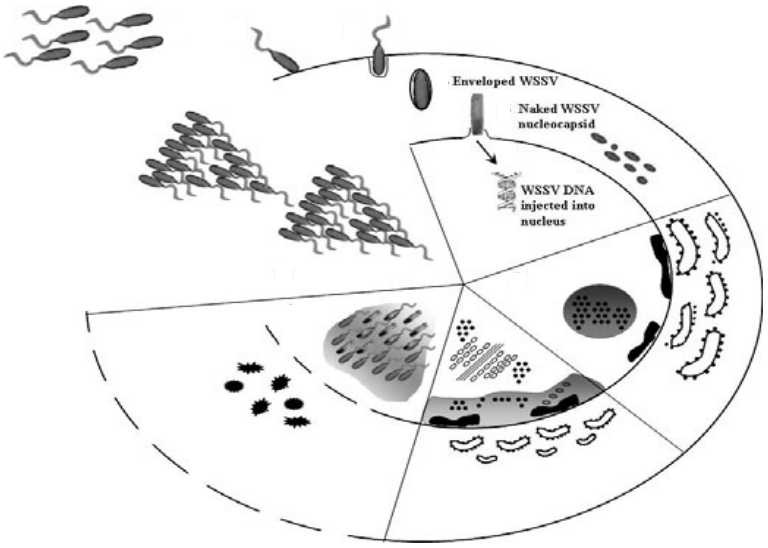

Figure 1.3 A proposed model of the morphogenesis of white spot syndrome virus (Taken from Escobedo-Bonilla *et al*., 2008).

Because of its serious impact on shrimp farming, there is an urgent need to understand virus–host interactions and unveil the underlying mechanisms involved in WSSV entry and pathogenesis in shrimp. Although considerable progress has been made in characterizing the virus, information on the cellular partners of WSSV in shrimp cells is still unclear.

1.2.3. Acute hepatopancreatic necrosis syndrome (EMS/AHPNS)

The shrimp-farming industry in Asia, the largest and most productive region in the world, was affected in 2009 by an emerging disease called early mortality syndrome or, more descriptively, acute hepatopancreatic necrosis syndrome. AHPNS began to cause significant production losses in southern China and by 2012 had spread to farms in Vietnam, Malaysia and Thailand. (Flegel 2012). EMS affects both *P. monodon* and *Litopenaeus vannamei* and is characterized by mass mortalities during the first 20 to 30 days of culture in growout ponds. Clinical signs of the disease include slow growth, corkscrew swimming, loose shells and pale coloration. Affected shrimp consistently show abnormal shrunken, small, swollen or discolored

hepatopancreases. Studies by the University of Arizona Aquaculture Pathology Laboratory (Prof. Donald Lightner) identified the causative agent for AHPNS as a unique strain of *Vibrio parahaemolyticus* that is infected by a virus known as a phage, which causes it to release a potent toxin. However, this need to be confirmed and the infectivity of this disease requires further study.

1.3. Shrimp immune responses

Shrimp immune defense comprises of two major responses, which are cellular mediated and humoral innate immune responses to combat invading pathogens (Figure 1.4). The major defense responses are carried in the hemolymph, which contains three different principal types of hemocytes that are defined as the hyaline, granular and semigranular hemocytes (Martin and Graves 1985). Cellular defense components include all those reactions performed directly by hemocytes, such as phagocytosis, encapsulation, nodule formation, blood coagulation and cytotoxicity system. Whereas, the humoral components related to production of soluble component playing roles in the defense system such as anticoagulant proteins, agglutinin, prophenoloxidase (ProPO), antimicrobial peptides (AMPs), cytokine-like factors and proteinase inhibitors (Holmblad and Söderhäll 1999, Jiravanichpaisal *et al.* 2006).

The first defense against microbial infections in innate immune response triggered diverse humoral and cellular activities via signal transduction pathways in both insects and mammals (Borregaard *et al.* 2001). Toll, IMD and JAK/STAT pathways are main pathways regulating the immune response in shrimp (Li and Xiang 2013). Up to date, Toll pathway of shrimp responds not only to Gram-positive bacteria, Gram-negative bacteria, but also to WSSV (Labreuche *et al.* 2009, Wang *et al.* 2011b). The components of IMD pathway, IMD and Relish, have been identified in shrimp, indicating that IMD pathway should be existed in shrimp and might play important roles in regulating the immune response of shrimp to bacteria and virus infection (Li *et al.* 2009, Wang *et al.* 2009). The transcription of STAT in shrimp was modulated after WSSV infection, suggesting that a putative JAK/STAT pathway might exist in shrimp and be very important to virus infection (Chen *et al.* 2008).

The ProPO-activation pathway is a phenoloxidation cascade comprising of pattern recognition proteins, several serine proteases, and inhibitors (Soderhall and Cerenius 1998). This proPO cascade was induced by pathogen infection after that pro-enzymes in this cascade were activated step by step to produce the melanin for killing and limiting the pathogen invasion. In penaeid shrimp, enzymes in the proPO system are localized in the semigranular and granular cells (Perazzolo and Barracco 1997). This is in accordance with the former studies showing that *P. monodon* proPO and PPAE mRNAs as well as a *L. vannamei* proPO mRNA are expressed only in hemocytes (Sritunyalucksana and Söderhäll 2000, Ai *et al.* 2009, Amparyup *et al.* 2009, Charoensapsri *et al.* 2009, Charoensapsri *et al.* 2011). Previous reports revealed that RNAi-mediated silencing of two *P. monodon* proPO genes (*Pm*proPO1 and *Pm*proPO2) and two *P. monodon* PPAE genes (*Pm*PPAE1 and *Pm*PPAE2) significantly decreased the total PO activity, leading to an increase in the bacterial number in *Vibrio harveyi*-infected shrimp and also enhanced their the mortality rate after infection (Amparyup *et al.* 2009, Charoensapsri *et al.* 2009, Charoensapsri *et al.* 2011). These results indicate that proPO and PPAE are important to proPO system as well as the innate immune response in crustaceans.

Hemolymph coagulation is part of the crustacean innate immune response; it prevents leakage of hemolymph from sites of injury and protects the invasion of pathogen throughout the body. Blood clotting in crayfish and shrimp results from the polymerization between free glutamine and lysine residues of clottable proteins (CPs), which is catalyzed by a calcium ion-dependent transglutaminase, TGase (Hall *et al.* 1999, Wang *et al.* 2001, Chen *et al.* 2005).

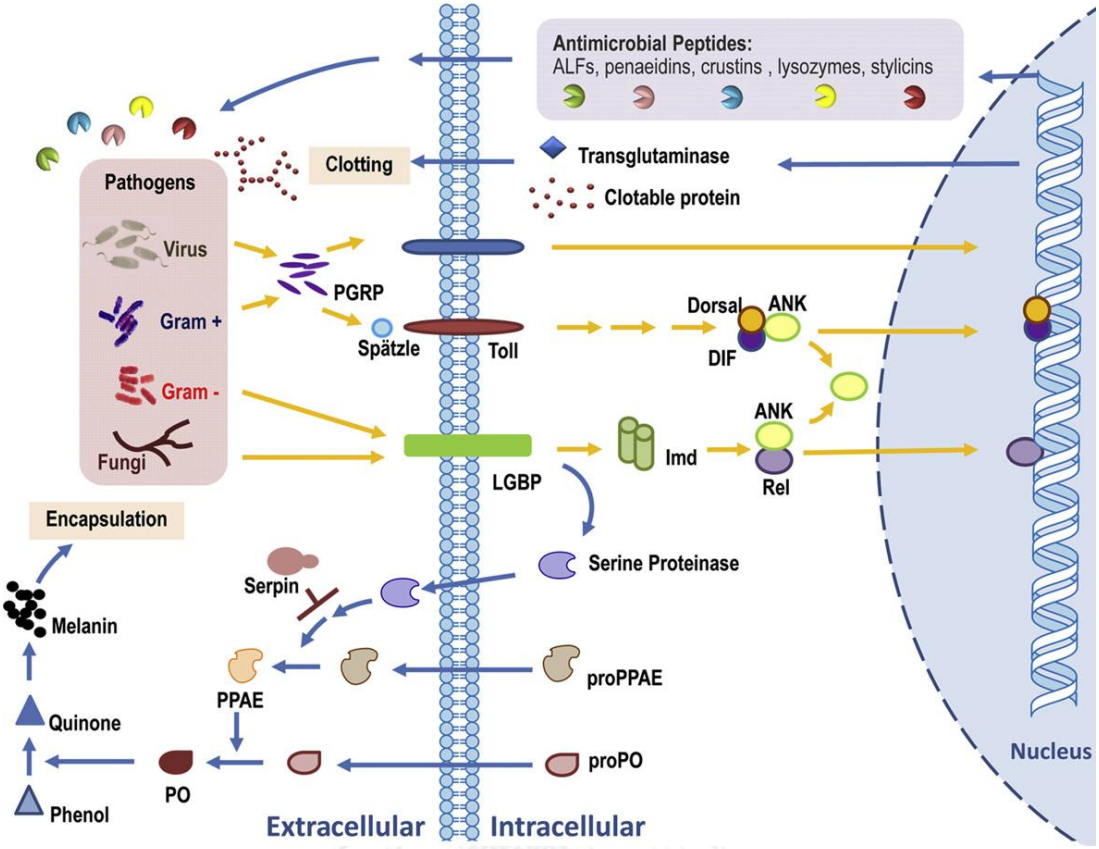

Figure 1.4 A schematic model of the shrimp immune system. (Taken from Tassanakajon *et al.*, 2013)

1.4. Antimicrobial peptide in crustacean

Antimicrobial peptides or proteins (AMPs) are one of the major components of the innate immune defense and are ubiquitously found in all kingdoms from bacteria to mammals, including fungi and plants. The AMP has activities against a broad range of microorganisms, including Gram-positive and Gram-negative bacteria, yeast, filamentous fungi, protozoans and enveloped viruses (Bulet *et al.* 2004, Yount *et al.* 2006, Guani-Guerra *et al.* 2010). Recent evidence has shown that in addition to their antimicrobial activity, AMPs may encompass a number of other diverse biological roles and are multifunctional molecules. It was demonstrated that these peptides have antitumor effects, mitogenic activity and, most importantly, participate

in immunoregulatory mechanisms by modulating signal transduction and cytokine production and/or release (Kamysz *et al.* 2003, Bowdish *et al.* 2005, Brown and Hancock 2006, Yount *et al.* 2006, Easton *et al.* 2009, Lai and Gallo 2009, Guani-Guerra *et al.* 2010).

The mechanism of how AMPs in general damage and kill micro-organisms can be divided into two categories; transmembrane pore formation and intracellular killing as shown in Figure 1.5 (Jenssen *et al.* 2006). Most AMPs appear to act on bacteria using a transmembrane pore-forming mechanism via interaction with the cell membrane components leading to pore formation and leakage of the bacterial cytoplasmic contents. To date, catagorized by the pore forming mechanisms, there have been 4 distinct models as follows; aggregate, barrel-stave, carpet, and toroidal-pore models. The other possibility is that once the AMPs pass through the cell membrane and enter the cells, they might bind to macromolecules and interrupt the synthesis of vital components, such as DNA, RNA and proteins, and so resulted in cell death. These two mechanisms are not necessarily mutually exclusive and nor is it known if different AMPs can act in concert, either additively or synergistically.

Several different models have been proposed to explain how, following initial attachment, antibacterial peptides insert into the bacterial membrane to form transmembrane pores, which result in membrane permeabilization. The aggregate model has been proposed (Wu *et al.* 1999). In this model peptides reorient to span the membrane as an aggregate with micelle-like complexes of peptides and lipid. In the toroidal pore model, peptides insert themselves in an orientation perpendicular to the membrane to form a pore, with the membrane also curving inward to form a hole with the head groups facing towards the center of the pore, and the peptides line this hole. Examples of antimicrobial peptides that are proposed to form torodial transmembrane pore include the magainins, melittin, and LL-37 (Matsuzaki *et al.* 1996, Yang *et al.* 2001, Hallock *et al.* 2003, Henzler-Wildman *et al.* 2004). In the barrel-stave model, peptides reorient to become the “staves” in a “barrel”-shaped cluster, which orients perpendicular to the plane of the membrane. Experimental evidence supports this mechanism of membrane permeabilization for the fungus-derived antimicrobial peptide alamethicin (He *et al.* 1996, Shimazaki *et al.* 1998) and

for the cyclic decameric cationic peptide gramicidin S (Zhang *et al.* 2001). The carpet model proposes that aggregates of peptide align parallel to the lipid bilayer, coating local areas in a carpet-like fashion. Cecropin (Gazit *et al.* 1995) and ovispirin (Yamaguchi *et al.* 2001) have been shown to from pore in carpet model.

From the review of (Brogden 2005), novel modes of action that have recently been demonstrated include inhibition of nucleic acid synthesis; buforin II (Park *et al.* 1998), defensins (Lehrer *et al.* 1989) and indolicidin (Subbalakshmi and Sitaram 1998). Some AMPs can inhibit protein synthesis and enzyme activity; pleurocidin (Patrzykat *et al.* 2001), dermaseptin (Mor and Nicolas 1994) and PR-39 (Boman *et al.* 1993, Boehr *et al.* 2003). Mersacidin (Brotz *et al.* 1995) and nisin (Brumfitt *et al.* 2002) have been reported to be able to inhibit cell wall synthesis.

The review from (Tassanakajon *et al.* 2010) reports on AMPs and their immune functions in shrimp. Shrimp AMPs are primarily expressed in hemocytes, which migrated to infection sites and AMPs are secreted into the circulation as well as site of infection to fight against pathogen invasion. In the white shrimp, *L. vannamei*, penaeidins is a family of antimicrobial peptides acting against gram-positive bacteria and fungi (Destoumieux *et al.* 1997). Penaeidins were found in many species of shrimp which are *Litopenaeus stylirostris, Litopenaeus schmitti, Farfantepenaeus brasiliensis, Fenneropenaeus chinensis, Fenneropenaeus penicillatus, Farfantepenaeus subtilis, Farfantepenaeus paulensis, L. vannamei, Litopenaeus setiferus* and *P. monodon* (Gross *et al.* 2001, Supungul *et al.* 2004, Tassanakajon *et al.* 2010). Different from other isoform, penaeidin 5 from the *P. monodon* was found to play a possible role in protection against viral infection (Woramongkolchai *et al.* 2011). Besides, referred to as the crustacean antimicrobial pepteides, crustins such as crustin*Ls* crustin*Lv*, and crustin*Pm* have been identified in the penaeid shrimp, *L. setiferus*, *L. vannamei* and *P. monodon* (Bartlett *et al.* 2002, Tassanakajon *et al.* 2010) They possess sequence identity with a family of proteinase inhibitory proteins, the whey acidic protein (WAP). Therefore, crustins play a role against Gram-positive and Gram-negative bacteria and also inhibit proteinase activity (Tassanakajon *et al.* 2010, Krusong *et al.* 2012). Anti-lipopolysaccharide factors (ALFs)

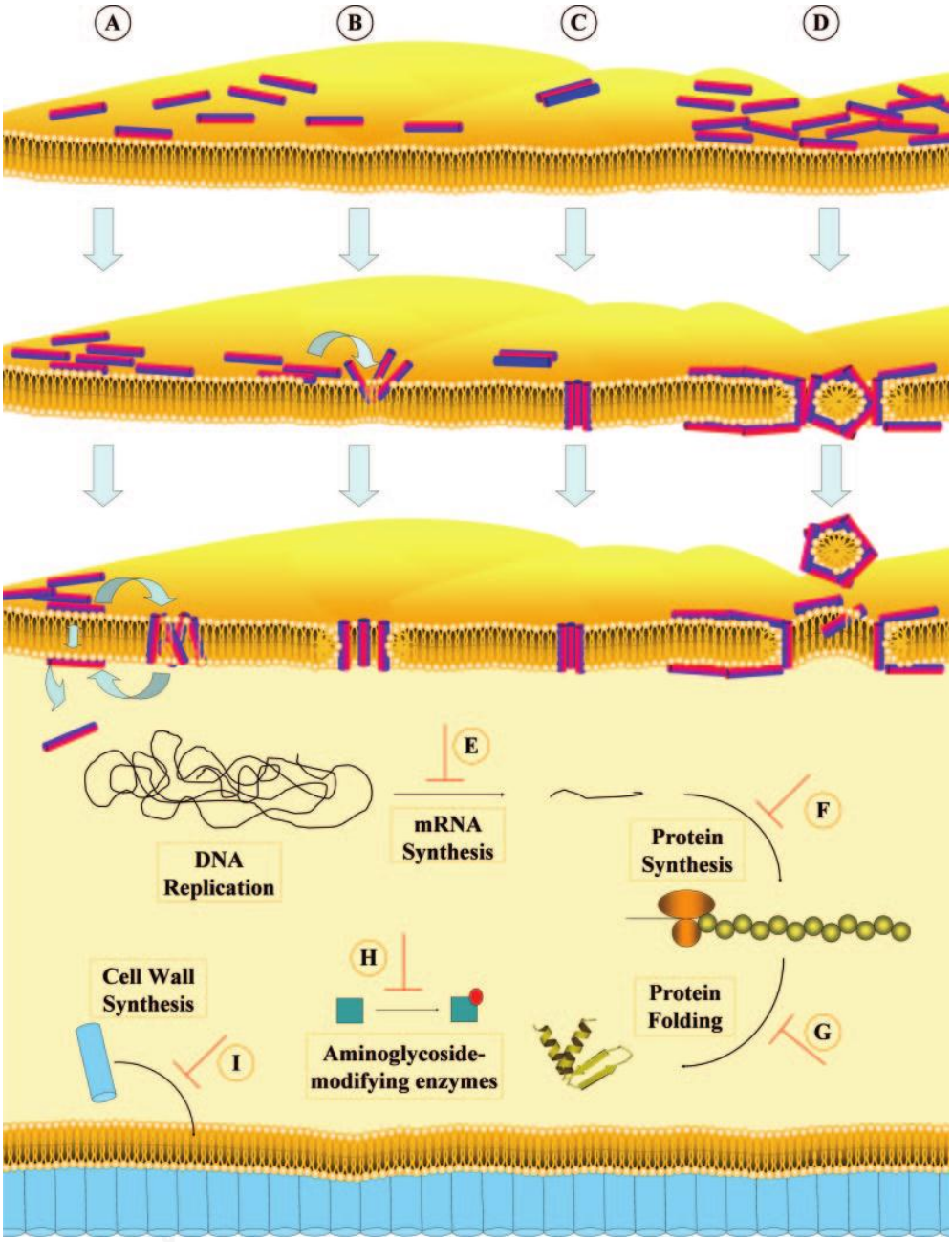

Figure 1.5 Mechanisms of action of antibacterial peptides. (Taken form Jenssen *et al.*, 2006). Models to explain mechanisms of membrane permeabilization are indicated (A to D), (A) Aggregate model, (B) Toroidal pore model, (C) Barrel-stave model and (D) Carpet model. The mechanisms of action of peptides which do not act by permeabilizing the bacterial membrane are depicted (E to I), (E) Inhibition of DNA and RNA synthesis at their MICs without destabilizing the membrane, (F) Inhibition of protein synthesis, (G) Inhibition of protein folding, (H) Inhibition of enzyme activity and (I) Inhibition of cell wall formation.

are AMPs identified in crustaceans. They have broad antimicrobial activities towards gram-positive and gram-negative bacteria, filamentous fungi, and viruses (Somboonwiwat *et al.* 2005, Liu *et al.* 2006, Li *et al.* 2008). The activities of ALFs against marine pathogens such as *V. harveyi* and WSSV have been reported (Liu *et al.* 2006, Ponprateep *et al.* 2009, Tharntada *et al.* 2009). In conclusion, AMPs play a major and effective role in host immune defense against diverse pathogens.

1.5. Anti-lipopolysaccharide factors (ALFs) in shrimp

ALFs are the antimicrobial peptides firstly isolated from the hemocytes of the horseshoe crabs, *Tachypleus tridentatus* and *Limulus polyphemus*, and are named because of their ability to specifically inhibit the lipopolysaccharide (LPS)-mediated activation of the *Limulus* coagulation system (Tanaka *et al.* 1982, Muta *et al.* 1987). Moreover, ALFs have been identified in other crustaceans including shrimp. ALFs have been discovered from the hemocytes of the black tiger shrimp, *P. monodon*, by a genomic approach (Supungul *et al.* 2002). So far, six isoforms of ALFs have been identified from the *P. monodon* EST databases (Tassanakajon *et al.* 2010). Of these six ALF*Pm* isoforms, ALF*Pm*3 is clearly the most abundant isoform (Supungul et al. 2004). From Rosa *et al.* (2013), shrimp ALFs were classified into four groups diverse in terms of primary sequence, biochemical properties, biological activities and gene expression. In previous, based on amino acid sequence, these variants were classified into three main groups: Group A (anionic and cationic ALFs), Group B (highly cationic ALFs) and Group C (cationic ALFs) (Tharntada *et al.* 2008, Ponprateep *et al.* 2012). In shrimp *Litopenaeus vannamei*, the newest isoform of ALF has been identified. Unlike other ALFs, a novel Group D ALFs is anionic peptide. Many residues of the LPS binding site of anionic ALF were absence leading to the lack of antimicrobial activity of the ALF. (Rosa *et al.* 2013). In 2008, it has been reported that the mortality of the ALF knockdown shrimp injected with *Vibrio penaeicida* is significantly higher than that of control group (de la Vega *et al.* 2008). Moreover, gene silencing study confirmed that ALF*Pm*3 is vital to shrimp and plays important role in the protection against microbial infection (Ponprateep *et al.* 2012). All known ALF sequences, including ALF*Pm*3, have two conserved cysteine residues and a cluster of positive

charges that are mainly within the disulfide loop (Aketagawa *et al.* 1986, Hoess *et al.* 1993). This positive charged cluster is defined as the putative LPS-binding site.

As compared to ALF, ALF*Pm*3 has a strong bactericidal effect on Gram-negative and Gram-positive bacteria and can bind to the main bacterial cell wall components of Gram-negative and Gram- positive bacteria, LPS and lipoteichoic acid (LTA) (Somboonwiwat *et al.* 2008), respectively, presumably via its LPS-binding site (Yang *et al.* 2009). The high antimicrobial activity against *V. harveyi* of rALF*Pm*3 suggests its potential use in the control or prevention of outbreaks of vibriosis in shrimp farming (Somboonwiwat *et al.* 2005). Indeed, rALF*Pm*3 has been reported to be able to completely neutralize *V. harveyi* (Ponprateep *et al.* 2009).

1.6. WSSV-inducible genes in shrimp

Due to the serious impact of WSSV on shrimp aquaculture, it is urgent to understand to the mechanisms involved in WSSV pathogenesis in shrimp. However, little information is available in relation to underlying mechanisms of host responses during the WSSV infection in naturally infected shrimp.

To gain more insight into viral infection and antiviral mechanisms in crustaceans, high throughput techniques were used to identify genes responding to WSSV infection including cDNA microarray (Dhar *et al.* 2003, Wang *et al.* 2006, Zeng and Lu 2009), suppression subtractive hybridization (Zheng *et al.* 2009, Prapavorarat *et al.* 2010), SSH combining with differential hybridization (He *et al.* 2005), ESTs (Leu *et al.* 2007), next-generation sequencing (Li *et al.* 2013).

Previous studies have discovered several immune-related genes responding to white spot syndrome virus (WSSV) infection in crustaceans. For example, many components in signal transduction pathways, which are Toll pathway, IMD pathway and JAK-STAT pathway, can be stimulated by WSSV challenge, such as Toll (Wang *et al.* 2012), Spätzle (Shi *et al.* 2009), Pelle (Wang *et al.* 2011a), TRAF6 (Wang *et al.* 2011b), Dorsal (Huang *et al.* 2010, Li *et al.* 2010), Relish (Huang *et al.* 2009, Li *et al.* 2010) and STAT (Chen *et al.* 2008, Sun *et al.* 2011). Ras superfamily is a group of small GTPases, regulated phagocytosis and endocytosis process. *Mj*Rab GTPase

formed a protein complex with beta-actin tropomyosin envelope protein VP466 of WSSV (Wu *et al.* 2008). Ran interacted with myosin in shrimp antiviral immune response (Liu *et al.* 2009). Some studies also indicated that virus could enter the host cells via clathrin-dependent endocytosis (Codran *et al.* 2006, Mercer *et al.* 2010). Nevertheless, some Rab protein, *Pm*Rab7, was shown binding to the WSSV structure protein VP28 and reduced WSSV replication (Sritunyalucksana *et al.* 2006).

The next-generation sequencing and bioinformatic techniques were used to observe the transcriptome differences of the shrimp between latent infection stage and acute infection stage. Genes in the Toll and IMD pathways (Spätzle, Toll-like receptors, MyD88, Tumor necrosis factor receptor-associated factor 6, dorsal, cactus, Ikkepsilon1 and relish), the Ras-activated endocytosis process (Ras, Rab, Rap, Rho, GAP, GEF, dynamin, myosin, clathrin, and actin), the RNA interference pathway, anti-lipopolysaccharide factors and many unknown genes, were found to be activated in shrimp from latent infection stage to acute infection stage. Moreover, the anti-bacterially proPO-activating cascade was firstly identified to be probably involved in antiviral process (Li *et al.* 2013). Moreover, high throughput approaches can be identified the unknown gene that might be involved in WSSV infection process. For example, the novel gene, hemocyte homeostasis-associated protein (HHAP), was found to be highly up-regulated at both the transcript and protein levels in WSSV-infected shrimp hemocytes. After knockdown *Pm*HHAP gene, shrimp hemocytes were damaged and a severe decrease in their numbers, suggesting the important role of *Pm*HHAP in hemocyte homeostasis (Prapavorarat *et al.* 2010).

1.7. WSSV-binding proteins

To understand how host shrimp respond to viral infections, the interactions between host and viral proteins, and particularly host virus-binding proteins that might play an important role in the viral infection process, should be characterized. The current knowledge on WSSV binding protein and its function has been reviewed by (Sritunyalucksana *et al.* 2013) and the interaction between WSSV-binding proteins and viral proteins as summarized in Table 1.2.

In shrimp, many virus-binding proteins have been identified, but their relationship to signaling pathways involved in immunity is still unclear. In present, several secreted and cell-surface viral-binding proteins have been reported from shrimp. The viral-binding protein can be interacted with virus into two types, which are non-specific interaction and specific interaction.

For non-specific interaction, a function of hemocyanin protein that can be found in shrimp hemolymph is the non-specific antiviral response of the black tiger shrimp, *P. monodon* (Zhang *et al.* 2004). Injection of the WSSV inoculum pre-incubated with the native hemocyanin resulted in no WSSV replication detected (Lei *et al.* 2008).

Many specific interactions between host and viral protein have been reported. In previous, major structural protein of WSSV can interact with host protein. For example, VP15, major nucleocapsid protein of WSSV, is involved in in genome packaging during virion formation (Witteveldt *et al.* 2005). This protein can be interacted with *Pm*FKBP46 which is FKBPs are a class of binding proteins of the immunosuppressive drug FK506 (Harding *et al.* 1989). The interaction between VP26, a major tegument protein of WSSV, with shrimp cytoskeletal protein β-actin was identified (Xie and Yang 2005b, Liu *et al.* 2011). The interaction between VP26 and β-actin might play an important role in WSSV infection. Moreover, VP26 protein also can bind with 3 kDa WSSV-binding protein (WBP). After incubation WBP with WSSV, the viral replication was reduced in WBP dose dependent manner (Youtong *et al.* 2011).

Lectin, a WSSV binding protein identified, is the host glycoprotein that can bind with carbohydrates expressed on different cell surfaces. Some lectins have been characterized as non-self-recognition molecules in vertebrate and invertebrate immunities including crustaceans and also have been reported to inhibit influenza A virus infection (Marques and Barracco 2000, Chang *et al.* 2010). From previous report, shrimp lectin also can interact with many WSSV proteins. Lectin from *Penaeus chinensis*, FcLec3 was shown to bind to the WSSV envelope protein VP28 (Wang *et al.* 2009). A recombinant LvCTL1 from *P. vannamei* (rLvCTL1) can bind to several envelope proteins of WSSV including VP95, VP28, VP26, VP24, VP19 and VP14 (Zhao

et al. 2009). After LvCTL1 was incubated with WSSV, shrimp survival rate was increased. In *Marsupenaeus japonicus*, three novel MjLecs (MjLecA, MjLecB and MjLecC) were identified. MjLecs also can bind to many WSSV protein and these MjLecs have diverse functions in antiviral immunity (Song *et al.* 2010).

The interaction of viral proteins with the host cell membrane is an important process for both viral pathogenesis and for the host antiviral response. A number of cell-surface receptors for WSSV have been reported, including β-integrin (Li *et al.* 2007), chitin-binding protein (Chen *et al.* 2007, Chen *et al.* 2009) and an F_1-ATP synthase beta subunit (Liang *et al.* 2010). β-integrin, which is the cell surface protein, can be interacted with VP187, envelope protein of WSSV. Knockdown of integrin expression resulted in inhibition of WSSV infection leading to higher shrimp survival rate. Chitin-binding protein, also cell-surface binding protein, can bind with chitin and VP53A. Injection of a recombinant fragment comprising the C-terminus of *Pm*CBP was able to block WSSV infection. From *P. vannamei*, F_1-ATP synthase beta subunit can be interacted with WSSV. Whether this protein is a WSSV receptor that can also function, as an astakine receptor remains to be determined. Some of viral proteins act as triggers for host receptors, the predominant viral activators are nucleic acids. PlgC1qR, receptor for globular head domain of complement component C1q, could bind to VP15, VP26, and VP28 of WSSV. Silencing of PlgC1qR resulted in higher replication of WSSV. These results suggested that PlgC1qR might control an antiviral mechanism (Watthanasurorot *et al.* 2010).

Some of the WSSV non-structural proteins can be interacted with host protein. The non-structural protein VP9 of WSSV is an interacting partner of activated protein kinase C1 homolog that has been identified from the hemocytes of *P. monodon* (*Pm*-RACK1) (Tonganunt *et al.* 2009).

Other intracellular shrimp proteins reported to be capable of interacting with WSSV proteins. The binding of shrimp Hsc70 to VP28 was also demonstrated to be specific and dependent on ATP and Hsc70 concentration (Xu *et al.* 2009). Shrimp ubiquitin-conjugating (Ubc) enzymes, PvUbc and FcUbc, were shown to interact with the RING domain (WRD) of RING domain-containing proteins of WSSV (Chen *et al.* 2011). Injection of FcUbc can inhibit viral replication and reduced shrimp mortality. In

conclusion, the effect of FcUbc-inhibited WSSV replication might come from the induction of ubiquitination of WRDs by FcUbc or direct binding of FcUbc to WRDs blocks other host proteins to interact with WRDs leading to antiviral effect. From previous report, shrimp serine/threonine protein phosphatase (PP) was involved in the latent-lytic life cycle of WSSV. This protein can interact with WSSV ORF427 that has been reported to be a WSSV latency-associated gene (Lu and Kwang 2004) and also WSSV403, a WRD protein involved in the regulation of WSSV latency (He and Kwang 2008). Further studies on shrimp PPs may reveal a novel target for a new anti-WSSV strategy.

The endosomal protein, VP28-binding protein, is PmRab7 isolated from the hemocytes of *P. monodon* (Sritunyalucksana *et al.* 2006). After PmRab7 silencing, the replication of WSSV was decreased. (Ongvarrasopone *et al.* 2008). These results suggested that PmRab7 functions as an important regulator of intracellular trafficking used. Study of PjRab in *P. japonicus* confirmed that PjRab protein was important to the antiviral response by formation of a complex with β-actin, tropomyosin and the WSSV envelope protein VP466 that led to hemocytic phagocytosis of the virus (Wu *et al.* 2008).

Table 1.2 Summary the protein-protein interaction between WSSV-binding protein and viral proteins (Sritunyalucksana *et al.* 2013).

Viral proteins	Shrimp species	Viral binding proteins	Possible mechanisms involved
WSSV proteins			
VP53A	*P. monodon*	PmCBP	Rececptor/cofactor candidate for WSSV, function like lectin
VP28	*P. chinensis*	FcLec3	Prevent virus to entering the shrimp cell
	P. monodon	PmRab7	Endocytosis
	P. clarkii	Hsc70	WSSV assembly pathway
WSSV protein	*P. vannamei*	F_1-ATP synthase beta subunit (BP53)	–
VP187	*P. japonicus* *P. clarkii*	β-integrin	Cellular receptor for WSSV infection
WSSV427	*P. vannamei*	Phosphatase (PPs)	Regulation of WSSV's life cycle
WSSV403	*P. vannamei*	Phosphatase (PPs)	
VP26	*P. clarkii*	Actin	Virus entry
	P. chinensis	β-actin/HmFc	Mediate the viral nucleocapsid movement
	P. vannamei	WBP	Inhibit the invasion of WSSV into host cells
VP26, VP28, 90 kDa and 100 kDa	*P. japonicus*	MjLecA	Recognize WSSV, and may act as pattern recognition proteins
VP28, 72 kDa and 90 kDa		MjLecB	
VP28, 90 kDa and 100 kDa		MjLecC	
Purified WSSV	*P. monodon*	Hemocyanin	–
VP15	*P. monodon*	PmFKBP46	Viral genome packaging
VP15, VP26, VP28	*P. leniusculus*	PlgC1qR	Interfere with WSSV replication
VP9	*P. monodon*	Pm-RACK1	Mediating intracellular VP9 functions
VP95, VP28, VP26, VP24, VP19, and VP14	*P. vannamei*	LvCTL1	Block the virus from entering cells
WSSV249	*P. vannamei*	PvUbc	Host cell pathogenesis
WSSV277 and WSSV304	*P. chinensis*	FcUbc	Inhibits replication of WSSV
VP644	*P. japonicus*	PjRab	Phagocytosis

1.8. Purposes of the thesis

To understand molecular mechanism of immune-related proteins from *P. monodon* in response to pathogen infection, I am interested in two genes/proteins that involved in shrimp immunity, which are anti-lipopolysaccharide factor isoform 3 (ALF*Pm*3) and a novel viral responsive protein 15 (*Pm*VRP15).

In contrast to other AMPs, the antibacterial mechanism of shrimp AMPs so far remains largely unknown. Therefore, the first part of this research, I focused on the effects of ALF*Pm*3 against major bacterial pathogen in shrimp, *V. harveyi.* Firstly, the binding activity of ALF*Pm*3 on bacteria was investigated by immune-localization technique using specific antibody against ALF*Pm*3. Subsequently, the permeability of this protein that can damage the outer and inner membrane of bacteria was determined. The morphology of the bacterial cell after treated with ALF*Pm*3 was observed by electron microscopy. From this research, we will sum up the effect of ALF*Pm*3 against bacteria, *V. harveyi.*

In the second part of my thesis, a novel viral responsive gene, namely "viral responsive protein 15 kDa (*Pm*VRP15)" was studied for the involvement in WSSV propagation by RNA interference technique. Because of the unknown function of *Pm*VRP15 protein, the partner protein that can interact with *Pm*VRP15 protein was identified by yeast-two hybrid screening to facilitate prediction of *Pm*VRP15 function. If the function of *Pm*VRP15-interacting protein was still unknown, this protein function might be characterized. Moreover, regulation of *Pm*VRP15 was characterized. Genome organization of *Pm*VRP15 gene was identified and promoter activity was tested. The narrow down on *Pm*VRP15 promoter and promoter activity assay were performed to identify the region of *Pm*VRP15 promoter that might be involved in gene regulation. Next, the transcription factor binding sites on promoter region were predicted by computational analysis. The site-directed mutagenesis was used to confirm the transcription factor binding sites that can regulate *Pm*VRP15 gene expression.

CHAPTER II
MATERIALS AND METHODS

2.1.Equipments

Avanti J-30I high performance centrifuge (Beckman coulter)

Amicon Ultra concentrators (Millipore)

Autoclave model # MLS-3750 (SANYO E&E Europe (UK Branch) UK Co.)

Automatic micropipette P10, P20, P100, P200 and P1000 (LioPette/ Select BioProduct/ Gilson Medical Electrical)

ÄKTA Prime Plus FPLC Purification System (GE Healthcare)

Balance PB303-s (Mettler Teledo)

Biophotometer (Eppendrof)

Centrifuge 5804R (Eppendrof)

Centrifuge AvantiTM J-301 (Beckman Coulter)

-20°C Freezer (Whirlpool)

-80°C Freezer (Thermo Electron Corporation)

Force mini centrifuge (Select BioProducts)

Gel Documention System (GeneCam FLEX1, Syngene)

GelMate2000 (Toyobo)

Gene pulser (Bio-RAD)

0.45 mm glassbeads

Incubator 30°C (Heraeus)

Incubator 37°C (Memmert)

Innova 4080 incubator shaker (New Brunswick Scientific)

Laminar Airflow Biological Safety Cabinets ClassII Model NU-440-400E (NuAire, Inc., USA)

Microcentrifuge tube 0.6 ml and 1.5 ml (Axygen® Scientific, USA)

Minicentrifuge (Costar, USA)

Minipulser electroporation system (Bio-RAD)

Mini-PROTEAN® 3 Cell (Bio-RAD)

Nipro disposable syringes (Nissho)

Optima™ L-100 XP Ultracentrifuge (Beckman Coulter)

Orbital shaker SO3 (Stuart Scientific, Great Britain)

PCR Mastercycler (Eppendrof AG, Germany)

PCR thin wall microcentrifuge tubes 0.2 ml (Axygen® Scientific, USA)

PD-10 column (GE Healthcare)

pH-meter pH 900 (Precisa, USA)

Pipette tips 10, 100 and 1000 µl (Axygen® Scientific, USA)

Power supply, Power PAC3000 (Bio-RAD Laboratories, USA)

Refrigerated incubator shaker (New Brunswick Scientific, USA)

Refrigerated microcentrifuge MIKRO 22R (Hettich Zentrifugen, Germany)

Sonicator (Bandelin Sonoplus, Germany)

SpectraMax M5 Multi-Mode Microplate Reader (Molecular Devices)

Touch mixer Model#232 (Fisher Scientific)

Trans-Blot®SD (Bio-RAD Laboratories)

Water bath (Memmert)

Whatman® 3 MM Chromatography paper (Whatman International Ltd., England)

96-well cell culture cluster, flat bottom with lid (Costar)

2.2.Chemicals and Reagents

100 mM dATP, dCTP, dGTP and dTTP (Promega)

5-bromo-4-chloro-3-indolyl-b-D-galactopyranoside (X-Gal) (Fermentas)

5-bromo-4-chloro-3-indolyl phosphate (BCIP) (Fermentas)

Absolute alcohol, C_2H_5OH (Hayman)

Acetic acid glacial, CH_3COOH (Merck)

Acrylamide, C_3H_5NO (Merck)

Agarose, low EEO, Molecular Biology Grade (Research Organics)

Agar powder, Bacteriological (Hi-media)

Alkaline phosphatase-conjugated rabbit anti-mouse IgG (Jackson ImmunoResearch Laboratories, Inc.)

Ammonium persulfate, $(NH_4)_2S_2O_8$ (Bio-Rad)

Anti-His antibody (GE Healthcare)

Benchmark™ Pre-stained Protein Ladder (Invitrogen)

Benchmark™ Unstained Protein Marker (Invitrogen)

Bovine serum albumin (Fluka)

Bromophenol blue (Merck, Germany)

Casein Enzyme Hydrolysate, Type-I, Tryptone Type-I (Hi-media)

Casein Peptone (Hi-media)

Chloroform, $CHCl_3$ (Merck)

Coomassie brilliant blue G-250 (Fluka)

Coomassie brilliant blue R-250 (Sigma)

D-Glucose anhydrous (Ajax)

Diethyl pyrocarbonate (DEPC), $C_6H_{10}O_5$ (Sigma)

Ethylene diamine tetraacetic acid disodium salt, EDTA (Ajax)

Ethidium bromide (Sigma)

GeneRuler™ 100bp DNA ladder (Fermentas)

GeneRuler™ 1kb DNA ladder (Fermentas)

Glycerol, $C_3H_8O_3$ (Ajax)

Glycine, USP Grade, NH_2CH_2COOH (Research organics)

Hybond™-ECL membrane (GE Healthcare)

Hydrochloric acid (HCl) (Merck)

HiTrap SP Sepharose™ Fast Flow column (GE Healthcare)

Imidazole (Fluka)

Isopropanol, C_3H_7OH (Merck)

Isopropyl-β-D-thiogalactoside (IPTG), $C_9H_{18}O_5S$ (USBiological)

Magnesium chloride, $MgCl_2$ (Merck)

Methanol, CH_3OH (Merck)

0.22 μM and 0.45 μM Millipore membrane filter (Millipore)

N, N, N´, N´-tetramethylethylenediamine (TEMED) (BDH)

N, N´-methylenebisacrylamide, $C_7H_{10}N_2O_2$ (USB)

Ni Sepharose 6 Fast Flow (GE Healthcare)

Nitroblue tetrazolium (NBT) (Fermentas)

Paraformaldehyde (Sigma)

Phenol:chloroform:isoamyl alcohol (Sigma)

Phosphoric acid (Labscan)

Prestained protein molecular weight marker (Fermentas)

Skim milk powder (Mission)

Silver nitrate (Merck)

Sodium carbonate anhydrous (Carlo Erba)

Sodium chloride, NaCl (Ajax)

Sodium citrate, $Na_3C_6H_5O_7$ (Carlo Erba)

Sodium dodecyl sulfate, $C_{12}H_{25}O_4SNa$ (Vivantis)

Sodium hydrogen carbonate, $NaHCO_3$ (BDH)

Sodium dihydrogen orthophosphate, $NaH_2PO_4.H_2O$ (Ajax)

di-Sodium hydrogen orthophosphate anhydrous, NaH_2PO_4 (Ajax)

Sodium hydroxide, NaOH (Merck)

Triton® X-100 (Merck)

TriReagent® (Molecular Research Center)

Tris (Vivantis)

Tryptic soy broth (Difco)

Tween™-20 (Fluka)

Unstained protein molecular weight marker (Fermentas)

Urea (Affy Metrix USB)

2.3.Kits

2-D Quant kit (GE healthcare)

High-speed plasmid mini kit (Geneaid)

Matchmaker™ Gold Yeast Two-Hybrid System (Clontech)

Nucleospin® Extract II kit (Macherey-Nagel)

RevertAID™ first strand cDNA synthesis kit (Fermentas)

RQ1 RNase-free DNase (Promega)

SsoFast™ EvaGreen® Supermix (Biorad)

T&A cloning vector kit (RBC Bioscience)

pGEM-T easy vector system (Promega)

T7 RiboMAX™ Express RNAi System (Promega)

Yeastmaker™ Yeast Transformation System 2 (Clontech)

Effectene transfection reagent (Qiagen)

Dual-luciferase® Reporter assay (Promega)

2.4.Enzymes

Advantage® 2 Polymerase Mix (Clontech)

*Bam*HI (Biolabs)

*Dra*I (Biolabs)

*Eco*RI (Biolabs)

*Eco*RV (Biolabs)

*Hin*dIII (Biolabs)

*Nde*I (Biolabs)

*Nco*I (Biolabs)

*Pvu*II (Biolabs)

*Sac*I (Biolabs)

*Stu*II (Biolabs)

*Xho*I (Biolabs)

Ex *Taq* polymerase (Takara)

KOD *Taq* polymerase (TOYOBO)

Phusion® Hot Start High-Fidelity DNA polymerase (Finnzymes)

Taq DNA polymerase (RBC Bioscience)

Ligation High Ver.2 (TOYOBO)

T4 DNA ligase (Biolabs)

2.5.Antibiotics

100x antimicrobial antibiotic (Gibco, Life technology)

Aureobasidin A (Clontech)

Ampicillin (BioBasic)

Kanamycin (BioBasic)

100x Penicillin-Streptomycin (Gibco, Life technology)

Tetracycline (BioBasic)

2.6.Bacterial, yeast and virus strains

Escherichia coli strain XL-1-Blue

E. coli strain 363

E. coli strain BL21(DE3)

E. coli strain MG1655

E. coli strain TOP10

Pichia pastoris strain KM71

Saccharomyces cerevisiae strain AH109 (Clontech)

Saccharomyces cerevisiae strain Y187 (Clontech)

Saccharomyces cerevisiae strain Y2HGold (Clontech)

Vibrio harveyi strain 639

White spot syndrome virus (WSSV) Thai isolated

2.7.Softwares

BlastN, BlastX (http://www.ncbi.nlm.nih.gov/blast/Blast.cgi)

ClustalW (http://www.ebi.ac.uk/Tools/msa/clustalw2/)

ExPASy ProtParam (http://au.expasy.org/tools/protparam.html)

GENETYX version 7.0 program (Software Development Inc.)

SECentral (Scientific & Educational Software)

SignalP (http://www.cbs.dtu.dk/services/SignalP/)

SPSS statistic 17.0 (Chicago, USA)

2.8.Vectors

pBAD/Myc-His A (Invitrogen)

pET-16b (Novagen®, Germany)

phRL-null (Promega)

pGBKT7 (Clontech, USA)

pGEMT-easy vector (Promega)

pGL3-basic (Promega)

2.9.Animal culture

Specific pathogen free (SPF) black tiger shrimp, *Penaeus monodon*, of about 15-20 g bodyweight were obtained from a farm in Nakhon Si Thammarat Province, Thailand. The animals were reared in laboratory tanks at ambient temperature (28 ± 4 °C), and maintained in aerated water with a salinity of 15 ppt for at least 7 days before use. For RNAi experiments, *P. monodon* of about 3-5 g in weight were purchased from local farms in Thailand or a farm in Nakhon Si Thammarat Province, Thailand, and were maintained as above.

2.10. General protocol purpose

2.10.1. Quantiative method for DNA determination

The concentration of DNA fragment was determined by measuring the A_{260} and estimated in µg/ml using an equation (1)

$$[\text{DNA}]\ (\mu g/ml) = A_{260} \times \text{dilution factor} \times 50 \qquad (1)$$

For one A_{260} corresponds to 50 µg/ml of DNA (Sambrook 1989).

2.10.2. Primers design

PCR primer pairs were designed based on nucleotide sequences of the template DNA using the SECentral (Scientific & Educational Software). Each primer in the pair should have about the same T_m values. They were checked for minimal self-priming and primer dimer formation.

2.10.3. Competent cell preparation and transformation

There are two types of *E. coli* competent cells used in this study, electro-competent cells and $CaCl_2$-trated cells.

A single colony of *E. coli* strain XL-1-Blue, BL21 (DE3) or TOP10, were inoculated into fresh LB media (1% (w/v*)* tryptone type-I, 0.5% (w/v) bacto yeast extract, and 1% (w/v) NaCl) containing an appropriate antibiotic. The culture was grown overnight at 37 °C with 250 rpm shaking as a starter. The starter was diluted 1:100 in LB broth and incubated until OD_{600} reached 0.5-0.6.

2.10.3.1. Competent cell for electro-transformation

The cell suspension was cooled down by chilling on ice for 30 min, then harvested by centrifugation at 4,000 × g for 15 min at 4 °C. The cell pellet was washed twice using 1 and 0.5 volume, respectively, of sterile pre-cooled distilled water. Then, cell pellet was resuspended in an appropriate volume of iced-cooled 10% (v/v) glycerol. Forty microliters of cell suspension were aliquoted and immediately frozen at -80 °C until used.

2.10.3.2. Competent cell for $CaCl_2$-transformation

The 10 min pre-chilled culture was centrifuged at 4,000 × g for 5 min. Then, the cells were washed once with 0.5 volume of 10 mM $CaCl_2$ solution. The final cell pellet was resuspended in an appropriate volume of 100 mM $CaCl_2$ solution supplemented with 10% (v/v) glycerol and chilled on ice for about 30 min. One

hundred microliters of competent cells were taken into an aliquot and immediately frozen at -80 $^{\circ}$C until used.

2.10.4. Transformation

For electro-transformation, plasmid solution at the maximum volume of 2 µl per 40 µl cells was transformed into electro-competent cells. The plasmid was incubated with competent cells on ice for 1 min, and then the mixture was transferred into cooled and cleaned 0.2 cm electrode gap cuvette for electroporation. The mixture was pulsed using Minipulser electroporation system (Bio-Rad) at constant 2.5 kV. The mixture was immediately transferred into 1 ml fresh LB media.

For $CaCl_2$ transformation, up to 10 µl plasmid was mixed with 100 µl of competent cells. The plasmid and competent cells were mixed and chilled on ice for at least 30 min. After that, the reaction was incubated at 42 ℃ for 1 min and optional on ice for 3 min. One milliliter of fresh LB media was subsequently added to the mixture. Afterwards, 1 ml culture containing recombinant cell was incubated at 37 ℃ with shaking for 1 h. The cell suspension was spread onto LB agar plate supplemented with appropriate selective substances.

2.10.5. Plasmid DNA preparation

A recombinant bacterial clone was inoculated into 5 ml of Luria-Bertani (LB) medium containing appropriate antibiotic and grew overnight at 37 ℃ with shaking. The cells were collected by centrifugation for 10 min at 8,000 × g. The plasmid was extracted using High-speed plasmid mini kit (Geneaid). The cell pellet was resuspended in 200 µl of PD1 buffer containing RNase A. The 200 µl of PD2 buffer was added and mixed gently by inverting the tube 10 times to lyse the cells. The cell lysate was neutralized by adding 300 µl of PD3 buffer and mixed immediately by inverting the tube 10 times. After centrifugation at 15,000 × g for 3 min, the supernatant containing the plasmid was applied to a LP column by pipetting. The column was centrifuged at 15,000 × g for 1 min and the flow-through was discarded.

The column was washed twice with 400 µl of W1 buffer and 600 µl of wash buffer containing ethanol, respectively, and then centrifuged to remove residual ethanol from wash buffer. Finally, the plasmid DNA was eluted by adding 50 µl of pre-heated elution buffer to the center of each column, incubating at room temperature for 2 min and centrifugation at 15,000 × g for 2 min. The eluent containing the plasmid was then stored at -20 °C until use.

2.10.6. Purification of PCR product

The PCR product was purified by Nucleospin® Extract II kit (Macherey-Nagel). For 1 volume of PCR product, 2 volume of NT buffer was added into the tube. A NucleoSpin extract column was placed into a 2 ml collecting tube. The sample was loaded into the column and centrifuged at 11,000 × g for 1 min. The flow-through was discarded, and the column was washed with 600 µl of NT3 buffer and centrifuged at 11,000 × g for 1 min. After centrifugation, the silica membrane in column was dried by centrifugation at 11,000 × g for another 2 min to completely remove NT3 buffer. The column was placed into a clean 1.5 ml microcentrifuge tube. The DNA was eluted by adding 50 µl of NE buffer into the center of silica membrane, leaving at room temperature for 1 min to increase elution yield of eluted DNA and centrifugation for 1 min. The flow-through containing the DNA fragment was measured at A_{260} for its concentration and stored at -20 °C until used.

The PCR product was purified from agarose gel by Nucleospin® Extract II kit (Macherey-Nagel). The PCR band was excised from agarose gel with a clean sharp scalpel. Extra agarose was removed to minimize the size of the gel slice. The gel slice was weighted and transferred to a clean microcentrifuge tube. For each 100 mg of agarose gel, 200 µl of NT buffer was added into the tube. The sample was incubated at 55 °C for about 10 min or until gel was completely melted and loaded into column. Then purification was performed as described above.

2.10.7. Agarose gel electrophoresis

The 1-1.5% (w/v) agarose gel was prepared using 1X TBE buffer (89 mM Tris-HCl, 8.9 mM boric acid and 2.5 mM EDTA, pH 8.0). After melting the agarose gel, the solution was cooled down before pouring into a tray with a well-forming comb. The gel was placed onto the running chamber. DNA samples with 1/10 volumes of the 10X loading dye (50 mM Tris-HCl, 2.5 mg/ml bromophenol blue, 2.5 mg/ml xylene cyanol, 60% glycerol at pH 7.6) were loaded into the wells. A DNA ladder (100 bp or 1 kb marker, Fermentas) was used as standard DNA markers. The electrophoresis was performed in 1X TBE buffer at 100 volts for 30-40 min. The gels were stained with ethidium bromide solution for a while and de-stained in water for about 10-15 min. The DNA bands were visualized under the UV transilluminator.

2.10.8. Protein analysis

2.10.8.1. SDS-PAGE analysis

A discontinuous system of SDS-PAGE was used. The gel solutions were prepared (Wyckoff *et al.* 1977). The glass plates and spacers were assembled. Then, the separation gel solution was pipetted into the gel plate set and layered on top with distilled water to ensure a flat surface of gel. When the polymerization was completed, water of poured off. The stacking gel solution was prepared and poured on top of the separating gel. Then, a comb was placed immediately in position with excess gel solution overflowing the front glass plate. After the stacking gel was polymerized, the comb was removed and the wells were rinsed with distilled water to remove excess un-polymerized acrylamide.

The protein samples were prepared by resuspending the proteins in 1X SDS loading buffer (12 mM Tris-HCl, pH 6.8, 5% glycerol, 0.4% SDS, 0.02% bromophenol blue, and 2.88 mM 2-mercaptoethanol). The samples were then boiled for 10 min and spun down. The samples were either held at room temperature or kept on ice until loaded into gel.

Electrophoresis was performed in 1X SDS running buffer containing 25 mM Tris-HCl, pH 8.3, 192 mM glycine, and 0.1% (w/v) SDS at a constant current of 25 mA

per gel. The protein samples and the pre-stained protein marker were loaded into the wells. After electrophoresis, the gels were stained with Coomassie brilliant blue R250 staining solution (0.1% (w/v) Coomassie brilliant blue R250, 10% (v/v) acetic acid, 45% (v/v) methanol) at room temperature with gentle shaking for 30 min. After that, the gels were dipped into the destaining solution (10% (v/v) acetic acid, 10% (v/v) methanol) and shaken at room temperature with agitation for 1-3 h or overnight. The destaining solution was replaced regularly to assist the staining removal.

2.10.8.2. Western Blot analysis

After electrophoresis through the SDS-PAGE, the protein gel was removed from the glass plates. The nitrocellulose membrane, gel, and 2 pieces of thick-blotting papers were soaked in transfer buffer (25 mM Tris, 150 mM glycine and 20% methanol) for 15-30 min together with nitrocellulose membrane, which were cut to the size of gel. A pre-soaked thick-blotting paper was placed onto the Trans-Blot® SD (Bio-Rad). A pipette was rolled over the surface of thick-blotting paper to exclude all air bubbles, followed by the nitrocellulose membrane, the gel, and another piece of thick-blotting papers, respectively.

The transfer of protein was performed at constant 100 mA for 60 min. After protein was transferred, the nitrocellulose membrane was blocked in a blocking solution (5% (w/v) skim milk in 1X PBS buffer and 0.05% (v/v) Tween™-20 at pH 7.4, 1X PBS-T) at room temperature for overnight with gentle shaking. The membrane was washed 3 times for 10 min with 1X PBS-T. The membrane was then incubated with antibody specific to each protein that was diluted in 1X PBS-T containing 1% (w/v) skim milk for about 3 h at 37 °C with gentle shaking. Subsequently, the membrane was washed 3 times for 10 min each with 1X PBS-T and incubated with a alkaline phosphatase-conjugated mouse or rabbit anti-mouse IgG (Jackson ImmunoResearch Laboratories, Inc.) that was diluted in 1X PBS-T containing 1% (w/v) skim milk at room temperature for an hour. The membrane was washed 3 times for 10 min with 1X PBS-T at room temperature. The color development was performed by adding NBT

and BCIP (Fermentas) at the final concentration of 375 and 188 μg/ml, respectively, in 100 mM Tris-HCl, 100 mM NaCl and 50 mM $MgCl_2$, pH 9.5 until the desired band were detected. Finally, the membrane was washed with distilled water to stop the reaction.

2.10.8.3. Bradford assay

The protein concentration was measured according to the method of Bradford (Bradford 1976) using bovine serum albumin (Fluka) as a standard protein. This method was based on the binding of Coomassie brilliant blue G250 dye to proteins in sample converting the red dye color to blue. A sample solution of 100 μl was mixed with 1 ml of Bradford working buffer and incubated for 10 min at room temperature before A_{595} was measured. The Bradford working buffer (100 ml) was a mixture of 6 ml Bradford stock solution (350 g of Coomassie blue G250, 100 ml of 95% ethanol and 200 ml of 85% phosphoric acid), 3 ml of 95% ethanol, 6 ml of 85% of phosphoric acid and 85 ml of distilled water.

2.10.9. RNA extraction and first-strand cDNA synthesis

2.10.9.1. Total RNA extraction

Total RNA was extracted from each tissue using the TRI Reagent® (Molecular Research Center). After collect the sample, 1 ml of TRI Reagent® was added and homogenized immediately. Then, 200 μl of chloroform was added. The sample was vigorously mixed by vortex for 15 min and standed on the table at room temperature for 2-5 min before centrifugation at 12,000 × *g* for 15 min at 4 °C. The colorless upper aqueous phase was transferred to a fresh 1.5 ml microcentrifuge tube. The total RNA was precipitated with 1 volume of isopropanol. The mixture was left at room temperature for 5-10 min and centrifuged at 13,500 rpm for 15 min at 4 °C. The supernatant was removed. The pellet of total RNA was washed in 1 ml of 75% ethanol and centrifuged at 13,500 rpm for 15 min at 4 °C. The supernatant was removed. The RNA pellet was briefly air-dried for 5-10 min. The total RNA was

dissolved with an appropriate amount of diethyl pyrocarbonate (DEPC)-treated water and leaving it on ice until it was completely dissolved.

2.10.9.2. DNase treatment of total RNA samples

The obtained total RNA was further treated with RQ1 RNase-free DNase (Promega). The reaction contains 5 μg of total RNA in 1X RNase-free DNase buffer and 1 unit of RQ1 RNase-free DNase. The DNase treatment reactions were incubated at 37 °C for 30 min to remove the contaminating chromosomal DNA. Then, the RNA was purified by TRI Reagent® as described in section 2.10.9.1

2.10.9.3. Determination of the quantity of RNA samples

The quantity and quality of total RNA was spectrophotometrically measured at 260 nm based on the specific property of UV adsorption. The concentration of total RNA could be determined using equation (2):

$$[\text{RNA}]\ (\text{ng}/\mu\text{l}) = A_{260} \times \text{dilution factor} \times 40 \qquad (2)$$

One A_{260} corresponds to 40 μg/ml of RNA (Sambrook 1989). The relative purity of RNA samples was examined by measuring the ratio of $A_{260/280}$ and $A_{260/230}$. The maximum absorption of organic solvent, nucleic acid, and protein is at 230, 260, and 280 nm, respectively. The ratio of absorbance at 260 nm and 280 nm is used to assess the purity of RNA. An approximately ratio above 1.7 is generally accepted as pure RNA. If the ratio is appreciably lower, it may indicate the presence of protein, phenol or other contaminants that absorb strongly at or near 280 nm. The quality was further investigated through an agarose gel electrophoresis. The gel was stained with EtBr and visualized under UV light, respectively.

2.10.9.4. First-strand cDNA synthesis

The first strand cDNA was synthesized from 1-5 μg of the total RNA using the RevertAid™ First Strand cDNA Synthesis Kit (Fermentas). According to the kit's instruction, the reaction was performed in a final volume of 12 μl containing 1 μg of the total RNA, 0.5 μg of the oligo$(dT)_{18}$ primer and adjusted the volume by DEPC-treated water. The mixture of RNA was incubated at 65 °C for 5 min and chilled on ice for 5 min to anneal the primer. After that, 4 μl of 5X reaction buffer, 1 μl of RiboLock™ RNase inhibitor (20U/μl), 2 μl of 10 mM dNTP mix and 1 μl (200 U/μl) of RevertAid™ reverse transcriptase were added and gently mixed. The reaction mixture was incubated 42 °C for 1 h and finally heated at 70 °C for 15 min to terminate the reaction. The cDNA was stored at -20 °C until used.

2.11. Effect of rALF*Pm*3 treatment on bacterial cells

2.11.1. Preparation of the purified recombinant protein ALF*Pm*3 (rALF*Pm*3)

2.11.1.1. Expression of rALF*Pm*3 in yeast, *Pichia pastoris*

The freezing stock culture of *Pichia pastoris* strain KM71 containing recombinant plasmid pPIC9K-ALF*Pm*3 (Somboonwiwat *et al.* 2005) was streaked onto a YPD agar plate (1% yeast extract, 2% peptone, 2% dextrose and 1.5% agar) and incubated at 30 °C for 3-5 days. A single colony was grown in 20 ml of YPD broth (1% yeast extract, 2% peptone, and 2% dextrose) with shaking at 250 rpm, 30 °C for overnight. The starter was inoculated 1:100 in 300 ml of BMGY medium (1% yeast extract, 2% peptone, 100 mM potassium phosphate, pH 6.0, 1.34% YNB, 4×10^{-5}% biotin, and 1% glycerol). The culture was grown at 30 °C with shaking at 300 rpm until the OD_{600} reached 4-6. The cells were harvested by centrifugation at 8,000 × g for 10 min at room temperature. After that, the cell pellet was resuspended in 60 ml of BMMY medium (1% yeast extract, 2% peptone, 100 mM potassium phosphate, pH 6.0, 1.34% YNB, 4×10^{-5}% biotin, and 0.5% methanol) to induce the recombinant ALF*Pm*3 protein (rALF*Pm*3) expression. The pure methanol was added to the culture to a final concentration of 0.5% every 24 h in order to maintain the induction for 3

consecutive days. The supernatant was collected by centrifugation at 8,000 × g for 10 min at room temperature. The supernatant was kept and stored at -80 °C until use. The rALF*Pm*3 was analyzed by 15% Silver-stained SDS-PAGE.

2.11.1.2. Purification of the rALF*Pm*3 protein by cation exchange chromatography

The crude supernatant containing the rALF*Pm*3 was diluted 1:1 with the start buffer (20 mM Tris-HCl, 200 mM NaCl, pH 7.0) and purified by a strong cation exchange chromatography, HiTrap SP Sepharose™ Fast Flow column (GE Healthcare) using ÄKTA Prime Plus FPLC Purification System (GE Healthcare). The column was equilibrated with start buffer. Afterwards, the diluted protein was loaded on to the column, and washed with start buffer to remove unbound proteins until the A_{280} was decrease to zero. The elution was performed using the elution buffer (20 mM Tris-HCl, 1 M NaCl, pH 7.0). The flow rate was controlled at 1 ml/min throughout the purified process. The fractions were analyzed by 15% SDS-PAGE. The antimicrobial activity of the purified protein was performed against *E. coli* 363 as described in section 2.11.3 The fractions were then pooled and dialyzed overnight against distilled water at 4 °C to eliminate salt (Somboonwiwat *et al.* 2005). The purified rALF*Pm*3 was concentrated using lyophilizer (freeze-dry) and then the protein concentration was measured at A_{280} using equation (3). The purified protein was kept at -80 °C until use.

$$[\text{rALF}Pm3]\ (\text{M}) = \frac{A_{280} \times \text{dilution factor}}{33270} \qquad (3)$$

where extinction coefficient (ξ) = 33,270 L mol^{-1} cm^{-1}

2.11.2. Antimicrobial activity assay

The antimicrobial activity of rALF*Pm*3 was tested against *E. coli* 363, and *Vibrio harveyi* 639 (a shrimp pathogenic strain), using liquid broth assay. Minimum inhibitory concentration (MIC) values were then determined according to Somboonwiwat *et al.*, 2005. The overnight culture were diluted 1:100 with LB broth (for *E. coli* 363) or TSB (for *V. harveyi* 639) and incubated until an OD_{600} was about 0.1 and then diluted with poor broth containing 1% tryptone type-1, 0.5% NaCl, pH 7.5 (for *E. coli* 363) or saline peptone water containing 1.5% peptone, 1.5% NaCl, pH 7.2 (for *V. harveyi* 639) to an OD_{600} of 0.001. One-hundred-microliter aliquots of bacteria were mixed with 10 µl of rALF*Pm*3 at various concentrations in well of a 96-well microtiter plate. Aliquots of distilled water with fresh medium were used as control. The reactions were cultured for overnight under vigorous shaking at 180 rpm 30 °C. The growth of bacteria was measure at OD_{600} using a SpectraMax M5 Multi-Mode Microplate Reader (Molecular Devices). The MIC value was recorded as the range between the highest concentration of the peptide where bacterial growth was observed and the lowest concentration that cause 100% of inhibition bacterial growth.

2.11.3. Preparation of log phase of *Vibrio harveyi* 639 cell

V. harveyi which is a severe pathogenic bacterial of shrimp, is often used for investigation of shrimp antimicrobial peptide activity. In this research mid-exponential phase *V. harveyi* 639 (or *Escherichia coli* where stated) cells were used to study the effect of ALF*Pm*3 against this shrimp bacterial pathogen. *V. harveyi*-freezing stock was streaked on tryptone soya agar (TSA) plate and incubated at 30 °C for overnight (16-18 h). Single colony of *V. harveyi* was inoculated into tryptone soya broth (TSB) medium at 30 °C with shaking 250 rpm for overnight. An overnight culture of *V. harveyi* 639 was sub-cultured into fresh TSB medium at 30 °C with shaking 250 rpm until the OD_{600} of the culture reached 0.6.

2.11.4. Localization of ALF*Pm*3 binding on *V. haveyi* cell by immuno-detection assay

The *V. harveyi* 639 cells were incubated with the addition of either the purified rALF*Pm*3 protein (diluted in phosphate buffered saline (PBS) buffer (13.7 mM NaCl, 0.27 mM KCl, 1 mM Na_2HPO_4 and 0.2 mM KH_2PO_4, pH 7.4)) at the MIC or with the same volume of PBS buffer as a control for 10 min. After incubation, the bacterial cells were fixed with 4% (w/v) paraformaldehyde in PBS and then washed three times with PBS buffer. The fixed bacteria cells were smeared on a Polysine® slide (Thermo Scientific), air-dried and then permeabilized with Tris-buffered saline (TBS) buffer containing 0.2% gelatin and 0.5% Triton X-100. The slides were pre-incubated with PBSTB (PBST (PBS, 0.05% (v/v) Tween-20) with 1% (w/v) BSA and 1% (v/v) normal goat serum) for 1 h and washed three times with PBST. The rALF*Pm*3 localized on the cell surface was detected by probing the slides with the rabbit anti-rALF*Pm*3 polyclonal antibodies (PcAb) (1:500 dilution in PBST) at 37 °C for 2 h, then washed in PBST and subsequently probed with the alkaline phosphatase (AP)-conjugated anti-rabbit Ab (1:2,000 dilution in PBST) at room temperature for 1 h. Finally, after washing with PBST the AP chromogenic substrate NBT/BCIP was added to a final concentration of 0.33 and 0.165 mg/ml, respectively in the AP detection buffer (100 mM Tris–HCl (pH 9.5), 100 mM NaCl and 10 mM $MgCl_2$ and 1 mM levamisole) to develop the staining. The slides were mounted and observed under the light microscopy (Olympus CX31).

2.11.5. Analysis of the bacterial membrane permeabilization activity of ALF*Pm*3

2.11.5.1. Outer membrane permeabilization

Since *V. harveyi* 639 is a Gram-negative bacterium with 2 layers of lipid membrane surrounding the cells, the ability of rALF*Pm*3 to permeabilize the outer membrane of *V. harveyi* 639 was determined by the 1-N-phenylnapthylamine (NPN) uptake assay (Loh *et al.* 1984). Cells from mid-logarithmic phase cultures of *V. harveyi* 639 (section 2.12) were washed in 5 mM HEPES buffer (pH 7.2) and fixed in 5

mM potassium cyanide in HEPES buffer. NPN at a final concentration of 0.33 μM was mixed with the fixed bacterial cells and with rALF*Pm*3 at various concentrations (0-(control), 1-, 5-, 10-, 15- or 20-fold of the MIC), the fluorescence of NPN was measured using a spectrofluorometer (SpectraMax M5, Molecular Devices) at an excitation wavelength of 350 nm (A_{350}) and an emission wavelength of 420 nm (A_{420}). The fluorescence value of each sample was standardized relative to the level measured from bacterial cells permeabilized by 0.01% (v/v) Triton X-100 (nominal 100% level control), as in equation (4).

$$\%\text{NPN uptake} = 100*[(F-F_0)/ (F_t-F_0)] \quad (4)$$

Where F, F_0 and F_t are the fluorescence intensity of bacterial cells incubated with rALF*Pm*3, 5 mM potassium cyanide in HEPES buffer (control) and 0.01% (v/v) Triton X-100 (100% reference standard), respectively.

2.11.5.2. Inner membrane permeabilization

To access the bacterial inner membrane permeabilizing activity of rALF*Pm*3, the *o*-nitrophenyl-β-d-galactoside (ONPG) and the total nucleotide leakage assays were performed on *E. coli* and *V. harveyi* cells, respectively, as follows. The inner membrane permeabilization was determined by measuring the β-galactosidase activity of *E. coli* MG1655 lacY:Tn10dKan, a lactose permease deficient strain, using ONPG as a substrate as previously described (Krusong *et al.* 2012). In brief, the overnight culture of *E. coli* MG1655 was inoculated into fresh LB medium containing 1 mM IPTG to induce the expression of β-galactosidase. Mid-logarithmic phase cultures were then incubated with 0.5 μM rALF*Pm*3 or, for the controls, with either same volume of PBS buffer or PBS buffer plus 0.5 μM BSA. At each time point (0, 5, 10, 20, 30, 60, 120, 240 and 480 min), the supernatant was collected and ONPG was added to a final concentration of 0.4 mM and incubated at 37 °C for 10 min. Reactions were stopped by adding 2 M sodium carbonate. The β-galactosidase

activity was monitored by measuring the ONPG hydrolyzed product, o-nitrophenol (ONP), at an absorbance wavelength of 405 nm (A_{405}) with a microtiter plate reader (SpectraMax M5, Molecular Devices).

The total nucleotide leakage assay was performed to study the inner membrane leakage and the release of cytoplasmic contents of *V. harveyi* cells (Tang *et al.* 2009). Mid-logarithmic phase cultures of *V. harveyi* 639 were prepared as described in section 2.12 and then treated with rALF*Pm*3 at concentrations of 0.5-, 1- and 2-fold MIC in PBS buffer or, for the control, with either same volume of PBS buffer or PBS buffer plus 3 μM BSA. After 0, 5, 10, 20, 30, 60 and 120 min of incubation, the supernatant was collected, and the absorbance at 260 nm (A_{260}) was measured to determine the total nucleotide leakage.

2.11.6. Observation of the morphological structure and the ultrastructure of *V. harveyi* after ALF*Pm*3 treatment using electron microscopy

2.11.6.1. Scanning electron microscopy

Scanning electron microscopy (SEM) was used to observe the morphological change of *V. harveyi* 639 after treatment with rALF*Pm*3. Mid-logarithmic phase cultures of *V. harveyi* 639 were prepared as described in section 2.11.3 and then resuspended in fresh filtrated PBS buffer. *V. harveyi* 639 cells were mixed with MIC of ALF*Pm*3 for 1 h or with 10-fold MIC of rALF*Pm*3 and immediately collected. The untreated cells were used as a control. The collected cells were then fixed in 2.5% (v/v) glutaraldehyde in 0.1 M phosphate buffer (pH 7.4) for 2 h, washed three times with 0.1 M phosphate buffer (pH 7.4) and dehydrated through a graded ethanol series. After critical point drying, they were mounted on 1-cm stubs and gold-coated using an Ion Sputter Coater (Balzers, model SCD 040). The specimens were then observed with a JEOL scanning electron microscope (JSM-5410LV).

2.11.6.2. Transmission electron microscopy

Mid-logarithmic phase cultures of *V. harveyi* cells from section 2.12 was incubated with a 5-fold MIC of rALF*Pm*3 in PBS buffer, or just PBS buffer (negative control), for 1 h. The fixed bacterial cells were prepared as described for SEM analysis. The fixed cells were then dropped on Formvar-coated copper grids and negatively stained with 1% (w/v) uranyl acetate for 1 min. The grids were observed using a Hitachi/S-4800 transmission electron microscope.

2.12. Functional characterization of *Pm*VRP15 in shrimp viral immunity

2.12.1. Production of *Pm*VRP15 and GFP dsRNA

Double-stranded RNAs (dsRNAs) specific to *Pm*VRP15 gene was prepared according to T7 RiboMAX™ Express RNAi System (Promega) kit's instruction using *Pm*VRP15-recombinant plasmid as a template for producing sense and anti-sense DNA templates of *in vitro* transcription. DNA templates containing the T7 promoter sequence at the 5′-end were generated by PCR using oligonucleotide primers (*Pm*VRP15-T7-F and *Pm*VRP15-T7-R) (Table 2.1). The negative control was dsRNA of green fluorescent protein (GFP) prepared from pEGFP-1 vector (Clontech) template using GFPT7-F and GFP-R for the sense strand template, and with GFP-F and GFPT7-R (Table 2.1) for the antisense strand template. PCR condition for those primer pairs was 94 °C for 3 min, 30 cycles of 94 °C for 30 sec, 58 °C for 30 sec and 72 °C for 30 sec, and then a final extension at 72 °C for 5 min using Phusion® High-Fidelity DNA polymerase (New England, Biolabs). Each template was *in vitro* transcribed using T7 RiboMAX™ Express RNAi System (Promega) to produce complementary ssRNAs. Then, equal amounts of each of the complementary ssRNAs were mixed and incubated at 70 °C for 10 min, and slowly cooled down at room temperature to allow annealing to form dsRNA. The *Pm*VRP15 dsRNA solution was treated with 2 units of RQ1 RNase-free DNase (Promega) at 37 °C for 30 min. 1/10 vol. of 3 M Sodium acetate (pH 5.2) and 1 vol. of isopropanol were added and mixed to precipitate dsRNA on ice for 5 min. The dsRNA was washed with 0.5 ml of 75% ethanol, centrifuged briefly, and then all residual ethanol was removed. Air-dry the pellet for 15 min at room

temperature, and resuspend the RNA sample in Nuclease-Free Water. The quality of dsRNA was checked by agarose gel electrophoresis. The concentration of dsRNA was measured at A_{260} using spectrophotometer and kept at -80°C before used.

Table 2.1 List of primers used to perform dsRNA production

Primer name	Sequence (5´⟶3´)
*Pm*VRP15- T7-F	GGATCCTAATACGACTCACTATAGGCGCGACCGAGCCAAGAG
*Pm*VRP15- T7-R	GGATCCTAATACGACTCACTATAGGTGAGCTGACGGAAGGCC
*Pm*VRP15-F	TCACTCTTTCGGTCGTGTCG
*Pm*VRP15-R	CCACACACAAAGGTGCCAAC
GFP-F	ATGGTGAGCAAGGGGGAGGA
GFP-R	TTACTTGTACAGCTCGTCCA
GFP-FT7	GGATCCTAATACGACTCACTATAGGATGGTGAGCAAGGGGGAGGA
GFP-RT7	GGATCCTAATACGACTCACTATAGGTTACTTGTACAGCTCGTCCA
WSV399-T7-F	GGATCCTAATACGACTCACTATAGGTTCCACATCGCATTCGCA
WSV399-T7-R	GGATCCTAATACGACTCACTATAGG CACGGGGATCAATATCTTGGA
WSV399-RT-F	TTCCACATCGCATTCGCA
WSV399-RT-R	CACGGGGATCAATATCTTGGA

2.12.2. *Pm*VRP15 gene knockdown in hemocyte of WSSV-infected shrimp

P. monodon shrimps (about 3 g body weight) were divided into two groups of three individuals each. The first (control) group was injected with 10 µg/g shrimp of GFP-dsRNA, whilst the second group (*Pm*VRP15 knockdown) was injected with 10 µg/g shrimp *Pm*VRP15-dsRNA. After 24 h, 10 µg/g shrimp *Pm*VRP15-dsRNA or dsGFP was mixed with 30 µl of the 10,000-fold diluted WSSV solution (a dose that causes 100%

mortality of shrimp in 3 days post- injection (dpi)) and injected into the respective groups of shrimp to double inject dsRNA together with WSSV infection into shrimp.

2.12.2.1. Expression analysis of *Pm*VRP15 gene

Hemocytes of individual shrimp were collected at 24 hours post- infection (hpi) and total RNA was extracted (section 2.10.9.1) and treated with RNase-free DNase (section 2.10.9.2) to remove any residual DNA contamination. Total RNA concentration was determined using spectrophotometer (section 2.10.9.3). An equal amount of DNA-free total RNA from three shrimp was pooled and 1 μg of pooled total RNA was used for the first strand cDNA synthesis using the RevertAid First Strand cDNA Synthesis kit (section 2.10.9.4).

To confirm the *Pm*VRP15 gene transcript knockdown, RT-PCR was performed. The *Pm*VRP15-RT-F/R primers (Table 2.2) were used (100 nM) along with the elongation factor-1α (EF-1α) gene as an internal control using the EF-1-F/R primer pair (Table 2.2). The PCR conditions were 94 ℃ for 1 min, followed by 27 cycles of 95 ℃ for 30 sec, 58 ℃ for 30 sec, and 72 ℃ for 30 sec, and then a final extension at 72 ℃ for 5 min. The PCR products were analyzed by 1.5% (w/v) agarose gel electrophoresis.

2.12.2.2. Expression analysis of *Pm*VRP15 protein

The hemolymph of WSSV-infected *Pm*VRP15 gene knockdown shrimp and of the control was collected from 5 individuals. The hemocyte was separated by centrifugation at 800 × g for 10 min 4 ℃. The hemocytes were homogenized in PBS and centrifuged to collect the supernatant. The protein concentration of the hemocyte lysate (HLS) was measured by the Bradford method (section 2.10.8.3). After protein extraction, protein lysate from each individual were pooled. Seventy μg of HLS protein (per lane) was subjected to SDS-PAGE (15% (w/v) acrylamide resolving gel, section 2.10.8.1) resolution, transferred to nitrocellulose membrane and then the *Pm*VRP15 and β-actin protein was detected by Western-blot analysis (section

2.10.8.2) using purified rabbit polyclonal anti-r*Pm*VRP15 antiserum (dilution 1:1,000) and mouse anti-actin (dilution 1:10,000, Millipore) antibodies. The positive bands were detected by secondary antibodies conjugated with horseradish peroxidase (brown color) for mouse antibody or alkaline phosphatase (purple color) for rabbit antibody.

2.12.3. WSSV gene expression analysis of *Pm*VRP15 knockdown shrimp infected with WSSV

From section 2.12.2, first-strand cDNAs of *Pm*VRP15 and GFP (control group) knockdown WSSV-infected shrimp hemocyte were prepared. The involvement of *Pm*VRP15 silencing in WSSV-infected shrimp was investigated. Upon *Pm*VRP15 gene silencing, the expression level of WSSV genes including ie-1, wsv 477 and vp28 was determined by the RT-PCR and quantitative real-time PCR (qRT- PCR).

The expression level of viral genes at various stages of infection, which are ie-1 (immediate early gene), wsv477 (early gene) and vp28 (late gene), was determined by semi-quantitative RT-PCR using gene specific primer, ie1-F/R, wsv477-F/R, and vp28-F/R (Table 2.2). EF-1**α** gene as a reference gene was amplified using EF-1-F/R primers. One microliter of 5-fold diluted cDNA was used as a template for PCR amplification. The reaction contained 1X PCR buffer, 0.1 **μ**M each dNTP, 0.2 **μ**M primer each, 1.25 U RBC *Taq* polymerase (RBC Bioscience). The reaction was pre-denatured at 94 ℃ for 1 min and followed by 35 cycles of denaturation at 94 ℃ for 30 sec, annealing at 60 ℃ for 30 sec and extension at 72 ℃ for 30 sec. Final extension was carried out at 72 ℃ for 7-10 min. The PCR product was analyzed by 1.5% (w/v) agarose gel electrophoresis.

For quatitative RT-PCR was performed on the BioRad CFX96^{TM} Real-Time PCR system. For ie-1, wsv477 and vp28 genes amplification, gene specific primer pairs: ie1-qrt-F/R, wsv477-qrt-F/R and vp28-qrt-F/R, respectively, were used (Table 2.2). EF-1**α** gene as a reference gene was amplified using EF-1-F/R primers. Reactions were prepared in a total volume of 15 μl containing 7.5 μl SsoFast™ EvaGreen® Supermix (Bio-Rad), 1 μl cDNA template, 100 nM (for WSSV genes) and 400 nM (for EF-1**α** gene)

forward and reverse primers. Amplification profiles consisted of 95 ℃ for 5 min, and 40 cycles of 95 ℃ for 30 sec, 60 ℃ for 30 sec (for all WSSV genes) or 58 ℃ for 30 sec (for EF-1**α** gene) and 72 ℃ for 30 sec. Three replicate qPCRs were performed per sample. The $2^{-\Delta\Delta Ct}$ method was used to calculate the relative expression ratio (Pfaffl 2001). Expression of each gene was normalized relatively to the reference EF-1**α** gene in the same sample.

Table 2.2 List of primers used to study the effect of *Pm*VRP15 silencing on WSSV propagation

Primer name	Sequence (5′⟶3′)
*Pm*VRP15-RT-F	CGTCCTTCAGTGCGCTTCCATA
*Pm*VRP15-RT-R	ACAGCGACTCCAAGGTCTACGA
EF-1-F	GGTGCTGGACAAGCTGAAGGC
EF-1-R	CGTTCCGGTGATCATGTTCTTGATG
vp28-F	TCACTCTTTCGGTCGTGTCG
vp28-R	CCACACACAAAGGTGCCAAC
ie1-F	GACTCTACAAATCTCTTTGCCA
ie1-R	CTACCTTTGCACCAATTGCTAG
wsv477-F	CGCGGATCCATGTATATCTTCGTCGA
wsv477-R	CCGGAATTCTTATAAGAAATGTACAA
vp28-qrt-F	GGGAACATTCAAGGTGTGGA
vp28-qrt-R	GGTGAAGGAGGAGGTGTTGG
ie1-qrt-F	AGCAAGTGGAGGTGCTATGT
ie1-qrt-R	CCATGTCGATCAGTCTCTTC
wsv477-qrt-F	GGCCAAGTCATGGAGATCTA
wsv477-qrt-R	CCATCCACTTGGTTGCAGTA
wsv399-F	CGCCTCGAGGTTCCAGAAATGGTTTGAATCGTT
wsv399-R	GCCGAATTCGCTTTGTTTGATAATACAATTTTCACCTTGT

2.12.4. Effect of *Pm*VRP15 gene silencing on the cumulative mortality of WSSV-infected shrimp

To study the involvement of *Pm*VRP15 gene in WSSV infection in shrimp, the percentage of cumulative mortality of WSSV-infected *Pm*VRP15 knockdown shrimp was compared with those of WSSV infected GFP knockdown shrimp, the control group. Ten *P. monodon* shrimp of approximately 3 g body weight per group were injected with *Pm*VRP15 dsRNA or GFP dsRNA as described in section 2.12.1. The dosage of WSSV used in this experiment causes 100% mortality of shrimp in 4 dpi. The shrimp mortality was observed every 3 h after WSSV infection. This experiment was done in triplicate. Moreover, after WSSV infection, shrimp hemocyte was collected at 24, 36, 48 and 60 hpi. Total RNA was extracted (section 2.10.9.1). After DNase treatment and cDNA synthesis, *Pm*VRP15 gene expression was investigated by RT-PCR (section. 2.12.2) in order to determine *Pm*VRP15 gene recovery.

2.12.5. Data analysis

Data were analyzed using the SPSS statistics 17.0 software (Chicago, USA) and are presented as the mean ±1 standard deviation (SD). Statistical significance of differences between means was calculated by the paired-samples *t*-test, where significance was accepted at the $P < 0.05$ level.

2.13. Identification of *Pm*VRP15- interacting protein from WSSV by yeast two-hybrid screening

2.13.1. Construction of bait plasmids containing the N-, C-terminus and open reading frame (ORF) of *Pm*VRP15 gene

The open reading frame (ORF), N- and C- terminus of *Pm*VRP15 gene were amplified by PCR using gene specific primers (Table 2.3). The PCR conditions were 94 °C for 1 min, followed by 30 cycles of 95 °C for 30 sec, 58 °C for 30 sec, and 72 °C for 30 sec, and then a final extension at 72 °C for 5 min using RBC *Taq* polymerase (RBC bioscience). The PCR products were analyzed by 1.5 % (w/v) agarose gel

electrophoresis and purified using Nucleospin® Extract II kit (Macherey-Nagel) as described in section 2.10.6.1. The purified PCR products that double-digested with restriction enzymes were cloned in-frame into pGBKT7 vector (Figure 2.1), a bait vector, cut with the same restriction enzymes. The total 20 µl of ligation mixture contained 2 µl of 10X T4 ligation buffer, 50 ng of *Nco*I/*Bam*HI or *Nde*I/*Eco*RI digested pGBKT7 vector, 40 ng of *Nco*I/*Bam*HI digested ORF of *Pm*VRP15 or *Nde*I/*Eco*RI digested N- and C- terminus of *Pm*VRP15, and 1 µl of 400 U/µl T4 DNA ligase (New England Biolabs). The reaction was incubated at 4 °C for overnight (16-18 h). 10 µl of the ligation mixture was transformed into an *E. coli* XL1-blue using $CaCl_2$-transformation. The transformants were selected on LB agar plate with 30 µg/ml kanamycin. The recombinant plasmids were subjected to nucleotide sequencing to verify the sequences of inserts (Macrogen Inc., Korea).

Table 2.3 List of primers used to amplify *Pm*VRP15 gene for bait plasmids construction

Primer name	Sequence (5'- 3')
ORF-*Pm*VRP15-*Nco*I-F	GGCCATGGAG-TTAACAGAGGACTTA
ORF-*Pm*VRP15-*Bam*HI-R	ACGGATCCTTA-ATGCTCTACTGA
N-*Pm*VRP15-*Nde*I-F	GCGCATATG-TTAACAGAGGACTTAGTAAACCTG
N-*Pm*VRP15-*Eco*RI-R	GTGCTGAATTCTTA-TGTTGAGACGAATGGTATGG
C-*Pm*VRP15-*Nde*I-F	GCGCATATG-TATGCTAGGGGGAAGTTCAAA
C-*Pm*VRP15-*Eco*RI-R	GCTCGGAATTCTTA-ATGCTCTACTGACATGTTGTG

2.13.2. Transformation bait vector into *Saccharomyces cerevisiae* strain Y2H Gold

2.13.2.1. Preparation of competent yeast cells

A single colony of *S. cerevisiae* strain Y2H Gold was cultured and used as starter in 3 ml of YPDA medium cultured at 30 °C with shaking at 250 rpm for 8-12 h. Then, 5 µl of the culture were transferred to 50 ml of YPDA medium and grown

overnight to an OD_{600} 0.15-0.3. The cells were pelleted by centrifugation at 700 × g for 5 min at room temperature. The cell pellet was resuspended to a final volume of 100 ml in fresh YPDA medium and incubated at 30 °C until OD_{600} reached 0.4-0.5. The culture was centrifuged at 700 × g for 5 min at room temperature. The pellet was washed by resuspending in a total of 60 ml of deionized water, gently mixed and centrifuged. The pellet was resuspended in 1.5 ml of 1.1X TE/LiAc. This cell suspension was equally transferred to two respective 1.5 ml microcentrifuge tubes and centrifuged at 15,000 × g for 15 sec. Finally, each cell pellet was resuspended in 600 µl of 1.1X TE/LiAc. The cells were now ready to be transformed with plasmid DNA.

2.13.2.2. Transformation of competent yeast cells

The bait vector, pGBKT7-ORF-*Pm*VRP15, pGBKT7-N-*Pm*VRP15 or pGBKT7-C-*Pm*VRP15, was transformed into *S. cerevisiae* Y2H Gold using Yeastmaker™ Yeast Transformation System 2 (Clontech). A 50 µl aliquot of *S. cerevisiae* Y2H Gold competent cells was kept on ice and gently mixed with 100 ng of bait plasmid, 50 µg of yeast maker carrier DNA, and 500 µl of PEG/LiAc. The mixture of cell was incubated 30 °C for 30 min. DMSO (20 µl) was added, mixed gently and incubated at 42 °C for 15 min. The yeast cells were pelleted by centrifugation at 15,000 × g for 15 sec. The cell pellet was resuspended in YPD plus medium, incubated at 30 °C with shaking 250 rpm for 90 min and centrifuged at 15,000 × g for 15 sec. The pellet yeast cells were resuspended in 0.9% (w/v) NaCl solution.

2.13.2.3. Determination of transformation efficiency

The cell suspension diluted at 10 and 100 folds in 0.9% NaCl were plated onto a selective medium SD medium lacking Tryptophan (SD/-Trp) and incubated at 30 °C until colonies appear. Then, the transformation efficiency was calculated using the following equation (5).

$$\text{Transformation Efficiency} = \frac{\text{cfu} \times \text{Suspension Volume (ml)}}{\text{Volume plated (ml)} \times \text{amount of DNA (µg)}} \quad (5)$$

2.13.2.4. Testing bait constructs for autoactivation and cell toxicity

The *Pm*VRP15 bait vectors were tested for autoactivation of reporter genes and cell toxicity before two-hybrid screening. The yeast transformant containing a bait plasmid, pGBKT7-*Pm*VRP15, pGBKT7-N-*Pm*VRP15 or pGBKT7-C-*Pm*VRP15, was tested for autoactivation. To confirm that *Pm*VRP15 protein and its fragments do not autonomously activate the reporter genes in *S. cerevisiae* Y2H Gold, in the absence of the prey protein, 100 ng of the bait plasmid was transformed into yeast using Yeastmaker™ Yeast Transformation System 2 (Clontech) as described in section 2.13.2.2. One hundred microliters of 10 and 100-fold diluted cell suspension were plated onto separate plates including SD/-Trp plates, SD/-Trp containing X-alpha-Gal (SDO/X) plates and SD/-Trp containing X-alpha-Gal and Aureobasidin A (SDO/X/A) plates. The plates were incubated at 30 °C until colonies appear. If the bait construction autoactivates the reporter genes of *S. cerevisiae* Y2H Gold the colonies with corresponding characters would appear on selective plates.

For toxicity test, the bait plasmids, pGBKT7-ORF-*Pm*VRP15, pGBKT7-N-*Pm*VRP15 or pGBKT7-C-*Pm*VRP15, transformed into the yeast cells, and cultured on solid medium would grow slower than control yeast. 100 ng of bait plasmid and 100 ng pGBKT7 plasmid (control) were transformed into *S. cerevisiae* Y2H Gold using Yeastmaker™ Yeast Transformation System 2 (Clontech) as described in section 2.13.2.2. The 100 µl of 10 and 100-fold diluted cell suspension was spreaded onto SD/-Trp plates and incubated at 30 °C until colonies appear. If the bait was toxic, the colonies containing the bait vector were significantly smaller than colonies containing the empty pGBKT7 vector.

2.13.2.5. Control mating experiments

The mated yeast clones bearing pGBKT7-53 and pGADT7-T plasmids were used as a positive control. A negative control was mated yeast containing pGBKT7-Lam and pGADT7-T plasmid. The control yeasts were plate onto separate plates, as followed: SD/-Trp plates, SD/-Leu plates, SD/-Leu/-Trp (DDO) plates and SD/-Leu/-Trp containing X-alpha-Gal and Aureobasidin A (DDO/X/A) plates and incubating at 30 °C until colonies appear. The expected results of positive interactions, the number of colonies on DDO should be the same on DDO/X/A agar plates and colonies on DDO/X/A were blue. For negative interactions, the colonies appear on DDO but no colonies on DDO/X/A agar plates.

2.13.3. Yeast mating

Due to the *Pm*VRP15 function is still unclear and *Pm*VRP15 transcript is highly up-regulated following WSSV infection, we would like to identify proteins from WSSV that might interact with *Pm*VRP15. The interacting protein partner of *Pm*VRP15 was screening from 2 yeast libraries which are WSSV-infected shrimp hemocyte prey library (Somboonwiwat et al., unpublished data) and WSSV ORF prey library (Sangsuriya *et al.* 2014).

To perform the Yeast Two-Hybrid screening in WSSV-infected shrimp hemocyte prey library, the *S. cerevisiae* strain Y2H Gold contained pGBKT7-*Pm*VRP15, pGBKT7-N-*Pm*VRP15 or pGBKT7-C-*Pm*VRP15 pre-cultured in 5 ml SD/-trp medium was mated with 1 ml aliquot WSSV-infected shrimp hemocyte prey library in *S. cerevisiae* strain Y187 as described in the Matchmaker™ Gold Yeast Two-Hybrid System (Clontech). The mating solutions were mixed in 45 ml of 2X YPDA broth containing 50 μg/ml of kanamycin. The mating culture was grown for 20-24 h at 30 °C with gentle swirling (50 rpm). The mating mixture was centrifuged at 1,000 × g for 10 min to collect the cell pellet that was resuspended in 10 ml of 0.5X YPDA containing 50 μg/ml of kanamycin.

The mating cultures were subsequently plated on the double dropout media lacking leucine and tryptophan (SD/-Leu/-Trp) containing X-alpha-Gal and

Aureobasidin A (DDO/X/A). Positive clones were the blue colonies from MEL1 reporter gene. MEL-1 encodes **α**-galactosidase, an enzyme occurring naturally in many yeast strains. As a result of two-hybrid interactions, **α** -galactosidase was expressed and secreted by the yeast cells. Yeast colonies that express MEL1 turn blue in the presence of chromagenic substrate X- **α** -Gal. After that positive clones were subsequently grown on the higher stringency quadruple dropout media in the absence of leucine, tryptophan, adenine and histidine (SD/-Leu/-Trp/-Ade/-His) containing X-alpha-Gal and Aureobasidin A (QDO/X/A).

One hundred microliters of mating cultures (1/10, 1/100, 1/1,000 and 1/10,000 dilution) were spread onto separate plates described above, as followed: SD/-Trp plates, SD/-Leu plates and SD/-Leu/-Trp containing X-alpha-Gal (DDO/X) plates and incubating at 30 °C until colonies appear. Then, the colonies were calculated the number of screened clones (diploids) from DDO/X and mating efficiency using the following equation (7 and 8).

$$\text{Number of screened clones} = \text{cfu/ml of diploids} \times \text{resuspension volumes (ml)} \quad (7)$$

$$\text{Mating efficiency} = \frac{\text{Number of cfu/ml of diploids} \times 10}{\text{Number of cfu/ml of limiting partner}} \quad (8)$$

To identify the WSSV protein that can interact with *Pm*VRP15, the *S. cerevisiae* strain AH109 contained pGBKT7-*Pm*VRP15, pGBKT7-N-*Pm*VRP15 or pGBKT7-C-*Pm*VRP15 was mated with the *S. cerevisiae* strain Y187 containing WSSV ORF prey library that performed by Dr. Saengchan Senapin, Mahidol University (Sangsuriya *et al.* 2014). After screening, the candidate colonies were selected by selective medium, which are DDO/X/A, and QDO/X/A plate as described above.

2.13.4. Rescue plasmid

In order to screen the real positive clones containing the interacting proteins, prey plasmid DNA (pGADT7 plasmid (Figure 2.2) containing interacting-protein partner gene) was isolated from positive clones grown on the QDO/X/A selective plate. Single colony was cultured in SD/-Leu broth with shaking 300 rpm at 30 ℃ for overnight. Cell was collected by centrifugation at 5,000 × g for 5 min at room temperature. The cell were washed by one milliliter of sterile H_2O and transferred into new 1.5 ml microcentrifuge tube. After discard the supernatant, 1 M sorbitol (400 μl) and 0.5 M EDTA (100 μl) were added and mixed by vortex. The yeast lytic enzyme, zymolyase, was added and let the cells incubated at 37 ℃ for 1 h. Lysis buffer containing 50 mM Tris-HCl, pH 7.4, 20 mM EDTA and 1% SDS-PAGE was added and incubated at 65℃ for 30 min. The total protein was precipitated by potassium acetate solution and pre-chilled on ice for 30 min. The supernatant was collected and subjected to phenol/ chloroform extraction. The 2.5 volume of absolute ethanol was added to precipitate DNA. The pellet was washed with 75% ethanol after that air-dry pellet at room temperature. DNA pellet was dissolved with TE buffer containing RNaseA. The rescued plasmid was transformed into *E. coli* XL-1-Blue to recover the plasmid for sequencing. The transformants were plated on LB agar plate containing ampicillin. The obtained sequences were searched against the GenBank database to identify the clones.

2.13.5. Confirmation of positive interaction by co-transformation

To confirm the screening results, each pGADT7 plasmid from positive clones containing interacting-protein partner gene was co-transformed with the interacting protein in pGBKT7-N-*Pm*VRP15 or pGBKT7-C-*Pm*VRP15 or, parental pGBKT7 plasmid into Y2H Gold strain as described in section 2.17.2 and plated on DDO/X and QDO/X/A according to the manufacturer's instruction (Clontech).

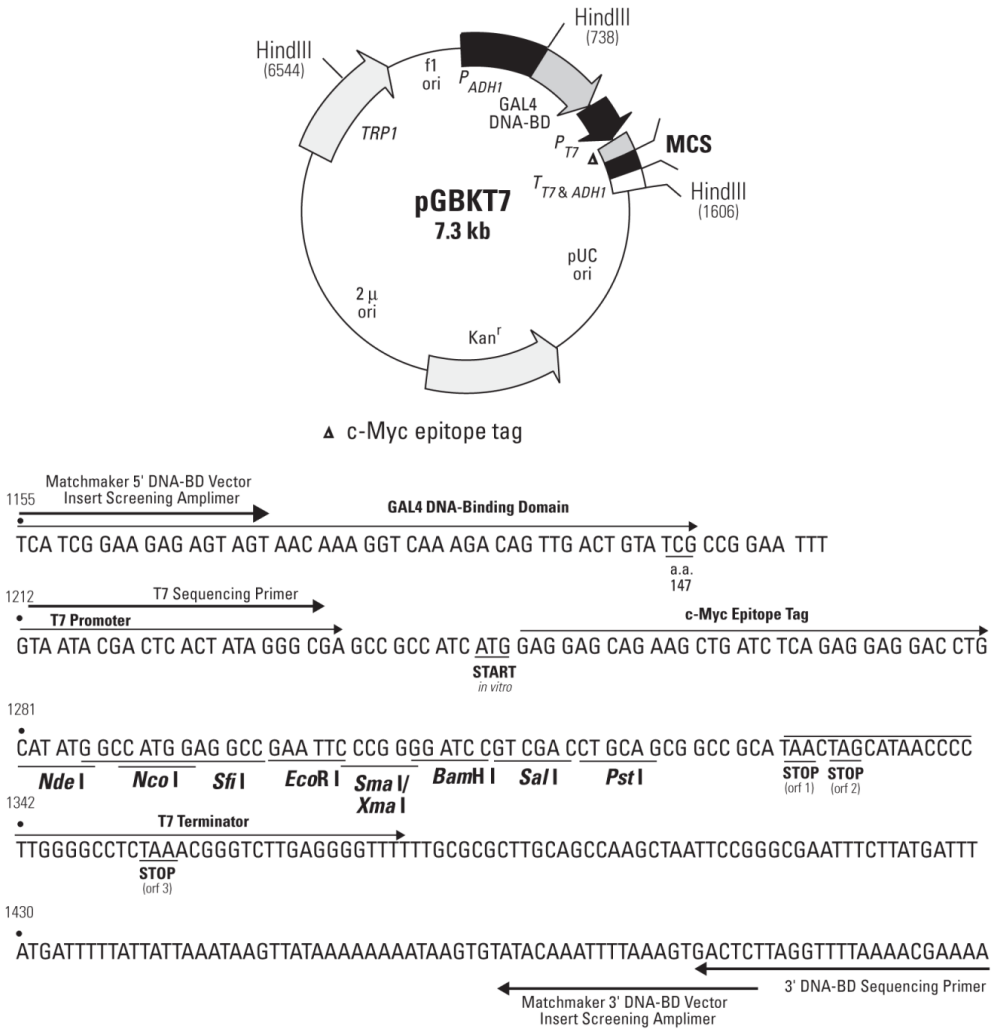

Figure 2.1 Map of pGBKT7 vector (Clontech)

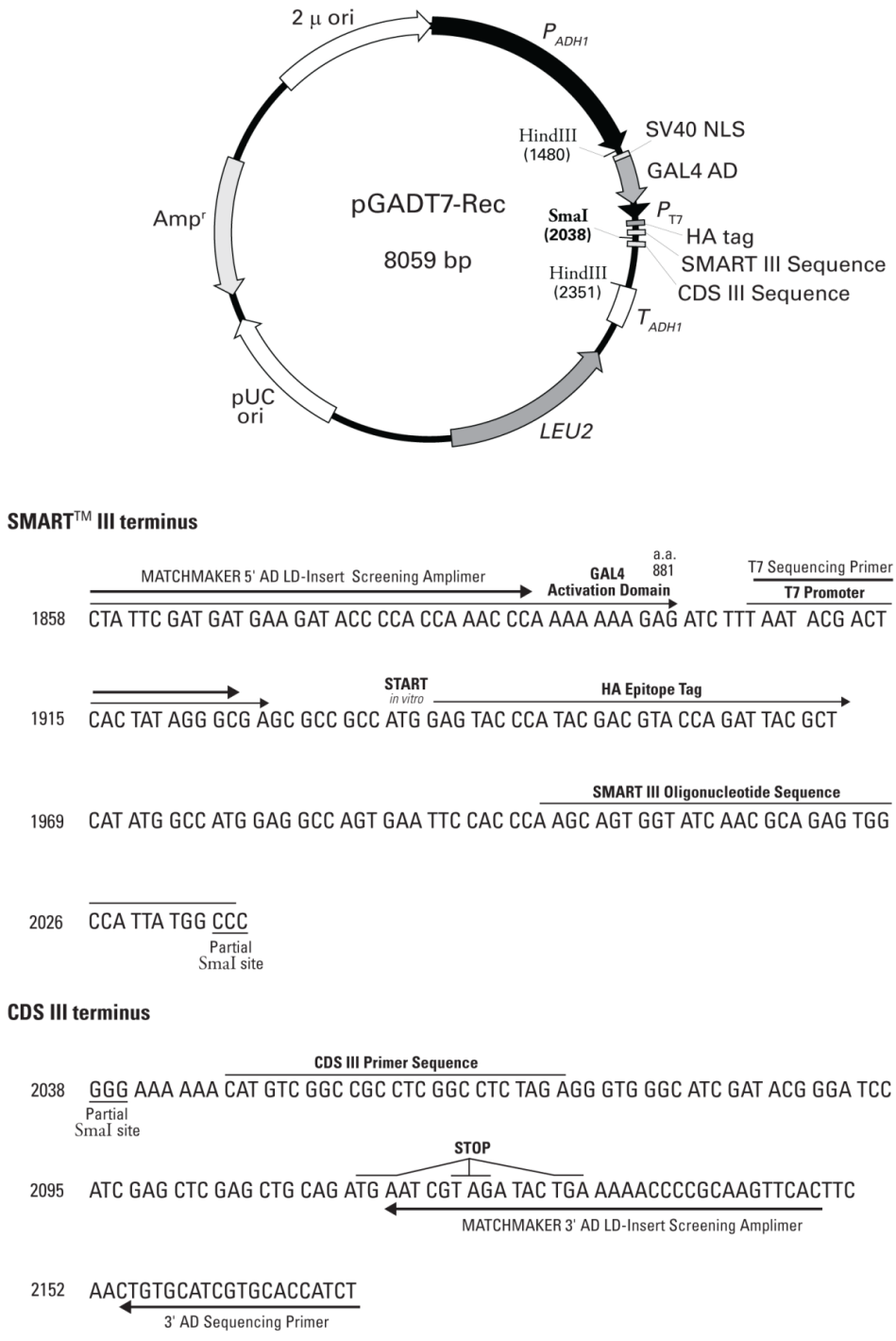

Figure 2.2 Map of pGADT7 vector (Clontech)

2.13.6. Confirmation of the protein-protein interaction by Co-immunoprecipitation

2.13.6.1. Recombinant *Pm*VRP15 protein expression

The freezing stock of *E. coli* stain C43 (DE3) containing recombinant plasmid pET22b^{+}-*Pm*VRP15 was streaked on LB-ampicillin (LB-amp) plate at 37 ℃ for overnight. The single colony was cultured in LB-amp medium with shaking at 250 rpm at 37 ℃ for overnight as a starter. The overnight culture was inoculated into fresh LB-amp medium until OD_{600} reached 0.5 then induced with IPTG to over-produce the r*Pm*VRP15. After 1 h of IPTG induction, the cell pellet was collected by centrifugation at 8,000 × g for 10 min, resuspended in 50 mM Tris-HCl, pH 7.0 and sonicated with a Bransonic 32 (Bandelin). Fraction containing r*Pm*VRP15 was collected by centrifugation at 10,000 rpm for 20 min. The soluble fraction collected was further centrifugated membrane protein part of *E. coli* including r*Pm*VRP15 by ultracentrifugation at 100,000 × g for 1 h and homogenized in ice-cold solubilization buffer (50 mM Tris-HCl, pH7.0, 20 mM Immidazole, 300 mM NaCl, 1% dodecyl-L-D-maltoside (DM) and 20% glycerol). The r*Pm*VRP15 was solubilized at 4℃ for overnight. The crude r*Pm*VRP15 protein was finally collected by ultracentrifugation at 100,000 × g for 30 min and subjected to purification through Nickle-NTA column (GE healthcare). The Ni-bead column was equilibrated in the equilibration buffer (50 mM Tris-HCl, pH 7.0, 20 mM Imidazole, 0.1% DM and 10% glycerol). Crude protein was loaded on to the column and incubated at 4 ℃ for up to 2 h. The unbound protein was discarded and the column was washed with washing buffer (50 mM Tris-HCl, pH 7.0, 50 mM Imidazole, 0.1% DM and 5% glycerol). The r*Pm*VRP15 was eluted by elution buffer (50 mM Tris-HCl, pH 7.0, 300 mM Immidazole, 0.1% DM and 5% glycerol). The eluted fraction was subjected to Amicon® Ultra-4 Centrifugal Filter Units cut-off 3 kDa (Millipore) dilution buffer (10 mM Tris-HCl, pH7.0, 0.07% DM and 2.5% glycerol) and concentrate the protein. The purified protein was analyzed using 15% SDS-PAGE (section 2.10.8.1). The concentration of protein was determined using the Bradford method (section 2.10.8.3).

2.13.6.2. Recombinant WSV399 protein expression in pBAD expression system

WSV399 gene was amplified by PCR using gene specific primer with *Xho*I and *EcoR*I restriction site, WSV399-*Xho*I-F: 5' CGCCTCGAGG-TTCCAGAAATGGTTTGAATCGTT 3' and WSV399-*Eco*RI-R: 5' GCCGAATTCGC-TTTGTTTGATAATACAATTTTCACCTTGT 3'. The PCR conditions were 94 °C for 1 min, followed by 30 cycles of 95 °C for 30 sec, 58 °C for 30 sec, and 72 °C for 30 sec, and then a final extension at 72 °C for 5 min using RBC *Taq* polymerase (RBC bioscience). The PCR products were analyzed by 1.5% (w/v) agarose gel electrophoresis and purified using Nucleospin® Extract II kit (Macherey-Nagel) as described in section 2.10.6. The purified PCR product was double digested with *Xho*I and *Eco*RI (New England Biolabs) and cloned into pBAD/*Myc*-His A (Invitrogen, Figure 2.3). The 20 µl ligation mixture contained 2 µl of 10X T4 ligation buffer, 50 ng of *Xho*I/*Eco*RI digested pBAD/*Myc*-His A vector, 40 ng of *Xho*I/*Eco*RI digested WSV399, and 1 µl of 400 U/µl T4 DNA ligase (New England Biolabs). The reaction was incubated at 4 °C for overnight. 10 µl of the ligation mixture was transformed into an *E. coli* TOP10 (invitrogen) using electro-transformation. The transformants were selected on LB agar plate with 100 µg/ml ampicillin. The recombinant plasmids were subjected to nucleotide sequencing to verify the sequences of inserts (Macrogen Inc., Korea).

The recombinant clone in the expression host was cultured and induced with L-arabinose (final concentration 0.1%) to over-produce the recombinant WSV399 (rWSV399). The rWSV399 protein was produced after L-arabinose induction at 4 h in *E. coli* TOP 10. The cell pellet was collected by centrifugation at 8,000 × g for 10 min, resuspended in 1X PBS, pH 7.4 and sonicated with a Bransonic 32 (Bandelin) for 4 min. The soluble protein was collected by centrifugation at 10,000 rpm for 20 min. The soluble form of rWSV399 was purified using Nickle-NTA column (GE healthcare). The Ni-bead column was equilibrated into equilibration buffer containing 50 mM Sodium phosphate buffer, pH 7.4, 300 mM NaCl, and 10 mM Imidazole. Crude protein was incubated Ni-NTA bead at room temperature for up to 2 h. Then the flow-through was discarded and the bead was washed with washing buffer (50 mM Sodium phosphate buffer, pH 7.4, 300 mM NaCl, and 20 mM Imidazole). The

r*Pm*VRP15 was eluted by elution buffer (50 mM Sodium phosphate buffer, pH 7.4, 300 mM NaCl containing 40, 80, 100, 250 and 500 mM Imidazole). The protein was analyzed using 12.5% SDS-PAGE (section 2.10.8.1). The concentration of protein was determined using the Bradford method (section 2.10.8.3). The purified protein from elution fractions was selected and dialyzed against 1X TBS, pH 7.4.

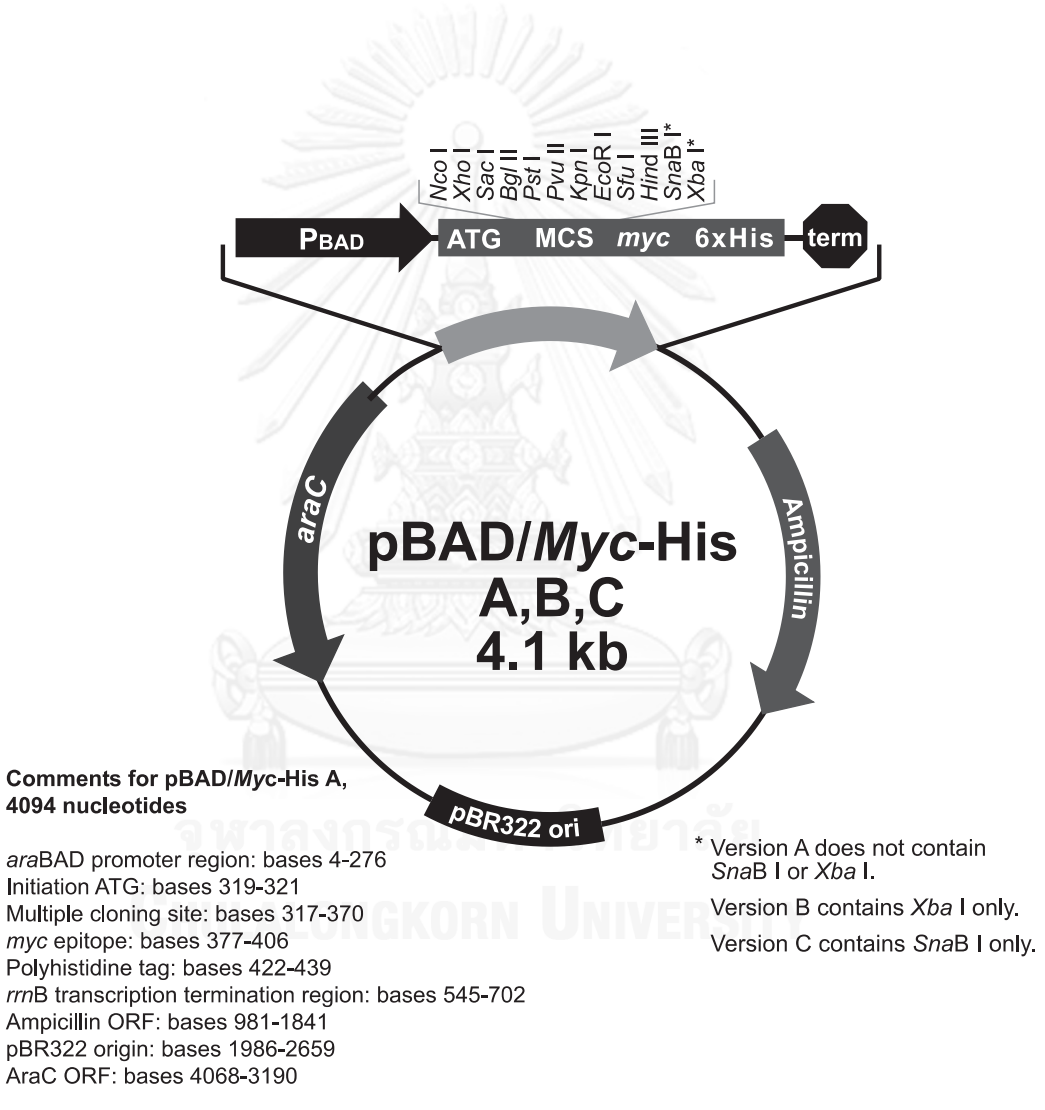

Figure 2.3 Map of pBAD/*Myc*-His A vector (Invitrogen)

2.13.6.3. Co-immunoprecipitation (Co-IP)

The co-immunoprecipitation experiment was performed according to instructions of the Pierce c-Myc Tag IP/Co-IP Kit (Thermo scientific). The interaction between WSV399 and *Pm*VRP15 was examined by incubating Myc-His-rWSV399 protein with His-r*Pm*VRP15 at 30 ℃ for 2 h with gentle rocking. Next, the anti-c-Myc antibody conjugated protein A bead (10 µl of 50% bed slurry) was incubated with mixture proteins between rWSV399 and r*Pm*VRP15 at 4 ℃ for overnight with gentle rocking. The beads were washed 10 times with 500 µl of Wash buffer (1X TBS) to remove non-specific binding protein. The SDS-loading sample buffer was mixed with the bead and heat at 100 ℃ for 15 min. The supernatant, which is the protein-protein complex, was collected by centrifugation. Then, protein-protein complex was analyzed by SDS-PAGE and western blot analysis. For detection of western blot experiment, the anti-c-Myc antibody (Clontech) and anti-His antibody (GE Healthcare) were used as primary antibodies. The first set of antibody detection, after transfer protein to nitrocellulose membrane and blocking, the anti-c-Myc antibody diluted 1:7,000 fold in 1X PBS-T buffer, was incubated with membrane at 37 ℃ for 3 h to detect rWSV399 protein. Then, secondary antibody, which is anti-IgG anti-mouse conjugated alkaline phosphatase (Jackson ImmunoResearch Laboratories, Inc.) (diluted 1:5,000 fold in 1X PBS-T buffer), was incubated at room temperature for 1 h. The band of rWSV399 was identified when NBT/BCIP solution, substrate of alkaline phosphatase enzyme were added. The second set of antibody detection was proceeded, after washing the membrane with 1X PBS-T for 3 times 15 min each, the anti-His antibody diluted 1:3,000 fold in 1X PBS-T was incubated with membrane at 37 ℃ for 3 h. This antibody can bind to r*Pm*VRP15 and rWSV399 proteins. Then, secondary antibody, which is anti-IgG anti-mouse conjugated alkaline phosphatase (diluted 1:7,000 fold in 1X PBS-T) was incubated at room temperature for 1 h. The bands of r*Pm*VRP15 and rWSV399 protein were identified using NBT/BCIP solution, substrate of alkaline phosphatase enzyme.

For control experiments, the anti-c-Myc antibody conjugated with protein A bead (10 µl of 50% bed slurry) was incubated with either r*Pm*VRP15 or rWSV399 and

followed the same steps. These controls were done simultaneously with the WSV399-*Pm*VRP15 interaction experiment.

2.14. Characterization of interacting protein (WSV399)

2.14.1. Recombinant WSV399 (rWSV399) expression in pET expression system for antibody production

2.14.1.1. Recombinant WSV399 plasmid construction

WSV399 ORF, whose size is 552 bp coding for 26 amino acid protein, was amplified by PCR using gene specific primer with *Nde*I and *Bam*HI restriction site, pET16b-WSV399-*Nde*I-F: 5' GCAGCCATATG-TTCCAGAAATGGTTTGAATC GT 3' and pET16b-WSV399-*Bam*HI-R: 5' GCAGCGGATCC-TTATTTGTTTGAT AATACAATTTTCACCT 3' and pGAD-T7 containing WSV399 ORF was used as a template. The PCR conditions were 94 °C for 2 min, followed by 30 cycles of 94 °C for 30 sec, 55 °C for 30 sec, and 68 °C for 30 sec, and then a final extension at 72 °C for 5 min using KOD *Taq* polymerase (TOYOBO). The PCR products were analyzed by 1.5% (w/v) agarose gel electrophoresis and purified using Gel/PCR DNA fragments extraction kit (Geneaid) as described in section 2.10.6. The purified PCR product was double digested with *Nde*I and *Bam*HI (New England Biolabs) and cloned into pET16b (Novagen®, Figure 2.4). The 10 µl ligation mixture contained 50 ng of *NdeI*/*Bam*HI digested pET16b vector, 40 ng of *NdeI*/*Bam*HI digested WSV399, and 5 µl of Ligation High Ver. 2 (TOYOBO). The reaction was incubated at 16 °C for 2 h. 5 µl of the ligation mixture was transformed into an *E. coli* DH5α (RBC Bioscience) using $CaCl_2$-transformation. The transformants were selected on LB agar plate with 100 µg/ml ampicillin. The recombinant plasmids were subjected to nucleotide sequencing to verify the sequences of inserts (MB mission biotech, Taiwan).

2.14.1.2. Recombinant WSV399 protein expression

The recombinant plasmid pET16b-WSV399 was transformed into expression host, *E. coli* BL21(DE3). The recombinant clone in the expression host was cultured

and induced with IPTG to over-produce the rWSV399. After 3 h incubation, the rWSV399 protein was over-produced. The cell pellet was collected by centrifugation at 8,000 × g for 10 min, resuspended in 1X PBS, pH 7.4 and sonicated with a Bransonic 32 (Bandelin) for 10 min. Inclusion bodies were collected by centrifugation at 10,000 rpm for 20 min to remove the supernatant liquid. The inclusion bodies were dissolved with 1.5% N-Lauroylsarcosine sodium salt (Sigma) in 1X PBS, pH 7.4. The crude rWSV399 was purified using Nickle-NTA bead (Qiagen). First, the Ni-bead was equilibrated with 1X PBS, pH 7.4 buffer after that the crude rWSV399 was incubated with Ni-bead. The bead was washed 10-column volume with 1X PBS, pH 7.4 buffer. The rWSV399 that bind with the Ni-bead and other protein fractions were analyzed by SDS-PAGE and western blot analysis. The concentration of protein was approximately determined by comparing with known amount of BSA standard protein on 12.5% SDS-PAGE. The rWSV399 protein was run onto SDS-PAGE. The expected size of rWSV399 is 26 kDa. The band corresponding to WSV399 protein was cut and sent to produce WSV399 antibody.

2.14.1.3. Antibody production

Mouse polyclonal antiserum against the purified r$(His)_6$-WSV399 protein (2 mg) was prepared commercially by Seeing Bioscience CO., LTD in Taipei, Taiwan R.O.C.

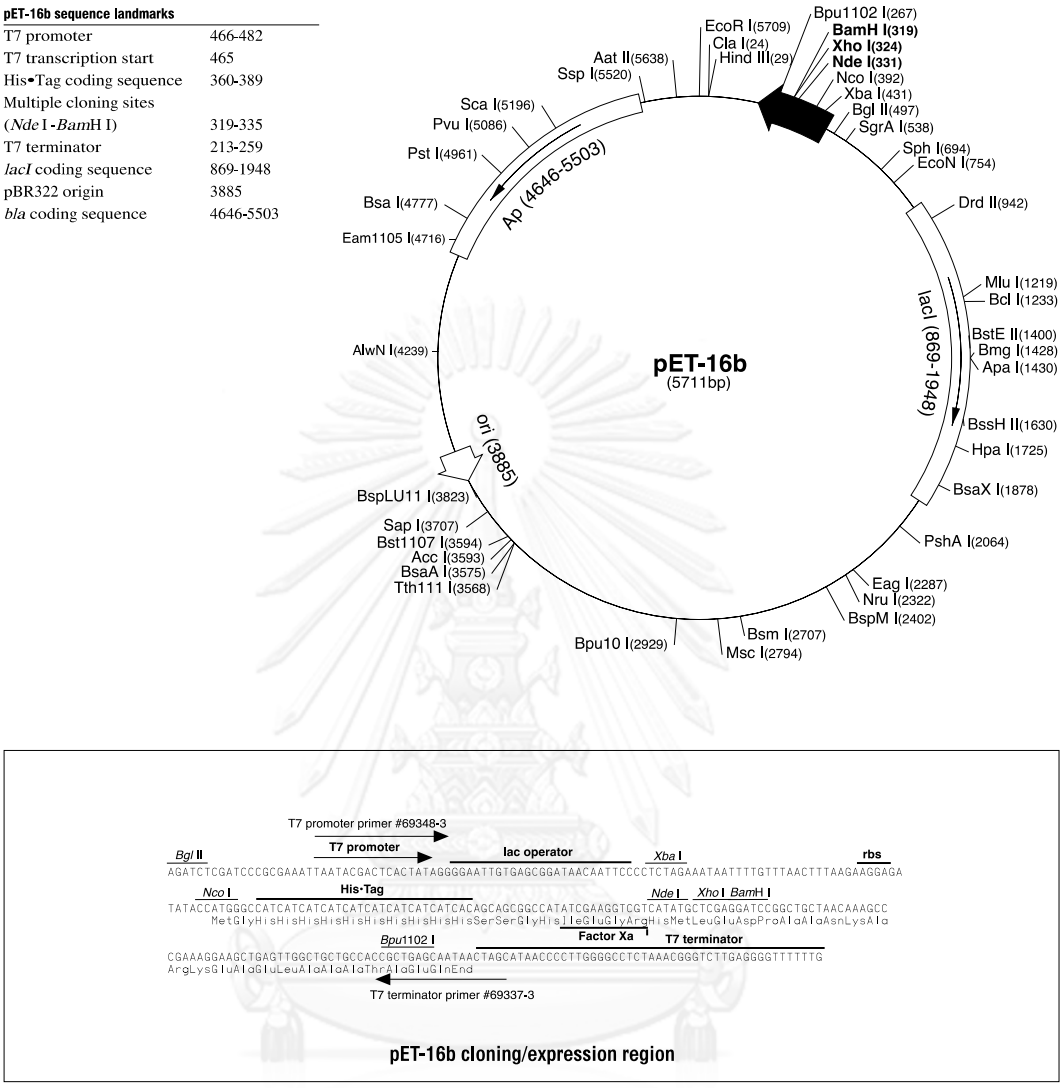

Figure 2.4 Map of pET16b vector (Novagen)

2.14.2. Localization of WSV399 protein on WSSV intact

2.14.2.1. Preparation and purification of WSSV intact

In this study, we used WSSV purified from crayfish, *Procambarus clarkia* prepared (Xie *et al.* 2005a). In brief, the crayfish, *P. clarkia*, (about 20-25 g) was acclimatized in freshwater at room temperature (25 °C). The virus stock, hemolymph of WSSV-infected shrimp *P. monodon*, was injected intramuscularly into healthy crayfish between the second and third abdominal segments. About 4-10 days post infection, WSSV-infected moribund crayfish were collected; all tissues excluding hepatopancreas and eye stock were homogenized for 2 min using homogenizer in TESP buffer (50 mM Tris-HCl, 5 mM EDTA, 500 mM NaCl, pH 8.5) containing 1 mM PMSF at the ratio of 1 g tissue: 10 ml TESP buffer and then centrifuged at 3,500 × g for 5 min. The pooled supernatant was filtered through nylon net (400 mesh) and centrifuged at 30,000 × g for 30 min. After the supernatant was discarded, the upper loose layer (pink pellet) of pellet was rinsed out carefully using a Pasteur pipette, and the lower compact layer (white pellet) was resuspended in TM buffer (50 mM Tris-HCl, 10 mM $MgCl_2$, pH 7.5). The virus suspensions were centrifuged at 3,000 × g for 5 min, and the supernatant was centrifuged again at 30,000 × g for 20 min. After the supernatant and pink loose layer were removed, the white pellet was resuspended in TM buffer containing proteinase inhibitor cocktail (Sigma), transferred to a 0.6 ml microcentrifuge tube and stored at -80 °C. The total protein of purified-WSSV was analyzed by 12.5% SDS-PAGE (section 2.10.8.1) and stained with Coomassie brilliant blue. The purity and intrigrity of the WSSV were evaluated by negative-staining transmission electron microscopy (TEM).

2.14.2.2. Preparation of the envelope and nucleocapsid fractions

To localize the WSV399 on WSSV virion, the purified WSSV was treated with TrironX-100 to separate envelope and nucleocapsid fractions of WSSV (Xie *et al.* 2006). In brief, the purified virus suspension was centrifuged at 20,000 × g for 30 min at 4 °C. The pellets were resuspended in TMN buffer (20 mM Tris- HCl, 150 mM NaCl,

2 mM $MgCl_2$, pH 7.5). Then, Triton X-100 was added to the final concentration of 1% and incubated at room temperature with gentle shaking for 30 min. Subsequently, the supernatant and pellet fractions were collected after centrifugation at 20,000 × g for 20 min at 4 °C. The supernatant was the envelope protein containing fraction. Then, the pellet was once again treated with TMN buffer containing 1% Triton X-100 as above. The resulting pellet was further rinsed with water to eliminate any residual supernatant solution and then resuspended in TMN buffer. The last fraction was nucleocapsid protein containing fraction. Finally, all samples were analyzed by SDS-PAGE stained with Coomassie brilliant blue.

2.14.2.3. Localization of WSV399 on purified-WSSV intact virion by immune-blot analysis

Ten micrograms of the purified WSSV virions were subjected to SDS-PAGE (section 2.10.8.1), and the separated proteins were then transferred to a polyvinylidene difluoride (PVDF) membrane. The membranes were incubated in blocking buffer containing 5% skim milk in 1X TBS-T (0.5% Tween 20 in Tris-buffered saline) at 4 °C overnight, followed by incubation with a purified polyclonal mouse anti-WSV399 antibody (1: 2,500 dilution in 2.5% skim milk, 1X TBS-T) for 3 h at room temperature. After the membrane was washed three times with TBS-T, it was incubated with a horseradish peroxidase-conjugated anti-mouse secondary antibody (Jackson ImmunoResearch Laboratories, Inc.) diluted 5,000-fold in 2.5% skim milk in 1X TBS-T for 1 h at room temperature. The membrane was washed as described above, and protein band specific to WSV399 was detected by a chemiluminescence reagent, Western Lightning® Plus-ECL, (Perkin-Elmer, Inc.) followed by exposure the membrane to film at the appropriate time. The result can be visualized after film exposure and development.

2.14.2.4. Localization of WSV399 on purified-WSSV intact virion by immuno electron microscopy

Following previous report (Leu *et al.* 2005), a purified WSSV virion (from section 2.14.2.1) suspension was adsorbed to Formvar-supported and carbon- coated nickel grids (150 mesh) and incubated for 5 min at room temperature. The primary antibody and preimmune mouse serum were diluted 1:50 in an incubation buffer (0.1% Aurion Basic-c, 15 mM NaN_3, 10 mM phosphate buffer, 150 mM NaCl, pH 7.4). The grids were blocked with the blocking buffer (5% bovine serum albumin, 5% normal serum, 0.1% cold water skin gelatin, 10 mM phosphate buffer, 150 mM NaCl, pH 7.4) for 15 min and then incubated with a diluted primary antibody or preimmune mouse serum for 3 h at room temperature. After several washes with incubation buffer, the grids were incubated with a goat anti-mouse secondary antibody conjugated with 18-nm-diameter gold particles (1:50 dilution in the incubation buffer) for 1 h at room temperature. The grids were then washed extensively with incubation buffer, washed twice more with distilled water to remove excess salt, and stained with 1% phosphotungstic acid (pH 7.2) for 2 min. Specimens were examined with a transmission electron microscope (TEM).

2.14.3. WSV399 gene expression profile in WSSV infected-shrimp hemocyte using RT-PCR technique

Semi-quantitative RT-PCR was used to examine the expression of interesting WSSV gene, WSV399, in WSSV-infected shrimp at various time points. *P. monodon* shrimp of approximately 15 g body weight were injected with 100 µl of the 10^{-5}-fold diluted WSSV solution (a dose that causes 100% mortality of shrimp in 5 dpi). Four WSSV-infected shrimp hemocytes were collected individually from four shrimp at 0, 3, 6, 12, 24, 36 and 48 hpi. Total RNA was extracted (section 2.10.9.1) and treated with RNase-free DNase (section 2.10.9.2) to remove any residual DNA contamination. Total RNA concentration was determined using spectrophotometer (section 2.10.9.3). An equal amount of DNA-free total RNA from three shrimp was pooled. One µg of DNase-free total RNA was used for the first strand cDNA synthesis using the RevertAid

First Strand cDNA Synthesis kit (section 2.10.9.4). To investigate the expression level of viral genes, which are ie-1 (immediate early gene), wsv477 (early gene), vp28 (late gene) and WSV399, RT-PCR was performed using gene specific primer, ie1-F/R, wsv477-F/R, vp28-F/R and wsv399-RT-F/R (Table 2.2). EF-1**α** gene as a reference gene was amplified using EF-1-F/R primers. One microliter of 5-fold diluted cDNA was used as a template for PCR amplification. The reaction contained 1X PCR buffer, 0.1 **μ**M each dNTP, 0.2 **μ**M primer each, 1.25 U RBC *Taq* polymerase (RBC Bioscience). The reaction was pre-denatured at 94 ℃ for 1 min and followed by 35 cycles of denaturation at 94 ℃ for 30 sec, annealing at 60 ℃ for 30 sec and extension at 72 ℃ for 30 sec, and final extension at 72 ℃ for 7-10 min. The PCR product was analyzed by 1.5% (w/v) agarose gel electrophoresis.

2.14.4. Expression of viral genes after WSV399 gene knockdown in WSSV-infected shrimp

The wsv399 dsRNA was prepared using WSV399-recombinant plasmid as a template for producing sense and anti-sense DNA templates of *in vitro* transcription as described in section 2.12.1. DNA templates containing the T7 promoter sequence at the 5′-end were generated by PCR using WSV399-T7-F and WSV399-R for the sense strand template, the other with WSV399-F and WSV399-T7-R (Table 2.1).

P. monodon shrimp of approximately 3 g body weight were divided into two groups of three individuals each. The first (control) group was injected with 10 μg/g shrimp of GFP-dsRNA, whilst the second and third groups were injected with 5 and 10 μg/g shrimp WSV399-dsRNA, respectively. After 24 h, 30 μl of the 10,000-fold diluted WSSV solution (a dose that causes 100% mortality of shrimps in 3 dpi) was injected into the respective group of shrimp. Hemocytes of individual shrimp were collected at 24 hpi and total RNA was extracted (section 2.10.9.1) and treated with RNase-free DNase (section 2.10.9.2) to remove any residual DNA contamination. Total RNA concentration was determined using spectrophotometer (section 2.10.9.3). An equal amount of DNA-free total RNA from three shrimp was pooled and 1 μg of total RNA was used for the first strand cDNA synthesis using the RevertAid First Strand cDNA Synthesis kit (section 2.10.9.4).

WSV399 gene expression was analyzed by RT-PCR. The wsv399-RT-F/R primers (Table 2.2) were used along with the EF-1**α** gene as an internal control using the EF-1-F/R primer pair (Table 2.2). The expression level of viral gene which is vp28, was determined by semi-quantitative RT-PCR using gene specific primer vp28-F/R (Table 2.2). The PCR conditions were 94 °C for 1 min, followed by 27 cycles of 95 °C for 30 sec, 58 °C (for EF-1**α**) or 60 °C (for wsv399 and vp28) 30 sec, and 72 °C for 30 sec, and then a final extension at 72 °C for 5 min. The PCR products were analyzed by 1.5% (w/v) agarose gel electrophoresis.

2.14.5. The effect of recombinant WSV399 on *Pm*VRP15 gene expression

P. monodon shrimp of approximately 5-7 g body weight were divided into three groups of four individuals each. The first (control) group was injected with buffer (20 mM Tris-HCl, pH 7.4), whilst the second and third groups were injected with 1 µg and 2 µg of rWSV399 (rWSV399 production was described in section 2.19.1.2), respectively. Hemocytes of individual shrimp were collected at 24 hpi and total RNA was extracted (section 2.10.9.1) and treated with RNase-free DNase (section 2.10.9.2) to remove any residual DNA contamination. Total RNA concentration was determined using spectrophotometer (section 2.10.9.3). An equal amount of DNA-free total RNA from three shrimp was pooled and 1 µg of total RNA was used for the first strand cDNA synthesis using the RevertAid First Strand cDNA Synthesis kit (section 2.10.9.4).

The *Pm*VRP15 gene transcript was identified by RT-PCR. The *Pm*VRP15-RT-F/R primers (Table 2.2) were used (100 nM) along with the EF-1**α** gene as an internal control using the EF-1-F/R primer pair (Table 2.2). The PCR conditions were 94 °C for 1 min, followed by 27 cycles of 95 °C for 30 sec, 58 °C for 30 sec, and 72 °C for 30 sec, and then a final extension at 72 °C for 5 min. The PCR products were analyzed by 1.5% (w/v) agarose gel electrophoresis.

2.15. Determination of genomic organization of *Pm*VRP15 gene

2.15.1. Extraction of *Penaeus monodon* shrimp genomic DNA

The genomic DNA of *P. monodon* was extracted from shrimp pleopods (swimming leg). Two to three pieces of the freezing shrimp swimming leg were mixed with extraction buffer (100 mM Tris-HCl, pH 9.0, 100 mM NaCl, 200 mM Sucrose and 50 mM Na_2EDTA, pH 8.0) and homogenized on ice. After that 10% SDS was added and incubated at 65 ℃ for 1 h. Proteinase K (50 ng/µl) was subsequently added and incubated continuously at 65 ℃ for another 3 h. Protein was precipitated after adding 5 M potassium acetate solution. After centrifugation at 12,500 x g 15 min, supernatant was transferred into a new microcentrifuge tube. The extracted DNA was treated with 1 µg of RNase A at 37 ℃ for 30 min. The contaminated-protein was removed by phenol: chloroform extraction. Genomic DNA was precipitated by adding 1/10 Vol. of 3 M sodium acetate, pH 5.2 and 2 Vol. of absolute ethanol. The pellet was washed with 75% ethanol. The pellet was air-dried and resuspended with TE buffer (10 mM Tris-HCl, pH 8.0, 1 mM EDTA, pH 8.0). Genomic DNA can be stored at 4 ℃ until used. The quality and quantity of genomic DNA were analyzed by running onto 1% agarose gel electrophoresis and measuring A_{260} using UV spectrophotometer.

2.15.2. Genomic organization of *Pm*VRP15 gene

To determine the organization of *Pm*VRP15 gene in genome, the primer pair specific to *Pm*VRP15 gene (ORF-*Pm*VRP15-F: ATGTTAACAGAGGACTTA and ORF-*Pm*VRP15-R: ATGCTCTACTGACATGTTGTG) were designed and used for amplification of genomic DNA by PCR. The PCR conditions were 94 ℃ for 2 min, followed by 30 cycles of 94 ℃ for 30 sec, 55 ℃ for 30 sec, and 68 ℃ for 30 sec, and then a final extension at 72 ℃ for 5 min using Advantage® 2 polymerase (Clontech). The PCR product was analyzed by 1% (w/v) agarose gel electrophoresis and the positive band was purified and cloned into T&A cloning vector (RBC Bioscience) and analyzed genomic DNA sequence (Macrogen Inc., Korea). The genomic sequence was then

compared to the *Pm*VRP15 cDNA sequences. The exon and intron regions of *Pm*VRP15 gene were identified (AG/GT method for distinguish between intron/exon).

2.16. Characterization of the *Pm*VRP15 promoter

2.16.1. Identification of the promoter of *Pm*VRP15 gene

2.16.1.1. Construction of *Penaeus monodon* genomic libraries

The promoter sequences of *Pm*VRP15 gene were identified using genome-walking technique. The genomic libraries were constructed using GenomeWalker universal kit (Clontech). *P. monodon* genomic DNA was completely digested by *Eco*RV, *Stu*I, *Pvu*II and *Dra*I respectively. The digested DNA was purified and ligated to Genomewalker adaptor to construct four genomic libraries of *P. monodon*. The genomic libraries were used as the template for PCR amplification.

2.16.1.2. Characterization of *Pm*VRP15 promoter sequence

In this experiment, we performed the genome walking for 2 times. For the first round genome walking, GSP1-1_*Pm*VRP15 and GSP2-1_*Pm*VRP15 were used. GSP1-2_*Pm*VRP15 and GSP2-2_*Pm*VRP15 were used for the second-round genome walking. These four gene-specific primers were designed according to the *Pm*VRP15 genomic sequence available (Table 2.4). Using each of four genomic DNA libraries as a template, primary PCRs were carried out with GSP1 and AP1 (adaptor primer, Clontech) as a primer. Secondary PCRs were performed using GSP2 and AP2 primer pair (adaptor nested primer, Clontech), using each primary PCR product as a template. The primary PCR condition was 94 ℃ for 2 min, followed by 30 cycles of 94 ℃ for 30 sec, 55 ℃ for 30 sec, and 68 ℃ for 30 sec, and then a final extension at 72 ℃ for 5 min. The PCR reaction contained 100 ng DNA template, 1x Advantage® 2 reaction buffer, 0.2 mM dNTP, 400 nM each primer and Advantage® 2 polymerase (Clontech). For nested-PCR condition was 94 ℃ for 2 min, followed by 30 cycles of 94 ℃ for 30 sec, 55 ℃ for 30 sec, and 68 ℃ for 30 sec, and then a final extension at 72 ℃ for 5 min. The PCR reaction was same as the primary PCR except that gene

specific primers, GSP1-2_*Pm*VRP15 and GSP2-2_*Pm*VRP15. The PCR products from the nested PCR were analyzed by 1% (w/v) agarose gel electrophoresis. The largest size of DNA fragment was purified from agarose gel by Nucleospin® Extract II kit (Macherey-Nagel) described in section 2.10.6. The purified DNA fragment was cloned into pGEM-T easy vector (Promega) and subjected to DNA sequencing (Macrogen Inc., Korea). The promoter sequences were then analyzed using freeware available e.g. Neural Network Promoter Prediction and Promoter 2.0 Prediction Server.

Table 2.4 List of primers used for genome walking experiment

Primer name	**Sequence (5'- 3')**
GSP1-1 *Pm*VRP15	AAGACGCCCAAGGGGCCCATATACAG
GSP2-1 *Pm*VRP15	TGAGACGAATGGTATGGAAGCGCACTGA
GSP1-2 *Pm*VRP15	TGTTCACTACGGGTGAGCCCACCCTGA
GSP2-2 *Pm*VRP15	TGGATTTTCTCGCATTTTCGAGGACTGCA
AP1	GTAATACGACTCACTATAGGGC
AP2	ACTATAGGGCACGCGTGG

2.16.2. Construction of the luciferase reporter plasmid containing the *Pm*VRP15 promoter

The promoter sequence of *Pm*VRP15 gene from -2047 to +612 position was cloned into pGL3-basic (Figure 2.5, Promega) which is the reporter plasmid containing the firefly luciferase gene for measuring promoter activity sequence required for. This recombinant plasmid was called the parental construction. The promoter sequences were narrowed down by PCR technique to identify the gene regulation of *Pm*VRP15 gene expression. For the narrow-down assay, several *Pm*VRP15 promoter constructs that contained the nucleotide position regions of -2047/+612, -1621/+612, -1147/+612, -907/+612, -727/+612, -525/+612, -427/+612, -387/+612, -287/+612, -208/+612, -92/+612 and -34/+612, were constructed. Each corresponding DNA fragment was amplified from *P. monodon* genomic DNA using the parental construct

as a template and specific primers containing restriction enzyme *Sac*I and *Xho*I at the 5' end of forward and reverse primers, respectively (Table 2.5). The PCR conditions were 94 °C for 2 min, followed by 30 cycles of 94 °C for 30 sec, 55 °C for 30 sec, and 68 °C for 30 sec, and then a final extension at 72 °C for 5 min using KOD *Taq* polymerase (TOYOBO). The PCR products from PCR were analyzed by 1% (w/v) agarose gel electrophoresis and purified by Gel/PCR DNA fragments extraction kit (Geneaid) as described in section 2.10.6. The purified PCR products cut with *Sac*I and *Xho*I were cloned in-frame into pGL3-basic vector, cut with the same restriction enzymes. For each construct, the 10 µl of ligation mixture contained 50 ng of *Sac*I/*Xho*I digested pGL3-basic vector, *Sac*I/*Xho*I digested *Pm*VRP15 promoter fragment, and 5 µl of Ligation High Ver. 2 (TOYOBO). The reaction was incubated at 16 °C for 2 h and 5 µl of the ligation mixture was transformed into an *E. coli* DH5-α (RBC Bioscience) using $CaCl_2$-transformation. The transformants were selected on LB agar plate with 100 µg/ml ampicillin. The recombinant plamid was extracted from the overnight culture of positive clones using High-speed plasmid mini kit (Geneaid) as described in section 2.10.5. The plasmid was double digested with restriction enzymes *Sac*I and *Xho*I and analyzed by 1% (w/v) agarose gel electrophoresis to confirm the existence of the insert. The constructed plasmids were subjected to nucleotide sequencing to verify the sequences of inserts (MB mission biotech, Taiwan). The pGL3 plasmids containing *Pm*VRP15 promoter regions, p(-2047/+612), p(-1621/+612), p(-1147/+612), p(-907/+612), p(-727/+612), p(-525/+612), p(-427/+612), p(-387/+612), p(-287/+612), p(-208/+612), p(-92/+612) and p(-34/+612) were purified using Qiagen plasmid mini kit (Qiagen). Plasmids were analyzed by 1% (w/v) agarose gel electrophoresis and measured plasmid concentration (A_{260}) and quality ($A_{260/280}$ and $A_{260/230}$) were examined by UV spectrophotometer before transfection.

Table 2.5 List of primers used to amplify *Pm*VRP15 promoter regions

Primer name	Sequence (5'-3')
promo-2047SacIF	5' CGCGGAGCTC-CCTAGATGGAAAGAAGAAAAAAAATACTTTTGA 3'
promo-1621SacIF	5' ACAGAGCTC-CCACTCAGGCCAGATGTGGTATACAGTT 3'
promo-1147SacIF	5' AGCGAGCTC-TGGGAGCTGCTCTTATCCAATGTGATGC 3'
promo-907SacIF	5' AGCAGGAGCTC-TGAGTCCGATGCTCTAACACTCG 3'
promo-727SacIF	5' AGCAGGAGCTC-GCTGAACCTGTGTTTTCTGCTTGT 3'
promo-427SacIF	5' AGCAGGAGCTC-TCACTCCTGCTCGGTTTTCC 3'
promo-525SacIF	5' TATGAGCTC-CCGTAGTGAACAGCTCCGGGTCTT 3'
promo-387SacIF	5' AGCAGGAGCTC-GTCGAGAGATTTTTTGTTGGGCATCA 3'
promo-208SacIF	5' AGCAGGAGCTC-ACCTATGCGCTGATAATGGCTT 3'
promo-287SacIF	5' AGCAGGAGCTC-TGAAGTATTTATATTTGTATTTTGTAACATTAATGA 3'
promo-92SacIF	5' GGCGAGCTC-CTTCAGGTTCAAGTGCAAAACGTCATCC 3'
promo-34SacIF	5' AGCAGGAGCTC-CTCAGTAATATAAAGCACAGTTCCCACG 3'
promo+612XhoIR	5' GCAGTCTCGAG-TGCGTAGCTAATGGGATGAGGA 3'

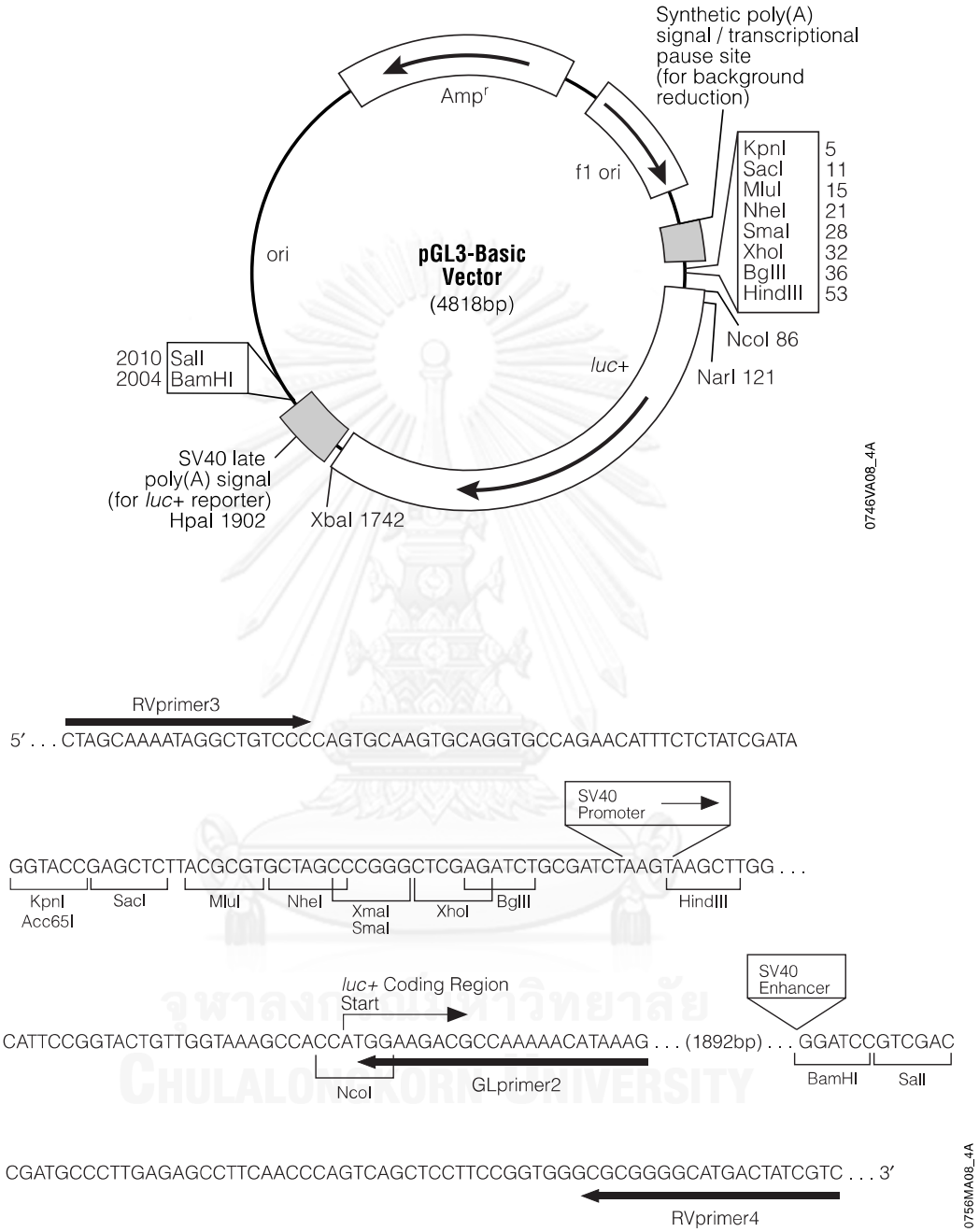

Figure 2.5 Map of pGL3-basic vector (Promega)

2.16.3. Promoter activity assay

Since no stable shrimp cell line was available, in this experiment, *Drosophila* Schneider 2 (S2) cell line, which is derived from hemocytes were used instead. For transfection experiment, S2 insect cells were seeded onto a 24-well plate (8×10^5 cells/well) and grown in the complete Schneider's Drosophila Medium containing 10% heat-inactivated FBS and antibiotic (50 units penicillin G and 50 µg streptomycin sulfate per milliliter of medium, Invitrogen) for overnight at 27 °C. The 200 ng of pGL3 plasmids containing *Pm*VRP15 promoter region or the pGL3-Basic, which was used as a negative control, were co-transfected with 5 ng of the Renilla luciferase plasmid phRL/AcMNPV *ie*1 into the S2 cells using the Effectene transfection reagent (Qiagen). The Renilla luciferase plasmid containing the Renilla luciferase reporter gene, was constructed by cloning the AcMNPV *ie*1 promoter into the phRL-null vector (Promega) (Liu *et al.* 2007) and it was used to monitor and normalize the transfection efficiency. Cells were collected at 60 h after transfection. The promoter activities were determined using Dual-Luciferase® Reporter Assay (Promega). Briefly, After 48 h post transfection, S2 cell was collected by centrifugation at 1,000 × g for 10 min at 4 °C and washed with 1X PBS buffer. The cell was lyzed with 1X PLB (Passive lysis buffer) and transfer to 96 well plate. The substrate of firefly luciferase, LARII solution, was added into well and then mixed. The firefly luciferase activity was determined by measuring the luminescence signal in Relative Luminescence Units (RLU) using SpectraMax M5 Multi-Mode Microplate Reader (Molecular device). After that Stop & Glo solution was added to stop the firefly luciferase activity and measure the luminescence signal of the Renilla luciferase activity. The RLU value of Firefly luciferase activity were normalized to that of the Renilla luciferase to correct for transfection efficiency, and data was expressed as the relative luciferase activity. Independent triplicate experiments were performed for each plasmid, and the mean and standard deviation (SD) were calculated.

2.16.4. Confirmation of the regulatory element by deletion assay

From the narrowed down promoter fragment experiment, the important parts of *Pm*VRP15 promoter that are required for *Pm*VRP15 gene expression were identified. The deletion construct of -525/-428 region was prepared using p(-727/+612) as a template and a primer pair; p(-727/+612) del(-525/-428)F and R (Table 2.6). The -287/-209 deletion plasmid, was constructed using p(-387/+612) as a template and primers such as p(-387/+612) del(-287/-209)F and R. The PCR conditions were 94 °C for 2 min, followed by 30 cycles of 94 °C for 30 sec, 55 °C for 30 sec, and 68 °C for 7 min, and then a final extension at 72 °C for 30 min using KOD *Taq* polymerase (TOYOBO). The PCR products were analyzed by 1% (w/v) agarose gel electrophoresis and purified by Gel/PCR DNA fragments extraction kit (Geneaid) as described in section 2.10.6. The 10 µl ligation mixture contained the purified PCR product of p(-727/+612) del(-525/-428) or p(-387/+612) del(-287/-209) fragments and 5 µl of Ligation High Ver. 2 (TOYOBO). The reaction was incubated at 16 °C for 2 h. An aliquot of 5 µl ligation mixture was transformed into an *E. coli* DH5α (RBC Bioscience) using $CaCl_2$-transformation. The transformants were selected on LB agar plate with 100 µg/ml ampicillin. The plasmid was extracted from positive clones using High-speed plasmid mini kit (Geneaid) as described in section 2.10.5. The constructed plasmids were subjected to nucleotide sequencing to verify the sequences (MB mission biotech, Taiwan). The promoter activity of p(-727/+612) del(-525/-428) or p(-387/+612) del(-287/-209) was compared with p(-727/+612) or p(-387/+612), respectively, using Dual-Luciferase® Reporter Assay (Promega) as described in section 2.21.3.

Table 2.6 List of primers used to study promoter deletion assay

Primer name	Sequence (5'-3')
p(-727/+612) del(-525/-428)F	5' TCACTCCTGCTCGGTTTTCCCGCC 3'
p(-727/+612) del(-525/-428)R	5' GTGAGCCCACCCTGACCCCAGGT 3'
p(-387/+612) del(-287/-209)F	5' ACCTATGCGCTGATAATGGCTTT 3'
p(-387/+612) del(-287/-209)R	5' AAAAGTATGTAAAATTAGATACTAACGCTTCTTATC 3'

2.16.5. Predication of transcription factor binding site on *Pm*VRP15 promoter fragments by bioinformatics approach

Upon the identification of *Pm*VRP15 promoter regulatory sequence, the transcription factor binding sites that are located on that sequences were predicted by programs TF search Ver.1.3, Match 1.0 (TRANSFAC® Public database) and Alibaba (TRANSFAC® Public database) programs. The results were confirmed by comparing with JASPAR database to confirm DNA sequence of the transcription factor binding site.

2.16.6. Identification of transcription factor regulating *Pm*VRP15 gene expression by site-directed mutagenesis technique

The predicted transcription factor binding sites of *Pm*VRP15 promoter were mutated to confirm the importance of the transcription factor binding site in regulatory *Pm*VRP15 gene expression. A pair of specific primer was designed for site-directed mutagenesis of each transcription factor binding site on *Pm*VRP15 promoter. From prediction results, the (-525/-427) promoter fragment has many transcription factor binding sites including Myb binding site (-517/-511), Rel binding site (-508/-499), IRF binding site (-484/-476) and NFYB binding site (-480/-427). The (-287/-209) promoter fragment also has many transcription factor binding sites including Oct-1 at -275/-268 position, C/EBP at -268/-260 position, NFAT at -229/-224 position and Ubx at -257/-252 position. The mutated constructs of these transcription factor binding sites were prepared by rolling PCR using their specific primers (Tables 2.7 and 2.8). The PCR conditions were 94 °C for 2 min, followed by 30 cycles of 94 °C for 30 sec, 55 °C for 30 sec, and 68 °C for 7 min, and then a final extension at 72 °C for 30 min using KOD *Taq* polymerase (TOYOBO). The PCR products were analyzed by 1% (w/v) agarose gel electrophoresis and purified by Gel/PCR DNA fragments extraction kit (Geneaid) as described in section 2.10.6. The 10 µl ligation mixture containing mutated-*Pm*VRP15 promoter fragment and 5 µl of Ligation High Ver. 2 (TOYOBO) was incubated at 16 °C for 2 h. Five microliters of the ligation mixture was transformed into an *E. coli* DH5α (RBC Bioscience) using $CaCl_2$-transformation. The transformants

were selected on LB agar plate containing 100 µg/ml ampicillin. The plasmid extracted from positive clones were extracted using High-speed plasmid mini kit (Geneaid) as described in section 2.10.5 and subjected to nucleotide sequencing to verify the sequences (MB mission biotech, Taiwan). The promoter activity of mutated-transcription factor binding site construct were measured and compared with wild type *Pm*VRP15 promoter plasmid using Dual-Luciferase® Reporter Assay (Promega) as described in section 2.16.3.

Table 2.7 List of primers used for site-directed mutagenesis of transcription factor binding sites on *Pm*VRP15 promoter region, p(-525/+612)

Name	Sequence (5'-3')
p(-525/+612)muC/EBP_F	5' CTTAAACCGTACGGGTCTGA 3'
p(-525/+612)muC/EBP_R	5' CCATTGATAGAGCGCGATCT 3'
p(-525/+612)muPU.1_F	5' ACCATGAAACCGATAGATCGC 3'
p(-525/+612)muPU.1_R	5' GAATTGTAGTGAAAGACCCGGA 3'
p(-525/+612)muMyb_F	5' ATTTCCGGGTCTTTCACTACAAAAGAGGATG 3'
p(-525/+612)muMyb_R	5' GCGCACTACGGGAGCTCGGTA 3'
p(-525/+612)muRel_F	5' TGGCACTACAAAAGAGGATGAAACC 3'
p(-525/+612)muRel_R	5' GATTCGGAGCTGTTCACTACGGG 3'
p(-525/+612)muIRF_F	5' CAATAGATCGCGCTCTATCTTTGGC 3'
p(-525/+612)muIRF_R	5' GCGTCATCCTCTTTTGTAGTGAAAGA 3'
p(-525/+612)muNFYB_F	5' GCAAGATCGCGCTCTATCTTTGG 3'
p(-525/+612)muNFYB_R	5' GATTTCATCCTCTTTTGTAGTGAAAGACCC 3'

Table 2.8 List of primers used for site-directed mutagenesis of transcription factor binding sites on *Pm*VRP15 promoter region, p(-287/+612)

Name	**Sequence (5'-3')**
p(-287/+612)muOct-1_F	5' ATCGTTTGTAACATTAATGATAATGTCA 3'
p(-287/+612)muOct-1_R	5' TACGATAAATACTTCAGAGCTCGG 3'
p(-287/+612)muC/EBP_F	5' ATGGCATTAATGATAATGTCATATAATCTT 3'
p(-287/+612)muC/EBP_R	5' AAGGTACAAATATAAATACTTCAGAGCTCG 3'
p(-287/+612)muNFAT_F	5' GGAAAGAAATGAGAATAAACCTATGC 3'
p(-287/+612)muNFAT_R	5' TAATTCTAAAGATTATATGACATTATCATTAATG 3'
p(-287/+612)muUbx_F	5' CAATAATGTCATATAATCTTTAGAAGGAAAAAAG 3'
p(-287/+612)muUbx_R	5' TCGATGTTACAAAATACAAATATAAATACTTCA 3'

CHAPTER III
RESULTS

3.1. Antibacterial mechanism of ALF*Pm*3

From a previous report, recombinant ALF*Pm*3 (rALF*Pm*3) protein exhibits antimicrobial activity against both Gram-negative and Gram-positive bacteria as well as fungi and can bind to the main bacterial cell wall components of Gram-negative and Gram- positive bacteria, LPS and lipoteichoic acid (LTA), respectively (Somboonwiwat *et al.* 2008). The high antimicrobial activity against *Vibrio harveyi* of rALF*Pm*3 suggests its potential use in the control or prevention of outbreaks of vibriosis in shrimp farming (Somboonwiwat *et al.* 2005). Indeed, rALF*Pm*3 has been reported to be able to completely neutralize *V. harveyi* infection in shrimp (Ponprateep *et al.* 2009).

In contrast to other AMPs, the antibacterial mechanism of shrimp AMPs so far remains largely unknown. In this research, the effects of ALF*Pm*3 against *V. harveyi* were investigated. We confirmed the localization of ALF*Pm*3 on the *V. harveyi* cells *in vivo* and then the membrane permeabilization of *V. harveyi* after treatment with rALF*Pm*3. The morphology and ultrastructure of rALF*Pm*3-treated bacteria were observed by scanning electron microscopy (SEM) and transmission electron microscopy (TEM), respectively.

3.1.1. Expression and purification of the recombinant protein ALF*Pm*3 (rALF*Pm*3) in yeast, *Pichia pastoris*

To study the effect of ALF*Pm*3 on *Vibrio harveyi*, the rALF*Pm*3 protein was over-produced in yeast, *Pichia pastoris*. After induction, the crude rALF*Pm*3 protein secreted into BMMY medium were analysed by 15% SDS-PAGE and silver staining. The expected size of rALF*Pm*3 at about 11 kDa was shown in Figure 3.1. The antimicrobial activity assay of the crude protein against *Escherichia coli* 363 was performed to check the efficiency of rALF*Pm*3. Afterwards, the crude protein was

purified by cation exchange chromatography, SP Sepharose High Performance column. As expected, the purified rALF*Pm*3 protein was eluted by high salt buffer containing 20 mM Tris-HCl, pH 7.4 and 1 M NaCl. The purity of rALF*Pm*3 was verified by 15% silver stained- SDS-PAGE (Figure 3.2). The antimicrobial activity of the purified rALF*Pm*3 was analyzed. Dialysis against steriled- distilled water was performed to desalt the purified protein. The purified rALF*Pm*3 was concentrated by lyophilyzation. The total purified ALF*Pm*3 protein obtained for this batch was approximately 1.7 mg. Prior to use for further investigation, the MIC values of ALF*Pm*3 against *E. coli* 363 and *V. harveyi* 639 were confirmed.

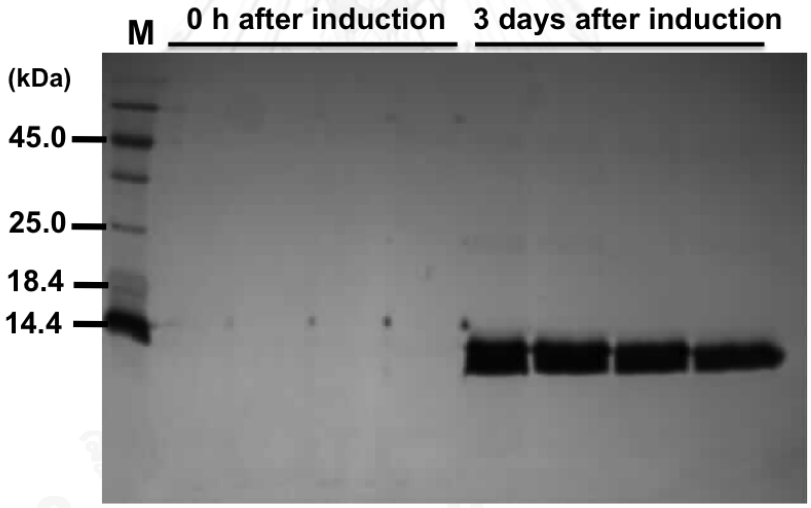

Figure 3.1 The silver stained- 15% SDS-PAGE of rALF*Pm*3 expression from *Pichia pastoris.* The crude rALF*Pm*3 was analyzed at 0 and 3 days after induction. Lane M: unstained protein marker (Fermentas).

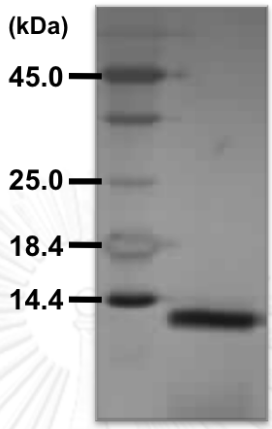

Figure 3.2 The silver stained- 15% SDS-PAGE of the purified rALF*Pm*3. Lane M: unstained protein marker (Fermentas).

To confirm the activity of rALF*Pm*3, the antimicrobial activity against *E. coli* 363 was determined. The purified-rALF*Pm*3 showed high activities against *E. coli* 363. The MIC value against *E. coli* 363 is 0.095–0.19 μM as the same with previous report (Somboonwiwat et al., 2008). In the present study, the antibacterial action of rALF*Pm*3 on a shrimp pathogenic bacterium, *V. harveyi* 639, was investigated. Prior to the experiments on the antibacterial activity on *V. harveyi* 639 cells, the MIC value and the binding capacity of ALF*Pm*3 on *V. harveyi* 639 were first determined. The MIC value of purified rALF*Pm*3 against *V. harveyi* 639 was found to be 0.78–1.56 μM and so for calculating the fold-MIC value for subsequent experiments a MIC value of 1.5 μM was used. To study the effect of ALF*Pm*3 on *V. harveyi* cells, multiple complementary assays carried out under quite different experimental conditions were used. Here, we performed all assays at the peptide concentrations that were related to their MIC value, always using the same culture medium (TSB broth) and the same bacterial density. Therefore, the results of the different experiments can be compared.

3.1.2. Immunolocalization of rALF*Pm*3 on *V. harveyi* 639 cells *in vivo*

To visually illustrate how the rALF*Pm*3 interacted with bacterial cells, the *V. harveyi* cells were incubated with the rALF*Pm*3 at a MIC and the bound rALF*Pm*3 was detected by immunocytochemistry using the Polyclonal antibody specific to rALF*Pm*3 and alkaline phosphatase conjugated secondary antibody (Figure 3.3). The positive cells were stained dark purple as compared to the untreated control cells (Figure 3.3A). The dark purple staining demonstrated the localization of rALF*Pm*3 on the *V. harveyi* cells (Figure 3.3B).

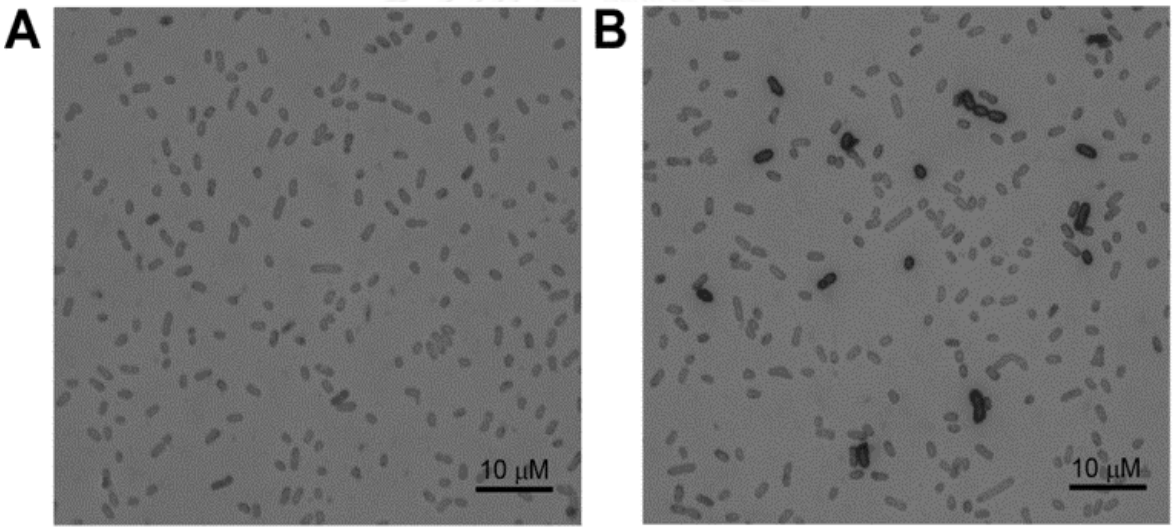

Figure 3.3 Immunolocalization of rALF*Pm*3 on *Vibrio harveyi* 639 cells. The cells were incubated in PBS with a (A) 0- (negative control) or (B) 1-fold MIC (1.5 μM) of rALF*Pm*3 for 10 min, and then probed with anti-rALF*Pm*3 PcAb and AP-conjugated secondary Ab with NBT/BCIP detection.

3.1.3. Analysis of the bacterial membrane permeabilization activity of ALF*Pm*3

The ability of ALF*Pm*3 to bind to the cell wall and membrane component of bacterial cell led us to suspect that the ALF*Pm*3 might be able to penetrate the membrane of *V. harveyi*. There are two layers of membrane in *V. harveyi*; an outer membrane made up of lipopolysaccharides and an inner cytoplasmic membrane. In order to investigate that, NPN uptake assay was performed to study *V. harveyi* outer membrane permeabilization and *E. coli* MG1655, the lactose permease deficient stain, was used instead to study inner membrane permeabilization. Moreover, we have confirmed the inner membrane permeabilizing activity of rALF*Pm*3 on *V. harveyi* cell by measuring the total nucleotide leakage.

3.1.3.1. Permeabilization of *V. harveyi* outer membrane by rALF*Pm*3

We first tested the ability of the rALF*Pm*3 to permeabilize the *V. harveyi* outer membrane, the NPN was used as a probe for the outer membrane integrity. If the outer membrane is disrupted, the NPN is able to penetrate the membrane then strongly fluoresces in the hydrophobic environment of a biological membrane but has a low fluorescence in an aqueous environment. Therefore, the NPN probe was used to demonstrate the permeabilization of the bacterial outer membrane. The membrane permeabilization, as shown by the increasing fluorescent intensity due to the NPN uptake, was clearly evident in *V. harveyi* cells treated with rALF*Pm*3 compared to the control. The results suggested that the outer membrane of *V. harveyi* was permeabilized by rALF*Pm*3 in an almost linearly dose-dependent manner (Figure 3.4).

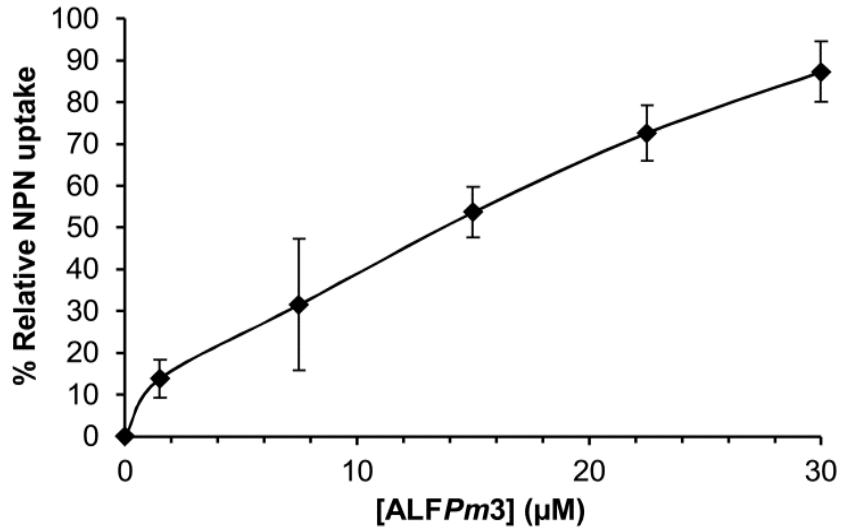

Figure 3.4 *Vibrio harveyi* permeabilization activity of rALF*Pm*3 by NPN uptake assay. The increase in fluorescence intensity (NPN uptake) in *V. harveyi 639* cells treated with various doses of rALF*Pm*3 (0- to 20- fold MIC, or 0 – 30 μM), expressed as relative to that seen with 0.01% (v/v) Triton X-100 permeabilized cells (set at 100%). Data are shown as the mean ± 1 SD and are derived from three independent repeats.

3.1.3.2. Permeabilization of *E. coli* inner membrane by rALF*Pm*3

The inner membrane permeabilization was investigated using the *E. coli* MG 1655 isolate that lacks lactose permease, an enzyme that functions in uptaking lactose from the outside media into the bacterial cell, using ONPG as the chromogenic substrate for the β- galactosidase activity assay. This Gram-negative bacterium (*E. coli*) is also known to be bound and be killed by rALF*Pm*3 and so was used in place of *V. harveyi* due to the absence of lactose permease deficient *V. harveyi* strains. The ONP produced upon cleavage of ONPG by β-galactosidase was detected spectrophotometrically as the A_{405} value. In the case that the inner membrane of *E. coli* was permeabilized by the rALF*Pm*3, the β-galactosidase activity would be detected outside the bacterial cell. After exposure to rALF*Pm*3 a rapid

increase in the A_{405} value (β-galactosidase activity) in the supernatant was observed from 0 to 60 min and thereafter remained almost the same (Figure 3.5). This result suggested that the rALF*Pm*3 rapidly permeabilized the inner membrane of *E. coli*.

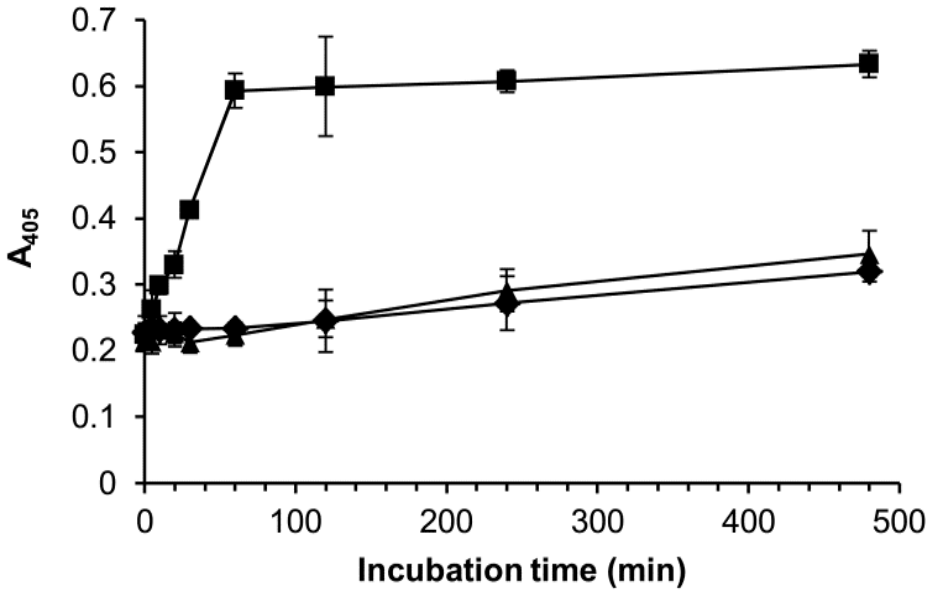

Figure 3.5 Kinetics of the membrane permeabilization of *E. coli* MG1655 cells by rALF*Pm*3. The induced *E. coli* MG1655 cells were incubated in PBS buffer alone (♦) or supplemented with either 0.5 μM rALF*Pm*3 (■) or 0.5 μM BSA (▲), for the indicated time. The supernatant was then collected and measured for β-galactosidase activity by determining the level of ONG formed from ONPG by measuring the absorbance at 405 nm. Data are shown as the mean ± 1 SD and are derived from three independent repeats.

3.1.3.3. Permeabilization of *V. harveyi* inner membrane by rALF*Pm*3

Given the rapid permeabilization of the bacterial inner cell membrane, we explored whether the loss of the membrane integrity resulted in the leakage of cytoplasmic contents leading to cell death. To this end, the leakage of cytoplasmic contents from *V. harveyi* 639 cells was determined by measuring the total (principally) nucleotide leakage as the increase in the A_{260} value. The total nucleotide

leakage (A_{260}) increased after exposure to rALF*Pm*3 in a concentration- and time-dependent manner, reaching the maximal level after around 60 min of exposure time for all three tested rALF*Pm*3 concentrations (Figure 3.6). Thus, it is likely that rALF*Pm*3 binds to the bacterial membrane, permeabilizes the inner membrane and leads to the leakage of the cytoplasmic contents resulting in bacterial death.

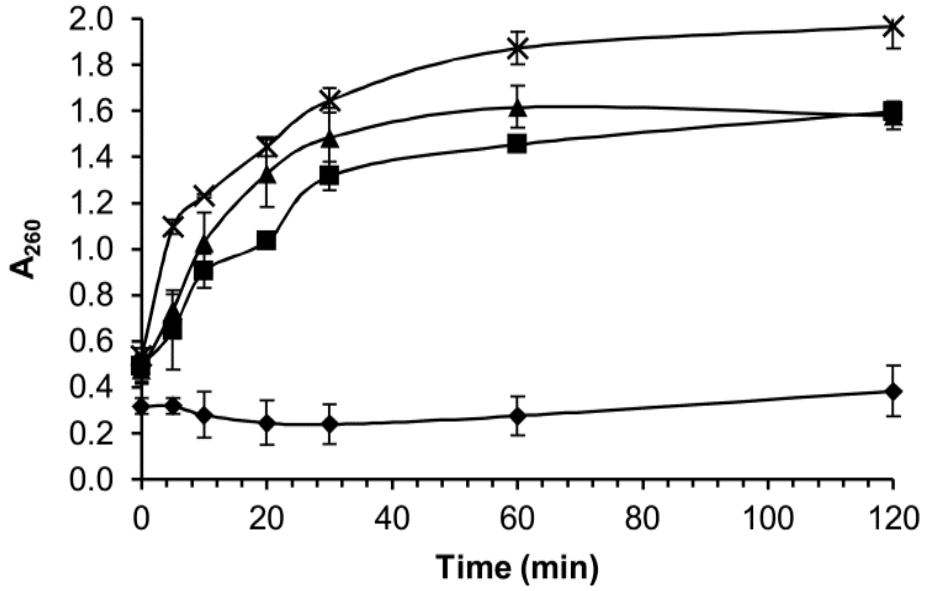

Figure 3.6 Total nucleotide leakage assay. The leakage of cytoplasmic contents of *V. harveyi* was detected in terms of the increased nucleotide level, evaluated as the absorbance at 260 nm, after incubation with a 0- (control) (♦), 0.5- (■), 1- (▲), and 2-fold MIC (3.0 μM) (✕) of rALFPm3 in PBS buffer for the indicated time periods. Data are shown as the mean ± 1 SD and are derived from three independent repeats.

3.1.4. Observation of the morphological structure and the ultrastructure of *V. harveyi* after ALF*Pm*3 treatment using electron microscopy

3.1.4.1. Scanning electron microscopy (SEM)

The previous results suggested that rALF*Pm*3 could permeabilize the inner bacterial membrane leading to cytoplasmic content leakage and bacterial cell death. Here, SEM was performed to investigate the morphological changes in *V. harveyi* cells after exposure to rALF*Pm*3. At low concentration (a MIC or 1.5 μM), the morphological changes of *V. harveyi* cell membrane were observed (Figures 3.7-3.8). Compared to the control (Figure 3.7A), rALF*Pm*3-induced blebs started to form and protruded from the microbial surface (Figure 3.7B). Shrinkage of the bacterial cell was also observed, which might be caused by leakage of the cytoplasmic content (Figure 3.7C). Finally, the bacterial cell was lysed leaving ghost cells and cell debris (Figure 3.7D). SEM images of *V. harveyi* cells after treatment with 10- fold MIC (15 μM) of rALF*Pm*3 showed the bactericidal effect of ALF*Pm*3 on *V. harveyi* cells that were visibly lysed and damaged (Figure 3.8).

3.1.4.2. Transmission electron microscopy (TEM)

The effect of rALF*Pm*3 on the ultrastructure of *V. harveyi* cells was determined by TEM. The bacterial cells were treated with rALF*Pm*3 at five times the MIC (7.5 μM) for 1 h, fixed, negative stained with uranyl acetate and then visualized under TEM (Figure 3.9). The dark areas indicate a high electron density, whereas the light areas indicate a low electron density. Similar to that observed by the SEM, the control cells were uniformly shaped with an intact cell membrane (Figure 3.9A), whereas several distinct signs of damage on the bacterial membrane were clearly observed by TEM. On the rALF*Pm*3-treated cells, the loss of membrane integrity (Figure 3.9B), the presence of blebs protruding from bacterial surface (Figure 3.9C), the potential pore formation indicated by the absence of staining of some parts of the bacterial membrane (Figures 3.9C and D), and with ghost-like cells, were evident (Figure 3.9D).

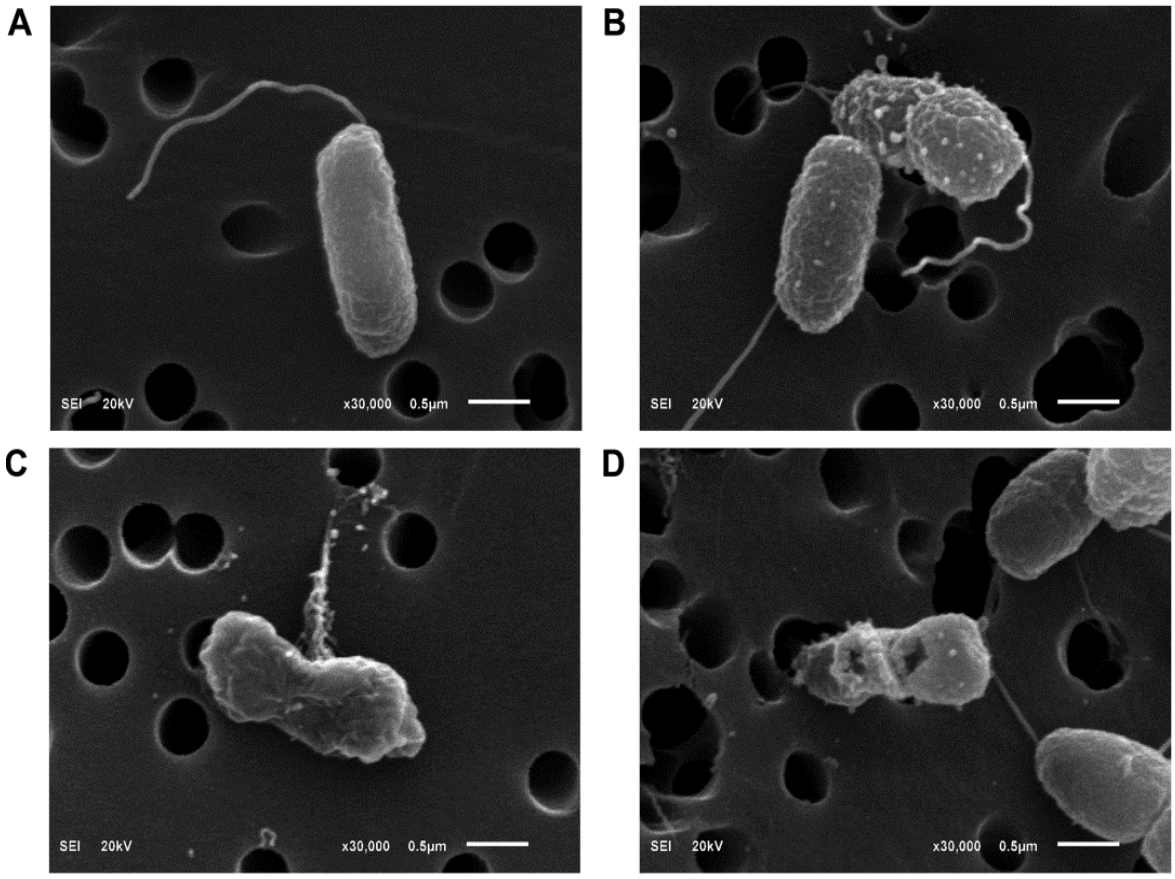

Figure 3.7 Representative SEM micrographs of *Vibrio harveyi* cells after incubation with (A) 0 µM (control) or (B-D) a 1-fold MIC (1.5 µM) of rALF*Pm*3 in PBS buffer. When exposed to rALF*Pm*3 many distinct signs of cell damage were clearly observed, such as (B) bleb formation, (C) cytoplasmic content leakage and (D) lysed cells.

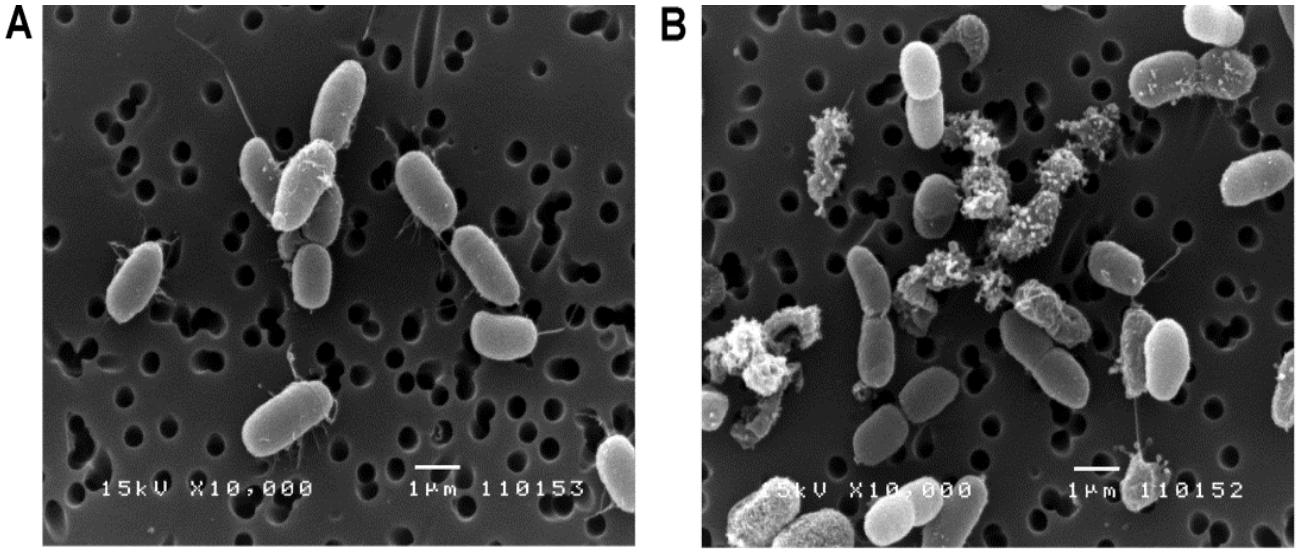

Figure 3.8 Representative SEM micrographs of the *Vibrio harveyi* cells after incubaion with rALF*Pm*3. *V. harveyi* cells were treated with (A) 0 µM (control) or (B) a 10-fold MIC (15 µM) of rALF*Pm*3 in PBS buffer immediately.

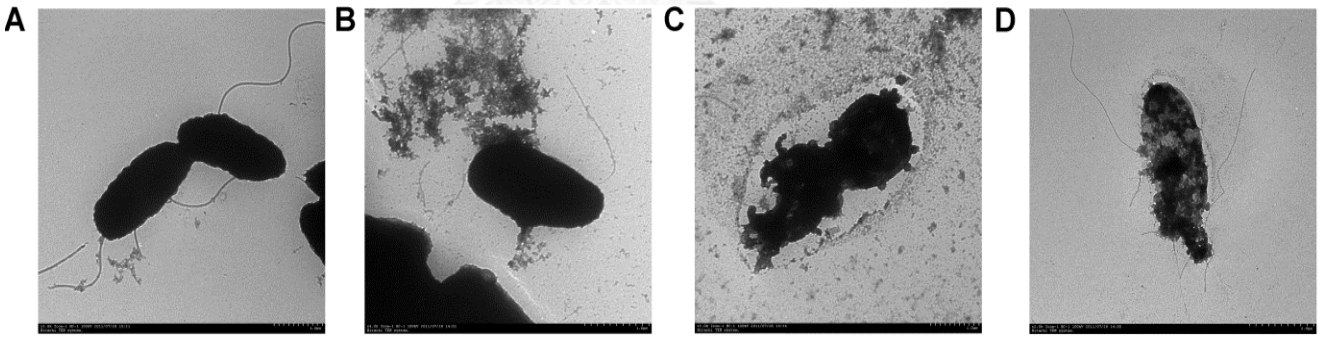

Figure 3.9 Representative TEM micrographs of ALF*Pm*3- treated *Vibrio harveyi* cells. The control was cell incubated in PBS alone (A) for 1 h. *V. harveyi* cells treated with a 5-fold MIC (7.5 µM) of rALF*Pm*3 (B-D) were observed at 1 h after incubation. The rALF*Pm*3 treated cells showed different ultrastructural changes, such as (B) cytoplasmic leakage, (C) bleb formation and (D) ghost-like appearance.

3.2. Functional characterization and gene regulation of *Pm*VRP15 gene

3.2.1. Determination of *Pm*VRP15 gene and protein expression after *Pm*VRP15 knockdown

Since *Pm*VRP15 transcript and protein were found to be highly up-regulated in the hemocytes of WSSV-infected shrimp (Vatanavicharn *et al*., 2014), then to identify the function of *Pm*VRP15 gene that involved WSSV propagation, *Pm*VRP15 gene RNA silencing in WSSV-infected shrimp was performed.

3.2.1.1. Production of *Pm*VRP15 and GFP dsRNA

The template for *Pm*VRP15 dsRNA construction was amplified by PCR using gene specific primer containing T7 promoter sequence. PCR product of *Pm*VRP15 dsRNA and GFP dsRNA (control dsRNA) template was analyzed by 1.5% agarose gel electrophoresis. The size of *Pm*VRP15 and GFP dsRNA template is about 400 and 700 bp, respectively (Figure 3.10). They were subjected to purification and used for the *Pm*VRP15 and GFP dsRNA production by *in vitro* transcription. The quality of dsRNA was investigated by agarose gel electrophoresis (Figure 3.10) and the concentration of dsRNA was measured at A_{260} using spectrophotometer.

3.2.1.2. The expression of *Pm*VRP15 gene and protein after *Pm*VRP15 gene silencing

To confirm that the dsRNA *Pm*VRP15 specifically suppressed the *Pm*VRP15 transcription levels in shrimp hemocytes at 24 hpi whereas GFP dsRNA had no effect on *Pm*VRP15 mRNA expression levels, the expression of *Pm*VRP15 gene in WSSV-infected shrimp injected with either *Pm*VRP15 dsRNA or GFP dsRNA was determined (Figure 3.11A). Moreover, the suppression of *Pm*VRP15 expression at the translational level was also confirmed. Twenty-four hours after knocking-down *Pm*VRP15 gene in WSSV-infected shrimp, *Pm*VRP15 protein expression level in the shrimp hemocyte lysate was compared with that of the control WSSV-infected shrimp with GFP dsRNA injection. The result showed that *Pm*VRP15 protein expression level in WSSV-

challenge shrimp was significantly decreased after *Pm*VRP15 gene silencing (Figure 3.11B).

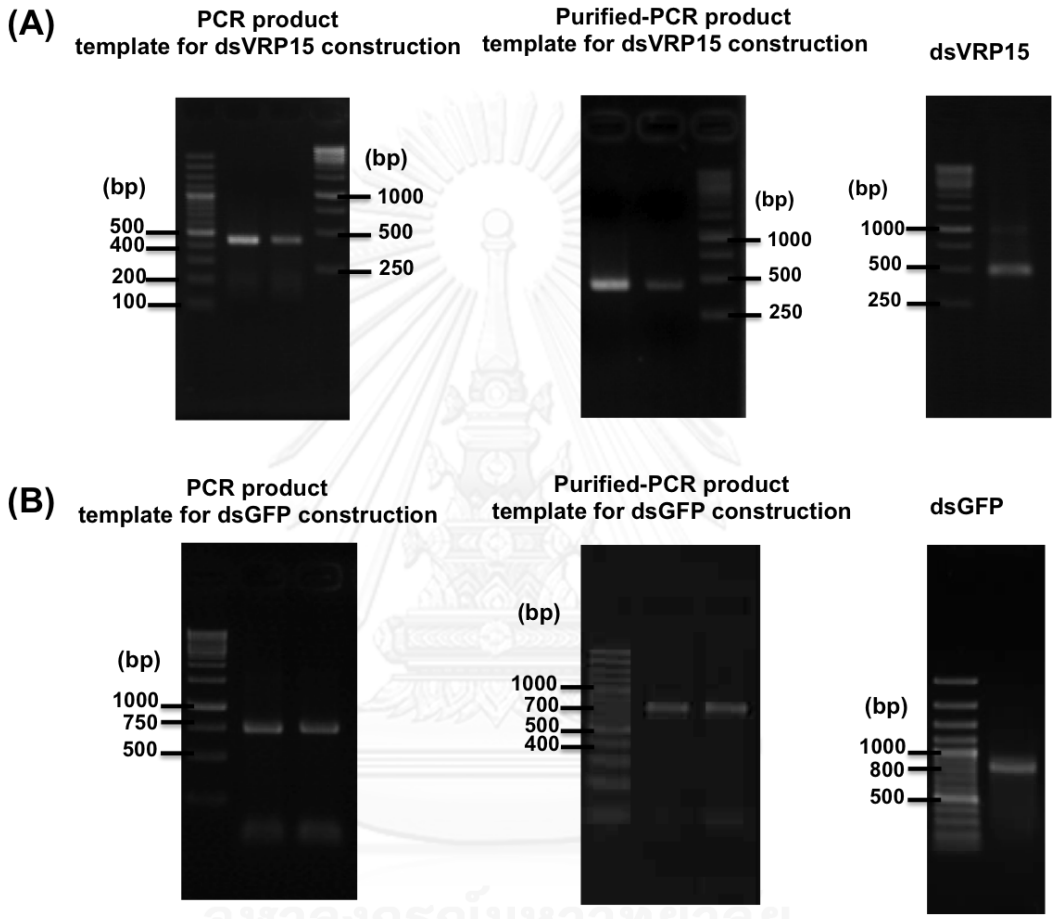

Figure 3.10 Production of *Pm*VRP15 dsRNA (A) and GFP dsRNA (B), control dsRNA.

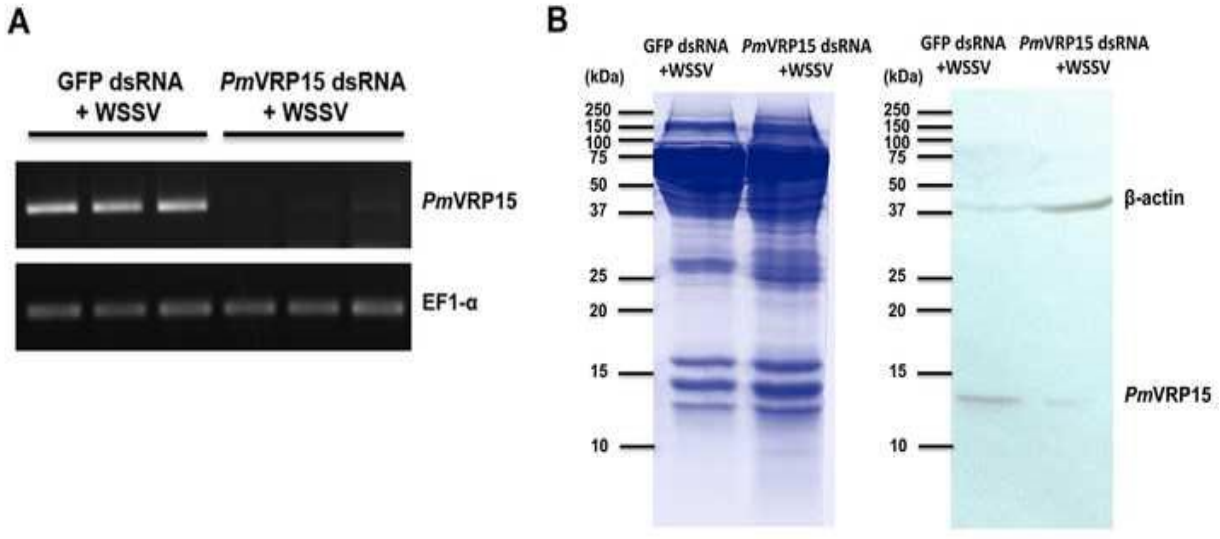

Figure 3.11 The *Pm*VRP15 gene silencing in WSSV- infected *Penaeus monodon* hemocytes. (A) Transcriptional level of *Pm*VRP15 transcripts after 24 h post-WSSV infection and -*Pm*VRP15 gene knockdown in the *P. monodon* hemocytes was determined by RT-PCR using gene specific primers. The control was shrimp that was injected with GFP dsRNA. Three individuals were used for each group and each experiment was performed in triplicate. (B) Protein expression level of *Pm*VRP15 was detected in both groups to confirm the success of *Pm*VRP15 knockdown. Hemocytes were collected at 24 h after *Pm*VRP15 gene knockdown in WSSV-infected shrimp. Seventy mgs of total HLS protein were analyzed by SDS-PAGE (left panel) and western blot analysis (right panel) using antibodies specific to *Pm*VRP15 and β-actin protein (an internal control).

3.2.2. Effect of *Pm*VRP15 gene knockdown on viral propagation in *P. monodon* hemocytes

The transcript expression level of representative WSSV genes for the three stages of WSSV infection; namely ie-1 (very early stage), wsv477 (early stage) and vp28 (late stage), was determined after *Pm*VRP15 knockdown in WSSV-infected shrimp by RT-PCR and qRT-PCR. For RT-PCR analysis, the viral gene expression level

was investigated by PCR using gene specific primer and analyzed by 1.5% agarose gel electrophoresis. From the RT-PCR result, the expression level of viral genes, which are ie-1, wsv477 and vp28, in *Pm*VRP15 knockdown WSSV-infected shrimp was decreased when compared with the control group, GFP knockdown WSSV-infected shrimp. Moreover, qRT-PCR was performed to quantitate and confirm the level of viral genes expression in *Pm*VRP15 silencing WSSV-infected shrimp using EF-1α as an internal control. It was found that transcript expression level of all three viral genes tested was considerably decreased in the *Pm*VRP15 knockdown shrimp by 83.5%, 85.5% and 94.8% for ie-1, wsv477 and vp28, respectively, as compared to the control shrimp (Figure 3.12). The decrease in WSSV transcript levels suggested that *Pm*VRP15 might participate in the WSSV propagation process.

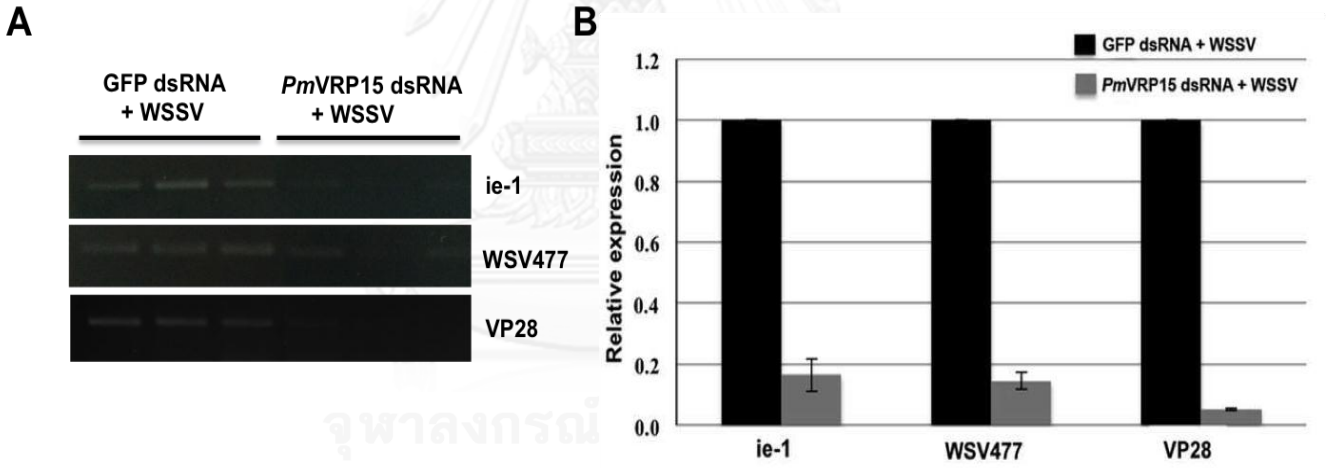

Figure 3.12 The effect of *Pm*VRP15 gene silencing on WSSV propagation in *Penaeus monodon* hemocytes. Transcript expression level of the WSSV genes: ie-1, wsv477 and vp28, in *Pm*VRP15 gene-silenced *P. monodon* hemocytes were determined by RT-PCR (A) and qRT-PCR (B). Data are shown as the mean ± 1 SD of three replicates and as the fold change of ie-1, wsv477 and vp28 after normalization to the EF-1α transcript levels (grey bar). The control group (GFP-dsRNA injected) are shown in the black bars.

3.2.3. Effect of *Pm*VRP15 gene silencing on cumulative mortality of WSSV-infected shrimp

In the previous experiment, after *Pm*VRP15 gene knockdown in WSSV-infected shrimp, the expression level of representative WSSV genes was significantly decreased suggesting the involvement of *Pm*VRP15 in the WSSV propagation. *Pm*VRP15 gene was silenced in WSSV-infected *P. monodon* and the mortality of shrimp was observed in parallel to those silenced with GFP dsRNA. The shrimp mortality of the control shrimp reached 100% at 90 h post- WSSV infection (hpi) whereas that of *Pm*VRP15 knockdown was slower and significantly different at 66-102 hpi with 50% lower. The cumulative mortality result showed that, after 66-102 hpi, mortality rate of *Pm*VRP15 knockdown group was 50% lower than that of control group. However, after 102 hpi, the cumulative mortality of *Pm*VRP15 knockdown shrimp was gradually increased and reached 100% at 144 hpi (6 dpi) (Figure 3.13A). Due to the fact that *Pm*VRP15 gene is highly up-regulated after WSSV infection, here, the *Pm*VRP15 gene recovery after *Pm*VRP15 dsRNA and WSSV injection was determined. Figure 3.13B showed that *Pm*VRP15 gene was recovered for about 50% at 36 hpi and to the same level as in the control at 60 hpi. According to the results, we confirmed that the absence of *Pm*VRP15 gene in shrimp affected the mortality of WSSV-infected shrimp.

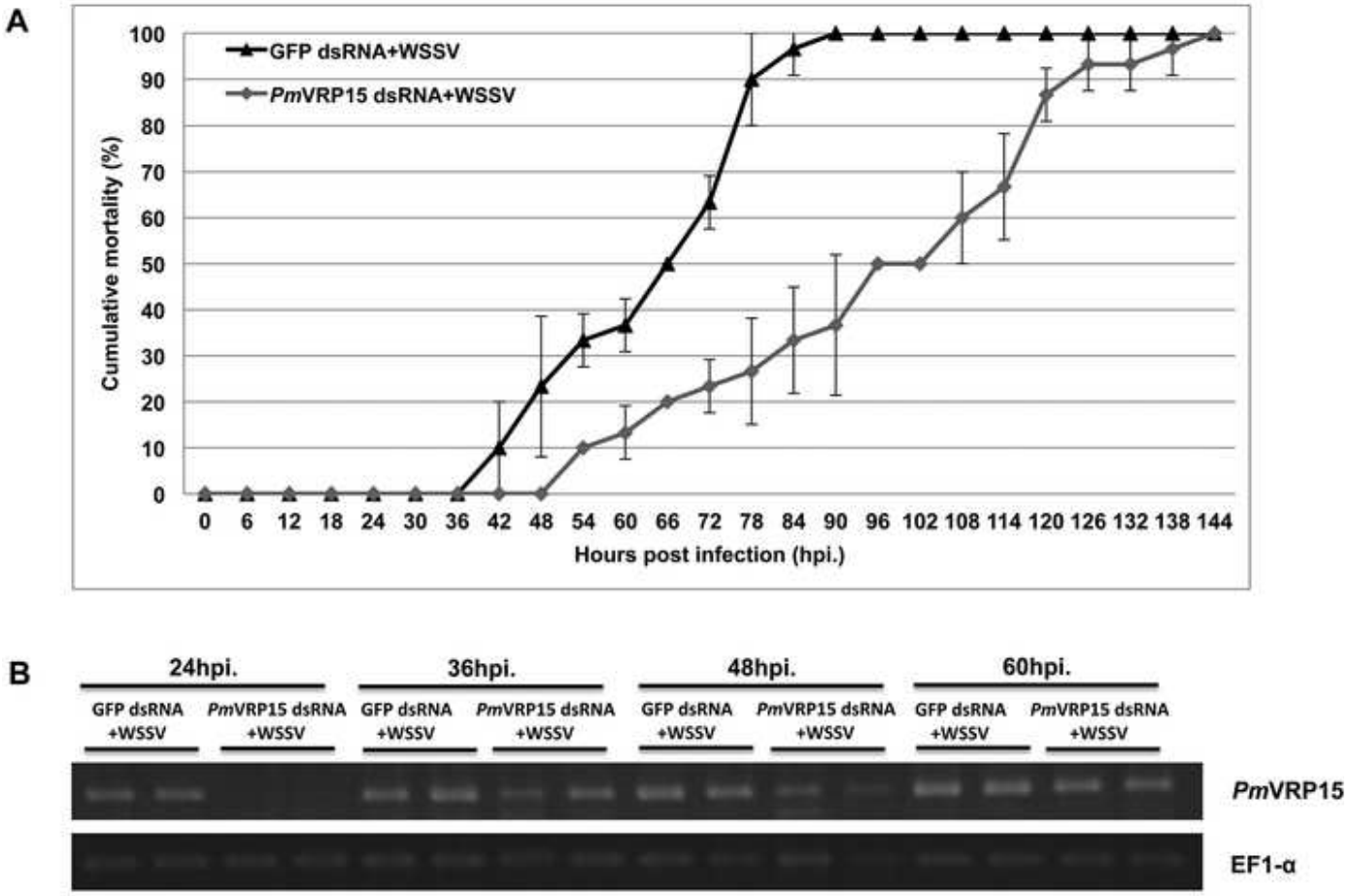

Figure 3.13 The involvement of knockdown *Pm*VRP15 gene in WSSV infection in shrimp. (A) Cumulative mortality of WSSV-infected *Pm*VRP15 gene knockdown shrimp (Grey line) was compared with that of the control, WSSV-infected GFP gene knockdown shrimp (Black line). Data are shown as the mean ±1 S.D. and are derived from three independent repeats. (B) After knockdown *Pm*VRP15 gene in WSSV-infected shrimp, *Pm*VRP15 gene recovery was observed after WSSV infection at 24, 36, 48 and 60 hpi.

3.2.4. Identification of *Pm*VRP15 interacting protein by yeast two-hybrid screening

From silencing experiment we found that *Pm*VRP15 involved in WSSV propagation. To characterize a novel *Pm*VRP15 protein function, yeast two-hybrid screening was performed to identify its interacting-partner protein from WSSV.

3.2.4.1. Construction of bait vectors which are open reading frame, N- and C-terminus of *Pm*VRP15 gene into pGBKT7 vector

The *Pm*VRP15 gene was amplified and cloned into pGBKT7 vector, which is a bait vector for the yeast two-hybrid screening. The open reading frame (ORF) of *Pm*VRP15 was amplified using gene specific primer containing restriction sites, *Nco*I and *Bam*HI. Because the transmembrane region of *Pm*VRP15 protein can interrupt protein translocation into nucleus causing failure of yeast two-hybrid assay, the N- and C- terminal parts of *Pm*VRP15 protein were constructed. The N- and C-terminus of *Pm*VRP15 gene were also amplified by PCR technique using gene specific primers containing restriction sites, *Nde*I and *EcoR*I. The PCR products were analyzed by agarose gel electrophoresis and the expected size of ORF, N- , and C- terminus of *Pm*VRP15 gene is 414, 114 and 231 bp, respectively (Figure 3.14). Then, the purified PCR product was digested with restriction enzymes and cloned into pGBKT7 vector, a bait vector, cut with the same enzymes. The ligation mixtures were transformed into *E. coli* strain XL-1 blue. The recombinant clones were screened and selected for plasmid preparation. Then, the recombinant plasmids (pGBKT7-ORF-*Pm*VRP15 for *Pm*VRP15 ORF, pGBKT7-N-*Pm*VRP15 for N-terminal fragment of *Pm*VRP15 and pGBKT7-C-*Pm*VRP15 for C-terminal fragment of *Pm*VRP15) were verified by restriction enzyme digestion with restriction enzymes as shown in Figure 3.14. DNA sequencing confirmed the correctness of sequences.

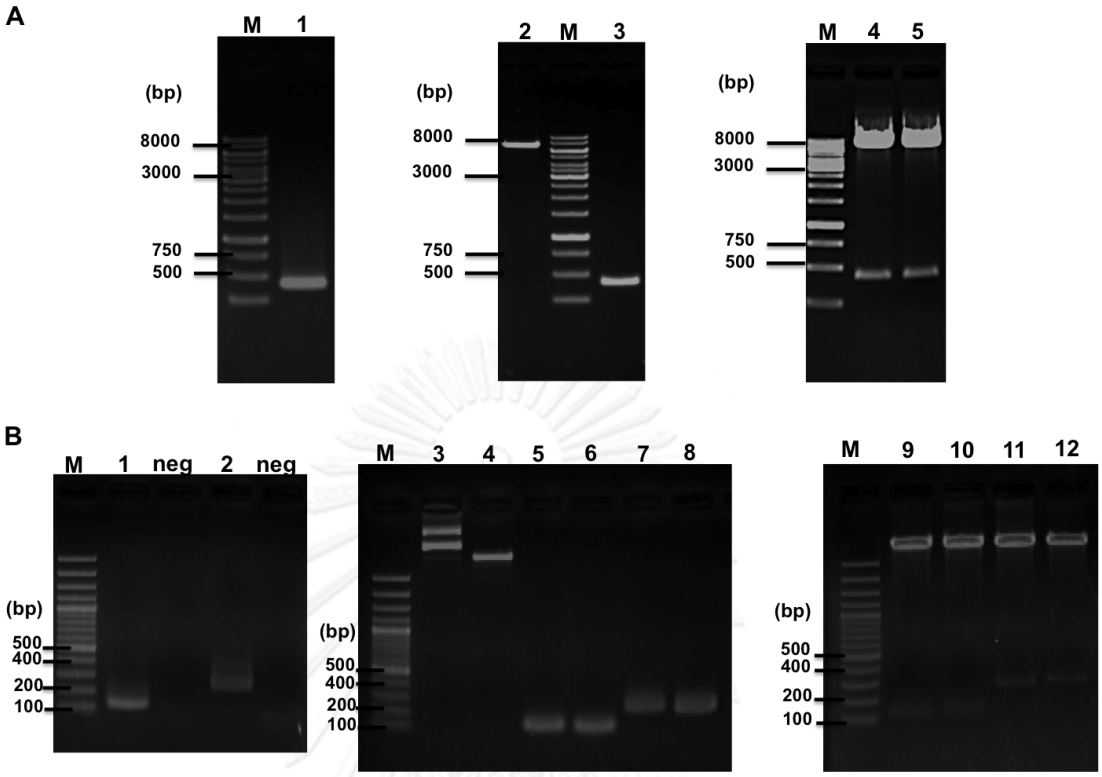

Figure 3.14 Bait plasmids construction. The bait plasmids are pGBKT7-ORF-*Pm*VRP15, pGBKT7-N-*Pm*VRP15 and pGBKT7-C-*Pm*VRP15. The pGBKT7-ORF-*Pm*VRP15 plasmids were constructed (A). Lane 1: PCR product of *Pm*VRP15 ORF (about 414 bp), Lanes 2 and 3: The purified pGBKT7 and *Pm*VRP15 ORF after double-digested with restriction enzymes, *Nco*I and *Bam*HI, respectively, Lanes 4 and 5: The recombinant plasmid was checked for insertion by restriction enzyme digestion. Also, the pGBKT7-N-*Pm*VRP15 and pGBKT7-C-*Pm*VRP15 plasmids were constructed (B). Lanes 1 and 2: PCR products of *Pm*VRP15 N- and C- terminal frangments whose size are 114 and 231, respectively, Lanes 3 and 4: pGBKT7 uncut and cut with restriction enzymes, *Nde*I and *Eco*RI, respectively, Lanes 5 and 7: purified *Pm*VRP15 N- and C- terminal frangments, Lanes 6 and 8: *NdeI/Eco*RI digested *Pm*VRP15 N- and C- terminal frangments, Lanes 9 and 10: The positive clones of pGBKT7-N-*Pm*VRP15 digested with *NdeI/Eco*RI, Lanes 11 and 12: The positive clones of pGBKT7-C-*Pm*VRP15 digested with *NdeI/Eco*RI, Lane M: DNA marker (Fermentas).

3.2.4.2. Checking auto-activation and toxicity of bait plasmid

Before yeast two-hybrid screening assay, bait plasmids were transformed into yeast, *Saccharomyces cerevisiae* strain Y2H Gold, to check auto-activation and toxicity. The colonies of Y2H Gold containing pGBKT7-ORF-*Pm*VRP15, pGBKT7-N-*Pm*VRP15 and pGBKT7-C-*Pm*VRP15 were white colonies suggesting that *Pm*VRP15 gene did not auto-activated. The representative results were shown in Figure 3.15. To test the toxicity of *Pm*VRP15 expression in yeast, the size of single colony of Y2H gold containing pGBKT7-ORF-*Pm*VRP15, pGBKT7-N-*Pm*VRP15 and pGBKT7-C-*Pm*VRP15 was compared with control which is Y2H gold containing empty pGBKT7 plasmid. Size of colonies containing each bait vector was same as that of control (Figure 3.16). In conclusion, the bait plasmids, pGBKT7-ORF-*Pm*VRP15, pGBKT7-N-*Pm*VRP15 and pGBKT7-C-*Pm*VRP15, did not auto-activated and were not toxic to yeast *S. cerevisiae* strain Y2H Gold.

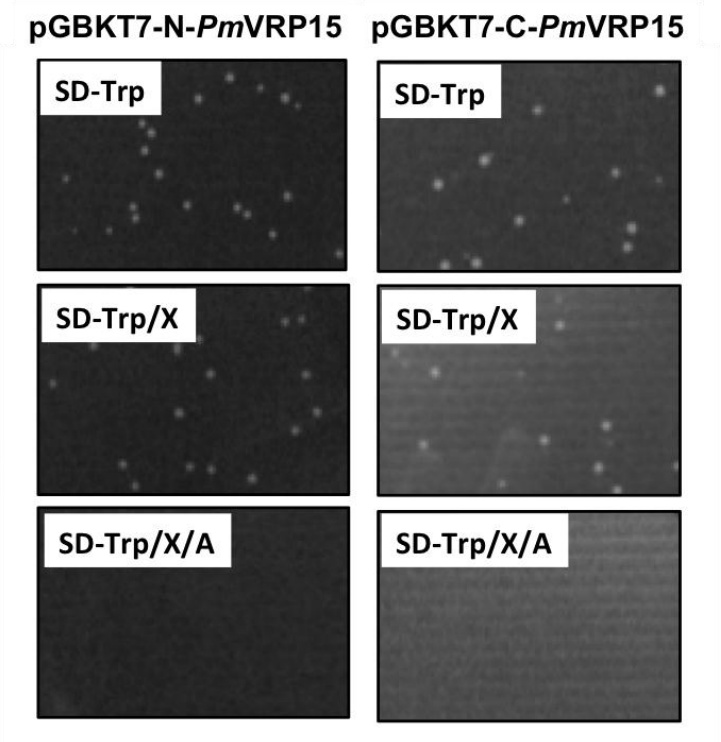

Figure 3.15 Yeast auto-activation assay of pGBKT7-N-*Pm*VRP15 and pGBKT7-C-*Pm*VRP15 in yeast, *Saccharomyces cerevisiae* strain Y2H Gold.

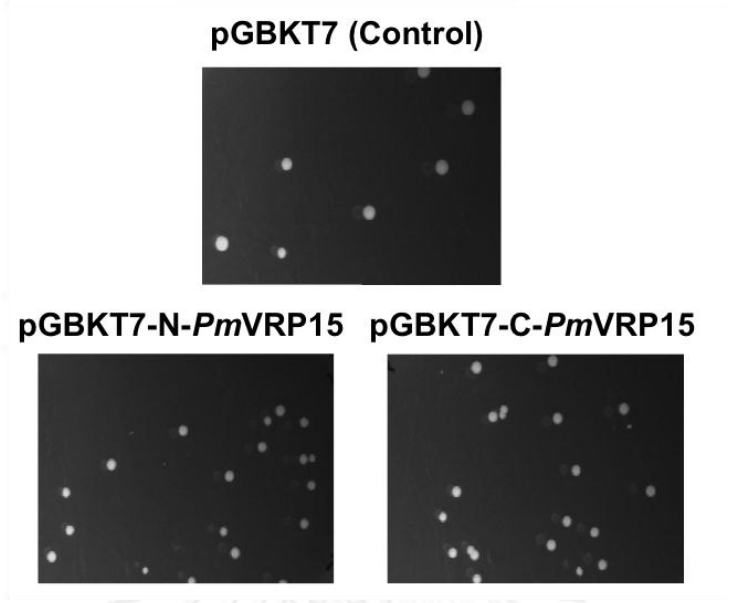

Figure 3.16 Toxicity assay of pGBKT7-N-*Pm*VRP15 and pGBKT7-C-*Pm*VRP15 in yeast, *Saccharomyces cerevisiae* strain Y2H Gold.

3.2.4.3. Identification of *Pm*VRP15 interacting protein in hemocyte of WSSV-infected shrimp and WSSV libraries

To identify the function of *Pm*VRP15 protein, yeast two- hybrid screening technique was used to find the interacting proteins. We do hope that the function of interacting protein might be a clue for *Pm*VRP15's function. Due to *Pm*VRP15 protein was up- regulated in WSSV-infected shrimp, the partners of *Pm*VRP15 protein were screened in WSSV- infected shrimp hemocyte and WSSV ORF libraries. Screening by yeast containing pGBKT7-ORF-*Pm*VRP15 bait vector showed no interaction between *Pm*VRP15 with any protein in both libraries. These might cause by the transmembrane part in *Pm*VRP15 protein blocked the protein translocation into nucleus. So, *Pm*VRP15 could not enter nucleus and interact with partner protein.

The *Pm*VRP15 gene was separated into 2 parts, which are N-terminus and C-terminus of *Pm*VRP15 and constructed into pGBKT7 vector. After yeast-two hybrid screening in WSSV-infected shrimp hemocyte library, 9 positive clones were found. One of them interacted with C-terminus of *Pm*VRP15 protein and 8 clones interacted

with N-terminus of *Pm*VRP15 protein. The *Pm*VRP15 interacting proteins from WSSV ORF library were screened in collaboration with Dr. Saengchan Senapin (Mahidol University). The candidate clones were confirmed by re-streaking on high stringency plate (QDO/X). Just only N-terminal fragment of *Pm*VRP15 protein can be interacted with WSSV proteins (about 40 clones).

To re-arrange the interacting protein with *Pm*VRP15 protein, the candidate clones were rescued the prey plasmid and organized by grouping the same size of insert gene using the restriction enzyme on pGADT7, *Hin*dIII. The plasmid of each group, was sequenced and analyzed using blastx program to identify the interacting protein. From WSSV-infected shrimp hemocyte library, 9 groups were found which are 1 clone interacting with C-terminus of *Pm*VRP15 protein and 8 clones interacting with N-terminus of *Pm*VRP15 protein (Table 3.1). From WSSV ORF library, only N-terminus of *Pm*VRP15 interacted with 3 candidated WSSV proteins (Table 3.2).

Table 3.1 Nine positives clones of WSSV infected shrimp hemocyte library with *Pm*VRP15 protein

Clone No.	Description	Frame
CHW 57-1	No significant similarity found	
NHW 6-2	Elongation factor 1-alpha [*Marsupenaeus japonicus*]	+1
NHW 7-1	No significant similarity found	
NHW 7-3	CD63 antigen [*Acromyrmex echinatior*]	+1
NHW 9-2	Hypothetical protein AaeL_AAEL008492 [*Aedes aegypti*]	+3/+1
NHW 19-1	Hypothetical protein DAPPUDRAFT_299952 [*Daphnia pulex*]	+3
NHW 35-2	No significant similarity found	
NHW 39-2	PREDICTED: vinculin-like [*Acyrthosiphon pisum*]	+2
NHW 61-3	No significant similarity found	

Table 3.2 Three positives clones of WSSV ORF library interacting with *Pm*VRP15 protein.

Clone No.	Description
NW2-1 (9)	wsv399 [Shrimp white spot syndrome virus]
NW2-2 (9)	wsv020 [Shrimp white spot syndrome virus]
NW1-14 (1)	wsv524 [Shrimp white spot syndrome virus]

3.2.4.4. Confirmation of interacting protein with *Pm*VRP15 protein by co-transformation

The candidate partner proteins were confirmed for the interaction with *Pm*VRP15 protein by co-transformation. The positive clones with blue colonies on DDO/X and QDO/X selective media were selected. Of those, only one candidate protein, which is WSV399 from WSSV ORF library, could interact with N-terminus of *Pm*VRP15 (Figure 3.17).

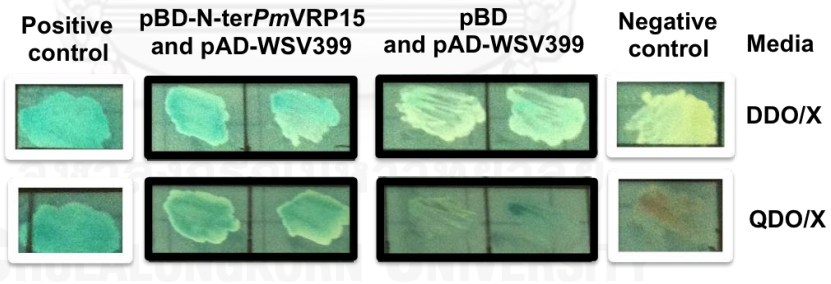

Figure 3.17 Confirmation of the interaction between N-terminus of *Pm*VRP15 and WSV399 protein by co-transformation. The transformants grown on selective media were restreaked onto DDO/X and QDO/X media. The negative control and the positive control are the yeast, *S. cerevisiae* strain Y2HGold, containing the murine p53 and either lamin or the SV40 large T antigen, respectively.

3.2.5. Confirmation of the protein-protein interaction by Co-immunoprecipitation

To further confirm the protein-protein interaction between *Pm*VRP15 and WSV399 proteins, co-immunoprecipitation (Co-IP) was performed. The recombinant proteins, which are r*Pm*VRP15 and rWSV399, were expressed and purified for the protein-protein interaction study.

The r*Pm*VRP15 was produced in *E. coli* stain C43 (DE3) and analyzed by 15% SDS-PAGE and western blot. The expected size of r*Pm*VRP15 is about 15 kDa as shown in Figure 3.18. After sonication, crude soluble protein was purified by Ni-NTA. The elution fractions of purified *Pm*VRP15 were determined by 15% coomessie stained SDS-PAGE (Figure 3.19).

For rWSV399 expression, the recombinant plasmid WSV399, pBAD-Myc/His containing WSV399, was constructed. WSV399 gene was amplified by PCR using gene specific primer. The expected size of PCR product is about 600 bp (Figure 3.20). After clone into pBAD-Myc/His vector, the positive clones were selected by restriction enzyme and checked WSV399 nucleotide sequence by DNA sequencing. The rWSV399 protein was produced in *E. coli* stain TOP10 and analyzed by 12.5% SDS-PAGE and western blot. The expected size of rWSV399 is about 26 kDa as shown in Figure 3.21. Crude protein was purified by Ni-NTA bead, affinity column. The elution fractions of purified WSV399 were determined by 12.5% coomessie stained SDS-PAGE (Figure 3.22).

To confirm the interaction between *Pm*VRP15 and WSV399, the co-immunoprecipitation assay was performed. In this experiment, r*Pm*VRP15 protein containing His_6-tag and rWSV399 containing c-*Myc* tag and His_6-tag were mixed and incubated with anti-*Myc* conjugated protein A bead. After washed unbound protein, protein A bead containing protein-protein complex was added with sample loading buffer and analyzed by western blot analysis (Figure 3.23). From the result in Figure 3.23, Lane 6, the r*Pm*VRP15 and rWSV399 can be detected indicating that PmVRP15 can interact with WSV399. In control experiment, anti-*Myc* conjugated protein A bead was incubated with only r*Pm*VRP15 or only rWSV399 and analyzed by western blot

with the same condition to check the false positive (Figure 3.23, Lanes 7 and 8, respectively). From Figure 3.23 in lane 7, no protein band can be detected indicating that *Pm*VRP15 protein cannot bind to anti-*Myc* conjugated protein A bead. From Figure 3.23 in lane 8 showed that rWSV399 can be detected on membrane because its normally can bind to the bead.

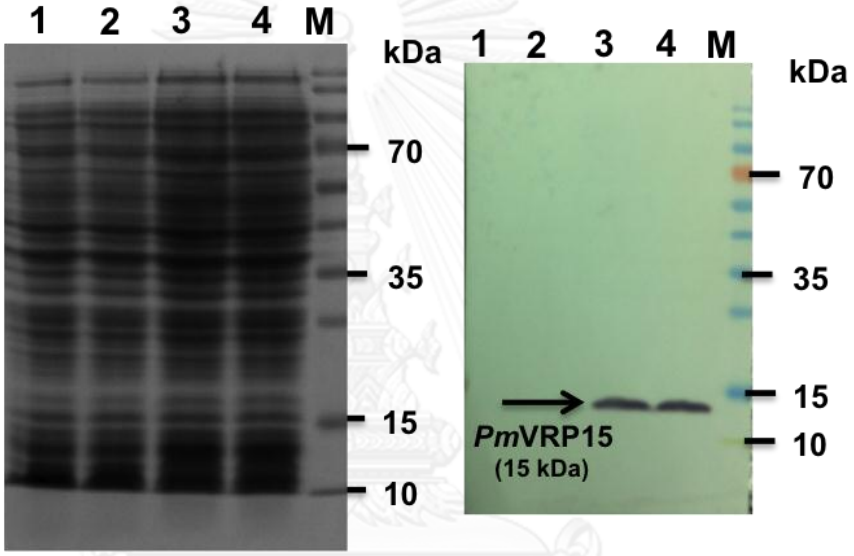

Figure 3.18 The expression of r*Pm*VRP15 from *E. coli* strain C43 (DE3). The crude protein was analyzed by 15% Coomassie-stained SDS-PAGE (left panel) and western blot analysis (right panel) using the anti-His antibody. Lane M: Prestained protein marker (Fermentas), Lanes 1 and 2: *Pm*VRP15 expression after 0 h induction, Lanes 3 and 4: *Pm*VRP15 expression after 1 h induction.

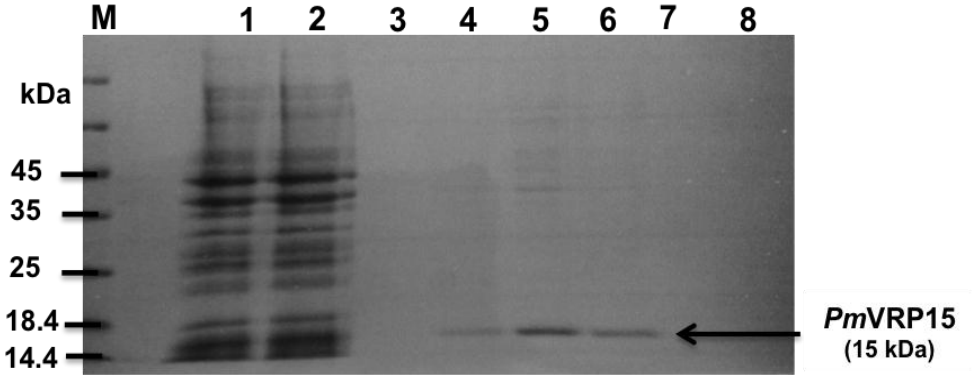

Figure 3.19 Purification of *Pm*VRP15 by Ni-NTA column. Lane M: unstained protein marker (Fermentas), Lane 1: crude r*Pm*VRP15, Lane 2: Flow-through fraction Lane 3; the last wash fraction, Lanes 4-6 Elution 1 fraction: fraction nos. 1-3 were eluted by elution buffer 1 (50 mM Tris-HCl, pH 7.0, 300 mM Imidazole, 0.1% DM and 5% glycerol), Lanes 7 and 8: Elution 2 fraction: fraction nos. 1-3 were eluted by elution buffer 2 (50 mM Tris-HCl, pH7.0, 500 mM Imidazole, 0.1% DM and 5% glycerol).

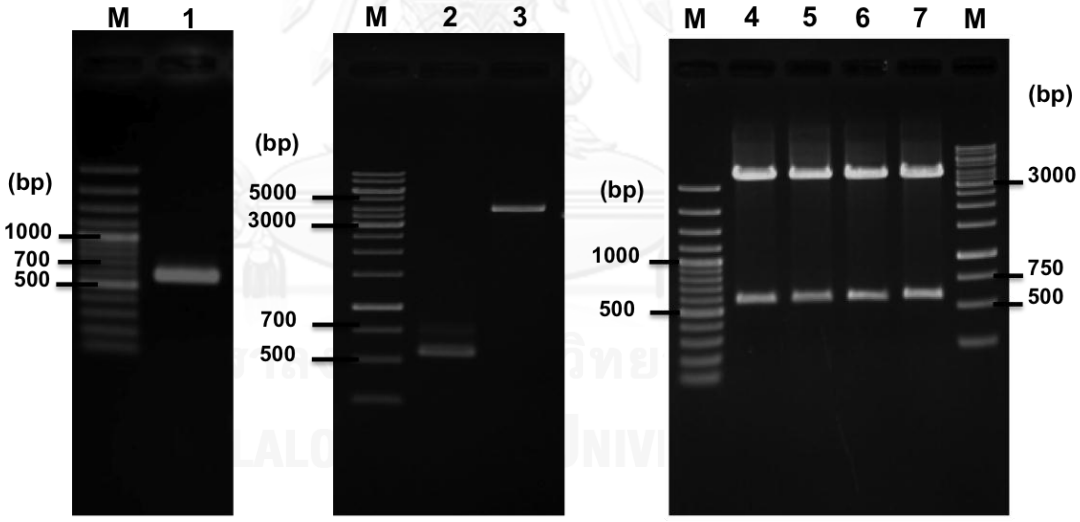

Figure 3.20 Construction of recombinant plasmid, pBAD-Myc/His-WSV399. Lane M: DNA marker (Fermentas), Lane 1: PCR product of ORF WSV399, Lane 2: the purified WSV399 gene after double digestion with *Xho*I and *Eco*RI, Lane 3: the purified pBAD-Myc/His vector after double digestion with *Xho*I and *Eco*RI, Lanes 4-7: the positive clones selected by *Xho*I/*Eco*RI double digestion

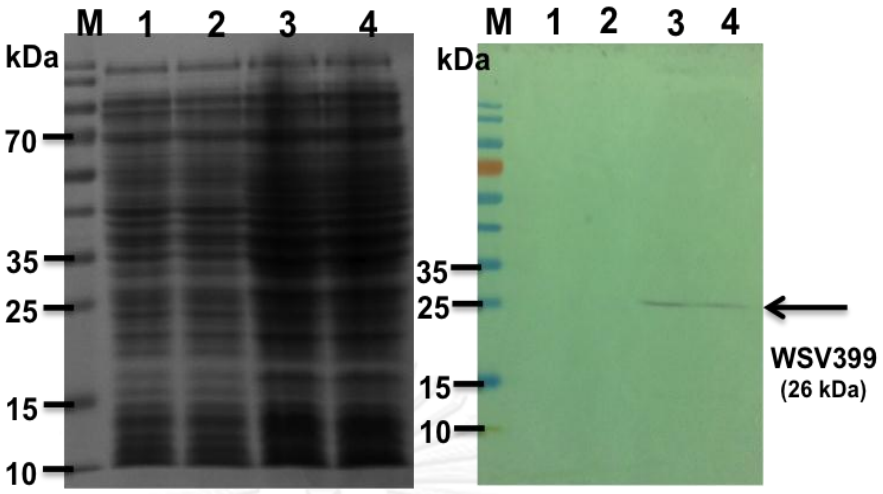

Figure 3.21 Expression of rWSV399 from *E. coli* strain TOP 10. The crude protein was analyzed by 12.5% Coomassie-stained SDS-PAGE and Western blot analysis using the anti-c-*Myc* antibody. Lane M: the prestained protein marker (Fermentas), Lanes 1 and 2: WSV399 expression after 0 h induction, Lanes 3 and 4: WSV399 expression after 4 h induction.

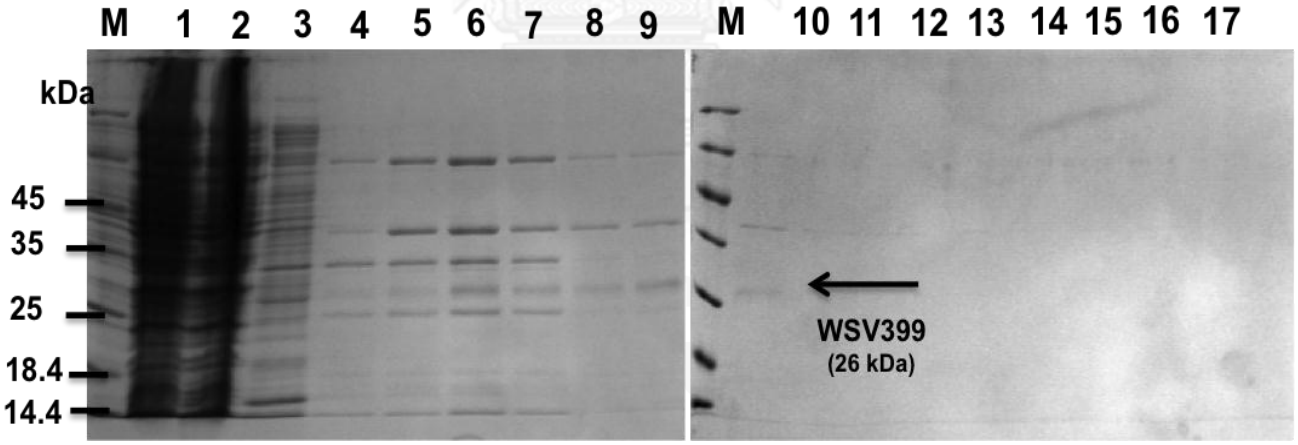

Figure 3.22 Purification of WSV399 by Ni-NTA column. Lane M: unstained protein marker (Fermentas), Lane 1: crude r*Pm*VRP15, Lane 2: flow-through fraction, Lane 3: wash fraction no.2, Lane 4 the last wash fraction, Lanes 5-7: Elution fraction no. 2, 4, 6 of elution buffer 1 (50 mM sodium phosphate buffer, pH 7.4, 300 mM NaCl and 40 mM Imidazole), Lanes 8-10: Elution fraction no. 2, 4, 6 of elution buffer 2 (50 mM sodium phosphate buffer, pH 7.4, 300 mM NaCl and 80 mM Imidazole), Lanes 11-13:

Elution fraction no. 2, 4, 6 of elution buffer 3 (50 mM sodium phosphate buffer, pH 7.4, 300 mM NaCl and 100 mM Imidazole), Lanes 14-16: Elution fraction no. 2, 4, 6 of elution buffer 4 (50 mM sodium phosphate buffer, pH 7.4, 300 mM NaCl and 250 mM Imidazole), Lane 17 Elution fraction of elution buffer 5 (50 mM sodium phosphate buffer, pH 7.4, 300 mM NaCl and 500 mM Imidazole).

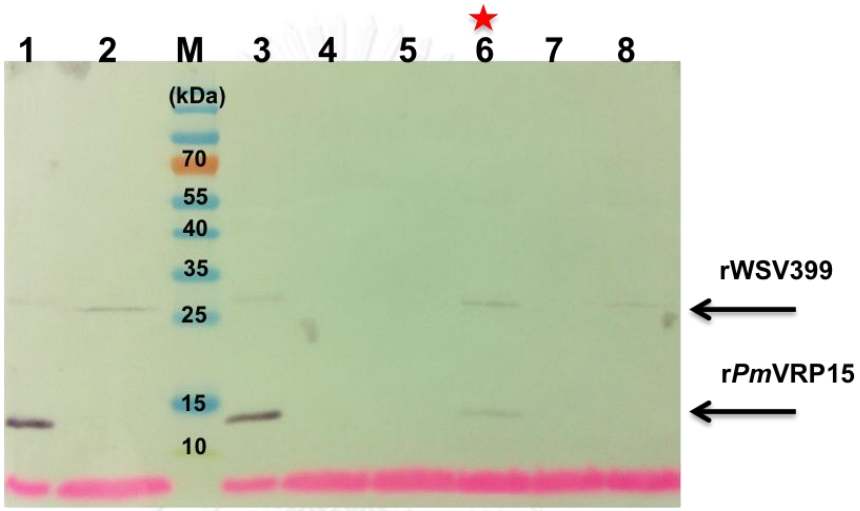

Figure 3.23 Confirmation of the interaction between *Pm*VRP15 and WSV399 by co-immunoprecipitation. The protein-protein complex was analyzed by western blot using specific antibodies, which are anti-His antibody for *Pm*VRP15 and anti-c-*Myc* antibody for WSV399. Lane M: prestained protein marker (Fermentas), Lane 1: the purified- r*Pm*VRP15 protein, Lane 2: the purified- rWSV399 protein, Lane 3: flow-through fraction from anti- c-*Myc* conjugated protein A incubated with mixture of *Pm*VRP15 and WSV399 proteins, Lanes 4 and 5: wash fraction no.1 and 2 from anti-c-*Myc* conjugated protein A incubated with mixture of *Pm*VRP15 and WSV399 proteins, Lane 6: Elution fraction from anti- c-*Myc* conjugated protein A incubated with mixture of *Pm*VRP15 and WSV399 protein, Lane 7: Elution fraction from anti- c-*Myc* conjugated protein A incubated with *Pm*VRP15 protein only, Lane 8: Elution fraction from anti- c-*Myc* conjugated protein A incubated with WSV399 protein only.

3.2.6. Characterization of a *Pm*VRP15 interacting protein (WSV399)

3.2.6.1. Expression of recombinant WSV399 (rWSV399) expression in pET expression system for anti-WSV399 antiserum production

Although, wsv399 gene was successfully cloned into pBAD-Myc/His A vector, the expression level of rWSV399 protein is quite low. To obtain an adequate amount of protein for production of the antibody specific to WSV399, the rWSV399 expressing plasmid was constructed and expressed using pET expression system.

The expression plasmid for WSV399 protein was constructed. wsv399 gene was amplified by PCR using gene specific primer. The size of wsv399 gene is 552 bp (Figure 3.24). After double digestion with restriction enzymes, *Nde*I and *Bam*HI, wsv399 gene was cloned into pET16b that digested with the same restriction enzymes. The positive clones were confirmed by digestion with restriction enzymes *Nde*I and *Bam*HI (Figure 3.24) and sequencing. The rWSV399 containing 6x- His tag protein was produced in *E. coli* stain BL21 (DE3) and analyzed by 12.5% SDS-PAGE and western blot. The expected size of rWSV399 is about 26 kDa as shown in Figure 3.25. Inclusion bodies protein was solubilized and purified by Ni-NTA bead, affinity column. The partial purified rWSV399 was determined by 12.5% Coomassie stained SDS-PAGE (Figure 3.26). The rWSV399 protein was separated on SDS-PAGE, the band corresponding to WSV399 protein was cut and used for anti- WSV399 antibody production (Seeing Bioscience CO., LTD, Taiwan R.O.C.). The specificity and quality of anti-WSV399 antibody was determined by western blot analysis. The purified rWSV399 was clearly detected by anti-WSV399 antibody (Figure 3.27).

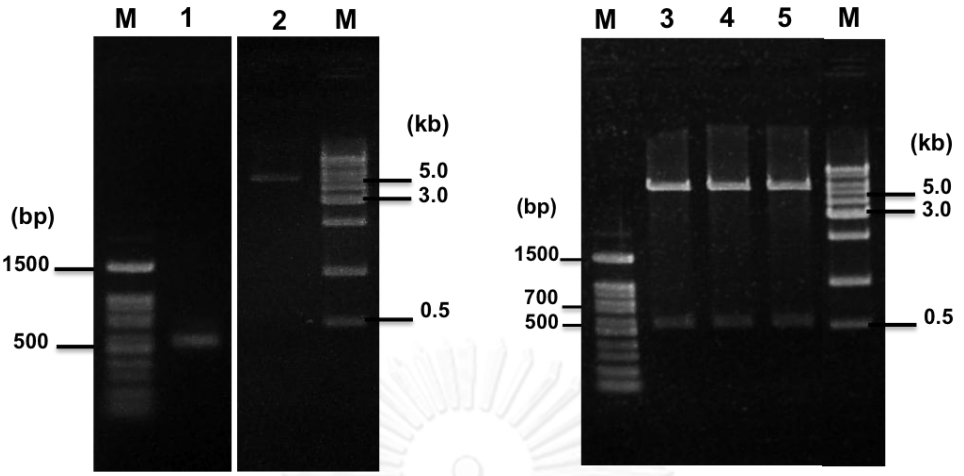

Figure 3.24 Construction of recombinant plasmid, pET16b-wsv399. Lane M: DNA marker, Lane 1: *Nde*I/*Bam*HI digestion of purified- PCR product of wsv399, Lane 2: *Nde*I/*Bam*HI digestion of pET16b vector, Lanes 3-5: The positive clones selected by *Nde*I/*Bam*HI digestion.

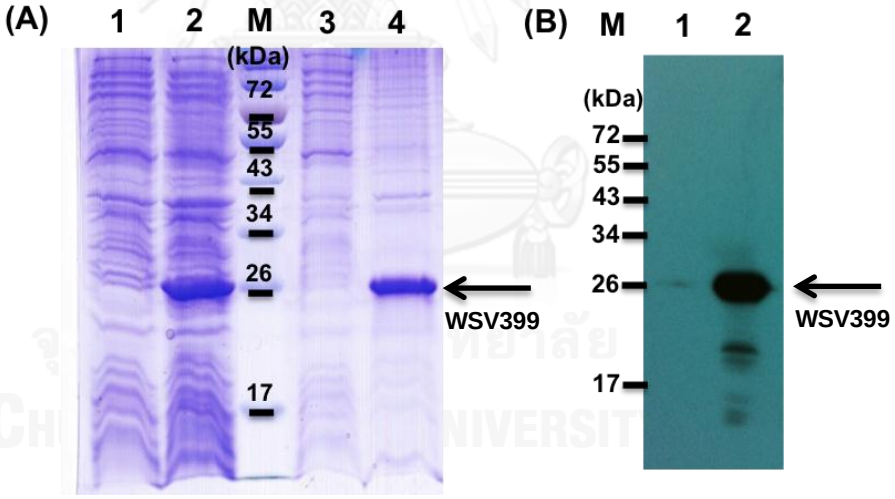

Figure 3.25 Expression of rWSV399 from *E. coli* strain BL21 (DE3). The crude protein was analyzed by 12.5% Coomassie-stained SDS-PAGE (A) and western blot (B). Lane M: Prestained protein marker (Fermentas), Lane 1: WSV399 expression after 0 h induction, Lane 2: WSV399 expression after 3 h induction, Lane 3: Soluble form of WSV399, Lane 4: Inclusion body of WSV399.

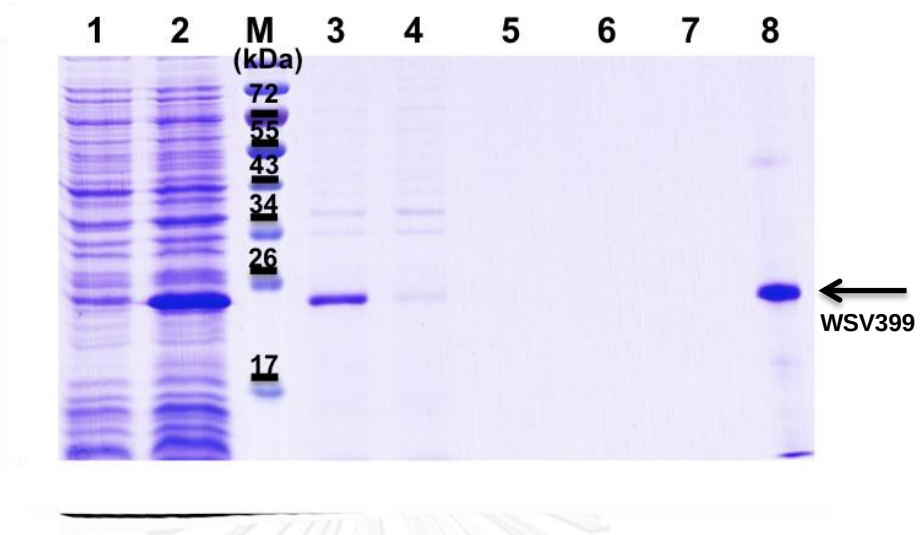

Figure 3.26 Purification of rWSV399 by Ni-NTA column. Lane M: Prestained protein marker, Lane 1: rWSV399 expression after 0 h induction, Lane 2: rWSV399 expression after 3 h induction, Lane 3: solubilized rWSV399 from inclusion bodies, Lane 4: flow-through fraction from Ni-NTA column, Lanes 5-7: wash fraction no.1-3 from Ni-NTA column, Lane 8: elution fraction of rWSV399 from Ni-NTA column.

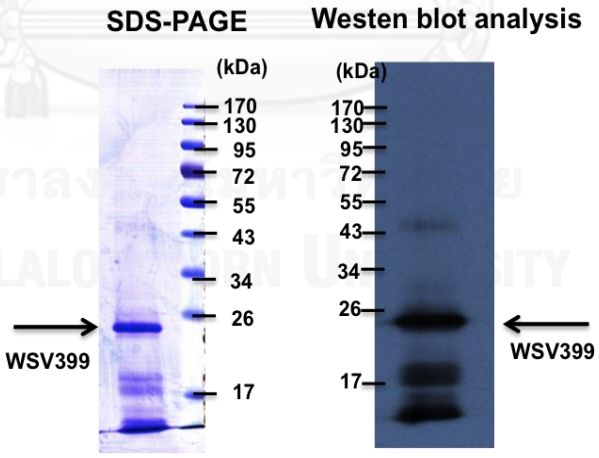

Figure 3.27 Specificity of anti-WSV399 antibody by Western blot analysis. The partial purified WSV399 was run on 12.5% SDS-PAGE and western blot analysis was performed using anti-WSV399 antibody.

3.2.6.2. Localization of WSV399 protein on WSSV virion

To study the localization of the WSV399 protein on WSSV virion, intact virus was extracted and purified from WSSV-infected crayfish, *Procambarus clarkii*. The proteins of the purified WSSV were analyzed by 12.5% Coomassie stained SDS-PAGE (Figure 3.28). The quality of WSSV preparation was investigated by negative-staining transmission electron microscopy (Figure 3.29). To localize WSV399 on WSSV virion, the purified WSSV protein was separated by 12.5% SDS-PAGE and detected by anti-WSV399 using western blot analysis. The result showed that WSV399 is a structural protein (Figure 3.30). WSSV virion consists of three parts of structure protein, which are envelope, tegument and nucleocapsid. WSSV fractions were prepared by treating WSSV with TritonX-100 solution, fractions of WSSV protein were analyzed by 12.5% Coomassie stained SDS-PAGE (Figure 3.31A). The separation efficiency was determined by detecting VP28 protein, a major known protein in the envelope fraction, using western blot analysis (Figure 3.31B). Moreover, WSV399 protein was localized on various WSSV fractions. WSV399 can be detected on both envelope and nucleocapsid fractions (Figure 3.32). This means that WSV399 might be a part of tegument protein on WSSV virion.

The localization of WSV399 protein on WSSV virion was confirmed by immunoelectron microscopy using gold particle labeling technique. The WSV399 was immuno-detected using the anti-WSV399 antibody and the anti-mouse IgG conjugated with 18 nm-diameter gold particles. The electron micrograph showed that the position of gold particles labeled-WSV399 protein was located on tegument part of WSSV (Figure 3.33). Therefore, we concluded that WSV399 is a tegument protein of WSSV.

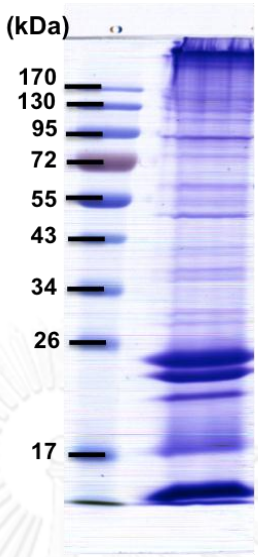

Figure 3.28 Analysis of protein from the purified WSSV by 12.5% Coomassie-stained SDS-PAGE.

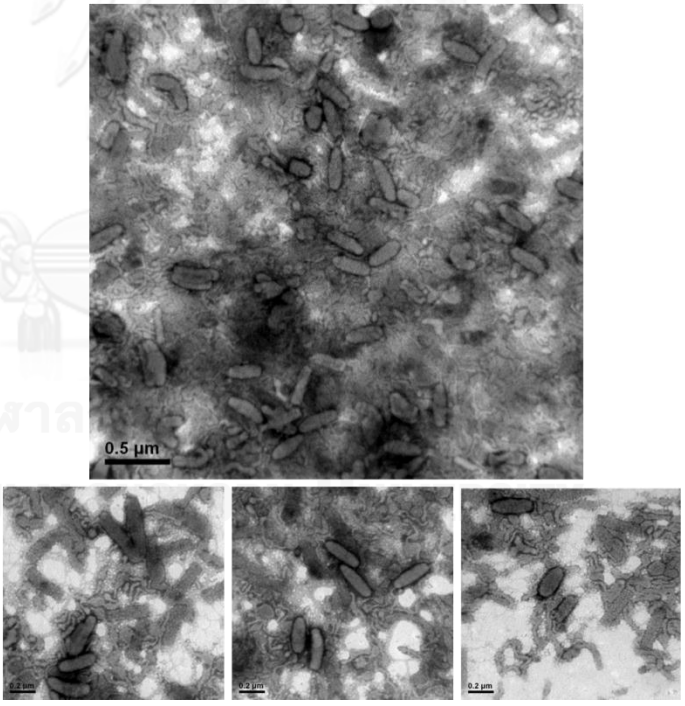

Figure 3.29 Investigation of WSSV virions by negative-staining transmission electron microscopy.

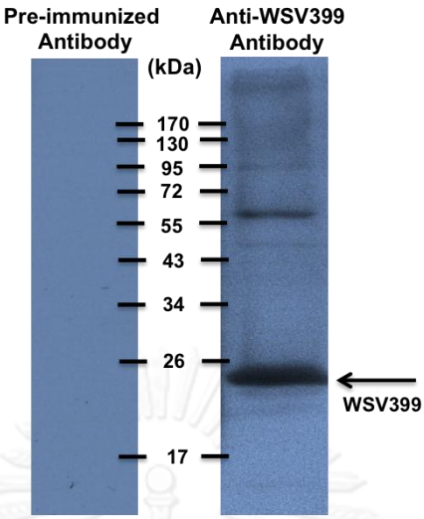

Figure 3.30 Localization of WSV399 on WSSV viron by Western blot analysis using anti-WSV399 antiserum. The pre-immunized antibody was used as a control.

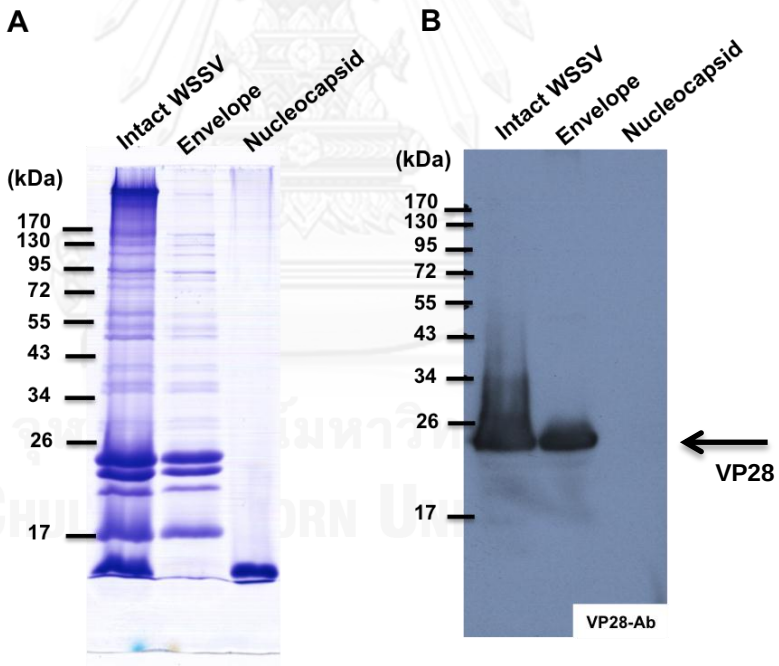

Figure 3.31 The structural proteins fractions including intact WSSV protein, envelope protein and nucleocapsid protein, were analyzed by 12.5% Coomassie-stained SDS-PAGE (A). The efficiency of the separated-WSSV fraction was investigated by immuno-detection assay using anti-VP28 antibody (B).

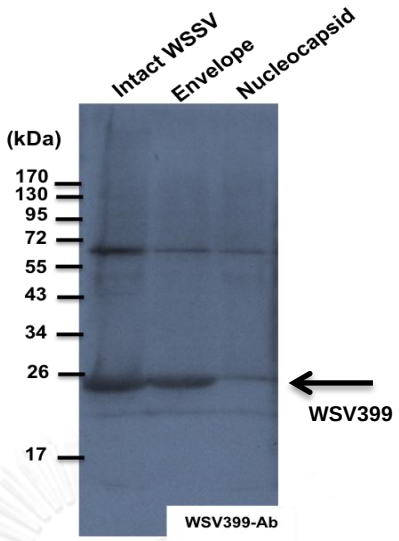

Figure 3.32 Localization of WSV399 on WSSV protein fractions. The presence of WSV399 protein on the intact WSSV virion protein, envelope protein and nucleocapsid protein was determined by western blot analysis using the purified anti-WSV399 polyclonal antibody.

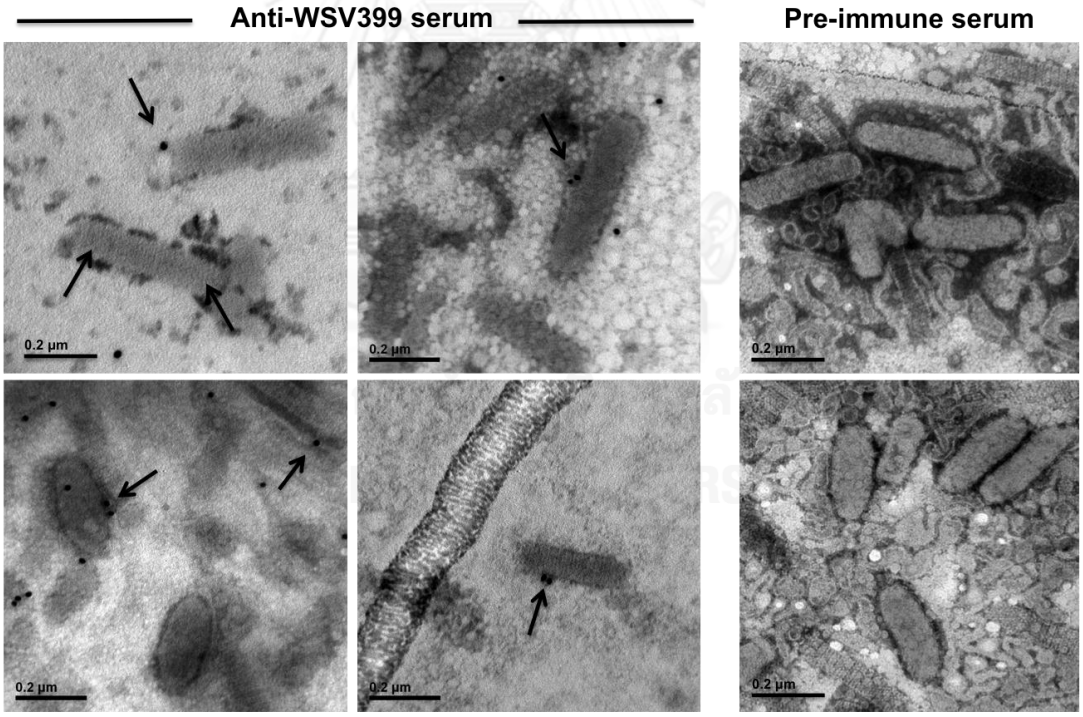

Figure 3.33 Localization of WSV399 on WSSV viron by immuno-electron microscopy using 18 nm-diameter gold particles labeling WSV399 protein.

3.2.6.3. WSV399 gene expression profile in WSSV-infected shrimp hemocyte using RT-PCR technique

The expression profile of WSV399 gene in WSSV-infected shrimp *P. monodon* was investigated by RT-PCR. In this study, the viral genes expression at different stages of viral replication, which are ie-1 (immediate early stage), wsv477 (early stage) and vp28 (late stage), was used as marker genes. After hemocyte of WSSV-infected shrimp at 0, 3, 6, 12, 24, 36 and 48 hpi, was collected. The gene expression level of these viral genes was analyzed by RT-PCR using EF-1α as an internal control. We found that wsv399 expressed at 24 hpi, the gene expression pattern is same as that of vp28 gene indicating that wsv399 transcript was expressed in late stage of viral replication (Figure 3.34).

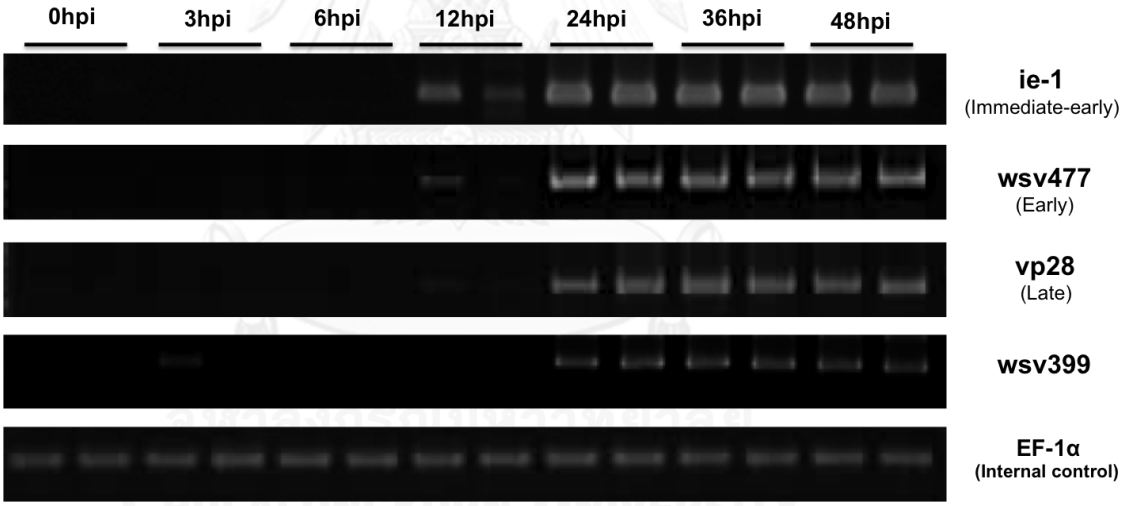

Figure 3.34 The expression profile of WSV399 gene in hemocyte of WSSV- infected shrimp *P. monodon* after 0, 3, 6, 12, 24, 36 and 48 hpi. The expression level of viral gene in various stages which are ie-1 (immediate early stage), wsv477 (early stage) and vp28 (late stage), was used as marker genes. EF-1α gene was used as an internal control. Four individuals were used for each group. The representative data of two individuals per group is shown.

3.2.6.4. Expression of viral gene after WSV399 gene knockdown in WSSV infected shrimp

To identify the function of wsv399 that involved in WSSV replication, wsv399 silencing was performed in WSSV-infected shrimp. After wsv399 gene knockdown, the level of vp28 gene expression was same as that of control shrimp injected with GFP dsRNA (Figure 3.35). We concluded that wsv399 might not be important to WSSV replication. However, the wsv399, which is the tegument protein, might have the other functions. Therefore, the function of wsv399 awaits further characterization.

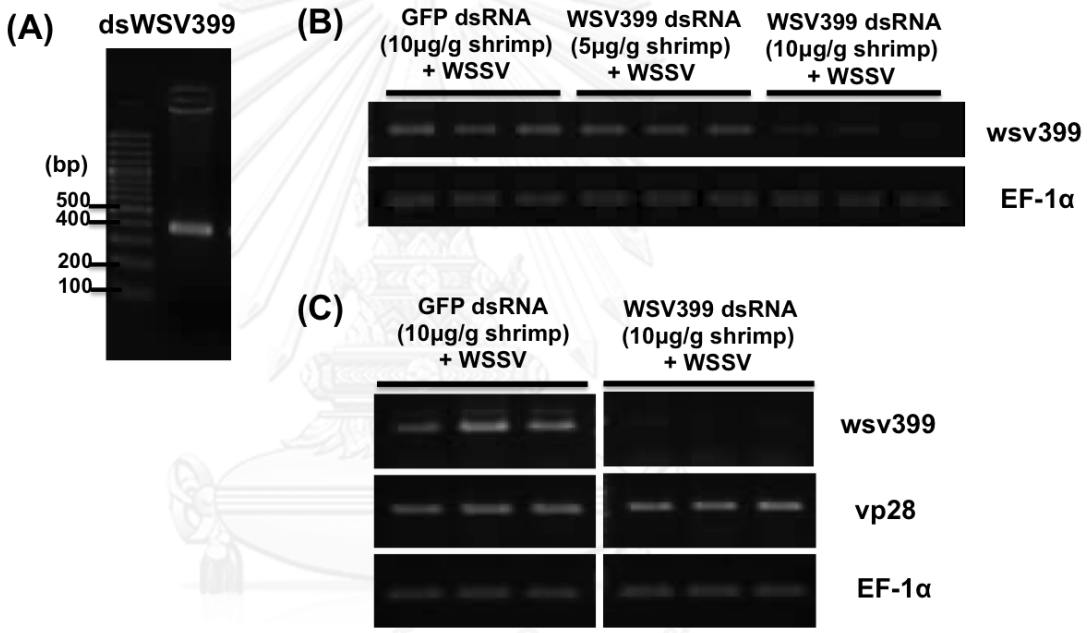

Figure 3.35 The effect of wsv399 gene silencing in WSSV-infected *P. monodon* hemocytes. (A) Production of wsv399 dsRNA. (B) Expression level of wsv399 transcripts after 24 h post-WSSV infection was determined after wsv399 gene knockdown by RT-PCR using gene specific primers. The control was shrimp that was injected with GFP dsRNA. Three individuals were used for each group and each experiment was performed in triplicate. (C) The effect of wsv399 gene silencing on WSSV replication in *P. monodon* hemocytes. Expression level of the WSSV gene, vp28, in wsv399 gene-silenced shrimp hemocytes were determined by RT-PCR.

3.2.6.5. The effect of recombinant WSV399 on *Pm*VRP15 gene expression

Due to the up-regulation of *Pm*VRP15 gene after WSSV infection, we supposed that its partner protein WSV399 identified here as the viral tegument protein, might be involved in the *Pm*VRP15 gene regulation. So, the rWSV399 protein was injected into normal shrimp *P. monodon*. The result showed that *Pm*VRP15 gene in rWSV399-injected shrimp expressed at the same level as the control (Figure 3.36). From this result we can conclude that, WSV399 protein is not involved in *Pm*VRP15 gene regulation, but might be the partner protein that can interact with *Pm*VRP15 protein for some other reason. This should be further explored.

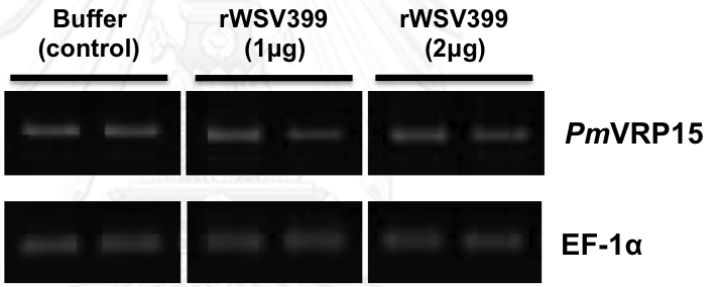

Figure 3.36 The effect of recombinant WSV399 on *Pm*VRP15 gene expression. The rWSV399 (1 and 2 µg) was injected into *P. monodon* and *Pm*VRP15 gene expression was determined by RT-PCR using gene specific primer. The control was shrimp that was injected with buffer only. Four individuals were used for each group. The representative data of two individuals per group is shown.

3.2.7. Determination of genomic organization of *Pm*VRP15 gene

To characterize the genome organization of *Pm*VRP15 gene, *P. monodon* genomic DNA was extracted from pleopod of shrimp using phonol-chloroform method. The quality of *P. monodon* genomic DNA was checked by 1.0% (w/v) agarose gel electrophoresis (Figure 3.37). The open reading frame of *Pm*VRP15 gene was amplified using gene specific primers. The amplicon size amplified from genomic DNA was about 1 Kb which is larger than that of product amplified from cDNA (about 400 bp) as shown in Figure 3.38. The genomic DNA fragment was cloned into T&A cloning vector. The sequence of PCR product was analyzed by DNA sequencing and then compared with the *Pm*VRP15 cDNA sequence. The exon and intron bounderies (AG/GT) of *Pm*VRP15 gene were identified. The *Pm*VRP15 gene contained 3 exons interrupt by 2 introns. Furthermore, the 5' upstream sequence of *Pm*VRP15 gene was identified by 5' genome walking, another exon and intron were identified. In conclusion, the *Pm*VRP15 gene contains 4 exons interrupted by 3 introns and the start codon is located in exon 2 (Figure 3.38).

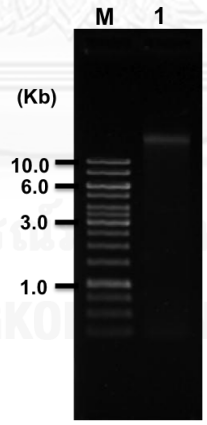

Figure 3.37 Genomic DNA from shrimp *Penaeus monodon.* Lane M: DNA marker, Lane 1: Genomic DNA of shrimp, *P. monodon*.

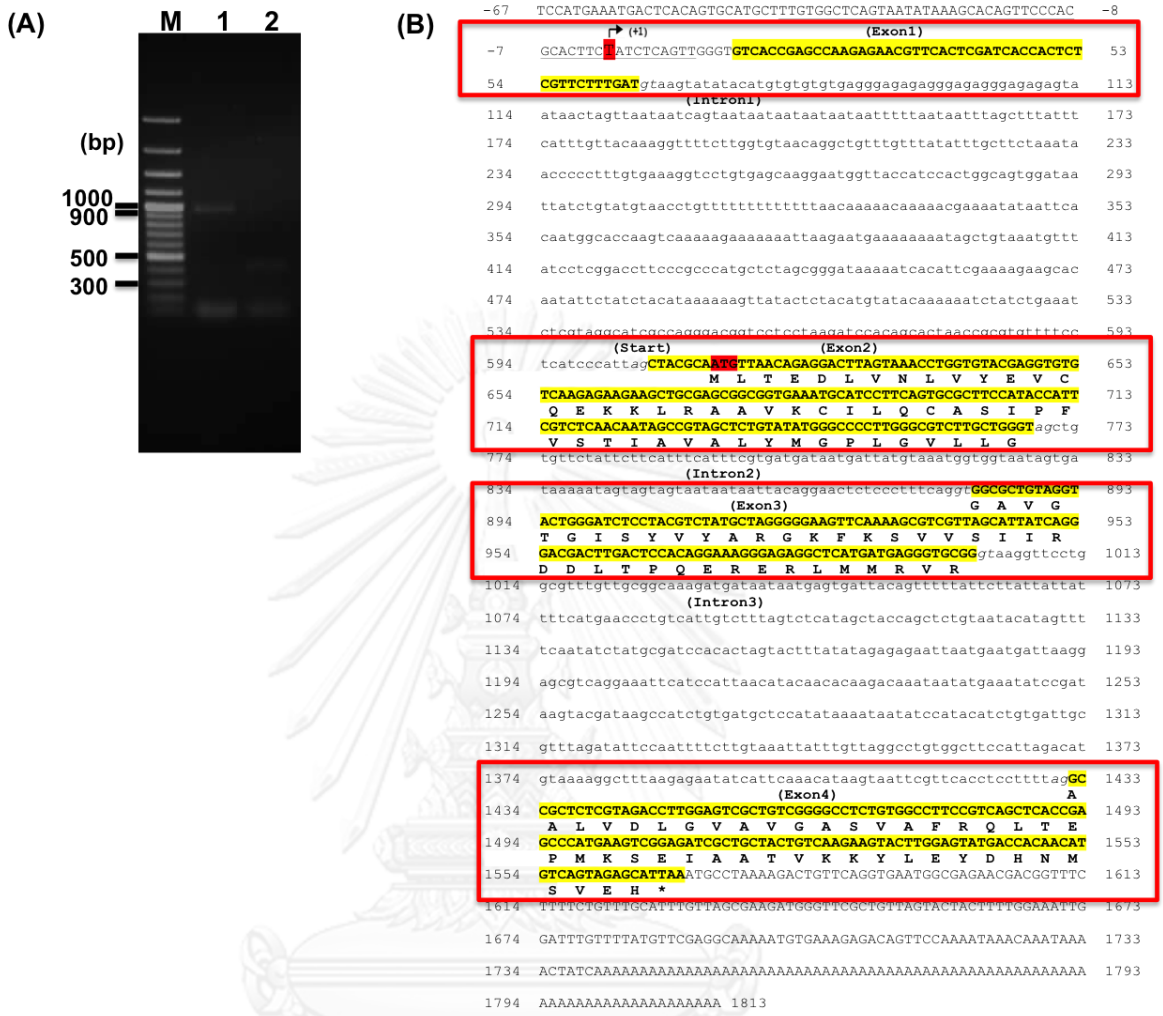

Figure 3.38 Genome organization of *Pm*VRP15 gene. The *Pm*VRP15 gene was amplified from genomic DNA of *P. monodon* (A). Lane M: DNA marker, Lane 1: PCR product of *Pm*VRP15 gene that was amplified from genomic DNA, Lane 2: PCR product of *Pm*VRP15 gene that was amplified from cDNA. The full-length DNA sequence of *Pm*VRP15 gene containing 4 exons interrupted by 3 introns (B).

3.2.8. Characterization of *Pm*VRP15 gene regulation

3.2.8.1. Identification of the promoter of *Pm*VRP15 gene

To study regulation of *Pm*VRP15 gene expression, promoter sequence of *Pm*VRP15 gene was identified by genome walking technique. Four genomic libraries derived from *P. monodon* DNA digested with *Eco*RV, *Stu*I, *Pvu*II and *Dra*I were used as templates. The PCR products of primary and nested PCR were analyzed by 1.0% (w/v) agarose gel electrophoresis (Figure 3.39). The adapter primer was amplified to detect any false positive result using adaptor primer (AP2/AP2). The major band from nested PCR whose size is about 1.4 Kb, was cut (arrow) and cloned into pGEM-T easy vector to identify the DNA sequence. It should be noted that 700 bp from 3'-end out of 1.4 Kb contained exon 1 and intron 1; therefore, the remaining promoter sequence of *Pm*VRP15 gene is about 700 bp. In general, the promoter of the eukaryotic gene is up to 2 Kb in size. So, genome walking was performed once again. The PCR product was analyzed by 1.0% (w/v) agarose gel electrophoresis (Figure 3.40). The major band of new nested PCR was about 1.5 Kb. When the sequence from both genome walking experiments were combined, the size of *Pm*VRP15 promoter sequence obtained was about 2 Kb. The transcription factor start site and TATA box were then predicted (Figure 3.41).

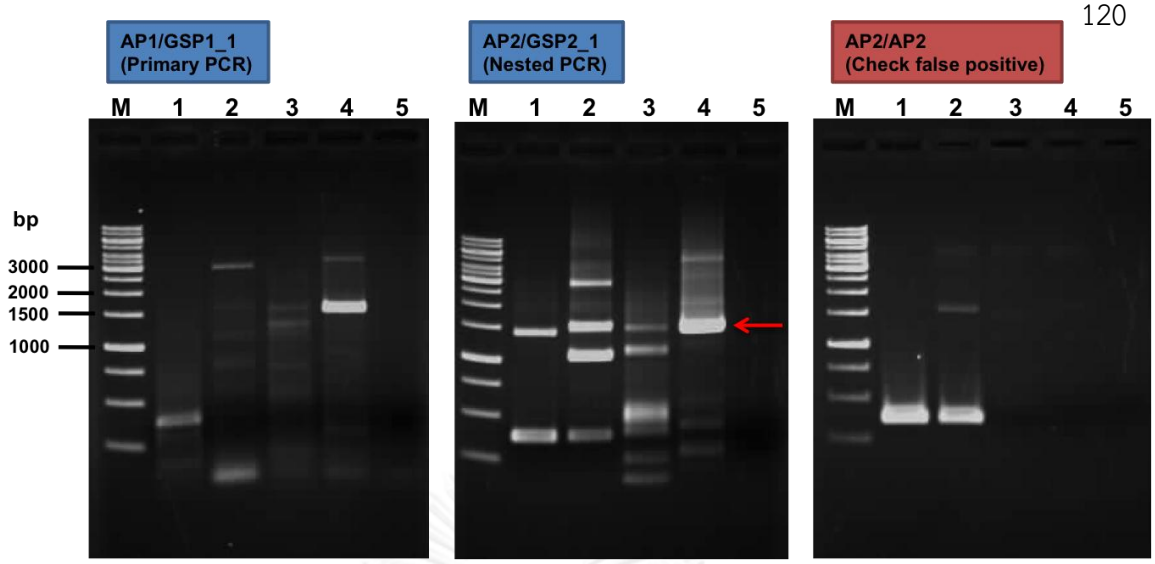

Figure 3.39 Genome walking of *Pm*VRP15 gene (the first trial). Four genomic libraries, *Eco*RV (Lane 1), *Stu*I (Lane 2), *Pvu*II (Lane 3) and *Dra*I (Lane 4) were used as template for amplification using gene specific primers (GSP1_1 and GSP2_1) and adapter primers (AP1 and AP2). The negative control was represented in Lane 5. The major band of nested PCR product is indicated by the arrow.

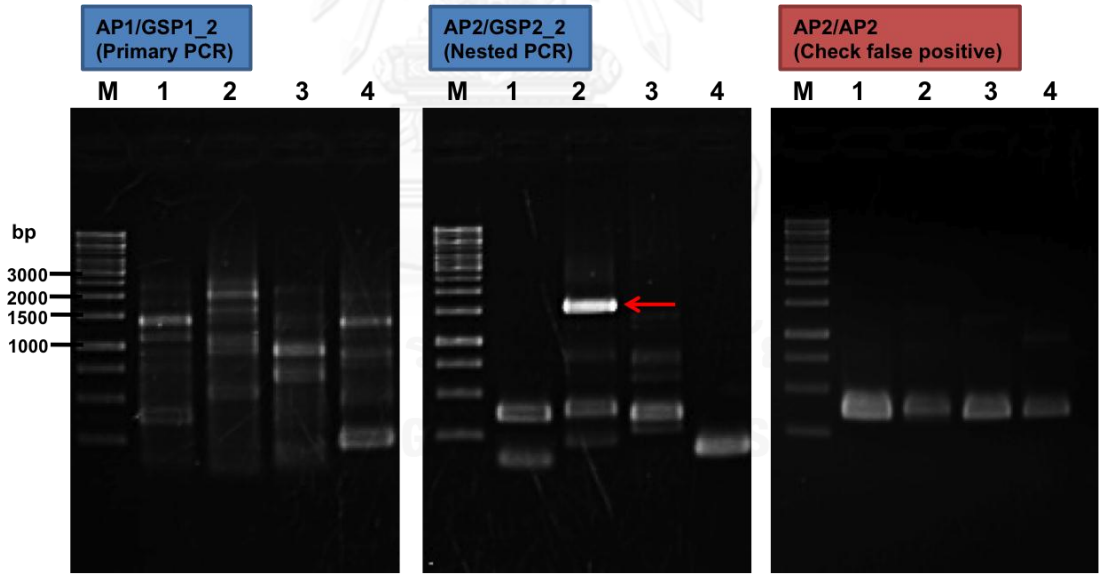

Figure 3.40 Genome walking of *Pm*VRP15 gene (the second trial). The construction of four genomic libraries, *Eco*RV (Lane 1), *Stu*I (Lane 2), *Pvu*II (Lane 3) and *Dra*I (Lane 4) were used as templates for PCR amplification using gene specific primers (GSP1_2 and GSP2_2) and adapter primers (AP1 and AP2). The major band of nested PCR product is shown by the arrow.

Figure 3.41 Genomic and deduced amino acid sequences of *Pm*VRP15. The nucleotide sequence is archived in GenBank (accession number KC250016). Putative cis-acting elements in the 5-flanking promoter region are underlined and designated according to bioinformatic analysis. The position of transcription factor start site (+1) was predicted using Neural Network Promoter Prediction and TATA box located on -25 position is highlighted in dark grey. Sequences of the four exons are highlighted in light grey and the deduced amino acids are shown underneath in single letter code. The start codon (ATG) and stop codon (TAA) are boxed. The polyadenylation signal (AATAAA) is dotted underlined.

3.2.8.2. Narrow down assay of *Pm*VRP15 promoter activity in *Drosophila* S2 cell

The important parts of *Pm*VRP15 promoter sequence that are involved in regulation of *Pm*VRP15 gene expression was identified by promoter narrow down assay. The promoter sequence of *Pm*VRP15 gene containing TATA box and transcription factor binding sites to translation start site (ATG, start codon) was amplified and cloned into a pGL3-basic vector containing the firefly luciferase gene for promoter activity assay. In the first set, *Pm*VRP15 promoter sequences were randomly narrowed down into 5 parts including (-2047/+612), (-1621/+612), (-1147/+612), (-525/+612) and (-92/+612). Each DNA fragment was amplified by PCR using a pair, analyzed by 1.0% agarose gel electrophoresis (Figure 3.42) and cloned into pGL3 vector. The recombinant plasmids, p(-2047/+612), p(-1621/+612), p(-1147/+612), p(-525/+612) and p(-92/+612), were co-transfected into *Drosophila* S2 cell with phRL-null containing AcMNPv *ie*-1 promoter (Control) and promoter activity was determined. As compared to the control, all constructs exhibited the promoter activity but at different level. Of those, at the nucleotide position -1147 to -93 showed significantly high level of activity (Figure 3.43) suggesting that it might take part in controlling *Pm*VRP15 gene expression. Anyway, this promoter region is still too long and the specific regulatory sites cannot be identified. So, the promoter sequence between -1147 to -93 position was narrowed down further. The smaller promoter regions such as (-907/+612), (-727/+612), (-427/+612) and (-208/+612) nucleotide positions, were amplified (Figure 3.42) and cloned into pGL3 vector. The recombinant plasmids, p(-1147/+612), p(-907/+612), p(-727/+612), p(-525/+612), p(-427/+612), p(-208/+612) and p(-92/+612), were transfected into *Drosophila* S2 and their promoter activity were tested. The promoter sequences between -525 to -428 nucleotide positions might have the repressor-binding site because the promoter activity was sharply increased after deletion promoter region (-525/-428) as shown in Figure 3.44. Moreover, the promoter sequence between position -427 to -92 might has the activator binding site, suggested by the significant decrease of promoter activity of p(-92/+612) as compare with that of p(-427/+612). However, the range of promoter region is needed to be narrowed down from -427 position. A serie of

deletion plasmid bearing (-387/+612), (-287/+612) and (-34/+612) nucleotide position of *Pm*VRP15 promoter, was constructed. Upon PCR amplification, the promoter regions were analyzed by 1.0% agarose gel electrophoresis (Figure 3.42) and cloned into pGL3 vector. The recombinant plasmids, p(-427/+612), p(-387/+612), p(-287/+612), p(-208/+612), p(-92/+612) and p(-34/+612), were transfected into *Drosophila* S2. The promoter activity assay showed that the p(-208/+612) has 38% lower in promoter activity as compared to that of p(-287/+612) (Figure 3.45). This indicated that (-287/-209) promoter region might have the activator-binding site.

In conclusion, the *Pm*VRP15 promoter region between -525 to -428 nucleotide position might have the repressor-binding site. The *Pm*VRP15 promoter region between -287 to -209 nucleotide position might have the activator-binding site.

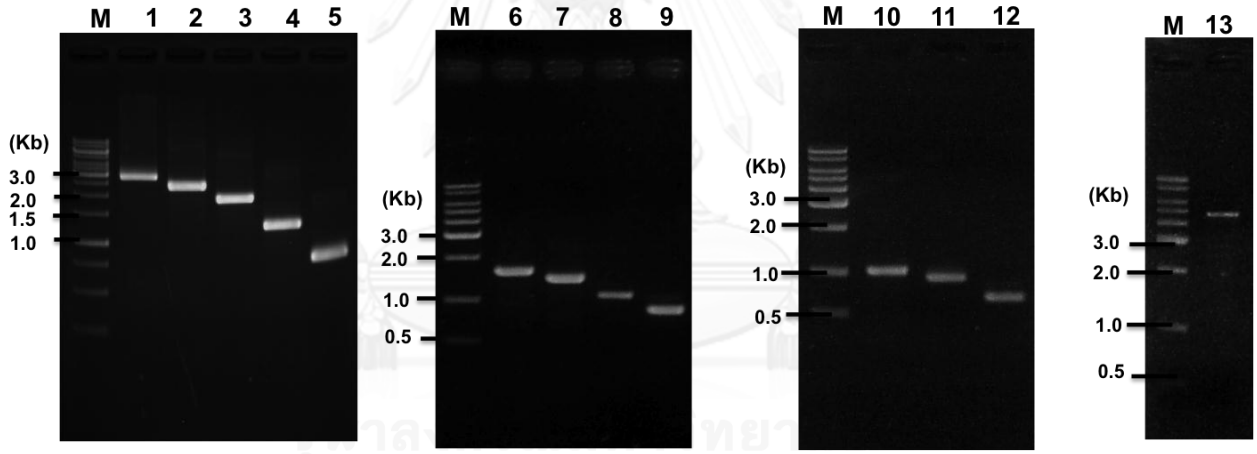

Figure 3.42 Amplification of *Pm*VRP15 promoter regions by PCR. The *Pm*VRP15 promoter regions, such as Lane 1: (-2047/+612), Lane 2: (-1621/+612), Lane 3: (-1147/+612), Lane 4: (-907/+612), Lane 5: (-727/+612), Lane 6: (-525/+612), Lane 7: (-427/+612), Lane 8: (-387/+612), Lane 9: (-287/+612), Lane 10: (-208/+612), Lane 11: (-92/+612) and Lane 12: (-34/+612), were amplified from *P. monodon* genomic DNA. Each promoter region was cloned into pGL3 plasmid (Lane 13) containing firefly luciferase, reporter gene to detect the promoter activity.

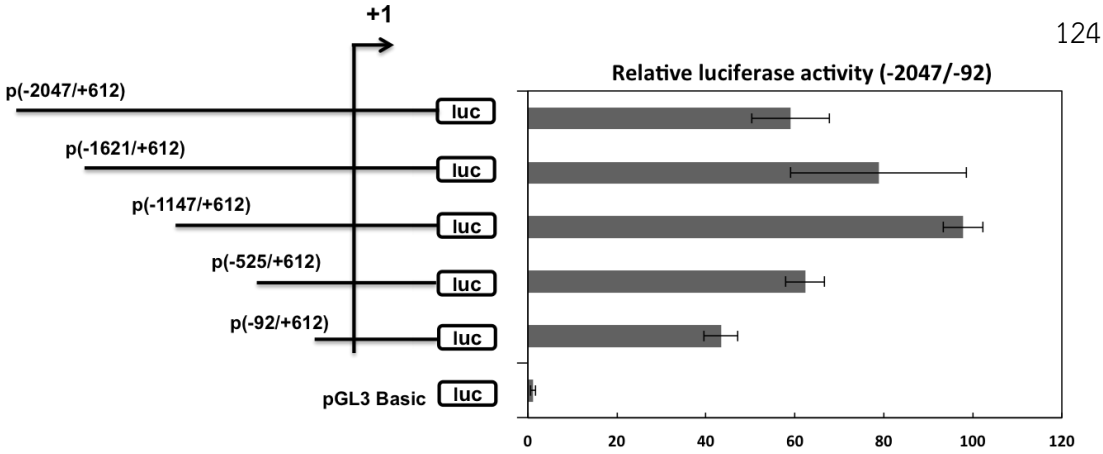

	pGL3	pGL3-promoter VRP15				
		-92	-525	-1147	-1621	-2047
Mean value (%)	1.12	43.37	62.30	97.78	78.85	59.01

Figure 3.43 Functional mapping of the deletion *Pm*VRP15 promoter from positions -2047 to -92. Relative luciferase activity has been normalized to the activity of the p(-1147/+612) plasmid which is arbitrarily set to 100%. Data represents the means from triplicate experiments. Error bars show ± 1 SD. The plasmid numbers in parentheses specify the beginning and end positions of the promoter fragments, and the arrow labeled +1 marks the transcription start site.

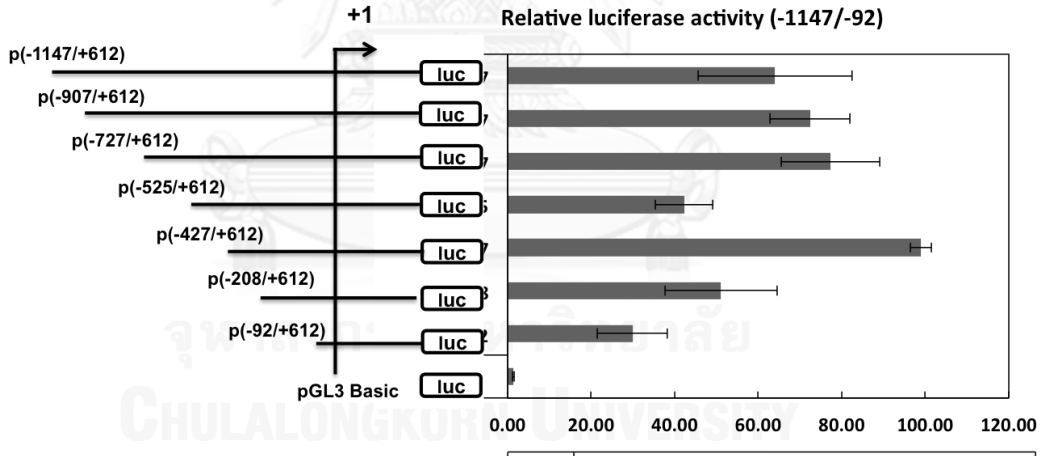

	pGL3	promoter VRP15						
		-92	-208	-427	-525	-727	-907	-1147
mean value (%)	1.36	29.87	51.06	98.96	42.30	77.30	72.40	63.98

Figure 3.44 Functional mapping of the deletion *Pm*VRP15 promoter from position -1147 to -92. Relative luciferase activity has been normalized to the activity of the p(-427/+612) plasmid which is arbitrarily set to 100%. Data represents the means from triplicate experiments. Error bars show ± 1 SD. The plasmid numbers in parentheses specify the beginning and end positions of the promoter fragments, and the arrow labeled +1 marks the transcription start site.

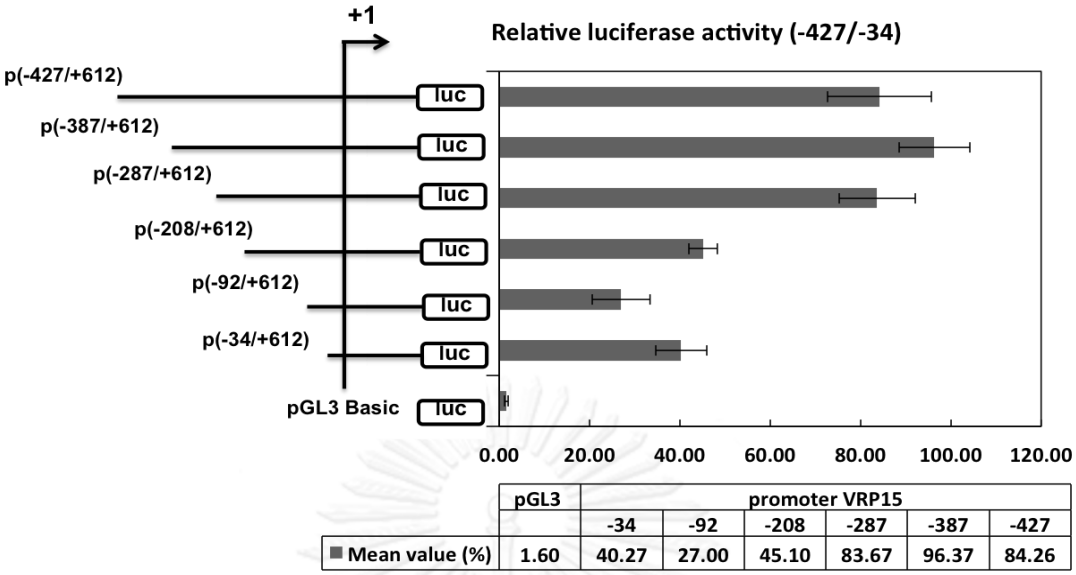

	pGL3	promoter VRP15					
		-34	-92	-208	-287	-387	-427
Mean value (%)	1.60	40.27	27.00	45.10	83.67	96.37	84.26

Figure 3.45 Functional mapping of the deletion *Pm*VRP15 promoter from position -427 to -34. Relative luciferase activity has been normalized to the activity of the p(-387/+612) plasmid which is arbitrarily set to 100%. Data represents the means from triplicate experiments. Error bars show ± 1 SD. The plasmid numbers in parentheses specify the beginning and end positions of the promoter fragments, and the arrow labeled +1 marks the transcription start site.

3.2.8.3. Confirmation of regulatory element by deletion assay

From previous experimental results, the promoter regions, (-525/-428) and (-287/-209) were found to be involved in *Pm*VRP15 gene regulation. These promoter regions were deleted and assay for the promoter activity to confirm the result. For (-525/-428) promoter region deletion, p(-727/+612) was used as a template for rolling PCR to create the -525 to -428 deletion construct, p(-727/+612) del(-525/-428). The promoter activity of deletion plasmid was compared with parental plasmid. The result (Figure 3.46) showed that the promoter activity of p(-727/+612) del(-525/-428) was 35.7% higher than that of p(-727/+612) indicating that the promoter sequence between -525 to -428 region has the repressor-binding site. To study the importance of -287 to -209 region in *Pm*VRP15 gene regulation, p(-387/+612) was used as a template to construct the (-287/-209) deletion plasmid, p(-387/+612) del(-287/-209). After transfection and promoter activity determination, the promoter activity of

p(-387/+612) del(-287/-209) was decreased for 34% when compare with the control p(-387/+612) as shown in Figure 3.47. In conclusion, the promoter region between -287 to -209 nucleotide position contains the activator-binding site.

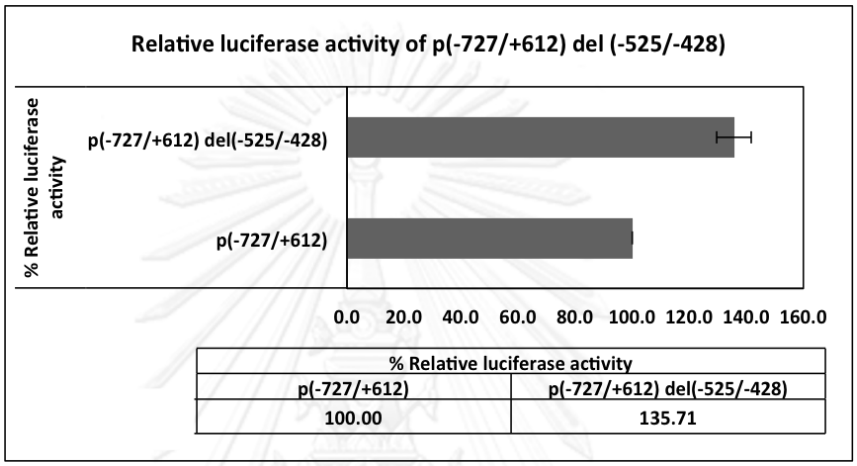

% Relative luciferase activity	
p(-727/+612)	p(-727/+612) del(-525/-428)
100.00	135.71

Figure 3.46 Effect of deleting the (-525/-428) nucleotide fragment from the *Pm*VRP15 promoter region. The deletion plasmid construct, p(-728/+612) del (-525/-428) where (-525/-428) region of the *Pm*VRP15 promoter is missing, was assayed for promoter activity in comparison with the parental plasmid p(-728/+612). The experiment was performed in triplicate. The relative luciferase activity is expressed as mean ± 1 SD.

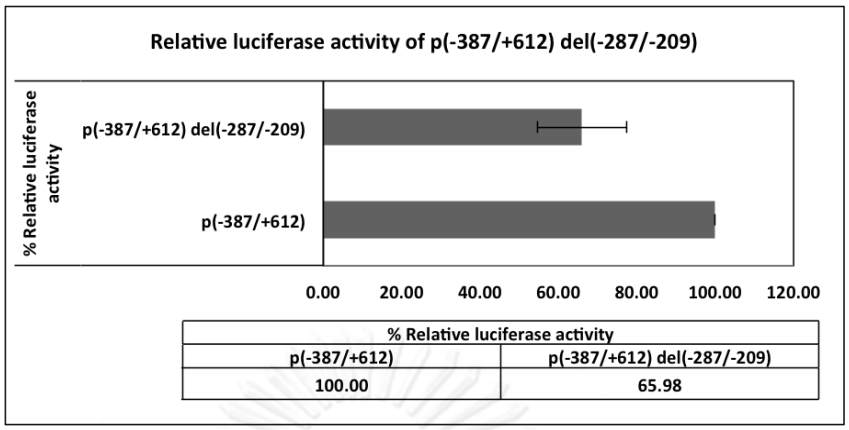

Figure 3.47 Effect of deleting the (-287/-209) nucleotide fragment from the *Pm*VRP15 promoter region. The deletion plasmid construct, p(-387/+612) del (-287/-209) where the (-287/-209) region of the *Pm*VRP15 promoter is missing, was assayed for promoter activity in comparison with the parental plasmid p(-387/+612). The experiment was performed in triplicate. The relative luciferase activity is expressed as mean ± 1 SD.

3.2.8.4. Predication of transcription factor binding site from *Pm*VRP15 promoter fragments by bioinformatics analysis

The DNA sequences at positions (-525/-428) and (-287/-209) of *Pm*VRP15 promoter region was predicted for the transcription factor binding sites by computational analysis. Many computer programs and transcription factor binding site databases, which are TF search ver.1.3, Match 1.0 (TRANSFAC® Public database) and Alibaba (TRANSFAC® Public database) were used to identify transcription factor binding site on *Pm*VRP15 promoter region. In the (-525/-428) promoter region, the repressor-binding site, many transcription factor binding sites were found which are CCAAT/enhancer binding protein (C/EBP) on the nucleotide positions -460 to -452, spleen focus forming virus (SFFV) proviral integration oncogene spi1 (PU.1) on the nucleotide positions -493 to -484, Myb proto-oncogene protein (Myb) on the nucleotide positions -517 to -511, proto-oncogene c-Rel transcription factor (Rel) on the nucleotide positions -508 to -499, interferon regulatory factor (IRF) on the nucleotide positions -485 to -481 and -437 to -433 and nuclear transcription factor Y

subunit beta (NFYB) on the nucleotide positions -480 to -475 (Figure 3.46A). In the (-287/-209) promoter region, the activator-binding site, many transcription factor binding sites were found which are octamer transcription factor binding site 1 (Oct-1) on the nucleotide positions -275 to -268, CCAAT/enhancer binding protein (C/EBP) on the nucleotide positions -268 to -260, nuclear factor of activated T-cells transcription factor (NFAT) on the nucleotide positions -229 to -224 and Ultrabithorax (Ubx) on the nucleotide positions -257 to -252 (Figure 3.47A).

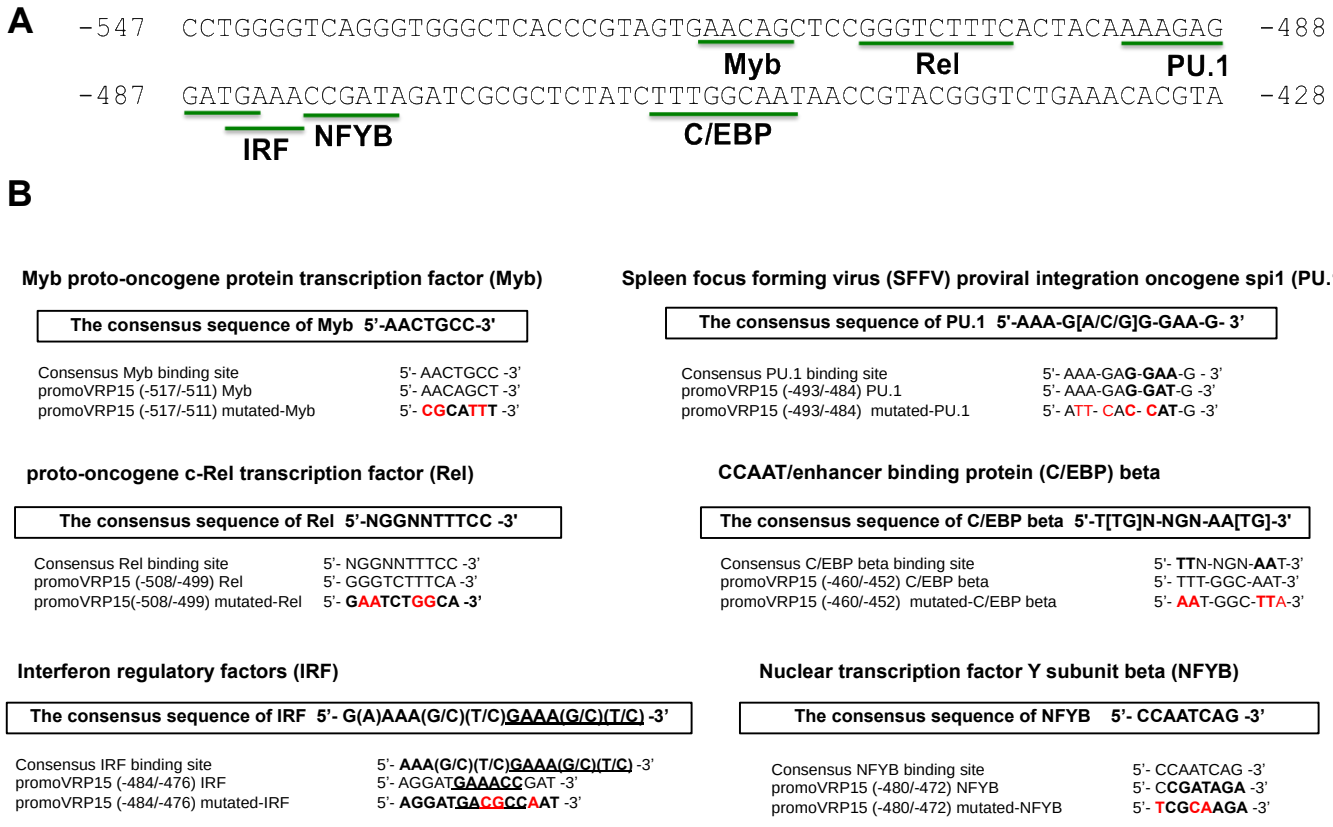

Figure 3.48 Transcription factor binding site on the (-525/-428) *Pm*VRP15 promoter region. Prediction of the transcription factor binding site on the (-525/-428) *Pm*VRP15 promoter region was analyzed by computational analysis (A). Sequences of the consensus, wild-type, and mutated transcription factor binding sites are shown. The grey labeled letters indicate the mutated nucleotides (B).

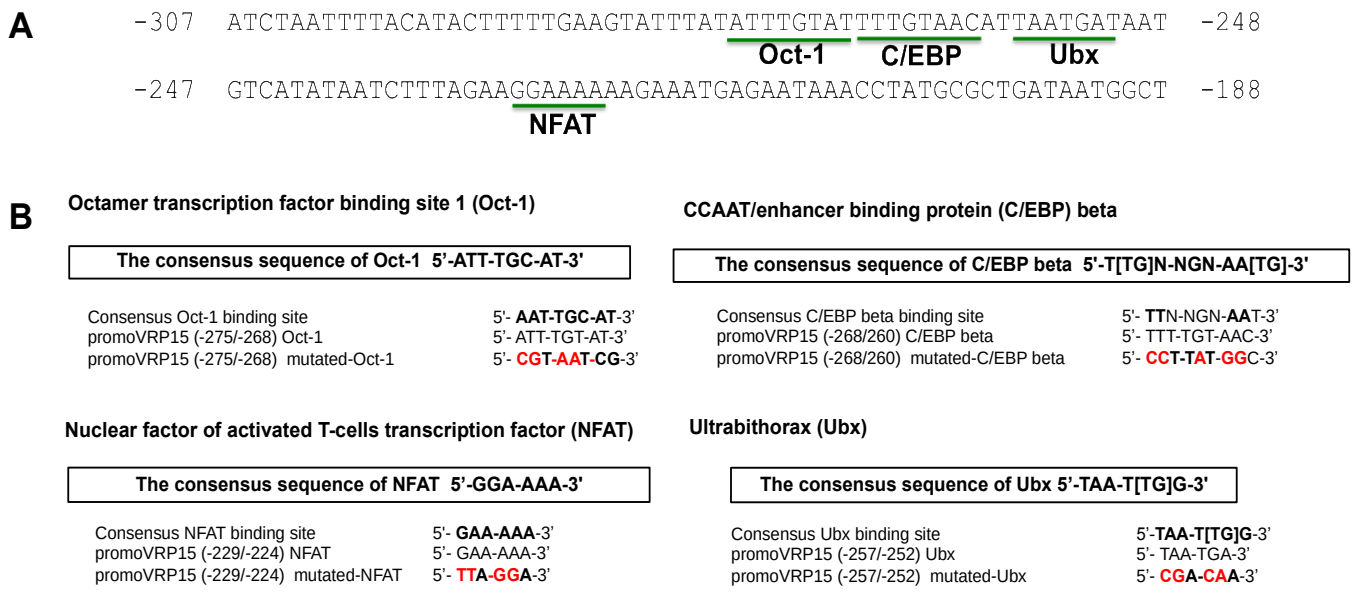

Figure 3.49 Transcription factor binding site on the (-287/-209) *Pm*VRP15 promoter region. Prediction of the transcription factor binding site on the (-287/-209) *Pm*VRP15 promoter region was analyzed by computational analysis (A). Sequences of the consensus, wild-type, and mutated transcription factor binding sites are shown. The grey labeled letters indicate the mutated nucleotides (B).

3.2.8.5. Identification of the transcription factor that can regulate *Pm*VRP15 promoter by site-directed mutagenesis technique

To further confirm that the predicted of transcription factor binding sites play role in regulating *Pm*VRP15 gene expression, site-directed mutagenesis was performed by rolling PCR. The gene specific primers containing mutated nucleotides of the conserved nucleotide on transcription binding site were used. For the -525/-428 *Pm*VRP15 promoter region, the mutation of transcription factor binding sites of Myb (-517/-511), Rel (-508/-499), IRF (-484/-476) and NFYB (-480/-427) was performed using p(-525/+612) as a template. The promoter activity was measured and compared with that of wild type, p(-525/-428). After mutation of IRF binding site, the promoter activity was increased for about 23% as compared with the control

(Figure 3.50) indicating that IRF transcription factor is a putative repressor binding to *Pm*VRP15 promoter.

Mutation on the -287/-208 *Pm*VRP15 promoter region, at different transcription factor binding sites such as Oct-1 (-275/-268), C/EBP (-268/-260), NFAT (-229/-224) and Ubx (-257/-252) was performed using p(-287/+612) as a template. The promoter activity of the mutated constructs was compared with that of parental plasmid p(-287/+612). After mutation of Oct-1 and NFAT binding sites, the promoter activity was decreased for about 60% and 49%, respectively, when compared with the control (Figure 3.51). These indicated that Oct-1 and NFAT transcription factors are the putative activator binding to *Pm*VRP15 promoter.

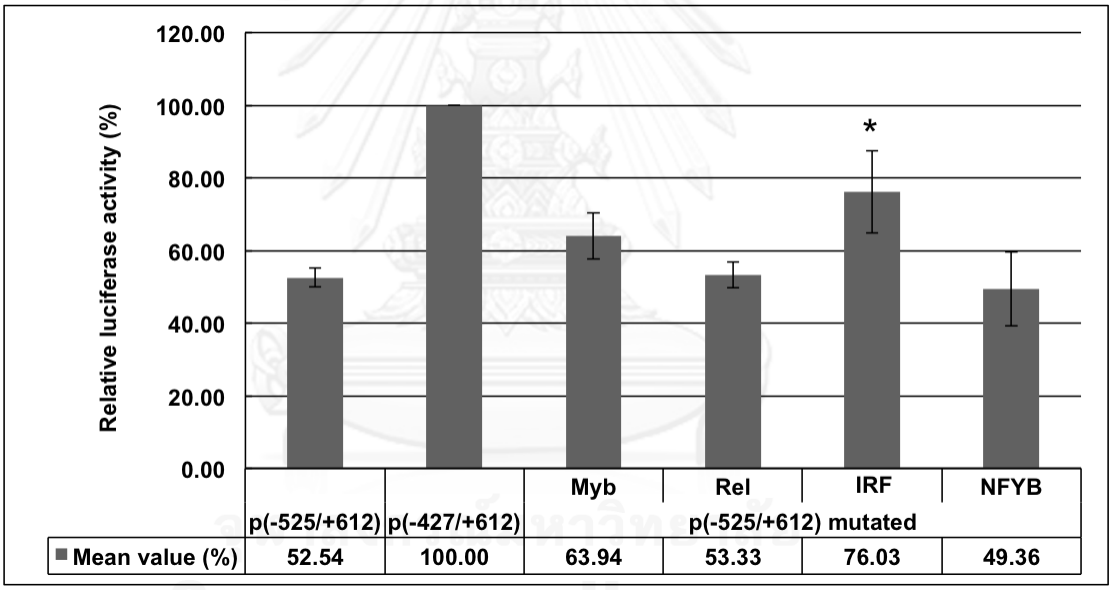

Figure 3.50 Site-directed mutagenesis of transcription factor binding sites on the (-525/-428) *Pm*VRP15 promoter region. Relative luciferase activity of *Pm*VRP15 p(-525/+612) promoter constructs with wild-type or mutated transcription factor binding sites (Myb, Rel, IRF and NFYB) were shown. Data represents the means ± SDs from three independent experiments. Means with an asterisk are significantly higher than control, p(-525/+612).

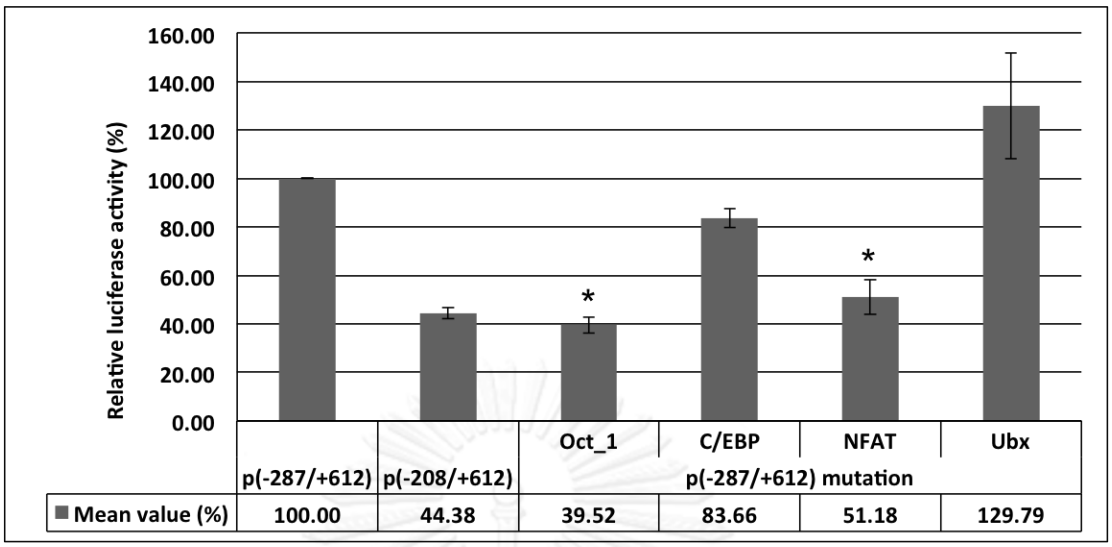

Figure 3.51 Site-directed mutagenesis of transcription factor binding sites on the (-287/-209) *Pm*VRP15 promoter region. Relative luciferase activity of *Pm*VRP15 p(-287/+612) promoter constructs with wild-type or mutated transcription factor binding sites (Oct-1, C/EBP, NFAT and Ubx) were shown. Data represents the means ± SDs from three independent experiments. Means with an asterisk are significantly lower than control, p(-287/+612).

CHAPTER IV
DISCUSSION

Effect of the anti-lipopolysaccharide factor isoform 3 (ALF*Pm*3) from *Penaeus monodon* on *Vibrio harveyi* cells

So far, several AMPs have been identified in shrimp. They are such as crustins, penaeidins, ALFs and stylicins. Among them, ALF*Pm*3 exhibits the broadest reported range of antimicrobial activity (Somboonwiwat *et al.* 2005, Amparyup *et al.* 2008, Supungul *et al.* 2008, Rolland *et al.* 2010). Compared to crustin*Pm*7 (a cationic peptide) and *Ls*-stylicins 1 (an anionic peptide), ALF*Pm*3 exhibits the strongest antibacterial activity against *V. harveyi*, which is an important shrimp bacterial pathogen (Somboonwiwat *et al.* 2005, Amparyup *et al.* 2008, Rolland *et al.* 2010). The MIC value of rALF*Pm*3 on *V. harveyi* 639 determined in this study (0.78–1.56 μM) was the same as that reported previously for *V. harveyi* 1526 (0.78–1.56 μM) (Somboonwiwat *et al.* 2005).

According to the 3D structure, ALF*Pm*3 contains three α-helices packed against four strands of β-sheet. By comparative molecular modeling, the hypothetical LPS-binding domain is located on the S2–S3 β-hairpin that is stabilized by a disulfide bond. This binding site consists of six positively charged amino acid residues (four Lys and two Arg) that might bind to the hydrophilic and phosphate groups of lipid A on the bacterial membrane (Yang *et al.* 2009). ALF*Pm*3 has been shown to be able to bind to the principal bacterial cell wall components of Gram-negative (LPS) and Gram-positive (LTA) bacteria, as well as to whole (intact) *E. coli* 363 and *Bacillus megaterium* cells (Somboonwiwat *et al.* 2008). We showed here that rALF*Pm*3 could also bind to *V. harveyi* cells, which may suggest a common mechanism of rALF*Pm*3 binding on various bacteria. In this scenario, the peptide initially binds to the cell wall of bacteria through the ionic interactions between the cationic peptide and the negatively charged of bacterial cell wall components.

Typically, most cationic AMPs have been reported to operate through membrane permeabilization/disruption, but interactions with intracellular targets or

disruption of cellular processes have also been reported (Brogden 2005, Nicolas 2009). Although the ALF from the Indian mud crab *Scylla serrata* has been reported to be able to permeabilize artificial membranes *in vitro* (Yedery and Reddy 2009), we reported for the first time the *in vivo* study of rALF*Pm*3 permeabilization activity on the outer and inner membranes of *V. harveyi.* The shrimp AMP, crustin*Pm*7, has been reported recently to be able to permeabilize the inner membrane of *E. coli* MG1655 but with a lower activity compared to that reported here for rALF*Pm*3 (Krusong *et al.* 2012). The rALF*Pm*3-treated *V. harveyi* cells showed a significant increase in the nucleotide leakage, indicating that after rALF*Pm*3 binding to the membrane lipid it causes membrane permeabilization to varying extents and this was in a time- and concentration-dependent manner, as inferred from the deduced levels of the induced nucleotide leakage. Thus, rALF*Pm*3 likely penetrates across the bacterial membrane and forms a transmembrane pore leading to the leakage of the bacterial cytoplasmic contents. However, the pores size on *V. harveyi* membrane after ALF*Pm*3 disruption has not measured yet. To investigate pore size on bacterial membrane after AMPs treatment, several techniques could be applied such as Atomic force microscopy (AFM) (Meincken *et al.* 2005) and Neutron diffraction (Yang *et al.* 1999). Besides, the artificial membrane containing various sizes of fluorescence dye can also be used to estimate the pore size on bacterial membrane (Ladokhin *et al.* 1997). Lacticin Q is a pore-forming bacteriocin and its antimicrobial activity is in the nanomolar range as of ALF*Pm*3. Liposomes containing green fluorescent protein, protein from live bacterial cells and dextran (diameter of 4.6 nm), were treated with Lacticin Q resulted in the dextran leakage implying that Lacticin Q can produce 4.6 nm pores on bacterial membrane (Yoneyama *et al.* 2009). According to our results, it should be noted that the pore size on *V. harveyi* cells treated with rALF*Pm*3 should be big enough for macromolecule like β-galactosidase and nucleotide to pass through.

The intracellular killing model is another possible mode of antimicrobial action of AMPs. AMPs translocate into bacterial cell and inhibit the cellular processes such as DNA, RNA and protein synthesis as well as enzyme activity. For example, mode of action of BuforinII and tachyplesin is involved binding to DNA/RNA that

cause inhibition of the cellular function (Yonezawa *et al.* 1992, Park *et al.* 1998). Pleurocidin, dermaseptin, PR-39, HNP-1/2 and indolicidin, can inhibit nucleic acid and protein synthesis of bacterial cell (Lehrer *et al.* 1989, Boman *et al.* 1993, Subbalakshmi and Sitaram 1998, Patrzykat *et al.* 2002). In some cases, AMPs employ both membrane disruption and intracellular killing for their antimicrobial acitivity. For example, at a higher concentration of pleurocidin, 5-MIC, it can inhibit macromolecular synthesis and also disrupt the bacterial cell membrane (Mason *et al.* 2007). In this research, I only focused on the membrane disruption mechanism of ALF*Pm*3; therefore, the intracellular mechanism of ALF*Pm*3 will be further investigated.

Previously, several studies showed that the cellular damages of bacterial cells treated with AMP were continued to accumulate behind the time required for antimicrobial killing. For example, *Pseudomonas aeruginosa* exposed to SMAP19 and CAP18 was killed in 15 min; however, the ultrastructural damage continued for up to 8 h (Kalfa *et al.* 2001). SEM and TEM evaluation of the changes in the ultrastructure of the *V. harveyi* cells after rALF*Pm*3 incubation for up to 1 h revealed several distinct signs of cell damage in support of the above postulated pore formation by rALF*Pm*3, such as cytoplasmic content leakage, bleb formation and potential pore formation. The blebs protruded on the surface of *V. harveyi* cells after rALF*Pm*3-treating, might be caused by the positive charge on the LPS-binding site of rALF*Pm*3 substituting for the cations, such as K^{+}, Ca^{2+} and Mg^{2+}, on the outer membrane of the bacteria leading to the outer membrane of bacteria being destabilized. After that, the inner membrane was permeabilized and the cytoplasmic content leaked to the periplasmic space resulting in the protruding of the outer membrane from the bacterial surface (da Silva and Teschke 2003).

Overall, we conclude that rALF*Pm*3 can bind to *V. harveyi* cells leading to the permeabilization of the bacterial membranes, and that this is likely to be pore formation. The cytoplasmic contents of the bacterial cell can then leak from the inside to the outside of the cells leading to cell death. The understanding of mechanism of action of rALF*Pm*3 is essential for its development as a therapeutic agent.

Functional characterization and promoter analysis of a viral responsive protein 15 (*Pm*VRP15) gene from black tiger shrimp, *Penaeus monodon*

From the previous report (Li and Xiang 2013), the shrimp antiviral immune pathways were reviewed. Toll pathway, Imd pathway and JAK/STAT pathway are activated upon viral infection and the signal are transmitted resulting in the production of the antiviral proteins that can inhibit viral infection. However, the functions of the antiviral proteins are still unclear.

Previously, the viral responsive protein 15 (*Pm*VRP15) has been identified by suppression subtractive hybridization (SSH) (Prapavorarat, 2010) but it is a novel protein with unknown function. *Pm*VRP15 gene expression was the highest up-regulated (9,000 fold) at 48 h after WSSV infection (late stage of infection) as compared with the uninfected-shrimp and its gene transcripts were mainly expressed in the hemocytes. The *Pm*VRP15 protein expression was localized on the uninfected and WSSV-infected shrimp hemocytes. After WSSV infection, *Pm*VRP15 protein was also over-expressed when compared with control and located around nuclear membrane (Vatanavicharn *et al.* 2014). Nuclear membrane proteins have been reported in many vertebrates to act as a path of infection for viruses, such as influenza virus (Hutchinson and Fodor 2012) and herpes virus (Bjerke and Roller 2006, Lee and Chen 2010). However, such protein functions remain unknown in invertebrates. Therefore, the role of *Pm*VRP15 in WSSV infection needed to be elucidated.

Many WSSV inducible genes in shrimp were identified which are genes in Toll and Imd pathways, the Ras-activated endocytosis process, the RNA interference pathway, anti-lipopolysacharide factors and many novel genes with unknown function (Li *et al.* 2013). At present, the RNA interference was used to identify function of various viral-inducible genes. From the previous report (Ongvarrasopone *et al.* 2008), after silencing of *Pm*Rab7 gene, the vp28 gene and also protein expression in WSSV-infected shrimp, which is WSSV major envelope protein, was decreased. This means that *Pm*Rab7 plays important roles for WSSV replication in shrimp. After *Pm*VRP15 gene knockdown, viral gene expression in various stages of WSSV infection, which are ie-1 for immediate early stage, wsv477 for early stage and

vp28 for late stage, was reduced and also the cumulative mortality of WSSV-infected *Pm*VRP15 knockdown shrimp was lower than control, WSSV-infected shrimp. Our results indicated that *Pm*VRP15 was involved in WSSV infection and important to WSSV replication in shrimp.

To further characterize the involvement of *Pm*VRP15 in WSSV-infection in shrimp, we used yeast-two hybrid screening to identifiy the protein partner that can interact with *Pm*VRP15 protein. Because *Pm*VRP15 was highly expressed after WSSV-infected shrimp, WSSV-infected shrimp hemocyte and WSSV ORF libraries was used for screening. The mature *Pm*VRP15 protein was screened in both libraries and no interacting protein was found. This might be because of transmembrane structure of *Pm*VRP15 protein, blocks the localization of *Pm*VRP15 into nucleus as a result it cannot interact with other proteins and show no transcription of reporter gene. Therefore, *Pm*VRP15 protein was separated into 2 parts, which are N- and C- terminus fragments without transmembrane protein portion. Yeast two-hybrid screening of *Pm*VRP15 fragments identified a WSSV protein, WSV399, which can interact with *Pm*VRP15 N-terminus fragment. No interacting-protein with C- terminus fragment was found. Co-immunoprecipitation technique was confirmed the interaction between the mature *Pm*VRP15 and WSV399 proteins.

Unfortunately, the function of WSV399 was still unidentified. Therefore, we performed WSV399 localization on WSSV virion by western blot analysis as well as immune electron microscopy. We confirmed that WSV399 was a tegument protein of WSSV. Like others WSSV tegument proteins such as VP26 (the major tegument protein of WSSV), VP36A, VP39A and VP95. WSV399 was found on both envelope and nucleocapsid parts of WSSV when virion was fractionated by Triton X-100 in the low salt condition (Tsai *et al.* 2006). Like the known tegument protein of WSSV, VP26, WSV399 protein was detected on unenveloped WSSV virion by immunogold electron microscopy.

From our results, *Pm*VRP15 could interact with WSV399, which is a tegument protein of WSSV. Previously, it has been reported that the tegument protein of WSSV, VP26 can bind to shrimp proteins such as β- actin, WSSV-binding protein (WBP), MjLecA, LvCTL1 and PlgC1qR, and 3 KDa WSSV-binding protein (WBD) (Youtong *et al.*

2011, Sritunyalucksana *et al.* 2013). Liu *et al.* (2011) showed that VP26 can interact with cell membrane of the *Fenneropenaeus chinensis* hemocyte and β- actin. The function of viral interacting protein, β- actin, might be involved in the viral nucleocapsid movement that can help WSSV replication in shrimp. Upon neutralization of WSSV with WBD protein, viral replication was reduced depends on WBD protein concentration. Other WSSV viral tegument proteins such as VP24, VP95 and VP26, could interact with LvCTL1, a C-type lectin from *Litopenaeus vannamei* (Zhao *et al.* 2009). After recombinant LvCTL1 binding to WSSV protein, the shrimp survival rate was significantly increased after WSSV infection. *Pl*gC1qR protein from fresh water crayfish, *Pacifastacus leniuslus*, the interacting protein of VP28 (envelope protein), VP26 (tegument protein) and VP15 (nucleocapsid protein), plays role in controlling antiviral mechanism as revealed by increase of viral replication upon *Pl*gC1qR silencing (Watthanasurorot *et al.* 2010).

The expression profile of wsv399 gene was characterized in hemocyte of WSSV-infected shrimp at various time points. The result showed that wsv399 gene was produced at 24 hpi, late stage of WSSV replication. Like *Pm*VRP15 gene expression profiling was also up-regulated at 24 hpi. So, this result confirmed the involvement of *Pm*VRP15 and wsv399 in WSSV infection in shrimp. Accoding to the above information, the shrimp proteins that can bind to the tegument proteins of WSSV have several possible roles; therefore, function of *Pm*VRP15 is needed to be characterized.

Because the function of WSV399 was unknown, knocking down of wsv399 gene was performed in order to reveal its importance in viral replication. Unfortunately, wsv399 gene knockdown did not affect the level of vp28 gene expression indicating that wsv399 might be not important to WSSV replication. However, the viral tegument protein of Herpes simplex virus type I has many functions for example capsid transport during entry and egress; targeting of the capsid to the nucleus; regulation of transcription, translation and apoptosis; DNA replication; immune modulation; cytoskeletal assembly; nuclear egress of capsid; and viral assembly and final egress (Kelly *et al.* 2009). According to our results, *Pm*VRP15 gene expression was highly up-regulated after WSSV infection and could interact with

tegument protein of WSSV, WSV399. We hypothesized that *Pm*VRP15 gene expression might be regulated by WSV399 protein. The effect of recombinant WSV399 protein in regulating *Pm*VRP15 gene expression was investigated. Unfortunately, the expression of *Pm*VRP15 gene was not changed in the presence of WSV399 indicating that *Pm*VRP15 gene was not regulated by WSV399 protein. Therefore, the function of tegument protein, wsv399, will need further investigation.

The *Pm*VRP15 gene expression was the highest up-regulated after WSSV infection that about 9,000 times compared with uninfected-shrimp. Therefore, gene regulation of *Pm*VRP15 gene expression was interesting to be characterized. We first characterized its genome organization. It contained 4 exons interrupted by 3 introns. The putative transcription start site was predicted at 612 bp before start codon.

Narrow down of the 5' flanking promoter sequence and deletion assay were used to identify specific region that are involved in gene regulation. After deletion of the promoter region at position (-525/-428), the promoter activity was increased but after deletion of the promoter region at position (-287/-209), the promoter activity was decreased. From this result, we concluded that *Pm*VRP15 promoter regions on the positions (-525/-428) and (-287/-209) contained repressor and activator binding sites, respectively. The transcription factor binding sites on both regions were predicted by computational analysis and confirmed by site-directed mutagenesis.

On the position (-525/-428), the interferon regulatory factor (IRF) binding site was identified as the repressor binding site that regulated *Pm*VRP15 gene expression. Many report revealed the involvement of IRFs in viral infection by controlling the host immune responses. IRF acted as the activator to induce interferon expression but some of them also acted as the repressor. The IRFs family comprises 9 members: IRF1, IRF2, IRF3, IRF4 IRF5, IRF6, IRF7, IRF8 and IRF9. An IRF was identified in virus, Kaposi's sarcoma–associated herpes virus (KSHV), and called viral interferon regulatory factor (vIRF) (Taniguchi *et al.* 2001). The IRF genes were up-regulated after viral infection or interferon stimulation. For example, IRF1 induced transcriptional activation of interferon genes, IFN-**α/β**, could be repressed by IRF2 (Harada *et al.* 1990). Virus produced the interferon regulatory factor (vIRF) to inhibit the activation-induced cell death (Kirchhoff *et al.* 2002). The function of vIRFs was not only

inhibited IFN-mediated innate immune response, but also degraded the host cell growth control mechanism (Lee *et al.* 2009).

IFNs carry out a wide range of biological effects, which include inhibition of pathogen replication and cell growth as well as modulation of the immune responses and of the expression of several genes (Pestka 2007). In 2005, the interferon-like protein (IntlP) was found in WSSV-resistance shrimp, *Penaeus japonicas* (He *et al.* 2005) amd known as the antiviral factor The expression of the IntlP protein transcript has increased in virus-resistant shrimp and the non-specific antiviral activity of IntlP protein was shown by its ability to inhibit SGIV (grouper iridovirus) in GP cells (grouper embryo cells). Moreover, the IntlP has the antibacterial activity against three Gram-negative bacteria, *Vibrio alginolyticus, Vibrio parahemolyticus* and *Vibrio vulnificus* (Mai *et al.* 2009). The intlP shows structural and functional properties similar to mammalian type I IFNs. On the contrary, there is a report suggested that IntlP is in fact a portion of the mitochondrial F0-ATP synthase (60–73% identity with insect F0-ATP synthase β -chain) but not a homologue of mammalian type I interferon (Rosa and Barracco 2008). However, the involvement of IRFs in innate and adaptive immune responses that are regulated by Toll-like receptors and cytosolic pattern-recognition receptors has been reported (Honda and Taniguchi 2006). Due to the possible involvement of IRF in viral infection, knowledge of *Pm*VRP15 gene regulation by IRF is interested to be explored.

The Octamer transcription factor binding site (Oct-1) and Nuclear factor activated T-cell binding site (NFAT) located at position (-287/-209) were identified as the activator binding site that regulated *Pm*VRP15 gene expression. The octamer-binding proteins (Oct) are groups of highly conserved transcription factors belonging to the POU domain family. The Oct transcription factor can bind to the octamer motif (ATGCAAT). The Oct family comprises 11 proteins (Oct-1 to Oct-11) but only 8 genes can be encoded Oct proteins, which are Oct1, Oct2, Oct3/4, Oct6, Oct7, Oct8, Oct19 and Oct11 (Zhao 2013). From our reseach, the putative Oct-1 binding site on *Pm*VRP15 promoter might activate *Pm*VRP15 gene expression after viral infection. Oct-1 proteins have been reported to be involved in viral response. (Nogueira *et al.* 2004) reported that, the immediate early gen (IE) of Herpes simplex virus (HSV)

needed to be activated by Oct-1 transcription factor. The Oct-1 protein formed complex with viral transactivator protein (VP16) and host protein (cellular cofactor host cell factor 1). Oct-1 is also involved in the viral assembly process of HSV. The Oct-1 protein as a stress sensor is also important to modulate the gene activity that involved in cellular response to stress (Tantin *et al.* 2005)

The nuclear factor activated T-cell (NFAT) was shown here to be a regulator of *Pm*VRP15 gene expression and acted as the activator. The NFAT family consists of five members: NFAT1, NFAT2, NFAT3 NFAT4 and NFAT5 (Rao *et al.* 1997, Miyakawa *et al.* 1999). All NFAT proteins have a highly conserved DNA-binding domain that belongs to the Rel-family transcription factors. The conserved core region of NFAT proteins consists of two tandem domains; a regulatory domain, which are also known as the NFAT-homology region (NHR), and a DNA binding domain called RHR. The NHR is moderately conserved among NFAT proteins and contains a potent transactivation domain. The NFAT proteins function was involved in calcium signaling pathway. After Ca^{2+} was up-taken into cytoplasm, the NFAT protein in cytoplasm was de-phospholyrated and translocated into nucleus for regulation of gene expression (Hogan *et al.* 2003). The NFAT proteins have crucial roles in the development and function of the immune system. NFAT targets include many genes that control alternative functions in activated T cells, such as cell-cycle progression and activation-induced cell death. The highly flexible structure of the NFAT DNA-binding domain allows several surfaces to be available for interactions with different transcriptional partners on DNA, thereby allowing NFAT to integrate many signaling pathways (Macian 2005). Moreover, NFAT play a role in Simian Virus 40 (SV40) infection. After inhibition of NFAT activity, the infectivity of SV40 was reduced suggesting the importance of NFAT in the transcription of viral gene (Manley *et al.* 2008).

The information above suggested that *Pm*VRP15 which is predicted to be positively by NFAT, might be a part of a signaling pathway that is activated upon WSSV infection and play a key role in WSSV infectivity. Although, the putative transcription factor binding sites which are IRF, Oct-1 and NFAT, were identified on *Pm*VRP15 promoter and the site-directed mutagenesis was performed to confirm

their involvement in *Pm*VRP15 gene regulation as well as the previous report showed the function of these putative transcription factor in viral infection response, all putative transcription factor binding sites should be further confirmed. The candidates of transcription factor will be produced. The function of transcription factor that can regulate *Pm*VRP15 promoter will be further characterized.

CHAPTER V

CONCLUSION

1. To better understand how ALF*Pm*3 perform its antibacterial activity, I have studied the effect of ALF*Pm*3 on the *Vibrio harveyi* cell. The disruption of the outer and inner membrane as well as the leakage of the nucleic acid were observed in the rALF*Pm*3-treated bacteria. Many distinct signs of damages on the bacterial cells such as the cytoplasmic content leakage, the bleb formation and the pore formation were clearly observed. I concluded here that the bacterial killing action of rALF*Pm*3 was via the membrane permeabilizing activity.
2. Function of a novel viral responsive protein 15 (*Pm*VRP15) have been studied using RNA interference technique. In *Pm*VRP15 knockdown shrimp infected with WSSV, the expression of representative WSSV genes at various stages of WSSV infection including ie-1 (immediate early stage), wsv477 (early stage) and vp28 (late stage), was significantly decreased by 83.5%, 85.5% and 94.8%, respectively. The significant decrease in the cumulative mortality rate of WSSV-infected shrimp following *Pm*VRP15 knockdown compared with WSSV-infected shrimp injected with GFP dsRNA, control. I summarized that *Pm*VRP15 is important to viral propagation as its knockdown leads to decrease in viral infection in *P. monodon*.
3. WSV399 protein was identified as a *Pm*VRP15 binding protein by yeast two-hybrid assay and confirmed co-immunoprecipitation. The localization of WSV399 on WSSV virion was identified as the tegument protein.
4. Study of *Pm*VRP15 gene regulation was performed by narrow down promoter activity assay. The *Pm*VRP15 gene consists of 4 exons interrupted by 3 introns. About 2 kb fragment upstream the putative transcription start site was obtained. The upstream sequence analysis of the *Pm*VRP15 gene revealed that a potential TATA box located at 25 nucleotide upstream from the transcriptional start site. (-525/-428) and (-287/-209) nucleotide positions of *Pm*VRP15 promoter might have regulatory parts, which are repressor and activator binding sites, respectively. The computational analysis and mutation of transcription factor binding sites; indicated that interferon regulatory factor (IRF) might be a repressor and Octamer transcription factor (Oct-1) and Nuclear factor activated T-cell (NFAT) might be activators.

REFERENCES

Ai, H. S., Liao, J. X., Huang, X. D., Yin, Z. X., Weng, S. P., Zhao, Z. Y., Li, S. D., Yu, X. Q. and He, J. G. (2009). "A novel prophenoloxidase 2 exists in shrimp hemocytes." Dev Comp Immunol **33**(1): 59-68.

Aketagawa, J., Miyata, T., Ohtsubo, S., Nakamura, T., Morita, T., Hayashida, H., Miyata, T., Iwanaga, S., Takao, T. and Shimonishi, Y. (1986). "Primary structure of limulus anticoagulant anti-lipopolysaccharide factor." J Biol Chem **261**(16): 7357-7365.

Amparyup, P., Charoensapsri, W. and Tassanakajon, A. (2009). "Two prophenoloxidases are important for the survival of *Vibrio harveyi* challenged shrimp *Penaeus monodon*." Dev Comp Immunol **33**(2): 247-256.

Amparyup, P., Kondo, H., Hirono, I., Aoki, T. and Tassanakajon, A. (2008). "Molecular cloning, genomic organization and recombinant expression of a crustin-like antimicrobial peptide from black tiger shrimp *Penaeus monodon*." Mol Immunol **45**(4): 1085-1093.

Austin, B. and Zhang, X. H. (2006). "*Vibrio harveyi*: a significant pathogen of marine vertebrates and invertebrates." Lett Appl Microbiol **43**(2): 119-124.

Bartlett, T. C., Cuthbertson, B. J., Shepard, E. F., Chapman, R. W., Gross, P. S. and Warr, G. W. (2002). "Crustins, homologues of an 11.5-kDa antibacterial peptide, from two species of penaeid shrimp, *Litopenaeus vannamei* and *Litopenaeus setiferus*." Mar Biotechnol (NY) **4**(3): 278-293.

Bjerke, S. L. and Roller, R. J. (2006). "Roles for herpes simplex virus type 1 UL34 and US3 proteins in disrupting the nuclear lamina during herpes simplex virus type 1 egress." Virology **347**(2): 261-276.

Boehr, D. D., Draker, K. A., Koteva, K., Bains, M., Hancock, R. E. and Wright, G. D. (2003). "Broad-spectrum peptide inhibitors of aminoglycoside antibiotic resistance enzymes." Chem Biol **10**(2): 189-196.

Boman, H. G., Agerberth, B. and Boman, A. (1993). "Mechanisms of action on *Escherichia coli* of cecropin P1 and PR-39, two antibacterial peptides from pig intestine." Infect Immun **61**(7): 2978-2984.

Borregaard, N., Theilgaard-Monch, K., Sorensen, O. E. and Cowland, J. B. (2001). "Regulation of human neutrophil granule protein expression." Curr Opin Hematol **8**(1): 23-27.

Bowdish, D. M., Davidson, D. J., Scott, M. G. and Hancock, R. E. (2005). "Immunomodulatory activities of small host defense peptides." Antimicrob Agents Chemother **49**(5): 1727-1732.

Bradford, M. M. (1976). "A rapid and sensitive method for the quantitation of microgram quantities of protein utilizing the principle of protein-dye binding." Analytical Biochemistry **72**(1–2): 248-254.

Brogden, K. A. (2005). "Antimicrobial peptides: pore formers or metabolic inhibitors in bacteria?" Nat Rev Microbiol **3**(3): 238-250.

Brotz, H., Bierbaum, G., Markus, A., Molitor, E. and Sahl, H. G. (1995). "Mode of action of the lantibiotic mersacidin: inhibition of peptidoglycan biosynthesis via a novel mechanism?" Antimicrob Agents Chemother **39**(3): 714-719.

Brown, K. L. and Hancock, R. E. (2006). "Cationic host defense (antimicrobial) peptides." Curr Opin Immunol **18**(1): 24-30.

Brumfitt, W., Salton, M. R. and Hamilton-Miller, J. M. (2002). "Nisin, alone and combined with peptidoglycan-modulating antibiotics: activity against methicillin-resistant *Staphylococcus aureus* and vancomycin-resistant enterococci." J Antimicrob Chemother **50**(5): 731-734.

Bulet, P., Stocklin, R. and Menin, L. (2004). "Anti-microbial peptides: from invertebrates to vertebrates." Immunol Rev **198**: 169-184.

Chang, W. C., White, M. R., Moyo, P., McClear, S., Thiel, S., Hartshorn, K. L. and Takahashi, K. (2010). "Lack of the pattern recognition molecule mannose-binding lectin increases susceptibility to influenza A virus infection." BMC Immunol **11**: 64.

Charoensapsri, W., Amparyup, P., Hirono, I., Aoki, T. and Tassanakajon, A. (2009). "Gene silencing of a prophenoloxidase activating enzyme in the shrimp, *Penaeus monodon*, increases susceptibility to *Vibrio harveyi* infection." Dev Comp Immunol **33**(7): 811-820.

Charoensapsri, W., Amparyup, P., Hirono, I., Aoki, T. and Tassanakajon, A. (2011). "PmPPAE2, a new class of crustacean prophenoloxidase (proPO)-activating enzyme and its role in PO activation." Dev Comp Immunol **35**(1): 115-124.

Chen, A. J., Wang, S., Zhao, X. F., Yu, X. Q. and Wang, J. X. (2011). "Enzyme E2 from Chinese white shrimp inhibits replication of white spot syndrome virus and ubiquitinates its RING domain proteins." J Virol **85**(16): 8069-8079.

Chen, K.-Y., Hsu, T.-C., Huang, P.-Y., Kang, S.-T., Lo, C.-F., Huang, W.-P. and Chen, L.-L. (2009). "*Penaeus monodon* chitin-binding protein (PmCBP) is involved in white spot syndrome virus (WSSV) infection." Fish Shellfish Immunol **27**(3): 460-465.

Chen, L. L., Leu, J. H., Huang, C. J., Chou, C. M., Chen, S. M., Wang, C. H., Lo, C. F. and Kou, G. H. (2002). "Identification of a nucleocapsid protein (VP35) gene of shrimp white spot syndrome virus and characterization of the motif important for targeting VP35 to the nuclei of transfected insect cells." Virology **293**(1): 44-53.

Chen, L. L., Lu, L. C., Wu, W. J., Lo, C. F. and Huang, W. P. (2007). "White spot syndrome virus envelope protein VP53A interacts with *Penaeus monodon* chitin-binding protein (PmCBP)." Dis Aquat Organ **74**(3): 171-178.

Chen, M. Y., Hu, K. Y., Huang, C. C. and Song, Y. L. (2005). "More than one type of transglutaminase in invertebrates? A second type of transglutaminase is involved in shrimp coagulation." Dev Comp Immunol **29**(12): 1003-1016.

Chen, W. Y., Ho, K. C., Leu, J. H., Liu, K. F., Wang, H. C., Kou, G. H. and Lo, C. F. (2008). "WSSV infection activates STAT in shrimp." Dev Comp Immunol **32**(10): 1142-1150.

Chou, H. Y., Huang, C. Y., Wang, C. H., Chiang, H. C. and Lo, C. F. (1995). "Pathogenicity of a baculovirus infection causing white spot syndrome in cultured penaeid shrimp in Taiwan." Dis Aquat Organ **23**(3): 165-173.

Codran, A., Royer, C., Jaeck, D., Bastien-Valle, M., Baumert, T. F., Kieny, M. P., Pereira, C. A. and Martin, J. P. (2006). "Entry of hepatitis C virus pseudotypes into primary human hepatocytes by clathrin-dependent endocytosis." J Gen Virol **87**(Pt 9): 2583-2593.

da Silva, A., Jr. and Teschke, O. (2003). "Effects of the antimicrobial peptide PGLa on live *Escherichia coli*." Biochim Biophys Acta **1643**(1-3): 95-103.

de la Vega, E., O'Leary, N. A., Shockey, J. E., Robalino, J., Payne, C., Browdy, C. L., Warr, G. W. and Gross, P. S. (2008). "Anti-lipopolysaccharide factor in Litopenaeus vannamei (LvALF): a broad spectrum antimicrobial peptide essential for shrimp immunity against bacterial and fungal infection." Mol Immunol **45**(7): 1916-1925.

Destoumieux, D., Bulet, P., Loew, D., Van Dorsselaer, A., Rodriguez, J. and Bachere, E. (1997). "Penaeidins, a new family of antimicrobial peptides isolated from the shrimp *Penaeus vannamei* (Decapoda)." J Biol Chem **272**(45): 28398-28406.

Dhar, A. K., Dettori, A., Roux, M. M., Klimpel, K. R. and Read, B. (2003). "Identification of differentially expressed genes in shrimp (*Penaeus stylirostris*) infected with White spot syndrome virus by cDNA microarrays." Arch Virol **148**(12): 2381-2396.

Durand, S., Lightner, D. V., Nunan, L. M., Redman, R. M., Mari, J. and Bonami, J. R. (1996). "Application of gene probes as diagnostic tools for White Spot Baculovirus (WSBV) of penaeid shrimp." Dis Aquat Organ **27**(1): 59-66.

Durand, S., Lightner, D. V., Redman, R. M. and Bonami, J. R. (1997). "Ultrastructure and morphogenesis of White Spot Syndrome Baculovirus (WSSV)." Dis Aquat Organ **29**(3): 205-211.

Easton, D. M., Nijnik, A., Mayer, M. L. and Hancock, R. E. (2009). "Potential of immunomodulatory host defense peptides as novel anti-infectives." Trends Biotechnol **27**(10): 582-590.

Escobedo-Bonilla, C. M., Alday-Sanz, V., Wille, M., Sorgeloos, P., Pensaert, M. B. and Nauwynck, H. J. (2008). "A review on the morphology, molecular characterization, morphogenesis and pathogenesis of white spot syndrome virus." J Fish Dis **31**(1): 1-18.

Farmer, J. J., Janda, J. M., Brenner, F. W., Cameron, D. N. and Birkhead, K. M. (2005). "Genus I. *Vibrio* Pacini 1854, 411^{AL}." Bergey's Manual of Systematic Bacteriology **2**: 494–546.

Flegel, T. W. (1997). "Major viral diseases of the black tiger prawn (Penaeus monodon) in Thailand." World Journal of Microbiology and Biotechnology **13**(4): 433-442.

Flegel, T. W. (2007). "Update on viral accommodation, a model for host-viral interaction in shrimp and other arthropods." Dev Comp Immunol **31**(3): 217-231.

Flegel, T. W. (2012). "Historic emergence, impact and current status of shrimp pathogens in Asia." J Invertebr Pathol **110**(2): 166-173.

Gazit, E., Boman, A., Boman, H. G. and Shai, Y. (1995). "Interaction of the mammalian antibacterial peptide cecropin P1 with phospholipid vesicles." Biochemistry **34**(36): 11479-11488.

Gross, P. S., Bartlett, T. C., Browdy, C. L., Chapman, R. W. and Warr, G. W. (2001). "Immune gene discovery by expressed sequence tag analysis of hemocytes and hepatopancreas in the Pacific White Shrimp, *Litopenaeus vannamei*, and the Atlantic White Shrimp, *L. setiferus*." Dev Comp Immunol **25**(7): 565-577.

Guani-Guerra, E., Santos-Mendoza, T., Lugo-Reyes, S. O. and Teran, L. M. (2010). "Antimicrobial peptides: general overview and clinical implications in human health and disease." Clin Immunol **135**(1): 1-11.

Hall, M., Wang, R., van Antwerpen, R., Sottrup-Jensen, L. and Soderhall, K. (1999). "The crayfish plasma clotting protein: a vitellogenin-related protein

responsible for clot formation in crustacean blood." Proc Natl Acad Sci U S A **96**(5): 1965-1970.

Hallock, K. J., Lee, D. K. and Ramamoorthy, A. (2003). "MSI-78, an analogue of the magainin antimicrobial peptides, disrupts lipid bilayer structure via positive curvature strain." Biophys J **84**(5): 3052-3060.

Han, F., Xu, J. and Zhang, X. (2007). "Characterization of an early gene (wsv477) from shrimp white spot syndrome virus (WSSV)." Virus Genes **34**(2): 193-198.

Harada, H., Willison, K., Sakakibara, J., Miyamoto, M., Fujita, T. and Taniguchi, T. (1990). "Absence of the type I IFN system in EC cells: transcriptional activator (IRF-1) and repressor (IRF-2) genes are developmentally regulated." Cell **63**(2): 303-312.

Harding, M. W., Galat, A., Uehling, D. E. and Schreiber, S. L. (1989). "A receptor for the immunosuppressant FK506 is a cis-trans peptidyl-prolyl isomerase." Nature **341**(6244): 758-760.

He, F. and Kwang, J. (2008). "Identification and characterization of a new E3 ubiquitin ligase in white spot syndrome virus involved in virus latency." Virol J **5**: 151.

He, K., Ludtke, S. J., Heller, W. T. and Huang, H. W. (1996). "Mechanism of alamethicin insertion into lipid bilayers." Biophys J **71**(5): 2669-2679.

He, N., Qin, Q. and Xu, X. (2005). "Differential profile of genes expressed in hemocytes of White Spot Syndrome Virus-resistant shrimp (*Penaeus japonicus*) by combining suppression subtractive hybridization and differential hybridization." Antiviral Res **66**(1): 39-45.

Henzler-Wildman, K. A., Martinez, G. V., Brown, M. F. and Ramamoorthy, A. (2004). "Perturbation of the hydrophobic core of lipid bilayers by the human antimicrobial peptide LL-37." Biochemistry **43**(26): 8459-8469.

Hoess, A., Watson, S., Siber, G. R. and Liddington, R. (1993). "Crystal structure of an endotoxin-neutralizing protein from the horseshoe crab, Limulus anti-LPS factor, at 1.5 A resolution." Embo j **12**(9): 3351-3356.

Hogan, P. G., Chen, L., Nardone, J. and Rao, A. (2003). "Transcriptional regulation by calcium, calcineurin, and NFAT." Genes Dev **17**(18): 2205-2232.

Holmblad, T. and Söderhäll, K. (1999). "Cell adhesion molecules and antioxidative enzymes in a crustacean, possible role in immunity." Aquaculture **172**(1–2): 111-123.

Honda, K. and Taniguchi, T. (2006). "IRFs: master regulators of signalling by Toll-like receptors and cytosolic pattern-recognition receptors." Nat Rev Immunol **6**(9): 644-658.

Huang, C., Zhang, X., Lin, Q., Xu, X. and Hew, C. L. (2002a). "Characterization of a novel envelope protein (VP281) of shrimp white spot syndrome virus by mass spectrometry." J Gen Virol **83**(Pt 10): 2385-2392.

Huang, C., Zhang, X., Lin, Q., Xu, X., Hu, Z. and Hew, C. L. (2002b). "Proteomic analysis of shrimp white spot syndrome viral proteins and characterization of a novel envelope protein VP466." Mol Cell Proteomics **1**(3): 223-231.

Huang, R., Xie, Y., Zhang, J. and Shi, Z. (2005). "A novel envelope protein involved in White spot syndrome virus infection." J Gen Virol **86**(Pt 5): 1357-1361.

Huang, X. D., Yin, Z. X., Jia, X. T., Liang, J. P., Ai, H. S., Yang, L. S., Liu, X., Wang, P. H., Li, S. D., Weng, S. P., Yu, X. Q. and He, J. G. (2010). "Identification and functional study of a shrimp Dorsal homologue." Dev Comp Immunol **34**(2): 107-113.

Huang, X. D., Yin, Z. X., Liao, J. X., Wang, P. H., Yang, L. S., Ai, H. S., Gu, Z. H., Jia, X. T., Weng, S. P., Yu, X. Q. and He, J. G. (2009). "Identification and functional study of a shrimp Relish homologue." Fish Shellfish Immunol **27**(2): 230-238.

Hutchinson, E. C. and Fodor, E. (2012). "Nuclear import of the influenza A virus transcriptional machinery." Vaccine **30**(51): 7353-7358.

Jenssen, H., Hamill, P. and Hancock, R. E. (2006). "Peptide antimicrobial agents." Clin Microbiol Rev **19**(3): 491-511.

Jiravanichpaisal, P., Lee, B. L. and Soderhall, K. (2006). "Cell-mediated immunity in arthropods: hematopoiesis, coagulation, melanization and opsonization." Immunobiology **211**(4): 213-236.

Jiravanichpaisal, P., Miyazaki, T. and Limsuwan, C. (1994). "Histopathology, Biochemistry, and Pathogenicity of *Vibrio harveyi* Infecting Black Tiger Prawn *Penaeus monodon*." Journal of Aquatic Animal Health **6**(1): 27-35.

Kalfa, V. C., Jia, H. P., Kunkle, R. A., McCray, P. B., Jr., Tack, B. F. and Brogden, K. A. (2001). "Congeners of SMAP29 kill ovine pathogens and induce ultrastructural damage in bacterial cells." Antimicrob Agents Chemother **45**(11): 3256-3261.

Kamysz, W., Okroj, M. and Lukasiak, J. (2003). "Novel properties of antimicrobial peptides." Acta Biochim Pol **50**(2): 461-469.

Kelly, B. J., Fraefel, C., Cunningham, A. L. and Diefenbach, R. J. (2009). "Functional roles of the tegument proteins of herpes simplex virus type 1." Virus Res **145**(2): 173-186.

Kirchhoff, S., Sebens, T., Baumann, S., Krueger, A., Zawatzky, R., Li-Weber, M., Meinl, E., Neipel, F., Fleckenstein, B. and Krammer, P. H. (2002). "Viral IFN-regulatory factors inhibit activation-induced cell death via two positive regulatory IFN-

regulatory factor 1-dependent domains in the CD95 ligand promoter." J Immunol **168**(3): 1226-1234.

Krusong, K., Poolpipat, P., Supungul, P. and Tassanakajon, A. (2012). "A comparative study of antimicrobial properties of crustinPm1 and crustinPm7 from the black tiger shrimp *Penaeus monodon*." Dev Comp Immunol **36**(1): 208-215.

Labreuche, Y., O'Leary, N. A., de la Vega, E., Veloso, A., Gross, P. S., Chapman, R. W., Browdy, C. L. and Warr, G. W. (2009). "Lack of evidence for *Litopenaeus vannamei* Toll receptor (lToll) involvement in activation of sequence-independent antiviral immunity in shrimp." Dev Comp Immunol **33**(7): 806-810.

Ladokhin, A. S., Selsted, M. E. and White, S. H. (1997). "Sizing membrane pores in lipid vesicles by leakage of co-encapsulated markers: pore formation by melittin." Biophys J **72**(4): 1762-1766.

Lai, Y. and Gallo, R. L. (2009). "AMPed up immunity: how antimicrobial peptides have multiple roles in immune defense." Trends Immunol **30**(3): 131-141.

Lee, C. P. and Chen, M. R. (2010). "Escape of herpesviruses from the nucleus." Rev Med Virol **20**(4): 214-230.

Lee, H. R., Kim, M. H., Lee, J. S., Liang, C. and Jung, J. U. (2009). "Viral interferon regulatory factors." J Interferon Cytokine Res **29**(9): 621-627.

Lehrer, R. I., Barton, A., Daher, K. A., Harwig, S. S., Ganz, T. and Selsted, M. E. (1989). "Interaction of human defensins with *Escherichia coli* mechanism of bactericidal activity." J Clin Invest **84**(2): 553-561.

Lehrer, R. I., Barton, A., Daher, K. A., Harwig, S. S., Ganz, T. and Selsted, M. E. (1989). "Interaction of human defensins with Escherichia coli. Mechanism of bactericidal activity." J Clin Invest **84**(2): 553-561.

Lei, K., Li, F., Zhang, M., Yang, H., Luo, T. and Xu, X. (2008). "Difference between hemocyanin subunits from shrimp Penaeus japonicus in anti-WSSV defense." Developmental & Comparative Immunology **32**(7): 808-813.

Leu, J. H., Chang, C. C., Wu, J. L., Hsu, C. W., Hirono, I., Aoki, T., Juan, H. F., Lo, C. F., Kou, G. H. and Huang, H. C. (2007). "Comparative analysis of differentially expressed genes in normal and white spot syndrome virus infected *Penaeus monodon*." BMC Genomics **8**: 120.

Leu, J. H., Tsai, J. M., Wang, H. C., Wang, A. H., Wang, C. H., Kou, G. H. and Lo, C. F. (2005). "The unique stacked rings in the nucleocapsid of the white spot syndrome virus virion are formed by the major structural protein VP664, the largest viral structural protein ever found." J Virol **79**(1): 140-149.

Li, C., Zhao, J., Song, L., Mu, C., Zhang, H., Gai, Y., Qiu, L., Yu, Y., Ni, D. and Xing, K. (2008). "Molecular cloning, genomic organization and functional analysis of an anti-lipopolysaccharide factor from Chinese mitten crab *Eriocheir sinensis*." Dev Comp Immunol **32**(7): 784-794.

Li, D.-F., Zhang, M.-C., Yang, H.-J., Zhu, Y.-B. and Xu, X. (2007). "β-integrin mediates WSSV infection." Virology **368**(1): 122-132.

Li, F., Wang, D., Li, S., Yan, H., Zhang, J., Wang, B., Zhang, J. and Xiang, J. (2010). "A Dorsal homolog (FcDorsal) in the Chinese shrimp *Fenneropenaeus chinensis* is responsive to both bacteria and WSSV challenge." Dev Comp Immunol **34**(8): 874-883.

Li, F. and Xiang, J. (2013). "Signaling pathways regulating innate immune responses in shrimp." Fish Shellfish Immunol **34**(4): 973-980.

Li, F., Yan, H., Wang, D., Priya, T. A., Li, S., Wang, B., Zhang, J. and Xiang, J. (2009). "Identification of a novel relish homolog in Chinese shrimp *Fenneropenaeus chinensis* and its function in regulating the transcription of antimicrobial peptides." Dev Comp Immunol **33**(10): 1093-1101.

Li, H., Zhu, Y., Xie, X. and Yang, F. (2006). "Identification of a novel envelope protein (VP187) gene from shrimp white spot syndrome virus." Virus Res **115**(1): 76-84.

Li, L., Xie, X. and Yang, F. (2005). "Identification and characterization of a prawn white spot syndrome virus gene that encodes an envelope protein VP31." Virology **340**(1): 125-132.

Li, S., Zhang, X., Sun, Z., Li, F. and Xiang, J. (2013). "Transcriptome analysis on Chinese shrimp *Fenneropenaeus chinensis* during WSSV acute infection." PLoS One **8**(3): e58627.

Liang, Y., Cheng, J. J., Yang, B. and Huang, J. (2010). "The role of F1 ATP synthase beta subunit in WSSV infection in the shrimp, *Litopenaeus vannamei*." Virol J **7**: 144.

Lightner, D. V. (1993). Diseases of cultured penaeid shrimp. Hawaii: The oceanic Institute.

Lightner, D. V. (1996). A Handbook of Pathology and Diagnostic Procedures for Diseases of Penaeid Shrimp. Baton Rouge, Louisiana, USA.

Liu, B., Tang, X. and Zhan, W. (2011). "Interaction between white spot syndrome virus VP26 and hemocyte membrane of shrimp, *Fenneropenaeus chinensis*." Aquaculture **314**(1–4): 13-17.

Liu, H., Jiravanichpaisal, P., Soderhall, I., Cerenius, L. and Soderhall, K. (2006). "Antilipopolysaccharide factor interferes with white spot syndrome virus

replication in vitro and in vivo in the crayfish *Pacifastacus leniusculus*." J Virol **80**(21): 10365-10371.

Liu, W., Han, F. and Zhang, X. (2009). "Ran GTPase regulates hemocytic phagocytosis of shrimp by interaction with myosin." J Proteome Res **8**(3): 1198-1206.

Liu, W. J., Chang, Y. S., Wang, A. H., Kou, G. H. and Lo, C. F. (2007). "White spot syndrome virus annexes a shrimp STAT to enhance expression of the immediate-early gene ie1." J Virol **81**(3): 1461-1471.

Liu, Y., Wu, J., Song, J., Sivaraman, J. and Hew, C. L. (2006). "Identification of a novel nonstructural protein, VP9, from white spot syndrome virus: its structure reveals a ferredoxin fold with specific metal binding sites." J Virol **80**(21): 10419-10427.

Loh, B., Grant, C. and Hancock, R. E. (1984). "Use of the fluorescent probe 1-N-phenylnaphthylamine to study the interactions of aminoglycoside antibiotics with the outer membrane of *Pseudomonas aeruginosa*." Antimicrob Agents Chemother **26**(4): 546-551.

Lotz, J. M. (1997). "Viruses, biosecurity and specific pathogen-free stocks in shrimp aquaculture." World Journal of Microbiology and Biotechnology **13**(4): 405-413.

Lu, L. and Kwang, J. (2004). "Identification of a novel shrimp protein phosphatase and its association with latency-related ORF427 of white spot syndrome virus." FEBS Lett **577**(1-2): 141-146.

Macian, F. (2005). "NFAT proteins: key regulators of T-cell development and function." Nat Rev Immunol **5**(6): 472-484.

Mai, W., Hu, C. Q. and Wang, W. (2009). "In vitro activation of the antibacterial activity by virus-resistant shrimp (*Marsupenaeus japonicus*) recombinant interferon-like protein." Aquaculture **288**(1–2): 140-142.

Manley, K., O'Hara, B. A. and Atwood, W. J. (2008). "Nuclear factor of activated T-cells (NFAT) plays a role in SV40 infection." Virology **372**(1): 48-55.

Marques, M. R. F. and Barracco, M. A. (2000). "Lectins, as non-self-recognition factors, in crustaceans." Aquaculture **191**(1–3): 23-44.

Martin, G. G. and Graves, B. L. (1985). "Fine structure and classification of shrimp hemocytes." Journal of Morphology **185**(3): 339-348.

Mason, A. J., Marquette, A. and Bechinger, B. (2007). "Zwitterionic phospholipids and sterols modulate antimicrobial peptide-induced membrane destabilization." Biophys J **93**(12): 4289-4299.

Matsuzaki, K., Murase, O., Fujii, N. and Miyajima, K. (1996). "An antimicrobial peptide, magainin 2, induced rapid flip-flop of phospholipids coupled with pore formation and peptide translocation." Biochemistry **35**(35): 11361-11368.

Meincken, M., Holroyd, D. L. and Rautenbach, M. (2005). "Atomic force microscopy study of the effect of antimicrobial peptides on the cell envelope of *Escherichia coli*." Antimicrob Agents Chemother **49**(10): 4085-4092.

Mercer, J., Schelhaas, M. and Helenius, A. (2010). "Virus entry by endocytosis." Annu Rev Biochem **79**: 803-833.

Miyakawa, H., Woo, S. K., Dahl, S. C., Handler, J. S. and Kwon, H. M. (1999). "Tonicity-responsive enhancer binding protein, a rel-like protein that stimulates transcription in response to hypertonicity." Proc Natl Acad Sci U S A **96**(5): 2538-2542.

Mohan, C. V., Shankar, K. M., Kulkarni, S. and Sudha, P. M. (1998). "Histopathology of cultured shrimp showing gross signs of yellow head syndrome and white spot syndrome during 1994 Indian epizootics." Dis Aquat Organ **34**(1): 9-12.

Mor, A. and Nicolas, P. (1994). "The NH_2-terminal alpha-helical domain 1-18 of dermaseptin is responsible for antimicrobial activity." J Biol Chem **269**(3): 1934-1939.

Muta, T., Miyata, T., Tokunaga, F., Nakamura, T. and Iwanaga, S. (1987). "Primary structure of anti-lipopolysaccharide factor from American horseshoe crab, *Limulus polyphemus*." J Biochem **101**(6): 1321-1330.

Nadala, E. C., Jr. and Loh, P. C. (1998). "A comparative study of three different isolates of white spot virus." Dis Aquat Organ **33**(3): 231-234.

Nicolas, P. (2009). "Multifunctional host defense peptides: intracellular-targeting antimicrobial peptides." Febs j **276**(22): 6483-6496.

Nogueira, M. L., Wang, V. E., Tantin, D., Sharp, P. A. and Kristie, T. M. (2004). "Herpes simplex virus infections are arrested in Oct-1-deficient cells." Proc Natl Acad Sci U S A **101**(6): 1473-1478.

Ongvarrasopone, C., Chanasakulniyom, M., Sritunyalucksana, K. and Panyim, S. (2008). "Suppression of PmRab7 by dsRNA inhibits WSSV or YHV infection in shrimp." Mar Biotechnol (NY) **10**(4): 374-381.

Park, C. B., Kim, H. S. and Kim, S. C. (1998). "Mechanism of action of the antimicrobial peptide buforin II: buforin II kills microorganisms by penetrating the cell membrane and inhibiting cellular functions." Biochem Biophys Res Commun **244**(1): 253-257.

Park, I. Y., Park, C. B., Kim, M. S. and Kim, S. C. (1998). "Parasin I, an antimicrobial peptide derived from histone H2A in the catfish, *Parasilurus asotus*." FEBS Lett **437**(3): 258-262.

Patrzykat, A., Friedrich, C. L., Zhang, L., Mendoza, V. and Hancock, R. E. (2002). "Sublethal concentrations of pleurocidin-derived antimicrobial peptides inhibit macromolecular synthesis in *Escherichia coli*." Antimicrob Agents Chemother **46**(3): 605-614.

Patrzykat, A., Zhang, L., Mendoza, V., Iwama, G. K. and Hancock, R. E. (2001). "Synergy of histone-derived peptides of coho salmon with lysozyme and flounder pleurocidin." Antimicrob Agents Chemother **45**(5): 1337-1342.

Perazzolo, L. M. and Barracco, M. A. (1997). "The prophenoloxidase activating system of the shrimp *Penaeus paulensis* and associated factors." Dev Comp Immunol **21**(5): 385-395.

Pestka, S. (2007). "The interferons: 50 years after their discovery, there is much more to learn." J Biol Chem **282**(28): 20047-20051.

Pfaffl, M. W. (2001). "A new mathematical model for relative quantification in real-time RT-PCR." Nucleic Acids Res **29**(9): e45.

Ponprateep, S., Somboonwiwat, K. and Tassanakajon, A. (2009). "Recombinant anti-lipopolysaccharide factor isoform 3 and the prevention of vibriosis in the black tiger shrimp, *Penaeus monodon*." Aquaculture **289**(3–4): 219-224.

Ponprateep, S., Tharntada, S., Somboonwiwat, K. and Tassanakajon, A. (2012). "Gene silencing reveals a crucial role for anti-lipopolysaccharide factors from *Penaeus monodon* in the protection against microbial infections." Fish Shellfish Immunol **32**(1): 26-34.

Prapavorarat, A., Pongsomboon, S. and Tassanakajon, A. (2010). "Identification of genes expressed in response to yellow head virus infection in the black tiger shrimp, *Penaeus monodon*, by suppression subtractive hybridization." Dev Comp Immunol **34**(6): 611-617.

Rao, A., Luo, C. and Hogan, P. G. (1997). "Transcription factors of the NFAT family: regulation and function." Annu Rev Immunol **15**: 707-747.

Rolland, J. L., Abdelouahab, M., Dupont, J., Lefevre, F., Bachere, E. and Romestand, B. (2010). "Stylicins, a new family of antimicrobial peptides from the Pacific blue shrimp *Litopenaeus stylirostris*." Mol Immunol **47**(6): 1269-1277.

Rosa, R. D. and Barracco, M. A. (2008). "Shrimp interferon is rather a portion of the mitochondrial F_0-ATP synthase than a true alpha-interferon." Mol Immunol **45**(12): 3490-3493.

Rosa, R. D., Vergnes, A., de Lorgeril, J., Goncalves, P., Perazzolo, L. M., Saune, L., Romestand, B., Fievet, J., Gueguen, Y., Bachere, E. and Destoumieux-Garzon, D. (2013). "Functional divergence in shrimp anti-lipopolysaccharide factors (ALFs): from recognition of cell wall components to antimicrobial activity." PLoS One **8**(7): e67937.

Ruangpan, L., Danayadol, Y., Direkbusarakom, S., Siurairatana, S. and Flegel, T. W. (1999). "Lethal toxicity of *Vibrio harveyi* to cultivated *Penaeus monodon* induced by a bacteriophage." Dis Aquat Org **35**: 195–201.

Sambrook, J., and W. Russell David (1989). Molecular cloning: a laboratory manual. Vol. 3. , Molecular cloning: a laboratory manual. Vol. 3. .

Sangsuriya, P., Huang, J. Y., Chu, Y. F., Phiwsaiya, K., Leekitcharoenphon, P., Meemetta, W., Senapin, S., Huang, W. P., Withyachumnarnkul, B., Flegel, T. W. and Lo, C. F. (2014). "Construction and application of a protein interaction map for white spot syndrome virus (WSSV)." Mol Cell Proteomics **13**(1): 269-282.

Saulnier, D., Avarre, J. C., Le Moullac, G., Ansquer, D., Levy, P. and Vonau, V. (2000). "Rapid and sensitive PCR detection of *Vibrio penaeicida*, the putative etiological agent of syndrome 93 in New Caledonia." Dis Aquat Organ **40**(2): 109-115.

Shi, X. Z., Zhang, R. R., Jia, Y. P., Zhao, X. F., Yu, X. Q. and Wang, J. X. (2009). "Identification and molecular characterization of a Spatzle-like protein from Chinese shrimp (*Fenneropenaeus chinensis*)." Fish Shellfish Immunol **27**(5): 610-617.

Shimazaki, J., Shinozaki, N. and Tsubota, K. (1998). "Transplantation of amniotic membrane and limbal autograft for patients with recurrent pterygium associated with symblepharon." Br J Ophthalmol **82**(3): 235-240.

Soderhall, K. and Cerenius, L. (1998). "Role of the prophenoloxidase-activating system in invertebrate immunity." Curr Opin Immunol **10**(1): 23-28.

Somboonwiwat, K., Bachere, E., Rimphanitchayakit, V. and Tassanakajon, A. (2008). "Localization of anti-lipopolysaccharide factor (ALF*Pm*3) in tissues of the black tiger shrimp, *Penaeus monodon*, and characterization of its binding properties." Dev Comp Immunol **32**(10): 1170-1176.

Somboonwiwat, K., Marcos, M., Tassanakajon, A., Klinbunga, S., Aumelas, A., Romestand, B., Gueguen, Y., Boze, H., Moulin, G. and Bachere, E. (2005). "Recombinant expression and anti-microbial activity of anti-lipopolysaccharide factor (ALF) from the black tiger shrimp *Penaeus monodon*." Dev Comp Immunol **29**(10): 841-851.

Song, K. K., Li, D. F., Zhang, M. C., Yang, H. J., Ruan, L. W. and Xu, X. (2010). "Cloning and characterization of three novel WSSV recognizing lectins from shrimp *Marsupenaeus japonicus*." Fish Shellfish Immunol **28**(4): 596-603.

Spann, K. M. and Lester, R. J. G. (1997). "Viral diseases of penaeid shrimp with particular reference to four viruses recently found in shrimp from Queensland." World Journal of Microbiology and Biotechnology **13**(4): 419-426.

Sritunyalucksana, K. and Söderhäll, K. (2000). "The proPO and clotting system in crustaceans." Aquaculture **191**(1–3): 53-69.

Sritunyalucksana, K., Utairungsee, T., Sirikharin, R. and Srisala, J. (2013). "Reprint of: Virus-binding proteins and their roles in shrimp innate immunity." Fish Shellfish Immunol **34**(4): 1018-1024.

Sritunyalucksana, K., Wannapapho, W., Lo, C. F. and Flegel, T. W. (2006). "PmRab7 is a VP28-binding protein involved in white spot syndrome virus infection in shrimp." J Virol **80**(21): 10734-10742.

Subbalakshmi, C. and Sitaram, N. (1998). "Mechanism of antimicrobial action of indolicidin." FEMS Microbiol Lett **160**(1): 91-96.

Sun, C., Shao, H. L., Zhang, X. W., Zhao, X. F. and Wang, J. X. (2011). "Molecular cloning and expression analysis of signal transducer and activator of transcription (STAT) from the Chinese white shrimp *Fenneropenaeus chinensis*." Mol Biol Rep **38**(8): 5313-5319.

Supungul, P., Klinbunga, S., Pichyangkura, R., Hirono, I., Aoki, T. and Tassanakajon, A. (2004). "Antimicrobial peptides discovered in the black tiger shrimp *Penaeus monodon* using the EST approach." Dis Aquat Organ **61**(1-2): 123-135.

Supungul, P., Klinbunga, S., Pichyangkura, R., Jitrapakdee, S., Hirono, I., Aoki, T. and Tassanakajon, A. (2002). "Identification of immune-related genes in hemocytes of black tiger shrimp (*Penaeus monodon*)." Mar Biotechnol (NY) **4**(5): 487-494.

Supungul, P., Tang, S., Maneeruttanarungroj, C., Rimphanitchayakit, V., Hirono, I., Aoki, T. and Tassanakajon, A. (2008). "Cloning, expression and antimicrobial activity of crustin*Pm*1, a major isoform of crustin, from the black tiger shrimp *Penaeus monodon*." Dev Comp Immunol **32**(1): 61-70.

Tanaka, S., Nakamura, T., Morita, T. and Iwanaga, S. (1982). "Limulus anti-LPS factor: An anticoagulant which inhibits the endotoxin-mediated activation of Limulus coagulation system." Biochemical and Biophysical Research Communications **105**(2): 717-723.

Tang, Y.-L., Shi, Y.-H., Zhao, W., Hao, G. and Le, G.-W. (2009). "Discovery of a novel antimicrobial peptide using membrane binding-based approach." Food Control **20**(2): 149-156.

Taniguchi, T., Ogasawara, K., Takaoka, A. and Tanaka, N. (2001). "IRF family of transcription factors as regulators of host defense." Annu Rev Immunol **19**: 623-655.

Tantin, D., Schild-Poulter, C., Wang, V., Hache, R. J. and Sharp, P. A. (2005). "The octamer binding transcription factor Oct-1 is a stress sensor." Cancer Res **65**(23): 10750-10758.

Tassanakajon, A., Amparyup, P., Somboonwiwat, K. and Supungul, P. (2010). "Cationic antimicrobial peptides in penaeid shrimp." Mar Biotechnol (NY) **12**(5): 487-505.

Tharntada, S., Ponprateep, S., Somboonwiwat, K., Liu, H., Soderhall, I., Soderhall, K. and Tassanakajon, A. (2009). "Role of anti-lipopolysaccharide factor from the black tiger shrimp, *Penaeus monodon*, in protection from white spot syndrome virus infection." J Gen Virol **90**(Pt 6): 1491-1498.

Tharntada, S., Somboonwiwat, K., Rimphanitchayakit, V. and Tassanakajon, A. (2008). "Anti-lipopolysaccharide factors from the black tiger shrimp, *Penaeus monodon*, are encoded by two genomic loci." Fish Shellfish Immunol **24**(1): 46-54.

Tonganunt, M., Saelee, N., Chotigeat, W. and Phongdara, A. (2009). "Identification of a receptor for activated protein kinase C1 (*Pm*-RACK1), a cellular gene product from black tiger shrimp (*Penaeus monodon*) interacts with a protein, VP9 from the white spot syndrome virus." Fish Shellfish Immunol **26**(3): 509-514.

Tsai, J. M., Wang, H. C., Leu, J. H., Hsiao, H. H., Wang, A. H., Kou, G. H. and Lo, C. F. (2004). "Genomic and proteomic analysis of thirty-nine structural proteins of shrimp white spot syndrome virus." J Virol **78**(20): 11360-11370.

Tsai, J. M., Wang, H. C., Leu, J. H., Wang, A. H., Zhuang, Y., Walker, P. J., Kou, G. H. and Lo, C. F. (2006). "Identification of the nucleocapsid, tegument, and envelope proteins of the shrimp white spot syndrome virus virion." J Virol **80**(6): 3021-3029.

van Hulten, M. C., Reijns, M., Vermeesch, A. M., Zandbergen, F. and Vlak, J. M. (2002). "Identification of VP19 and VP15 of white spot syndrome virus (WSSV) and glycosylation status of the WSSV major structural proteins." J Gen Virol **83**(Pt 1): 257-265.

van Hulten, M. C., Westenberg, M., Goodall, S. D. and Vlak, J. M. (2000). "Identification of two major virion protein genes of white spot syndrome virus of shrimp." Virology **266**(2): 227-236.

Vatanavicharn, T., Prapavorarat, A., Jaree, P., Somboonwiwat, K. and Tassanakajon, A. (2014). "*Pm*VRP15, a novel viral responsive protein from the black tiger shrimp, *Penaeus monodon*, promoted white spot syndrome virus replication." PLoS One **9**(3): e91930.

Vlak, J. M., Bonami, J. R., Flegel, T. W., Kou, G. H., Lightner, D. V., Lo, C. F., Loh, P. C. and Walker, P. W. (2004). Nimaviridae. Amsterdam, 8th Report of the International Committee on Taxonomy of Viruses, Elsevier.

Wang, B., Li, F., Dong, B., Zhang, X., Zhang, C. and Xiang, J. (2006). "Discovery of the genes in response to white spot syndrome virus (WSSV) infection in *Fenneropenaeus chinensis* through cDNA microarray." Mar Biotechnol (NY) **8**(5): 491-500.

Wang, P. H., Gu, Z. H., Huang, X. D., Liu, B. D., Deng, X. X., Ai, H. S., Wang, J., Yin, Z. X., Weng, S. P., Yu, X. Q. and He, J. G. (2009). "An immune deficiency homolog from the white shrimp, *Litopenaeus vannamei*, activates antimicrobial peptide genes." Mol Immunol **46**(8-9): 1897-1904.

Wang, P. H., Gu, Z. H., Wan, D. H., Zhang, M. Y., Weng, S. P., Yu, X. Q. and He, J. G. (2011a). "The shrimp NF-kappaB pathway is activated by white spot syndrome virus (WSSV) 449 to facilitate the expression of WSSV069 (ie1), WSSV303 and WSSV371." PLoS One **6**(9): e24773.

Wang, P. H., Liang, J. P., Gu, Z. H., Wan, D. H., Weng, S. P., Yu, X. Q. and He, J. G. (2012). "Molecular cloning, characterization and expression analysis of two novel Tolls (LvToll2 and LvToll3) and three putative Spatzle-like Toll ligands (LvSpz1-3) from *Litopenaeus vannamei*." Dev Comp Immunol **36**(2): 359-371.

Wang, P. H., Wan, D. H., Gu, Z. H., Deng, X. X., Weng, S. P., Yu, X. Q. and He, J. G. (2011b). "*Litopenaeus vannamei* tumor necrosis factor receptor-associated factor 6 (TRAF6) responds to *Vibrio alginolyticus* and white spot syndrome virus (WSSV) infection and activates antimicrobial peptide genes." Dev Comp Immunol **35**(1): 105-114.

Wang, R., Liang, Z., Hal, M. and Soderhall, K. (2001). "A transglutaminase involved in the coagulation system of the freshwater crayfish, *Pacifastacus leniusculus*. Tissue localisation and cDNA cloning." Fish Shellfish Immunol **11**(7): 623-637.

Wang, X. W., Xu, W. T., Zhang, X. W., Zhao, X. F., Yu, X. Q. and Wang, J. X. (2009). "A C-type lectin is involved in the innate immune response of Chinese white shrimp." Fish Shellfish Immunol **27**(4): 556-562.

Watthanasurorot, A., Jiravanichpaisal, P., Soderhall, I. and Soderhall, K. (2010). "A gC1qR prevents white spot syndrome virus replication in the freshwater crayfish *Pacifastacus leniusculus*." J Virol **84**(20): 10844-10851.

Witteveldt, J., Vermeesch, A. M., Langenhof, M., de Lang, A., Vlak, J. M. and van Hulten, M. C. (2005). "Nucleocapsid protein VP15 is the basic DNA binding protein of white spot syndrome virus of shrimp." Arch Virol **150**(6): 1121-1133.

Wongteerasupaya, C., Vickers, J. E., Sriurairatana, S., Nash, G. L., Akarajamorn, A., Boonsaeng, V., Panyim, S., Tassanakajon, A., Withyachumnarnkul, B. and Flegel, T. W. (1995). "A non-occluded, systemic baculovirus that occurs in cells of ectodermal and mesodermal origin and causes high mortality in the black tiger prawn *Penaeus monodon*." Dis Aquat Organ **21**(1): 69-77.

Woramongkolchai, N., Supungul, P. and Tassanakajon, A. (2011). "The possible role of penaeidin5 from the black tiger shrimp, *Penaeus monodon*, in protection against viral infection." Dev Comp Immunol **35**(5): 530-536.

Wu, C. and Yang, F. (2006). "Localization studies of two white spot syndrome virus structural proteins VP51 and VP76." Virol J **3**: 76.

Wu, M., Maier, E., Benz, R. and Hancock, R. E. (1999). "Mechanism of interaction of different classes of cationic antimicrobial peptides with planar bilayers and with the cytoplasmic membrane of *Escherichia coli*." Biochemistry **38**(22): 7235-7242.

Wu, W., Wang, L. and Zhang, X. (2005). "Identification of white spot syndrome virus (WSSV) envelope proteins involved in shrimp infection." Virology **332**(2): 578-583.

Wu, W., Zong, R., Xu, J. and Zhang, X. (2008). "Antiviral phagocytosis is regulated by a novel Rab-dependent complex in shrimp *Penaeus japonicus*." J Proteome Res **7**(1): 424-431.

Wyban, J. A. (2007). Thailand's white shrimp revolution. Global Aquaculture Advocate**:** 56-58.

Wyckoff, M., Rodbard, D. and Chrambach, A. (1977). "Polyacrylamide gel electrophoresis in sodium dodecyl sulfate-containing buffers using multiphasic buffer systems: Properties of the stack, valid Rf– measurement, and optimized procedure." Analytical Biochemistry **78**(2): 459-482.

Xiao, N., Zhang, X., Dai, L., Yuan, L., Wang, Y., Zhang, M., Xu, T. and Dai, H. (2006). "Isolation and identification of a novel WSSV nucleocapsid protein by cDNA phage display using an scFv antibody." J Virol Methods **137**(2): 272-279.

Xie, X., Li, H., Xu, L. and Yang, F. (2005a). "A simple and efficient method for purification of intact white spot syndrome virus (WSSV) viral particles." Virus Res **108**(1-2): 63-67.

Xie, X., Xu, L. and Yang, F. (2006). "Proteomic analysis of the major envelope and nucleocapsid proteins of white spot syndrome virus." J Virol **80**(21): 10615-10623.

Xie, X. and Yang, F. (2005b). "Interaction of white spot syndrome virus VP26 protein with actin." Virology **336**(1): 93-99.

Xu, H., Yan, F., Deng, X., Wang, J., Zou, T., Ma, X., Zhang, X. and Qi, Y. (2009). "The interaction of white spot syndrome virus envelope protein VP28 with shrimp Hsc70 is specific and ATP-dependent." Fish Shellfish Immunol **26**(3): 414-421.

Yamaguchi, S., Huster, D., Waring, A., Lehrer, R. I., Kearney, W., Tack, B. F. and Hong, M. (2001). "Orientation and dynamics of an antimicrobial peptide in the lipid bilayer by solid-state NMR spectroscopy." Biophys J **81**(4): 2203-2214.

Yang, F., He, J., Lin, X., Li, Q., Pan, D., Zhang, X. and Xu, X. (2001). "Complete genome sequence of the shrimp white spot bacilliform virus." J Virol **75**(23): 11811-11820.

Yang, L., Harroun, T. A., Weiss, T. M., Ding, L. and Huang, H. W. (2001). "Barrel-stave model or toroidal model? A case study on melittin pores." Biophys J **81**(3): 1475-1485.

Yang, L., Weiss, T. M., Harroun, T. A., Heller, W. T. and Huang, H. W. (1999). "Supramolecular structures of peptide assemblies in membranes by neutron off-plane scattering: method of analysis." Biophys J **77**(5): 2648-2656.

Yang, Y., Boze, H., Chemardin, P., Padilla, A., Moulin, G., Tassanakajon, A., Pugniere, M., Roquet, F., Destoumieux-Garzon, D., Gueguen, Y., Bachere, E. and Aumelas, A. (2009). "NMR structure of rALF-Pm3, an anti-lipopolysaccharide factor from shrimp: model of the possible lipid A-binding site." Biopolymers **91**(3): 207-220.

Yedery, R. D. and Reddy, K. V. (2009). "Identification, cloning, characterization and recombinant expression of an anti-lipopolysaccharide factor from the hemocytes of Indian mud crab, *Scylla serrata*." Fish Shellfish Immunol **27**(2): 275-284.

Yoneyama, F., Imura, Y., Ohno, K., Zendo, T., Nakayama, J., Matsuzaki, K. and Sonomoto, K. (2009). "Peptide-lipid huge toroidal pore, a new antimicrobial mechanism mediated by a lactococcal bacteriocin, lacticin Q." Antimicrob Agents Chemother **53**(8): 3211-3217.

Yonezawa, A., Kuwahara, J., Fujii, N. and Sugiura, Y. (1992). "Binding of tachyplesin I to DNA revealed by footprinting analysis: significant contribution of secondary structure to DNA binding and implication for biological action." Biochemistry **31**(11): 2998-3004.

Yount, N. Y., Bayer, A. S., Xiong, Y. Q. and Yeaman, M. R. (2006). "Advances in antimicrobial peptide immunobiology." Biopolymers **84**(5): 435-458.

Youtong, W., Deachamag, P., Phongdara, A. and Chotigeat, W. (2011). "WSSV: VP26 binding protein and its biological activity." Fish Shellfish Immunol **30**(1): 77-83.

Zeng, Y. and Lu, C.-P. (2009). "Identification of differentially expressed genes in haemocytes of the crayfish (*Procambarus clarkii*) infected with white spot syndrome virus by suppression subtractive hybridization and cDNA microarrays." Fish Shellfish Immunol **26**(4): 646-650.

Zhang, L., Rozek, A. and Hancock, R. E. (2001). "Interaction of cationic antimicrobial peptides with model membranes." J Biol Chem **276**(38): 35714-35722.

Zhang, X., Huang, C. and Qin, Q. (2004). "Antiviral properties of hemocyanin isolated from shrimp *Penaeus monodon*." Antiviral Res **61**(2): 93-99.

Zhang, X., Huang, C., Tang, X., Zhuang, Y. and Hew, C. L. (2004). "Identification of structural proteins from shrimp white spot syndrome virus (WSSV) by 2DE-MS." Proteins **55**(2): 229-235.

Zhao, F. Q. (2013). "Octamer-binding transcription factors: genomics and functions." Front Biosci (Landmark Ed) **18**: 1051-1071.

Zhao, Z. Y., Yin, Z. X., Xu, X. P., Weng, S. P., Rao, X. Y., Dai, Z. X., Luo, Y. W., Yang, G., Li, Z. S., Guan, H. J., Li, S. D., Chan, S. M., Yu, X. Q. and He, J. G. (2009). "A novel C-type lectin from the shrimp *Litopenaeus vannamei* possesses anti-white spot syndrome virus activity." J Virol **83**(1): 347-356.

Zheng, G., Yampara-Iquise, H., Jones, J. E. and Andrew Carson, C. (2009). "Development of Faecalibacterium 16S rRNA gene marker for identification of human faeces." J Appl Microbiol **106**(2): 634-641.

Zhu, Y., Ding, Q. and Yang, F. (2007). "Characterization of a homologous-region-binding protein from white spot syndrome virus by phage display." Virus Res **125**(2): 145-152.

Zhu, Y., Xie, X. and Yang, F. (2005). "Transcription and identification of a novel envelope protein (VP124) gene of shrimp white spot syndrome virus." Virus Res **113**(2): 100-106.

Zhu, Y. B., Li, H. Y. and Yang, F. (2006). "Identification of an envelope protein (VP39) gene from shrimp white spot syndrome virus." Arch Virol **151**(1): 71-82.

APPENDIX

Publications

1. **Jaree, P.**, Tassanakajon, A., Somboonwiwat, K., Effect of the Anti-lipopolysaccharide Factor Isoform 3 (ALF*Pm*3) from *Penaeus monodon* on *Vibrio harveyi* cells, Developmental & Comparative Immunology (2012), Dev Comp Immunol., 38, pp. 554-560.
2. Vatanavicharn, T., Prapavorarat, A., **Jaree, P.**, Somboonwiwat, K., Tassanakajon, A. *Pm*VRP15, a novel viral responsive protein from the black tiger shrimp, *Penaeus monodon*, promoted white spot syndrome virus replication (2014). PLoS ONE, Volume 9, Issue 3, e91930.

Oral Presentation

1. Jaree, P., Somboonwiwat, K., Lo, C. F., Tassanakajon, A., Functional characterization and gene regulation of a novel viral responsive protein 15 (*Pm*VRP15) from *Penaeus monodon*. The RGJ-Ph.D. Congress XV, Chonburi, Thailand (2014).

   Award: The outstanding oral presentation, Session: Biological Sciences, RGJ-Ph.D. Congress XV., Chonburi, Thailand.
2. **Jaree, P.**, Somboonwiwat, K., Lo, C. F., Tassanakajon, A., Genome organization and promoter analysis of a highly WSSV-inducible gene, viral responsive protein 15 (*Pm*VRP15) from *Penaeus monodon*. 2014 Symposium on Emerging Trends in Aquatic Disease and Aquaculture Biotechnology, Tainan, Taiwan (2014).
3. **Jaree, P.**, Somboonwiwat, K., Lo, C. F., Tassanakajon, A., Genome organization and promoter analysis of a highly WSSV-inducible gene, viral responsive protein 15 (*Pm*VRP15) from *Penaeus monodon*. The 10th Asia-Pacific Marine Biotechnology Conference (APMBC 2014), Taipei, Taiwan (2014).
4. **Jaree, P.**, Somboonwiwat, K., Lo, C. F., Tassanakajon, A., Genomic organization and promoter characterization of a viral responsive protein 15 (*Pm*VRP15) from black tiger shrimp, *Penaeus monodon*. The 4th International Biochemistry and Molecular Biology Conference 2014, Bangkok, Thailand (2014).
5. **Jaree, P.**, Somboonwiwat, K., Lo, C. F., Tassanakajon, A., Functional characterization and promoter analysis of a viral responsive protein 15 (*Pm*VRP15)

gene from black tiger shrimp, *Penaeus monodon*. The science forum 2014, Chulalongkorn University, Bangkok, Thailand (2014).

Award: The first prize of the oral presentation, Session: Biological Sciences, The Science Forum 2014, Chulalongkorn University, Thailand

6. **Jaree, P.**, Somboonwiwat, K., Tassanakajon, A., ALF*Pm*3 exhibits the anti-vibrio activity using pore forming mechanism, The 16th Biological Sciences Graduate Congress, National University of Singapore, Singapore (2011).
7. **Jaree, P.**, Somboonwiwat, K., Tassanakajon, A., The pore forming peptide from the shrimp *Penaeus monodon*, The 37th Congress on Science and Technology of Thailand (STT37), Bangkok, Thailand (2011).
8. **Jaree, P.**, Somboonwiwat, K., Tassanakajon, A., The effect of anti-lipopolysaccharide isoform 3 (ALF*Pm*3) from *Penaeus monodon*, against *Vibrio harveyi*, The science forum 2011, Chulalongkorn University, Bangkok, Thailand (2011).

   Award: The first prize of the oral presentation, Session: Biological Sciences, The Science Forum 2011, Chulalongkorn University, Thailand

Poster Presentation

1. **Jaree, P.**, Somboonwiwat, K., Tassanakajon, A., Functional characterization of a novel viral reponseive protein 15 (*Pm*VRP15) from the black tiger shrimp *Penaeus monodon*. The science forum 2013, Chulalongkorn University, Bangkok, Thailand (2013).

   Award: The first prize of the poster presentation, Session: Biological Sciences, The Science Forum 2013, Chulalongkorn University, Thailand
2. **Jaree, P.**, Somboonwiwat, K., Tassanakajon, A., Genomic organization and promoter activity of a viral responsive protein from the black tiger shrimp, *Penaeus monodon*. 17th Biological Sciences Graduate Congress (BSGC), Bangkok, Thailand (2012).

Award: The Silver Medalist Winner for poster presentation, Session: Cell and Molecular Biology, The 17th Biological Sciences Graduate Congress 2012, Chulalongkorn University, Thailand

3. **Jaree, P.**, Somboonwiwat, K., Tassanakajon, A., RNAi knock-down of *Penaeus monodon* viral responsive protein 15 (*Pm*VRP15) reduces WSSV replication in shrimp. 13th FAOBMB Congress 2012, Bangkok, Thailand (2012).
4. **Jaree, P.**, Somboonwiwat, K., Tassanakajon, A., Antimicrobial action of anti-lipopolysaccharide factor isoform3 (ALF*Pm*3) from the black tiger shrimp *Penaeus monodon.* 2012 Niigata Graduate Research forum, Niigata University, Niigata, Japan (2012).

   Award: The excellent poster presentation award, 2012 Niigata Graduate Research forum, Niigata University, Japan

5. **Jaree, P.**, Somboonwiwat, K., Tassanakajon, A., Pore forming Mechanism Mediates the antibacterial acitivity of ALF*Pm*3 from the black tiger shrimp *Penaeus monodon.* The 3rd Biochemistry and Molecular Biology (BMB) Conference, Chiang mai, Thailand (2011).

VITA

Ms. Phattarunda Jaree was born on August 26, 1987 in Bangkok. She graduated with the degree of Bachelor of Science from the Department of Bichemistry, Faculty of Science, Chulalongkorn University in 2009. Then she got the scholarship from The Chulalongkorn University graduate scholarship to commemorate the 72nd Anniversary of His Majesty King Bhumibol Adulyadej and the Royal Golden Jubilee Ph.D. Program, Thailand Research Fund for the degree of doctor of philosophy of Science at the Department of Biochemistry, Faculty of Science, Chulalongkorn University since 2009.

She had published her works in the research journal, Developmental & Comparative Immunology, on the topic of “Effect of the Anti-lipopolysaccharide Factor Isoform 3 (ALFPm3) from Penaeus monodon on Vibrio harveyi cells” and the research journal , PLoS ONE, on the topic of “PmVRP15, a novel viral responsive protein from the black tiger shrimp, Penaeus monodon, promoted white spot syndrome virus replication”.